ADVANCES ON THIRDHAND SMOKE USING TARGETED AND UNTARGETED APPROACHES

Sònia Torres Gené

UNIVERSITAT ROVIRA i VIRGILI

Advances on Thirdhand Smoke using Targeted and Untargeted Approaches

Sònia Torres Gené

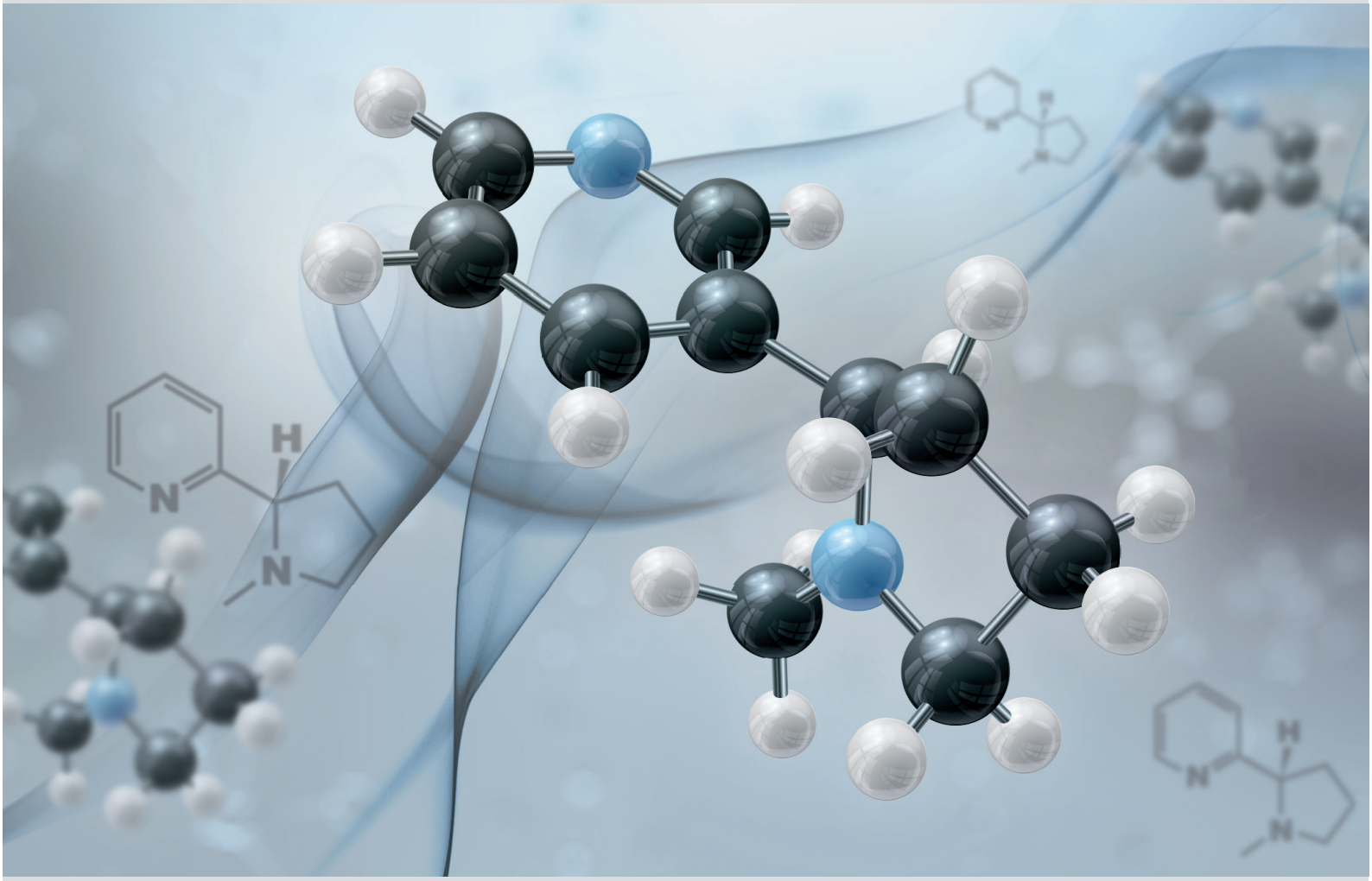

DOCTORAL THESIS
2020-2021

UNIVERSITAT ROVIRA I VIRGILI
ADVANCES ON THIRDHAND SMOKE USING TARGETED AND UNTARGETED APPROACHES
Sònia Torres Gené

Sònia Torres Gené

Advances on Thirdhand Smoke using targeted and untargeted approaches

DOCTORAL THESIS

Supervised by Dr. Noelia Ramírez and Dr. Xavier Correig

Departament d'Enginyeria Electrònica, Elèctrica i Automàtica

UNIVERSITAT ROVIRA I VIRGILI

Tarragona
2021

UNIVERSITAT ROVIRA I VIRGILI
ADVANCES ON THIRDHAND SMOKE USING TARGETED AND UNTARGETED APPROACHES
Sònia Torres Gené

UNIVERSITAT ROVIRA I VIRGILI
ADVANCES ON THIRDHAND SMOKE USING TARGETED AND UNTARGETED APPROACHES
Sònia Torres Gené

UNIVERSITAT ROVIRA I VIRGILI
ADVANCES ON THIRDHAND SMOKE USING TARGETED AND UNTARGETED APPROACHES
Sònia Torres Gené

UNIVERSITAT ROVIRA I VIRGILI

Escola Tècnica Superior d'Enginyeria

Departament d'Enginyeria Electrònica, Elèctrica i Automàtica

Av. Països Catalans 26

Campus Sescelades

43007 Tarragona

We STATE that the present study, entitled: Advances on thirdhand smoke using targeted and untargeted approaches, presented by Sònia Torres Gené for the award of the degree of Doctor, has been carried out under our supervision at the Department of Electronic, Electric and Automatic Engineering (DEEEA) of this university and meets the requirements to qualify for International Mention.

Tarragona, March 2021

Doctoral thesis supervisors

RAMIREZ GONZALEZ NOELIA - 39699685Y
Digitally signed by RAMIREZ GONZALEZ NOELIA - 39699685Y
Date: 2020.10.23 17:28:09 +02'00'

UNIVERSITAT ROVIRA I VIRGILI
Francesc Xavier Correig Blanchar - DNI 39849924D (AUT)
2020.10.23 20:29:22 +02'00'

Dr. Noelia Ramírez González

Dr. Francesc Xavier Correig Blanchar

UNIVERSITAT ROVIRA I VIRGILI
ADVANCES ON THIRDHAND SMOKE USING TARGETED AND UNTARGETED APPROACHES
Sònia Torres Gené

ACKNOWLEDGMENTS

Aquest matí, després d'un llarg dia de muntatge de documents, he enviat per fi la penúltima versió d'aquesta tesi, dient als meus directors que esperaba tenir els agraïements escrits per divendres, no sabia que posar! Després he escrit un wats app al grup dels companys donant-los la noticia de que això que tant a costat ja casi està aquí! Ràpidament alguns de vosaltres m'heu escrit per privat per quedar, fer un café i veuren's les cares. Llavors m'he adoant de que ho tenia clar, lo millor d'aquesta tesi, sou vosaltres, cada una de les persones que he conegut en aquest llarg camí. Que aquesta es l apart bona de que hagi set llarg, que n'he conegut moltes! Vaig aterrar a un Búnquer ple de nois, el "Dream team" dels programadors, titulars: Xavi Domingo, Pere Ràfols, Daniel Cañueto, Josep Gómez, Rubén Barrilero i Didac Vilalta, i jo allí, sense tenir ni idea de que era l'R! El Xavi es va oferir a fer-me unes classes, el Pere algún cop també va intentar alguna cosa…pero nois, ho sento pero no era lo meu! Això si, no he pogut riure més amb vosaltres, ni passar-m'ho millor en cada un dels cafés, sopars i moments que he compartit amb vosaltres. Sobretot vull agrair al Pere, la seva paciencia ensenyant-me com funcionava el MALDI i el ggplot del'R, ha estat tot un paler ser la teva companya de taula tants anys!

També volia donar les gràcies a tots els que heu anat entrant després, María, Lluch, Gerard Alex i Carla. Alex! Many thanks! I'll never forget our time in Florence! Carla, eres la persona mas trabajadora, buena, amable y generosa que he conocido (¡y mira que soy mayor!). Muchas gracias

por todas las veces que me has ayudado, te deseo lo mejor y mucho ánimo que en nada estas acabando tu tesis!

Y por último quiero agradecer miles de cosas a Sara, gracias por enseñarme mucho de lo que sé de metabolomica, Q-TOF, RMN y R. Pero sobretodo gracias por haberte convertido en una gran amiga y por estar ahí siempre y para todo.

"Research is what I'm doing when

I don't know what I'm doing"

Wernher von Braun

UNIVERSITAT ROVIRA I VIRGILI
ADVANCES ON THIRDHAND SMOKE USING TARGETED AND UNTARGETED APPROACHES
Sònia Torres Gené

ABSTRACT

Thirdhand smoke (THS) is a novel way of exposure to tobacco smoke compounds little known in our society. THS contamination begins when cigarette smoke is extinguished and airborne compounds deposit on surfaces near to the smoking area. These compounds remain for long periods of time in indoor environments, leading to their aging and the possibility of reacting with other compounds present in the environment to form secondary pollutants that could be more toxic than primary compounds. This type of contamination is of especial concern in homes of children with smoking parents, since the ways of exposure to THS toxicants are ingestion, dermal absorption and inhalation. Consequently, children habits like crawling, playing on the floor or bringing objects to mouth turns them into the most vulnerable population. Hence, it is crucial to have a broader knowledge of this type of contamination and the health effects associated to THS exposure, to protect children and people who live with smokers from this source of exposure.

Tobacco smoke is made up of thousands of compounds and many of them toxic and carcinogen. To date, research on the chemical characterization of THS has been mostly focused on the analysis of tobacco-specific compounds, as nicotine and carcinogenic tobacco specific nitrosamines (TSNAs). Since these compounds are found at very low concentrations in the environment and present different physic-chemical characteristics, robust and sensitive analytical methods are required for their determination. For the assessment of THS-induced health effects, research has mainly focused on the determination of exposure biomarkers in biological matrices and the evaluation of known

health markers in vivo and in vitro models to characterize the health effects derived from THS exposure.

However, for a comprehensive characterization of THS it is crucial the use more holistic approaches to achieve a better assessment of the risks associated to THS exposure and to broaden the current knowledge of THS-induced damage and health effects.

Hence, the main objective of this thesis is to advance on the current knowledge of THS by using novel target and untargeted approaches. To accomplish that, this thesis has been divided in two secondary objectives: to improve the chemical characterization of THS, and to advance on the health effects derived from THS exposure.

In this thesis, we have combined the determination of targeted tobacco-specific toxicants with non-target screening (NTS) to improve the chemical characterization of THS. The first study presented here focuses on the development of a novel analytical method for the simultaneous determination of nicotine, cotinine and four tobacco-specific nitrosamines (TSNAs) in household dust by using ultra high-performance liquid-chromatography (UHPLC) coupled to tandem mass spectrometry (LC-MS/MS) using a triple quadrupole (QQQ) mass spectrometer. The developed method, based on a QuEChERS (Quick, Easy, Cheap, Effective, Rugged, and Safe) extraction, is high-throughput, easy to automatize and more cost-effective than the methods reported by the literature.

In the second study included in this thesis, we have applied for the first time a combination of targeted and NTS strategies for the advance characterization of household dust from smokers' and non-smokers' homes. Results of the targeted analysis confirmed the ubiquitous presence of tobacco-specific toxicants, even in smoke-free homes. The untargeted workflow developed combined the acquisition by UHPLC coupled to high-resolution mass spectrometry (HR-MS) with the application of advanced data processing strategies, the statistical prioritization of relevant features and a novel strategy for compound annotation. Results presented in this thesis show that the combination of these two approaches provided for the first time the annotation of dozens of toxicants related to THS contamination.

We also present the application of multiplatform untargeted metabolomics to unravel the molecular alterations of liver from mice exposed to THS. We used two analytical platforms (UHPLC-HRMS and nuclear magnetic resonance, NMR) for a comprehensive determination of the altered metabolites in liver extracts, and mass spectrometry imaging (MSI) for the study of the differential spatial distribution of lipids in the liver tissues. The results presented in this thesis indicate that THS exposure dysregulate several hepatic metabolic pathways and abnormal lipid metabolism known as NAFLD, being oxidative stress the main mechanism for the alterations suffered. The lipid liver accumulation was confirmed by MSI, which permitted the visualization and determination of the lipid species that accumulate in liver.

The results presented in this thesis confirm the ubiquitous presence of THS contaminants, provide an improved chemical characterization and unravel new molecular alterations underlying THS exposure, thus confirming the health risks associated to this exposure. These results also demonstrate that the use of untargeted approaches in combination of robust targeted methods are key for the comprehensive study environmental health risks.

LIST OF ABBREVIATIONS

1D	1-dimension
2D	2-dimensions
2D-JRES	2-dimensional J-resolved spectrum
ACN	Acetonitrile
APCI	Atmospheric pressure chemical ionization
APPI	Atmospheric pressure photo ionization
$CDCl_3$	Deuterated Chloroform
CD_3OD	Deuterated Methanol
CH_3Cl	Chloroform
CI	Chemical ionizaiton
CO	Carbon monoxide
CO_2	Carbon dioxide
COSY	Correlation spectroscopy
C-trap	Curved linear trap
CV	Coeficient of variation
D_2O	Deuterated water
Da	Dalton
DCM	Dichloromethane
DDA	Data-dependent acquisition
DESI	Desorption electrospray ionization
DHA	Docosahexaenoic acid
DIA	Data independent acquisition
d-SPE	Dispersive solid phase extraction
ESI	Electron Spray Ionization
EPA	Environmental Protection Agency

ERETIC	Electronic reference to access In vivo concentrations
ESI	Electrospray Ionization
ETS	Environmental Tobacco smoke
FC	Fold change
FCTC	Framework convention on Tobacco control
FT	Fourier Transform
FT-ICR	Fourier transform ion cyclotron resonance
GC	Gas Chromatography
H_2O_2	Hydrogen peroxide
HCD	Higher-energy collisional dissociation
HILIC	Hydrophilic Interaction Liquid Chromatography
HONO	Nitrous acid
HPLC	High performance liquid chromatography
^{1}H-NMR	Proton Nuclear Magnetic Resonance
HPLC	High Performance Liquid Chromatography
HMDB	Human Metabolome Database
HRMS	High-resolution mass spectrometry
IARC	International Agency for Research on Cancer
IT	Ion Trap
J-Res	J-resolved spectroscopy
LC	Liquid chromatography
LC-MS	Liquid chromatography - mass spectrometry
LDI	Laser desorption ionization
LE	Liquid extraction
LOD	Limit of detection
LOQ	Limit of quantification
MAE	Microwave assisted extraction

MALDI	Matrix-assisted laser desorption ionization
MeOH	Methanol
MS	Mass Spectrometry
MS^2	Tandem mass spectrometry
MSI	Mass spectrometry imaging
MSPD	Matrix solid phase dispersion
MS/MS	Tandem mass spectrometry
MRM	Multiple reaction monitoring
m/z	mass-to-charge ratio
NAFLD	Non-alcoholic fatty liver disease
NASH	No-alcoholic steatohepatitis
NCD	Nitrogen chemiluminescence detector
NHANES	National health and nutrition examination survey
NIST	National Institute of Standards and Technology
NNA	1-(N-methyl-N-nitrosamino)-1-(3-pyridinyl)-4-butanal)
NNK	4-(methylnitrosamino)-1-(3-pyridinyl)-1-butanone
NNN	N-nitroso nornicotine
NOESY	Nuclear Overhauser effect spectroscopy
NMR	Nuclear Magnetic Resonance
NPLC	Normal phase liquic chromatography
PAHs	Polycyclic aromatic hydrocarbons
PCA	Principal Component Analysis
PLE	Pressurize dliquid extraction
PM	Particulate matter
PUFAs	Polyunsaturated fatty acids

Q	Quadrupole
Q-Orbitrap	Quadrupole Orbitrap
QQQ	Triple quadrupole
QuEChERS	Quick, Easy, Cheap, Effective, Rugged and Safe
Q-TOF	Quadrupole Time of Flight
ROS	Reactive oxygen species
RP	Reverse phase
RPLC	Reverse phase liquid chromatography
SALDI	Surface assisted laser desorption ionization
SD	Standard deviation
SHS	Secondhand smoke
SIMS	Secondary ion mass spectrometry
SPE	Solid phase extraction
SRM	Selected reaction monitoring
SWATH	Sequential window acquisition of all theoretical fragment-ion spectra
TD	Thermal desorption
TG	Tryglicerides
THS	Thirdhand smoke
THRMS	Tandem high-resolution mass spectrometry
TIC	Total ion count
TOCSY	Total Correlation Spectroscopy
TOF	Time of Flight
TSNAs	Tobacco specific Nitrosamines
UHPLC	Ultra-high performance liquid chromatography
VOCS	Volatile Organic Compounds
WHO	World Health Organization

LIST OF PUBLICATIONS

Publications included this thesis:

Sònia Torres, Carla Merino, Beatrix Paton, Xavier Correig and Noelia Ramírez. "Biomarkers of Exposure to Secondhand and Thirdhand Tobacco Smoke: Recent Advances and Future Perspectives" Int. J. Environ. Res. Public Health 2018, 15, 2693.DOI: 10.3390/ijerph15122693

Sònia Torres, Sara Samino, Pere Ràfols, Manuela Martins-Green, Xavier Correig and Noelia Ramírez."Unravelling the metabolic alterations of liver damage induced by Thirdhand Smoke" Environ. Int. 2020, 146 DOI: 10.1016/j.envint.2020.106242

Sònia Torres, Beatrix Paton, Rosa María Marcé, Francesc Borrull, Xavier Correig and Noelia Ramírez. "Development of a quick, easy, cheap, effective, rugged and safe (QuEChERS) extraction method to determine tobacco specific toxicants in house dust by liquid chromatography-tandem mass spectrometry" Analyst 2020 *(Submitted)*

Sònia Torres, Xavier Correig, Emma L. Schymanski and Noelia Ramírez. "Combination of Target and Non-target methods to advance on the chemical composition of Thirdhand Smoke in Household Dust" Environ Sci Technol *(In preparation)*

Publications from collaborations:

Pere Ràfols, **Sònia Torres**, Noelia Ramírez, Esteban del Castillo, Oscar Yanes, Jesús Brezmes and Xavier Correig. "rMSI: an R package for MS imaging data handling and visualization". Bioinformatics, 2017, 33, (15), pp 2427–2428. DOI:10.1093/bioinformatics/btx182

Pere Ràfols, Didac Vilalta, **Sònia Torres**, Raul Calavia, Bram Heijs, Liam A. McDonnell, Jesús Brezmes, Esteban del Castillo, Oscar Yanes, Noelia Ramírez and Xavier Correig. "Assessing the Potential of Sputtered Gold Nanolayers in Mass Spectrometry Imaging for Metabolomics Applications". PLoS One 2018, 13 (12), e0208908. DOI: 10.1371/journal.pone.0208908

Esteban Del Castillo, LLuc Sementé, **Sònia Torres**, Pere Ràfols, Noelia Ramírez, Manuela Martins-Green, Manel Santafe and Xavier Correig. "RMsikeyion: An Ion Filtering r Package for Untargeted Analysis of Metabolomic LDI-MS Images". Metabolites 2019, 9 (8). DOI: 10.3390/metabo9080162

LIST OF CONFERENCE COMMUNICATIONS

Sònia Torres, Pere Ràfols, Dídac Vilalta, Raul Calavia, Oscar Yanes, Noelia Ramírez and Xavier Correig. *"New technologies for metabolomics MS imaging"*.27-30/06/2016. 12th Annual Conference of the Metabolomics Society (http://metabolomics2016.org). Dublín, Ireland. **Oral communication**

Sònia Torres, Sara Samino, N. Adhami, Manuela Martins-Green, Xavier Correig, Noelia Ramírez. *"Targeted and untargeted metabolomics of urine of mice exposed to thirdhand tobacco smoke"*. 13-17/02/2017. EMBO Practical course on Metabolomics Bioinformatics for Life Scientists. (https://www.ebi.ac.uk/training/events/2017/embo-practical-course-metabolomics-bioinformatics-life-scientists-3). Cambridge, UK. **Poster communication.**

Sònia Torres, Sara Samino, Pere Ràfols, Neema Adhami, Manuela Martins-Green, Xavier Correig**,** Noelia Ramírez. *"Assessment of the THS exposition in animal models by multiplatform metabolomics analysis".* 26-31/08/2018. XXII International Mass Spectrometry Conference. (http://www.imsc2018.it). Florence (Italy). **Poster communication**.

Noelia Ramírez, Sara Samino, **Sònia Torres**, Neema Adhami, Manuela Martins-Green, Xavier Correig *"Multiplatform MS metabolomics reveals metabolic disorders in mice exposed to thirdhand tobacco smoke*". 27-30/06/2016. 12th Annual Conference of the Metabolomics Society (http://metabolomics2016.org). Dublín, Ireland. **Poster communication.**

Noelia Ramírez, **Sònia Torres**, Xavier Domingo, Lara Gundel, Hugo Destaillats, Rosa Maria Marcé, Francesc Borrull, Xavier Correig. *"Combination of multiple analytical platforms and nontargeted approaches for comprehensive risk assessment characterization: thirdhand tobacco smoke as case study"*. 9-16/10/2016. 26th Annual Meeting of the International Society of Exposure Science (http://ises2016.org). Utrecht, Netherlands. **Oral communication.**

Noelia Ramírez, Sara Samino, **Sònia Torres**, Beatrix Paton, Neema Adhami, Manuela Martins-Green, Xavier Correig *"Metabolomics reveals metabolic disorders in mice exposed to thirdhand tobacco*

smoke". 9-16/10/2016. 26th Annual Meeting of the International Society of Exposure Science (http://ises2016.org). Utrecht, Netherlands. **Poster communication.**

Pere Ràfols, Dídac Vilalta, **Sònia Torres**, Jesús Brezmes, Noelia Ramírez and Xavier Correig. *"rMSI: An R package for MSI data handling and visualization"*. 17-21/10/2016. OurConIV. (https://ms-imaging.org/wp/2016/01/19/ourcon-iv/). Ustron, Poland (2016). **Oral communication**

Noelia Ramírez, Sara Samino, **Sònia Torres**, Beatrix Paton, Neema Adhami, Manuela Martins-Green, Xavier Correig*. "Metabolomics reveals metabolic disorders in mice exposed to thirdhand tobacco smoke". 18-20/10/2017. International Workshop on* Environmental Omics, Integration & Modeling. Barcelona, Spain. *http://wenvomics2017.info*. **Oral communication.**

Noelia Ramírez, Sara Samino, **Sònia Torres**, Beatrix Paton, Neehma Adhami, Manuela Martins-Green, Xavier Correig. "Metabolomics reveals metabolic disorders in mice exposed to thirdhand tobacco smoke" 23-27/06/2019. 15th Annual Conference of the Metabolomics Society (http://metabolomics2019.org). The Hague, Netherlands. **Poster communication**

Emma L. Shymanski, **Sònia Torres**, Noelia Ramírez. "Environmental cheminformatics: Case of study Thirdhand smoke in house dust" 22-24/01/2020. European RFMF Metabomeeting (https://rfmf-mpf-2020.sciencesconf.org). Toulouse, France. **Oral Communication**

TABLE OF CONTENTS

ABSTRACT X
LIST OF ABBREVIATIONS XIII
LIST OF PUBLICATIONS XVI
LIST OF CONFERENCE COMMUNICATIONS XVII
TABLE OF CONTENTS XIX

1. Introduction 1
1.1 Thirdhand Smoke 1
1.2 Environmental Exposure 9
1.3 Analytical techniques 14
1.3.1 Mass Spectrometry 14
1.3.1.1 Tandem Mass Spectrometry 19
1.3.2 Liquid Chromatography 25
1.3.3 Mass Spectrometry Imaging 26
1.3.4 Nuclear Magnetic Resonance 29
1.4 Dust targeted analysis 32
1.5 Untargeted analysis 37
1.5.1 LC/MS experiments 38
1.5.2 MSI experiments 46
1.5.3 NMR experiments 51
1.5.4 Result Interpretation 54
1.6 Thesis motivation and objectives 55
1.7 Organization of the document 57
1.8 References 60

2. Biomarkers of Exposure to Secondhand and Thirdhand Tobacco Smoke: Recent Advances and Future Perspectives 76

2.1 Abstract 78

2.2 Introduction 78

2.3 Selection of the papers 81

2.4 Biological matrices 82

2.5 Tobacco-Specific Biomarkers 86

2.5.1 Nicotine 91

2.5.2 Nicotine Metabolites 92

2.5.3 Tobacco Specific Nitrosamines (TSNAs) 96

2.6 Tobacco-Related Biomarkers 98

2.6.1 Polycyclic Aromatic Hydrocarbons (PAHs) 98

2.6.2 Volatile Organic Compounds (VOCs) 99

2.6.3 Metals 101

2.6.4 Carbon Monoxide 103

2.7 Determination of Multiple Specific Biomarkers. Examples of Applications 104

2.7.1 Evaluation of SHS Exposure 104

2.7.2 Evaluation of THS Exposure 106

2.8 Conclusions 109

2.9 Supplementary Information 111

2.10 References 123

3. Development of a quick and cost-effective method for determining tobacco-specific toxicants in indoor dust 133

3.1 Abstract 135

3.2 Introduction 136

3.3 Experimental 138

3.3.1 Reagents and standards 138

3.3.2 Sample collection and pretreatment 140
3.3.3 Extraction 141
3.3.4 UHPLC-MS/MS analysis 142
3.4 Results and Discussion 143
3.4.1 UHPLC-MS/MS 143
3.4.2 Indoor dust extraction 144
3.4.2.1 Extraction technique and solvent selection 144
3.4.2.2 Solvent ratio 148
3.4.2.3 dSPE sorbent selection 150
3.5 Method validation 152
3.6 Application to indoor samples 155
3.7 Conclusions 158
3.8 References 160
4. Combination of Target and Non-target methods to advance on the chemical composition of Thirdhand smoke in household dust ... 163
4.1 Abstract 165
4.2 Introduction 166
4.3 Materials and methods 168
4.3.1 Sample collection and preparation 168
4.3.2 Dust extraction and analysis 170
4.3.3 Untargeted data analysis 172
4.4 Results and Discussion 174
4.4.1 Target results 174
4.4.2 Non-target results 180
4.5 Conclusions 184
4.6 Supplementary Information 185

4.7 References 190

5. Unravelling the metabolic alterations of liver damage induced by Thirdhand Smoke 195

5.1 Abstract 197

5.2 Introduction 198

5.3 Materials and methods 201

5.3.1 Animal models 201

5.3.2 Untargeted metabolomic analysis 202

5.3.3 Pathway analysis 206

5.3.4 Mass spectrometry Imaging 206

5.4 Results 207

5.4.1 Untargeted metabolomic results 207

5.4.2 Spatial distribution of lipids 218

5.4.3 Effects of THS exposure in liver metabolism 221

5.5 Discussion 222

5.6 Conclusions 227

5.7 Supplementary Information 228

5.8 References 235

6. General discussion and conclusions 240

6.1 SHS and THS biomarkers 242

6.2 Analytical procedures and characterization of the chemical composition of THS in indoor dust 244

6.3 Advance on the health impact of THS exposure 248

6.4 Future trends and perspectives 250

6.5 References 252

1. Introduction

1.1 Thirdhand smoke

Passive smoking is estimated to be the cause of about 1.0% of worldwide mortality, approximately 600,000 deaths each year [1]. Secondhand smoke (SHS), also known as environmental tobacco smoke (ETS), is composed by the mainstream smoke exhaled while smoking, and the side stream smoke emitted from the burning cigarette. This mixture contains over 4,700 chemicals including hazardous amines, carbonyls, hydrocarbons and metals, among others [2–4]. SHS hazards and health effects have been studied from different science branches such as medicine, psychiatry, toxicology and environmental science. Scientific evidence has unequivocally established that exposure to tobacco smoke causes death and diseases including, among others, lung and breast cancer, ischemic heart disease, and asthma in adults, and lower respiratory tract infection, sudden infant death syndrome, and low birth weight in children [5]. As a result of the globalization of the tobacco epidemic in 2003 there was the first international treaty for guiding national tobacco laws negotiated under the auspices of the World Health Organization (WHO); The WHO Framework Convention on Tobacco Control (WHO FCTC) [6]. These policies, made to promote public health and to protect people from tobacco smoke exposure in public places, have been adopted to date for 180countries including the USA and 50 WHO European member States[7]. They also allowed to bring the scientific knowledge of SHS health effects closer to the population. Although most of the population is aware of the hazards of tobacco consumption and SHS exposure, few people are aware that these hazards continue long after cigarette consumption through the so-called thirdhand smoke (THS).

THS is a novel pathway of tobacco smoke exposure produced by the accumulation of SHS particles and gases, which can absorb to indoor particles and surfaces, resuspend, reemit back into the air and react with oxidants or other environmental compounds to form secondary pollutants [8–12]. THS is a rather complex mixture, and its entire composition is yet to be elucidated. To date the constituents identified in THS include tobacco-specific toxicants, such as nicotine, tobacco-specific nitrosamines (TSNAs) and other nicotine alkaloids, and non-specific toxicants such as volatile nitrosamines, aromatic amines, polycyclic aromatic hydrocarbons (PAHs), and volatile carbonyls among others [12–16]. In order to better understand the complexity of THS chemical composition, during the elaboration of this doctoral thesis we have compiled the current knowledge of the organic compounds identified in THS samples. This list is part of the NORMAN Suspect list Exchange [17]—which is as a central access point to find suspect lists relevant for environmental monitoring— and it has been published at the CompTox Chemicals Dashboard (DSSTox) of the United States Environmental Protection Agency (EPA) website [18]. Table 1 shows the 95 compounds included in this list, classified by compound category, their chemical name, molecular formula and the DSSTox substance identifier (DTXSID).

Table 1. List of the 95 organic compounds identified to date in THS, their compound category, chemical name, molecular formula and DSSTox substance identifier (DTXSID) .

CATEGORY	COMPOUND: CHEMICAL NAME	MOLECULAR FORMULA	DSSTOX ID
NICOTINE AND NICOTINE ALKALOIDS	**Nicotine**: 3-(1-methylpyrrolidin-2-yl)pyridine	$C_{10}H_{14}N_2$	DTXSID1020930
	Cotinine: 1-methyl-5-(pyridin-3-yl)pyrrolidin-2-one	$C_{10}H_{12}N_2O$	DTXSID1047576
	3-hydroxycotinine: 3-Hydroxy-1-methyl-5-(3-pyridinyl)-2-pyrrolidinone	$C_{10}H_{12}N_2O_2$	DTXSID30873224
	Nicotyrine: Pyridine, 3-(1-methyl-1H-pyrrol-2-yl)-	$C_{10}H_{10}N_2$	DTXSID3075048
	2,3'-Bipyridine	$C_{10}H_8N_2$	DTXSID00206823
	N-Formylnornicotine: 2-(Pyridin-3-yl)pyrrolidine-1-carbaldehyde	$C_{10}H_{12}N_2O$	DTXSID30336006
	Nicotelline	$C_{15}H_{11}N_3$	DTXSID40197781
TOBACCO SPECIFIC NITROSAMINES (TSNAS)	**NNN**: N'-Nitrosonornicotine	$C_9H_{11}N_3O$	DTXSID4021476
	NNA: 4-(methylnitrosamino)-4-(3-pyridyl)butanal	$C_{10}H_{13}N_3O_2$	DTXSID00897139
	NNK: 4-(Methylnitrosoamino)-1-(3-pyridinyl)-1-butanone	$C_{10}H_{13}N_3O_2$	DTXSID3020881
	NNAL: 4-(methylnitrosamino)-1-(3-pyridyl)-1-butanol	$C_{10}H_{15}N_3O_2$	DTXSID8020880
	NAB: N-nitrosoanabasine	$C_{10}H_{13}N_3O$	DTXSID3021019
	NAT: N-nitrosoanatabine	$C_{10}H_{11}N_3O$	DTXSID40868005
SECONDARY PRODUCTS OF NICOTINE HETEROGENEOUS NITROSATION	**Methyl nicotinate**: 3-Pyridine carboxylic acid methyl ester	$C_7H_7NO_2$	DTXSID7044471
	N-methylnicotinamide: N-Methylpyridine-3-carboxamide	$C_7H_8N_2O$	DTXSID00870467

N-NITROSAMINES	**NDMA**: N-nitrosodimethylamine	$C_2H_6N_2O$	DTXSID7021029
	NMEA: N-nitrosomethylethylamine	$C_3H_8N_2O$	DTXSID6021036
	NDEA: N-nitrosodiethylamine	$C_4H_{10}N_2O$	DTXSID2021028
	NDPA: N-nitrosodi-n-propylamine	$C_6H_{14}N_2O$	DTXSID6021032
	NPyr: N-nitrosopyrrolidine	$C_4H_8N_2O$	DTXSID8021062
	Nmor: N-nitrosomorpholine	$C_4H_8N_2O_2$	DTXSID4021056
	Npip: N-nitrosopiperidine	$C_5H_{10}N_2O$	DTXSID8021060
	NDBA: N-nitrosodi-n-butylamine	$C_8H_{18}N_2O$	DTXSID2021026
AROMATIC AMINES	2-Methylaniline	C_7H_9N	DTXSID1026164
	2-Naphthylamine	$C_{10}H_9N$	DTXSID2020921
	2-Anisidine	C_7H_9NO	DTXSID5023877
	Aniline	C_6H_7N	DTXSID8020090
	4-aminobiphenyl	$C_{12}H_{11}N$	DTXSID5020071
	2,6-Dimethylaniline	$C_8H_{11}N$	DTXSID8026307
IARC LIST OF CARCINOGEN CONSTITUENTS OF TOBACCO SMOKE	9-nitroanthracene	$C_{14}H_9NO_2$	DTXSID5025730
	1-nitropyrene	$C_{16}H_9NO_2$	DTXSID6020983
	Benz[a]anthracene	$C_{18}H_{12}$	DTXSID5023902
	Benzo[b]fluoranthene	$C_{20}H_{12}$	DTXSID0023907
	Benzo[j]fluoranthene	$C_{20}H_{12}$	DTXSID8052691
	Benzo[k]fluoranthene	$C_{20}H_{12}$	DTXSID0023909
	Benzo[a]pyrene	$C_{20}H_{12}$	DTXSID2020139
	Dibenz[a,h]anthracene	$C_{22}H_{14}$	DTXSID9020409
	Dibenzo[a,i]pyrene	$C_{24}H_{14}$	DTXSID9059751
	Dibenzo[a,e]pyrene	$C_{24}H_{14}$	DTXSID3052690
	Indeno[1,2,3-cd]pyrene	$C_{22}H_{12}$	DTXSID8024153
	5-Methylchrysene	$C_{19}H_{14}$	DTXSID6063143
NITROGENATED VOCS	3-Vinylpyridine	C_7H_7N	DTXSID90149912
	2-Vinylpyridine	C_7H_7N	DTXSID1026667
	2-Methylpyridine	C_6H_7N	DTXSID9021899
	3-Methylpyridine	C_6H_7N	DTXSID9021897
	3-Ethylpyridine	C_7H_9N	DTXSID6060212
	Pyridine	C_5H_5N	DTXSID9021924
	Pyrrol	C_4H_5N	DTXSID5021910
	Acetonitrile	C_2H_3N	DTXSID7020009

	Propionitrile	C_3H_5N	DTXSID1021879
	Acrylonitrile	C_3H_3N	DTXSID5020029
AROMATIC HYDROCARBONS	2-Methylfuran	C_5H_6O	DTXSID9025611
	2,5-Dimethylfuran	C_6H_8O	DTXSID7022093
	Benzaldehyde	C_7H_6O	DTXSID8039241
	Benzene	C_6H_6	DTXSID3039242
	Benzo(b)furan	C_8H_6O	DTXSID6020141
	Dibenz(a,j)acridine	$C_{21}H_{13}N$	DTXSID4059758
	7H-Dibenzo[c,g]carbazole	$C_{20}H_{13}N$	DTXSID9059755
	Ethylbenzene	C_8H_{10}	DTXSID3020596
	Furan	C_4H_4O	DTXSID6020646
	Iso-Propylbenzene	C_9H_{12}	DTXSID1021827
	m-Ethyltoluene	C_9H_{12}	DTXSID6050386
	m,p-Xylene	C_9H_{12}	DTXSID80109469
	m-Xylene	C_9H_{12}	DTXSID6026298
	p-Xylene	C_9H_{12}	DTXSID2021868
	n-Propylbenzene	C_9H_{12}	DTXSID3042219
	Naphthalene	$C_{10}H_8$	DTXSID8020913
	1-Ethyl-2-methylbenzene	C_9H_{12}	DTXSID2050403
	o-Xylene	C_8H_{10}	DTXSID3021807
	p-Ethyltoluene	C_9H_{12}	DTXSID9029194
	Nitrobenzene	$C_6H_5NO_2$	DTXSID3020964
	Styrene	C_8H_8	DTXSID2021284
	Toluene	C_7H_8	DTXSID7021360
CARBONYLS AND CHLORINATED VOCS	2,3-Butanedione	$C_4H_6O_2$	DTXSID6021583
	2-Butanone	C_4H_8O	DTXSID3021516
	Acetaldehyde	C_2H_4O	DTXSID5039224
	Acetone	C_3H_6O	DTXSID8021482
	Acetophenone	C_8H_8O	DTXSID6021828
	Propenal	C_3H_4O	DTXSID5020023
	Methacrylaldehyde	C_4H_6O	DTXSID0052540
	Chloromethane	CH_3Cl	DTXSID0021541
	Dichloromethane	CH_2Cl_2	DTXSID0020868
	Solanesol	$C_{45}H_{74}O$	DTXSID60884580

ALKANES AND ALKENES	Butane	C_4H_{10}	DTXSID7024665
	Isobutane	C_4H_{10}	DTXSID1026401
	n-Decane	$C_{10}H_{22}$	DTXSID6024913
	n-Nonane	C_9H_{20}	DTXSID9025796
	1,3-Butadiene	C_4H_6	DTXSID3020203
	1,3-Pentadiene	C_5H_8	DTXSID3027160
	1-Butene	C_4H_8	DTXSID1026746
	1-Nonene	C_9H_{18}	DTXSID2059562
	1-Octene	C_8H_{16}	DTXSID6025804
	d-Limonene	$C_{10}H_{16}$	DTXSID1020778
	Isoprene	C_5H_8	DTXSID2020761

Nicotine and TSNAs have been widely studied as THS markers since they are tobacco-specific toxicants. Nicotine is the main compound in tobacco filler, ranging from 7.2 to 18.3 mg/cigarette depending on the cigarette brand [4], and, in consequence, it is the most abundant organic compound emitted during tobacco smoking, from 0.5 to 2 mg/cigarette in mainstream cigarette smoke [19]. Nicotine sorbed to indoor surfaces can react with ambient nitrous acid (HONO) and other common atmospheric oxidants to form TSNAs such as 1-(N-methyl-N-nitrosamino)-1-(3-pyridinyl)-4-butanal) (NNA), 4-(methylnitrosamino)-1-(3-pyridinyl)-1-butanone (NNK), and N-nitroso nornicotine (NNN) [20,21], see Figure 1. Of those TSNAs, NNK and NNN have been classified as carcinogenic to humans (Group 1) by the International Agency for Research on Cancer (IARC) [22]. Although NNK and NNN are frequently found in tobacco smoke in the range of 50-200 ng/cigarette [4], NNA has not been reported in tobacco smoke due to its reactivity and instability at high temperatures during tobacco pyrolysis [23]. Therefore, NNA could potentially be an exclusive tracer of THS.

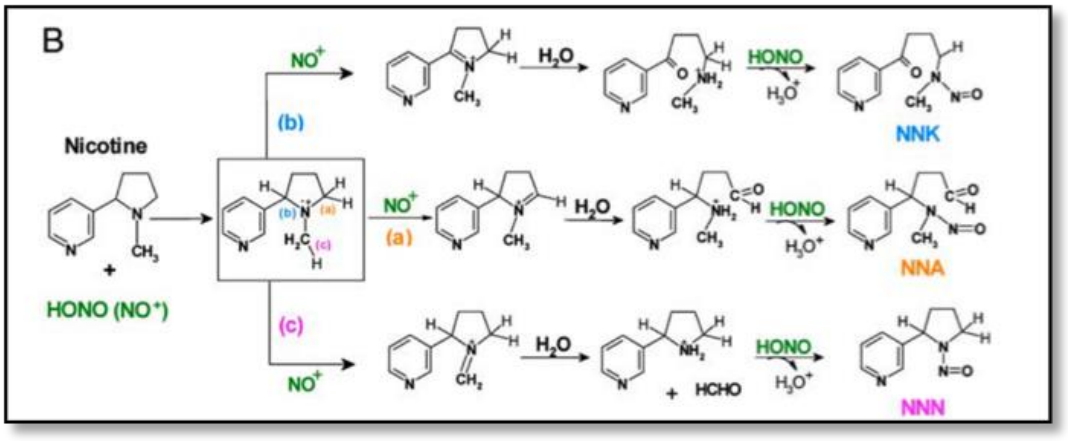

Figure 1. Proposed mechanism for the surface-mediated formation of TSNAs from nicotine in the presence of nitrous acid HONO (NO^+)[22].

The determination of tobacco-specific toxicants concentrations, such as nicotine and TSNAs, is key for the chemical characterization of THS, the detection of contaminated spaces and to understand the changes of THS chemical composition over time. To date, THS toxicants have been determined in dust and surfaces from smokers homes [24–27], cars [28] and public spaces such as hotels [29,30], a casino [31], and outdoor particles [32,33]. Conversely to SHS that can be easily removed by ventilation, THS can remain for long periods of time in indoor spaces [34], persisting in homes previously occupied by smokers [35,36], and at least for 6 months in homes occupied by smokers who quit smoking [37]. Hence, non-smokers living with smokers, including children with smoking parents, are exposed to tobacco toxicants even if they are not present when tobacco is consumed.

THS exposure occurs through ingestion, dermal absorption and, to a lesser extent, through inhalation [38]. These predominant ways of exposure make infants the most vulnerable population. Children are estimated to ingest more than twice dust than adults [39] because of their behaviour in the first years of life

and their hand-and object-to-mouth habit [40]. For the assessment of human exposure to THS, research has focused on the analysis of biomarkers in biological fluids.[41] However, it is still necessary to find reliable biomarkers able to differentiate between low SHS and THS exposure.

Regarding the impact of THS exposure in health, few exposure studies have been conducted on humans, besides most of them are limited to monitoring biomarkers in biofluids, hair and nicotine in hands. Despite the few studies conducted in humans THS exposure has been related to an increase of cough related-symptoms in children [42] and with higher levels of exhaled nitric oxide in kids with asthma [43]. It has also been found a linear relationship between respiratory symptoms and THS biomarkers levels in adolescents [44]. In a designed experiment for the study of the health effects of inhaled THS, nasal epithelium samples from healthy women revealed the differential expression of 389 genes compared to participants that inhaled clean air [45]. Since it is known that active smoking and SHS genotoxicity is one of the critical mechanisms responsible for many types of cancer [46] the genotoxic potential of THS has been tested [47–49]. Works conducted with cells showed that THS exposure causes alterations in both animal and human cellular functions [48], including mitochondrial stress and small alterations in gene expression [50], alteration of the gene expression of male murine reproductive cells [51] and structural changes in DNA in Human hepatocellular carcinoma (HepG2) cells [52]. In animal models, THS has been associated with an increased lung cancer risk [53], insulin resistance [54] the induction of hepatic steatosis [55] and a delayed wound healing and altered inflammatory response in the mice skin among others [56]. Of these studies only one has used a metabolomic approach, concluding that exposure to THS at very low concentrations causes metabolic changes in two different types of male

reproductive cells, including alterations in glutathione, nucleic acid and ammonia metabolisms [51].

Despite current evidences on THS health impact, knowledge about THS is yet to expand. In order to advance on THS characterization and health effects it is crucial the use of more holistic approaches for the study of the chemical composition of THS and the health effects associated to its exposure.

1.2 Environmental Exposure

Nowadays there is a worldwide growing interest in knowing how the chemicals and toxics to which we are exposed affect our health. The health effects of such exposure will depend on the intrinsic characteristics of the chemical, the degree of exposure as well as the concentration of the toxic and the characteristics of the individual such as, age sex and genotype [57,58]. To characterize the risks of such exposure, there are two main sciences that converge, in one hand analytical chemistry to identify and characterize those chemicals and pollutants and, on the other hand molecular biology and biochemistry, to understand how these chemicals interact with our body and affect our health.

A great challenge in environmental exposure is the control of the risks associated to mixtures of emerging contaminants. THS markers are emerging contaminants that deposit on surfaces and especially in indoor settled dust and particles. Indoor settled dust is a complex matrix that provides valuable information for the assessment of human indoor exposure and the compounds attached to house dust are indicators of both indoor and outdoor chemical contamination. Moreover, settled dust represents average levels of

contamination over long periods of time and can be useful for retrospective exposure assessment [59]. According to a recent European Commission report, Europeans spend 90% of their time in indoor environments and that indoor spaces can be at least twice polluted as outdoor environments [60]. Therefore, the characterization of indoor pollution is key in human exposure assessment.

Different methods have been developed for the analysis of organic contaminants in dust [61–63], and although these methods have been shown to be sensitive and selective, they aim to quantify and study only a small number of compounds. However, due to the number of compounds present in dust, generic analytical techniques to measure a broader range of compounds in a single study are becoming essential to overcome the challenges in analyzing complex matrices that contain many targeted and non-targeted compounds at different concentrations. Hence, High-resolution mass spectrometry (HRMS) is very suitable for these applications due to the high resolving power, mass accuracy, and sensitivity in full scan acquisition [64,65]. Nevertheless, few studies have been performed for the untargeted analysis of indoor dust using HRMS [66–68]. This is due to the fact that these approaches are not stablished enough in the environmental field. Since this problem has challenged environmental chemists for decades the capabilities and limitations of untargeted approaches have been evaluated. Two different collaborative nontarget screening trial on controlled test household dust samples have been organized by the EPA (EPA's Non-Targeted Analysis Collaborative Trial)[69] and by the NORMAN network (Network of reference laboratories, research centers and related organizations for monitoring of emerging environmental substances) [70]. The results of these initiatives highlighted the need for unified workflows to advance in the characterization of samples and in the search for new environmental markers.

Hence, one of the major trends in THS research is to develop fast and efficient analytical methods for the trace analysis of known and unknown compounds in settled dust. To date, no previous research has focused on the untargeted analysis of compounds related to THS in dust, thus opening the possibility of discovering new THS markers.

Analogously to the environmental field, for the assessment of THS-induced health effects it is crucial the use more holistic approaches. In this sense "omics" sciences of transcriptomics, proteomics and metabolomics seem to be the most suitable techniques. Among the omics sciences, metabolomics is particularly important for the assessment of progressive disease and environmental exposure since it offers a faster biological response to changes in the microenvironment compared to proteins or mRNA [71]. Therefore, metabolomics would be able to provide new insights on the health effects produced by THS exposure. As far as we know, only one previous study has used metabolomics to assess THS exposure [72].

Metabolomics is the study of endogenous and exogenous low molecular mass compounds (i.e. metabolites) in a cell, tissue or biofluid [73–75]. These metabolites include lipids, sugars and amino acids that serve as substrate and products of enzymatic reactions. Metabolites are influenced by gene, environmental factors, disease, nutrition and other aspects that can unbalance cell homeostasis. Therefore, the metabolome is the reflection of the combination of endogenous effects like genetics, and exogenous effects such as lifestyle and environmental factors. Metabolomics have been applied to multiple research fields including disease diagnosis, biomarker discovery, drug discovery and development, toxicology, food science and nutritional studies [76,77]. The basis of most of these applications is that the metabolic response to a natural or anthropogenic stressor is used to obtain information of the biological

state of the studied organism. Depending on the detected metabolites we can determine changes on the energetic, reproductive or oxidative status of the organism [57], as well as discover biomarkers and elucidate relationship between metabolite levels and external stressor [78]. Metabolome profiling is typically performed either by target and untargeted methods. However, due to the large chemical complexity of the metabolome, untargeted approaches using multiple analytical platforms are needed to analyse the entire range of metabolites [79].

Targeted approaches are based on the analysis of known compounds while for the analysis of unknowns, the development of untargeted methodologies is required. Targeted approaches are hypothesis-driven and refer to a method in which a small and well-defined set of known compounds are determined and commonly quantified. These compounds are usually at trace levels, therefore, their determination require analytical methods with high sensitivity, specificity and robustness [80]. Targeted analysis implies an important analytical effort for the optimization of all the steps involved in the analytical workflow, from sample collection, storage and preparation to the optimization of the instrumental parameters to achieve detection at trace levels. Data processing and interpretation are well stablished techniques and typically performed using vendor software.

In contrast untargeted approaches are hypothesis-free and provide a global analysis or comparative overview between two or more different sample groups. Untargeted methods require minimal and non-selective sample preparation, aiming to get coverage of a wider range of analytes by simple preparation steps. These minimum sample manipulation permits the use of multiplatform approaches, since no single analytical technique is suitable for the detection and identification of compounds with different chemical and physic characteristics. Compound identification is performed using existing

chemical repositories and libraries or in-house libraries [66]. The main differences between targeted and untargeted analytical strategies are summarized in Figure 2.

The principal advantage of untargeted approaches, either in the environmental and metabolomics field is that unexpected and novel responses are captured. Hypothesis-free studies provide the most appropriate route to detect changes in analyte concentrations, maximizing the number of analytes detected and providing the opportunity to observe changes. Therefore, for a holistic study of THS, this thesis focuses on the application of targeted and untargeted approaches to advance on the characterization of the chemical composition of THS as well as the study of targeted biomarkers and untargeted metabolomics to advance on the health effects derived from THS exposure.

	Targeted	Non-targeted
Analytical question	- Hypothesis-drive - Pre-defined analytes	- Hypothesis-free - Global analysis
Sample handling	- Selective - Complex	- Generic - Simple & high-throughput
Sample Analysis	- Selective - Sensitive	- Universal
Data processing	- Identification using chemical standards - Absolute quantification - Univariate statistics	- Compound assignment by matching with libraries - Relative quantification - Univariate/Multivariate statistics
Data Interpretation	- Assessment of target list values	- Identification of unknowns - Sample classification

Figure 2. Main differences between targeted and untargeted approaches throughout the analytical process (adapted from Spánik, et.al). [81]

1.3 Analytical techniques

The methods more used for the determination of trace organic analytes in environmental and biological samples are gas chromatography (GC) and liquid chromatography (LC) as separation techniques coupled to mass spectrometry (MS), being tandem mass spectrometer mode MS/MS the most reliable technique for identification purposes. For untargeted analysis high resolution tandem mass spectrometry instruments, coupled with soft ionization techniques to liquid and gas chromatography (LC-HRMS, GC-HRMS) allow sensitive and untargeted detection of thousands of compounds [82]. Moreover over the past two decades, nuclear magnetic resonance (NMR) has emerged as one of the principal analytical techniques used in metabolomics [83]. Furthermore, using mass spectrometry imaging (MSI), metabolites can be spectrometry spatially localized within biological specimens like vegetal or animal tissues and cell cultures[84].

A combination of the different techniques commented above have been used for the development of the different projects included in this thesis. A detailed explanation of the techniques and instruments used is provided in next sections.

1.3.1 Mass Spectrometry

Mass spectrometry (MS) is a powerful analytical technique used to identify and quantify analytes using the mass-to-charge ratio (m/z) of ions generated from a sample. Results are displayed in the form of a mass spectrum, which is a graphical representation of ion abundance versus m/z. Since molecules fragment in a unique manner under given conditions, it is possible to identify

the molecule based on the resulting molecular mass and the masses of its fragments [85].

Mass spectrometers are routinely coupled to chromatography systems in order to separate sample compounds prior to the identification by MS. Mass spectrometers typically consist of the following elements: inlet, source, mass analyzer and ion detection module [86].

a) **Inlet:** Is the injection system used to introduce the sample to the ionization source. The sample can be introduced manually in the case of direct injection or through a connection system working at high pressure in the case of coupled with chromatography instruments.

b) **Ionization source**: Is the module in which sample is ionized and transferred from the liquid phase into gas phase, generally by spraying the sample through a metal capillary by a turbulent air stream. The ionization consists of a physic-chemical process that converts neutral molecules to electrically charged molecules. There are two main types of ionization methods: soft ionization methods that leave the structure of the original molecule relatively unharmed; and hard ionization methods that fragment the compound molecular structure into smaller fragment ions (in-source fragmentation).

In LC-MS systems, three major soft ionization methods are available: electro spray ionization (ESI) mainly used in the characterization of biomolecules, ionic and very labile organic and organometallic compounds [87], atmospheric pressure chemical ionization (APCI) used for medium to non-polar organic compounds and synthetic polymers and atmospheric pressure photo ionization (APPI) which is less widespread. The most common ionization methods used in LC-MS are ESI and APCI [88,89].

Electrospray Ionization (ESI)

ESI uses electrical energy to produce ions using an electrospray in which a high voltage (e.g. 2.5-6.0 KV) is applied to a liquid to create an aerosol. ESI involves three steps: first dispersion of a fine spray of charge droplets, followed by solvent evaporation and ion ejection from the highly charged droplets. The charged droplets, generated at the exit of the electrospray tip, pass down a pressure and potential gradient toward the mass analyser of the spectrometer. The charged droplets are continuously reduced in size by the evaporation of the solvent acquired with and elevated ESI-source temperature and/or another stream of nitrogen drying gas [90]. A scheme of the ESI ionization from Forcisi, et.al. [91] is displayed in Figure 3. This soft ionization technique include little or no fragmentation thus enhancing the generation of $[M+zH]^{z+}$ ions in the case of positive ESI ionization and $[M-zH]^{z-}$ ions in the case of negative ESI ionization [92]. However, in ESI positive mode it is quite common the formation of adducts such as $[M+Na]^{+}$ or $[M+K]^{+}$, this ions can be easily formed in the gas phase by non-covalent interactions between the generated ions and the neutral solvent molecules [91].

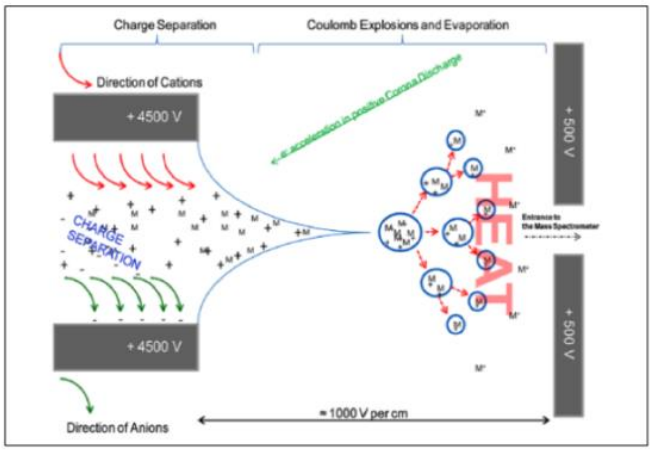

Figure 3. Scheme of the ESI ionization process [91].

Atmospheric pressure chemical ionization (APCI)

APCI is a soft ionization method that uses gas-phase ion-molecule reactions at atmospheric pressure (10^5 Pa). As it can be seen in Figure 4, in APCI the sample is dissolved in a solvent and pumped through a capillary inside an uncharged quartz tube. At the end of the capillary, the sample is converted into an aerosol and then vaporized with the help of nitrogen gas at very high temperature (~350-550 °C) condition. The gaseous solvent and sample are then ionized by a corona discharge, in which a highly charged electrode creates an electric field strong enough to ionize nearby molecules. A potential of several kilovolts applied to the electrode typically remove an electron from a neutral molecule, without depositing enough internal energy to cause fragmentation. The corona discharge may directly ionize an analyte molecule to form a radical cation ($M^{+\bullet}$). Different radical reactions can spontaneously occur between solvent and analyte radicals. The resulting analyte ions ($M^{+\bullet}$ or $[M+H]^+$) are then injected into the mass spectrometer for detection.[88,93]

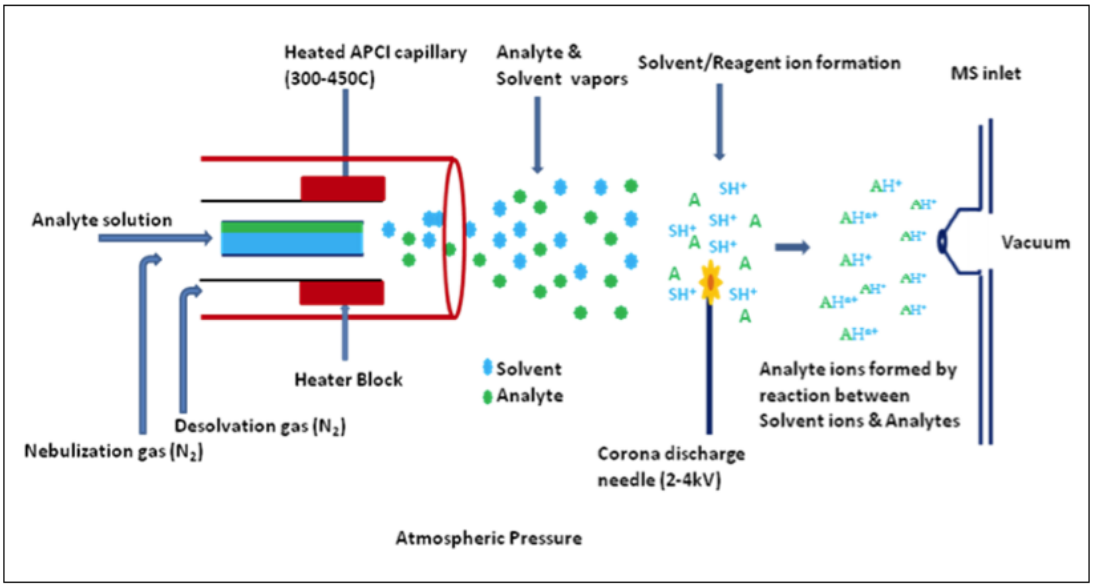

Figure 4. Schematic diagram of APCI process [94]

ii) **Mass analyzer:** Ions are analyzed using either beam type analyzers such as quadrupole, time-of-flight (TOF) or trapping mass analyzers (such as ion trap (IT) or Orbitrap). The main difference is that trapping systems resolve ions discontinuously while ion-beam instruments do it continuously [95]. Mass analyzers separate the ions according to their m/z by applying a differential equation of motion of charged particles. Mass analyzers use either static or dynamic fields, and magnetic or electric fields to accelerate, sort and drive ions to the detector. Ion trap (IT), Orbitrap, and Fourier transform ion cyclotron resonance (FTICR) mass analyzers separate ions based on their m/z resonance frequency, while quadrupoles (Q) use m/z stability of the ions trajectories in oscillating electric fields, and time-of-flight (TOF) analyzers uses time.[96]. As a consequence, each analyzer present different acquisition capabilities thus influencing the following parameters:

- Resolution: is defined as the ability to distinguish two peaks of different mass-to -charge ratios (ΔM/z), in a mass spectrum. Fundamentally, mass spectrometers can be classified as either unit-mass-resolution (the mass could only be measured to single-digit units: nominal mass) which is the case of quadrupole mass analyzers or high-resolution instruments (capable of mass measurements on several decimal places: accurate or exact mass) such as TOF and Orbitrap.
- Mass accuracy: is defined as the difference between the experimental and theoretical mass of a given sum formula. It can be calculated either as (Experimental mass – Theoretical mass) in Da or by:

$$\text{Mass accuracy} = \frac{Experimental\ mass - Theoric\ mass}{Theoric\ mass} \text{ x } 1{,}000{,}000$$

- Sensitivity: the minimal concentration of a compound leading to a peak intensity greater than a specified signal-to-noise ratio (s/n)
- Scan speed/rate: the frequency at which the instrument is recording ion abundances, it is measured as the number of duty cycles that can be performed in one second (Hz). Depending on the architecture of the analyzer and the detector, this speed can go from 1 to 100 Hz.
- Mass range: It is the range of m/z values at which the analyzer performs with maximal mass accuracy and sensitivity.

d) **Mass detector**: The detector records the charge induced (or a change in current) produced when an ion passes by or hits a surface, these are associated to abundance of the previously measured molecular ions, a task solved by the instrument software. Because the number of ions leaving the mass analyzer at a particular instant is quite small, typically electron multipliers are used to get an amplified signal [97].

1.3.1.1 Tandem Mass Spectrometry

Tandem mass spectrometry, also known as MS/MS or MS^2 offers increased selectivity by the selection of a compound-specific precursor ion in the first mass spectrometer, fragmentation of the precursor ion in a collision cell, and subsequent selection of the specific fragment or product ions in a second mass spectrometer [98,99]. There are different combinations of mass analyzers to carry out MS/MS experiments, the selection of the mass analyzer will depend on the purpose of the experiment. For instance, triple-quadrupole (QQQ) instruments are limited in resolution and mass accuracy, but they offer a high dynamic range and excellent sensitivity, which make them ideal instruments for targeted

analyses. On the other hand, the emergence of tandem high-resolution mass spectrometry (THRMS) provide accurate monoisotopic mass measurements and high-resolution MS/MS or MS^n spectra for target confirmation and for the identification of unknown compounds [100]. Time of Flight (TOF) and Orbitrap are the most widely used mass analyzers in THRMS. These hybrid mass spectrometers are designed for untargeted or targeted screening with high-confidence confirmation, and enable identification and quantitation of compounds with greater confidence, resulting in a broad range of qualitative and quantitative applications[101].

Triple quadrupole (QQQ)

Among the different possible combinations of MS instruments, triple quadrupole (QQQ) instruments have taken the lead in the analysis of target compounds, mainly due to the higher sensitivity and selectivity of applying tandem MS (MS/MS) operated in multi-reaction monitoring (MRM) mode [90]. Briefly, in a triple quadrupole QQQ, three quadrupoles (Q1, Q2, and Q3) are lined up in a row. A scheme of the QQQ instrument is displayed in Figure 5. Basically, precursor ions are selected in Q1 and sent to Q2 for dissociation (fragmentation). The generated product ions are sent to Q3 for mass scanning. However, Q1 and Q3 can work in different data acquisition modes, being the most used:

a) Product scan: the first quadrupole Q1 is set to select an ion of a known mass, which is fragmented in Q2, then Q3 is set to scan the entire m/z range, giving information on the sizes of the fragments made. The structure of the original ion can be deduced from the ion fragmentation information. This method is commonly performed to

study molecular structure and identify transitions used for quantification by tandem MS.

b) Selected reaction monitoring (SRM): both Q1 and Q3 are set at a specific mass, allowing only a distinct fragment ion from a certain precursor ion to be detected. If Q1 and/or Q3 are set to more than a single mass, this configuration is called multiple reaction monitoring (MRM). This method results in increased sensitivity and it is used for compound quantification [102].

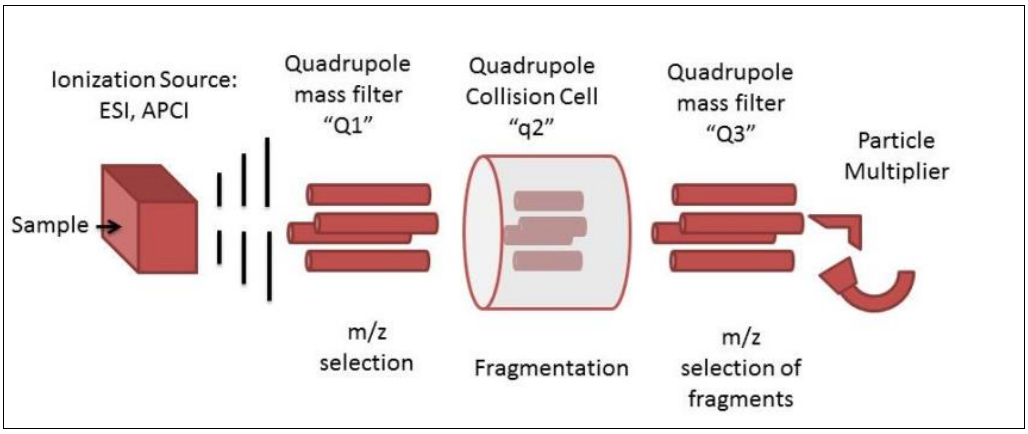

Figure 5. Scheme of a triple quadrupole instrument [94]

Quadrupole Time of Flight (Q-TOF)

Q-TOF systems use the high compound efficiency of quadrupole technology in combination with the rapid analysis speed and high mass resolution capability of time-of-flight. Q-TOF offer higher resolution than a single TOF (60.000 vs 20.000) but low mass accuracy (2ppm vs 1ppm) respectively [100]. Q-TOF, is the most widely used THRMS, and has its own unique advantages, including (i) fast acquisition speed and rapid determination of the sample, (ii) wide mass range up to 40 000 m/z. As can be seen in Figure 6 Q-TOF is

connected in series with a quadrupole mass analyzer and a TOF mass analyzer. The ions that are generated by the source first enter the quadrupole, then the ions that are stable oscillating in the quadrupole electric field will pass through the collision cell into the TOF mass analyzer. With this configuration the instrument can work in two distinct modes, full scan mode where all ions are transmitted to TOF to provide accurate mass scan of the unfragmented precursors ion, and MSMS mode that can use the quadrupole in filter mode, transmit ions into the collision cell and the subsequent product ions and any unfragmented precursor ion to the TOF analyzer [103].

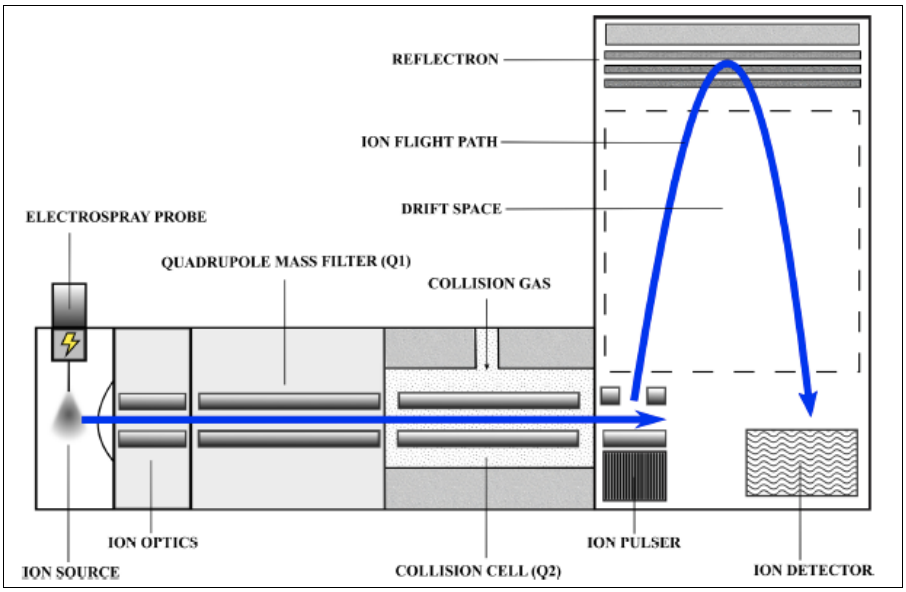

Figure 6. Scheme of the qTOF instrument [103]

Q-Orbitrap

The Quadrupole Orbitrap MS (Q-Orbitrap) is a Fourier Transform based hybrid instrument with a quadrupole as first mass analyzer followed by high resolution Orbitrap. It can combine high-performance quadrupole precursor selection with high-resolution and accurate-mass orbitrap detection. The

strongest point of Orbitrap is its high resolution (150.000 FWHM) and high mass accuracy which can reach up to 1ppm under standard internal calibration conditions [101].

As shown in Figure 7, the hybrid quadrupole-Orbitrap mass spectrometer mainly includes an ion source, which is APCI for most of these instruments, a stacked-ring ion guide (S-lens), a quadrupole mass filter, a curved linear trap (C-trap), a Higher-energy Collisional Dissociation (HCD) cell, and an Orbitrap mass analyzer.

In this configuration the quadrupole works as ion transmission device with the possibility to filter the transmitted ion according to its m/z ratios. The ions are transferred into the C-Trap and then injected into the Orbitrap mass analyzer to get mass spectra. In addition, ions are passed through the C-Trap into the High Energy Collisional Dissociation HCD cell to conduct MS/MS experiments in combination with the quadrupole mass filter.

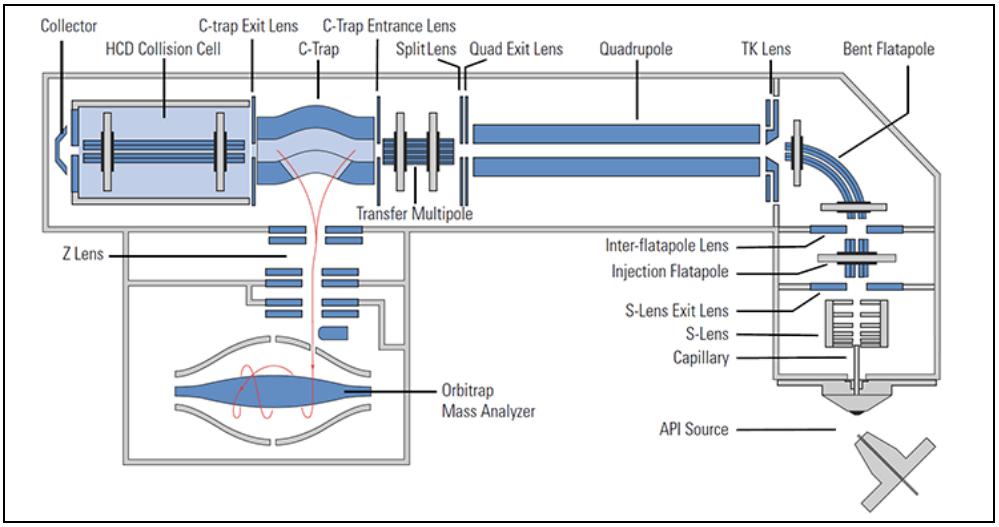

Figure 7. Scheme of the hybrid quadrupole-Orbitrap mass analyzer [104]

Both Q-TOF and Q-orbitrap instruments can perform data acquisition in target and non-target modes. In targeted acquisition the mass analyzer is

specifically optimized to detect only pre-determined compounds [105]. Untargeted acquisition can be classified in two groups:

a) Data-dependent acquisition (DDA): ion fragmentation is only performed if an ion complies with a certain condition in the full scan mode, meaning that in DDA the instruments are sequentially switching between full scan (MS1) and MS2 modes. This method allows predefined criteria e.g, signal intensity or a list of accurate mass to select ions [106]. Given the capability of DDA systems it is possible to obtain hundreds of MSMS spectra in a single experimental run, meaning that the identification process can be automatized. A disadvantage of DDA is that relevant analytes of low abundance may not be selected for further fragmentation[86].

b) Data independent acquisition (DIA): no pre-determined criteria for triggering the acquisition of product ion spectra is required thus allowing comprehensive MSMS data collection.

The most common method to generate DIA data is known as SWATH (Sequential Window Acquisition of All Theoretical Fragment-Ion Spectra). SWATH acquisition consists of a recurring cycle of a survey scan and a Q1 isolation strategy. In the first step, a survey scan with low collision energy covers the user-defined mass range (Q1 set to full transmission). The mass range then is consecutively scanned using predefined Q1 windows (typically 20 Da), applying a range of collision energies to produce product ion spectra[107]. Consequently, the SWATH MS data consists of highly multiplexed fragment ion maps that are deterministically recorded over the user-defined mass precursor mass range and chromatographic separation. This method has proven

advantageous in mass regions where precursor density is high; resulting in improved analyte separation and selectivity.[108]

1.3.2 Liquid Chromatography

Liquid chromatography (LC) is recognized as the most versatile technique due to the possibility to analyze an extensive range of compounds with a wide range of molecular weights, from 100s to 100,000s Da, without no volatility or thermal stability limitations [109].

HPLC relies on pumps to pass a pressurized liquid and a sample mixture through a column filled with a sorbent, leading to the separation of the sample components. Components are separated in the column based on each component's affinity for the mobile and stationary phases. The mobile phase is typically a mixture of solvents with different polarities (e.g. water, acetonitrile and/or methanol), its composition and temperature play a major role in the separation process by influencing the interactions taking place between metabolites and the stationary phase. The stationary phase or sorbent, is typically a granular material made of solid particles (e.g. silica, polymers, etc.), 2-50 micrometres in size [110]. Based on the stationary phase, liquid chromatography is divided in: a) normal phase liquid chromatography (NPLC), where the column to be used for the separation is more polar than the mobile phase; b)reverse phase liquid chromatography (RPLC) that uses a non-polar stationary phase with a polar mobile phase; and c) hydrophilic interaction liquid chromatography (HILIC) which is a variant of NPLC that uses high polar and hydrophilic stationary phases with reversed-phase type eluents capable of forming a water-rich layer in which hydrophilic compounds are retained based on their polar, ionic and hydrogen bonding interactions. The order of elution is

inverted compared to RPLC, with hydrophilic or polar compounds being retained longer than hydrophobic or non-polar compounds [111].

RPLC is the most widely used separation mode since it is suitable for a wide range of applications because of the various mobile and stationary phases available, being C_{18} silica column using an acidic water/organic mobile phase the standard choice [112]. However, very polar compounds are not retained in classical C_{18} stationary phases and elute within the void volume, in that cases HILIC provides an alternative approach to effectively separate small polar compounds on polar stationary phases [113].

In recent years HPLC has been improved in terms of chromatographic performance, resolution and time of analysis with the use of ultra-high performance liquid chromatography (UHPLC). UHPLC utilize capillary columns packed with sub -2µm particles which enable the use of higher pressure up to 4000 bar and high temperatures up to 200°C to decrease mobile-phase viscosity and polarity thus providing more efficiency and minimized band broadening [114,115].

1.3.3 Mass Spectrometry Imaging

Mass spectrometry imaging (MSI) is a technique used to visualize the spatial distribution of molecules like metabolites, peptides or proteins in a tissue. MSI is an attractive technique to explore the metabolic differences directly on tissues, which is essential for the comprehensive understanding of how multicellular organisms function.

Figure 8 shows a typical MSI experiment. As can be seen in the figure, a thin section of tissue is coated with a matrix in order to promote the ionization.

Once the tissue is prepared, it is placed inside the mass spectrometer where an ionization energy is applied at different points of the sample in order to desorb and ionize the compounds from the sample. Subsequently, molecular ions generated are detected by one of several different types of mass analyzers[116], resulting in a dataset that contains an array of spectra in which each spectrum is an independent molecular profile of the desorbed and ionized area.[117]

The most common ionization technologies in the field of MSI are desorption electrospray ionization (DESI), secondary ion mass spectrometry (SIMS) and laser-based systems: matrix-assisted laser desorption ionization (MALDI) and matrix-free or surface-assisted laser desorption ionization (SALDI).

- DESI: is a less destructive technique that consist of spraying the sample with an electrically charged solvent mist at an angle that causes the ionization and desorption of the molecular species. Although this technique has the poorest resolution (50 µm), it can create high-quality images from a large scan area, as a whole body section scanning.[118]

- SIMS is a hard ionization technique that use particle bombardment with a continuous beam of highly-focused energetic ions such as Cs^+, Au^{3+} and C^{60+}. SIMS provides the highest image resolution (< 100 nm), but the mass range it is limited to >1000 Da because of the extensive fragmentation produced(< 100 nm)[119].

- MALDI: an organic matrix is deposited over the tissue section to promote the ionization process, then a laser is responsible of transmitting the ionization energy which enables the desorption of the molecular ions. MALDI is currently the most common ionization method used in MSI since the laser focus can be precisely adjusted to

provide a high image resolution while offering softer ionization than SIMS [120]. A typical MALDI -MS workflow is represented in Figure 8.

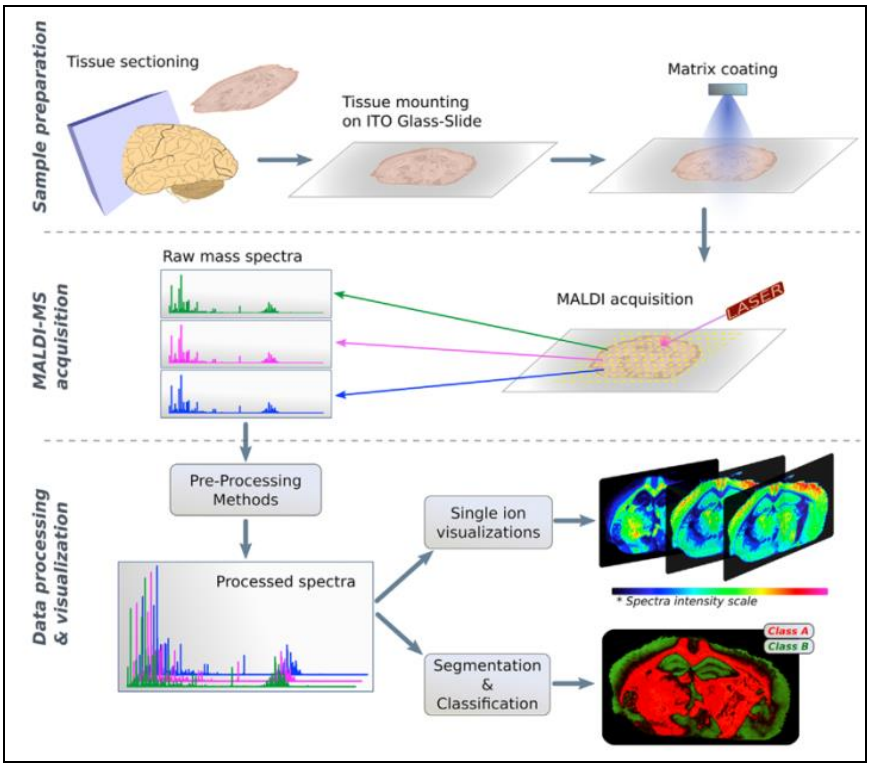

Figure 8. MALDI-MS experiment workflow [121]

- Matrix free LDI-MS: Commonly used matrix-free techniques are: surface-assisted laser desorption/ionization (SALDI), in which ionization is supported by the surface of the target plate; nanostructure-initiator mass spectrometry (NIMS) [16], which uses molecules of an initiator compound trapped in nanostructured surfaces promoting the ionization of the metabolites; and nanoparticle-assisted LDI (nanoPALDI) which uses nanoparticles and nanolayers of different metals and metal oxide to promote the ionization [122].

Time of flight (TOF) analyzers are the most commonly used detectors including the axial TOF spectrometer, which provides a mass-accuracy error between 10 and 20 ppm due to the initial velocity/drift of the generated ions [123,124].The addition of an ion reflector together with delayed ion extraction helps to compensate for this effect, which can result from non-flat sample morphology. Using this configuration, mass accuracies of 5–10 ppm can be achieved. Modern MALDI-TOF spectrometers which are equipped with an orthogonal reflector can provide mass error < 10ppm [121]. Other mass spectrometers used in MSI are the Fourier transform orbitrap (FT-orbitrap) and Fourier transform ion cyclotron resonance (FT-ICR), which provide mass errors <1 ppm at m/z 300 [125].

1.3.4 Nuclear Magnetic Resonance

Nuclear magnetic resonance spectroscopy, most commonly known as NMR spectroscopy, is a spectroscopic technique based on the observation of magnetic fields around atomic nuclei. Figure 9 shows the basic parts of a NMR instrument, as seen, the sample is placed in a tube inside the instrument, then a magnetic field and the NMR signal is produced by excitation of the nuclei sample with radio waves into nuclear magnetic resonance, which is detected with sensitive radio receivers. The intramolecular magnetic field around an atom in a molecule changes the resonance frequency, thus giving access to details of the electronic structure of a molecule and its individual functional groups. Besides identification, NMR spectroscopy provides detailed information about the structure, dynamics, reaction state, and chemical environment of molecules.[126]

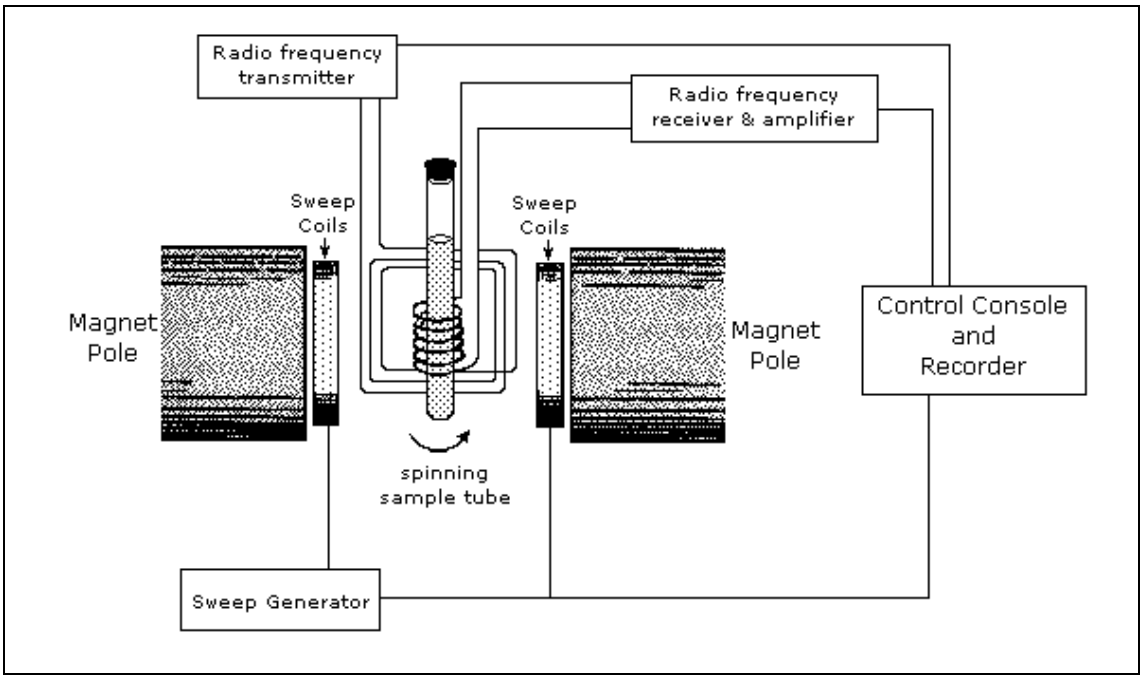

Figure 9: Scheme of the basic parts of a NMR instrument [127]

The atomic-resolution power of NMR is intrinsically linked to the occurrence of chemical shift. In an NMR spectrum, the magnitude or intensity of the resonance is displayed along a single frequency axis (in the case of 1D NMR) or several axis for multidimensional NMR. Chemical shift is usually expressed not in Hz but in ppm relative to the central vibration frequency of a standard:

$$\delta \text{ (ppm)} = 10^6 \cdot \frac{\upsilon - \upsilon_0}{\upsilon_0}$$

Where "$\boldsymbol{\nu}$" is the signal frequency in Hz and "$\boldsymbol{\nu}_0$" is the frequency of a reference compound. Thus, chemical shift in ppm can be compared between data sets recorded at different field strength. The chemical shift for ^{1}H NMR is determined as the difference (in ppm) between the resonance frequency of the observed proton and that of a reference proton present in a reference

compound.[128] Several chemical shift reference standards are available including tetramethylsilane (TMS) which is used in organic solvents because of its poor solubility in water and 2,2-dimethyl-2-silapentane-5-sulfonic acid (DSS), used for aqueous solutions. The measured chemical shifts vary: 0–10 ppm for ^{1}H; and from 0–250 ppm for ^{13}C. The signal intensity depends on the number of identical nuclei, which is used to perform quantification. The presence of complex samples does not interfere with the measured intensity [129].

NMR Acquisition can be performed in one dimensional (1D) or two-dimensional NMR (2D-NMR) pulses. 2D-NMR, is often used to facilitate the attribution of peaks and to achieve structural elucidation. Indeed, 2D experiments offer the advantage of spreading overlapped peaks along two orthogonal dimensions, thus limiting peak overlap while providing additional information on chemical structures[130]. 2D-NMR generates a large number of different spectra, which can be globally classified into homonuclear (i.e., 1H–1H-NMR) and heteronuclear (i.e.,1H–13C or 1H–15N) spectra[128]. There are also different pulse sequences designed to suppress or amplify particular types of resonances. As an example, in Nuclear Overhauser Effect (NOE) spectroscopy, the relaxation of the resonances is observed. As NOE depends on the proximity of the nuclei, quantifying the NOE for each nucleus allows the construction of a three-dimensional model of a molecule. Other methods used to generate the 2D-NMR spectra include correlation spectrometry (COSY), total correlation spectroscopy (TOCSY) or J-resolved spectroscopy (J-Res)[83].

COSY provides information on homonuclear correlations between coupled nuclei (1H-1H) while TOCSY is an extension of COSY, wherein the chemical shift of a given nucleus is correlated with the chemical shift of other nuclei within the total (or near total) spin system of a given compound. The J-Res experiment

simplifies spectral assignments by increasing the peak dispersion compared with a conventional 1D NMR experiment[83].

Although 2D-NMR gives additional and important information on the chemical properties and the structure of the compound is often restricted to the characterization of those compounds that cannot be identified with 1D-NMR spectra. The main reason why the use of multi-dimensional NMR is still not as widespread as it could be is the long experiment time required to record such spectra with sufficient resolution. 2D experiments typically need the repetition of several hundreds of 1D experiments, leading to experiment times between a few tens of minutes and several hours.[131]

1.4 Dust targeted analysis

Due to the complexity of indoor dust, sample preparation is a key step in targeted analysis. Indoor dust is an heterogenous mixture that contains fibers, inorganic and mostly organic particles [132]. Its high content of organic carbon difficulties the extraction and the determination of target compounds [61,62]. The most common extraction method of organic targeted compounds is solvent liquid extraction (LE) using an organic solvent or a mixture of them. Usually the obtained extracts need to be cleaned up and/or preconcentrated before analysis. The most commonly used extraction techniques in the analysis of organic compounds in dust include: solvent extraction assisted by sonication or mechanical agitation, Soxhlet extraction, and pressurized liquid extraction (PLE). These three techniques have been used in about 90% of the studies[133]. Other extraction techniques include microwave assisted extraction (MAE), ultrasonically assisted extraction (UAE), matrix solid phase dispersion (MSPD) and thermal desorption (TD) [133].

Soxhlet extraction is a conventional method that requires large volume of organic solvents, up to 500 mL and long extraction times, 8 to 24 hours [134]. PLE, MAE and UAE present extraction yields comparable to Soxhlet but reduced extraction time and lower organic solvent consumption due to the application of high pressure, high temperature, and/or supplementary energy. In contrast to Soxhlet, the use of these techniques requires specific equipment. However, these techniques are low selective and the obtained extracts usually contain many interfering substances which require the use of clean up steps after the extraction. PLE offers the possibility of performing a clean-up step on the same instrument and even in the same cell used in the extraction ("on cell" and "in cell" clean up).

MSPD also consume less organic solvent, it is performed under ambient conditions, it does not need special equipment and present high extraction yields. MSPD consist of an extraction with a sorbent and also offers the possibility to carry out an additional in-situ clean-up with a co-sorbent [135]. Finally, thermal desorption (TD) is a quick and easy method that presents high sensitivity. It does not consume organic solvents which avoids solvent extraction disadvantages like matrix extraction, concentration and clean-up steps which decrease the time, reduce likelihood of sample contamination and losses. In contrast, it has to deal with the volatility and the thermal stability of the targeted compounds [136].

As an alternative the Quick, Easy, Cheap, Effective, Rugged and Safe extraction technique (QuEChERS) has been recently applied for the chemical characterization of organic aerosols[137]. The QuEChERS method uses low quantities of solvent to perform the extraction, in combination with the addition of a salt to promote the extraction of the targeted compounds with

the salting out effect followed by a dispersive-SPE (d-SPE) for the elimination of interfering compounds [138].

Since most of the extraction methods are low selective, the clean-up step is necessary. This usually consist of a solid phase extraction (SPE) or a dispersive-solid phase extraction (d-SPE). Both techniques use the same principle; the sample is mixed with a solid that will retain specific interferences, then the sample is washed and finally the compounds of interest elute using the appropriate solvent. In the case of d-SPE the solid sorbent is directly added into the sample without the use of any cartridge or elution step. Figure 10 schematically shows the SPE and the d-SPE techniques.

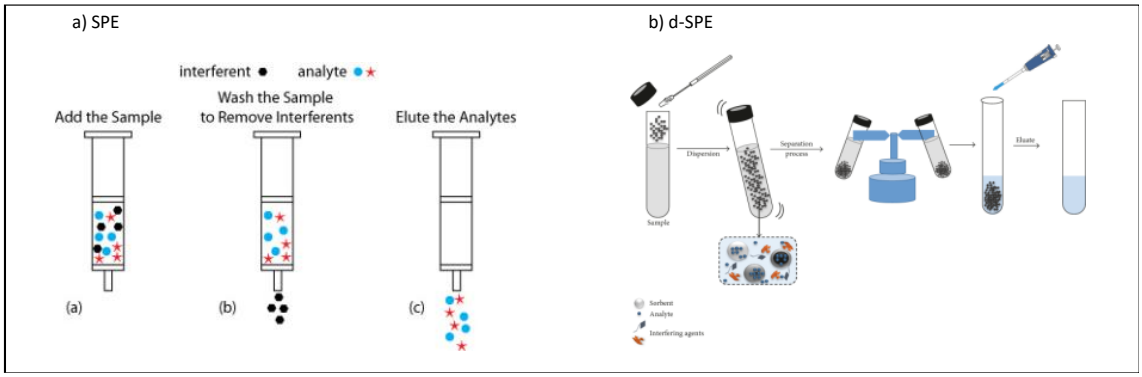

Figure 10. a) Steps performed in the SPE technique b) Steps performed in the d-SPE technique [139,140]

As can be seen in Table 2, for the analysis of nicotine and TSNAs in dust samples, the preferred extraction method is LE. However, few methods have analysed nicotine in combination with TSNAs. The main challenge in the combined analysis of these compounds is the optimization of the solvent used as well as the pH of the sample, since nicotine polarity and structure differs more from the TSNAs (Nicotine log P: 0.87 vs TSNAs log P: (0.33-0.77)).

TSNAs have been analysed either by GC and LC (see Table 2), GC is the preferred chromatographic technique for nicotine analysis due to its volatility

and medium polarity [logP=0.87]. However, for the rest of TSNAs high temperature can lead to the degradation of the compounds in the injection port. For this reason, when analysing TSNAs with GC, detectors such as nitrogen chemiluminescence detector (NCD) provide higher selectivity and sensitivity than MS instruments[15,25]. Consequently, for TSNAs the analytical technique most used is LC-MS/MS (See table 2). In LC-MS the main challenge is to prevent the coelution of some nitrosamines and the prevention of peak splitting of some TSNAs. Peak splitting arises when a Gaussian peak gets a shoulder or a twin. Although peak splitting can be caused by a number of factors including instrumental problems, in the case of nitrosamines this phenomenon has been experimented by different researchers. Some authors have reported that nitrosamines peak splitting is due to the fact that nitrosamines exist as mixture of E and Z isomers[141,142] while others have found that the split up of the signal was probably due to the formation of the protonated isomers[143]. Moreover some nitrosamines such as NNAL exists in their enantiomeric forms since they have a chiral centre in the carbonyl carbon and present 4 different structures (S,E), (S,Z), (R,E) and (R,Z)-NNAL. Peak splitting can be prevented working at the appropriate pH and optimizing column temperature and mobile phases.

Table2. Summary of the studies performed in dust that analyze Nicotine and/or TSNAs. The table summarized the compounds analyzed, the extraction technique, solvent, determination technique and the limit of detection of the method. * Limit of quantification (LOQ) is provided when LOD is not available in the research paper.

Compounds	Extraction method	Extraction solvent	Determination technique	LOD (ng/g dust)	Authors
Nicotine	LE	Diethyl ether	GC-MS	0.02	Kim, et.al [144]
Nicotine	LE	Toluene: butanol (70.30)	GC-MS	270	Whitehead, et.al [145]
Nicotine	LE	Dichloromethane (DCM)	GC-MS	20	Whitehead, et.al [146]
Nicotine	-	-	GC-MS	2000	Matt, et.al [147]
Nicotine	LE	Methanol	LC-MSMS	10*	Matt, et.al [148]
Nicotine, NNN, NAT, NAB, NNK, NNAL	PLE	Ethyl Acetate	GCxGC-NCD	Nic: 15.8 NNN: 8.7 NAT: 6.0 NAB: 5.6 NNK: 8.4 NNAL: 14.2	Ramírez, et.al [25]
Nicotine, NNN, NNK, NNA, NAB, NAT, Cotinine, Nicotinelle, Myosmine, N-formylnornicotine	LE	DCM/pentane/Ethyl Acetate (45:45:10)	LC-MSMS	-	Whitehead, et.al [149]
Nicotine, NNK, NNN, NAT, NAB	LE	Methanol	LC-MSMS	Nic: 10* NNK: 0.3* NNN: 1.25* NAT: 1.25* NAB: 0.3*	Matt, et.al [37]

1.5 Untargeted analysis

The typical untargeted workflow used in environmental analysis and metabolomics is shown in Figure 11 The workflow includes the following steps: a) sample preparation; whose aim is to extract a broad number compounds from the sample, b) sample analysis; which is performed using the most suitable analytical technique or combination of them, c) data pre-processing and data analysis; which consist of processing the spectral data obtained from the instrument and applying statistical univariant and/or multivariant analysis to highlight the differential compounds between samples or groups, d) compound identification and e) result interpretation [150].

A detailed explanation of the untargeted workflow is described in the following sections for each technique used in this thesis (including LC-MS, NMR and MSI). Note that particularities for the untargeted metabolomics workflow, are highlighted in each section. Moreover, result since the interpretation of the results is common for all techniques, it is presented at the end as a separate section.

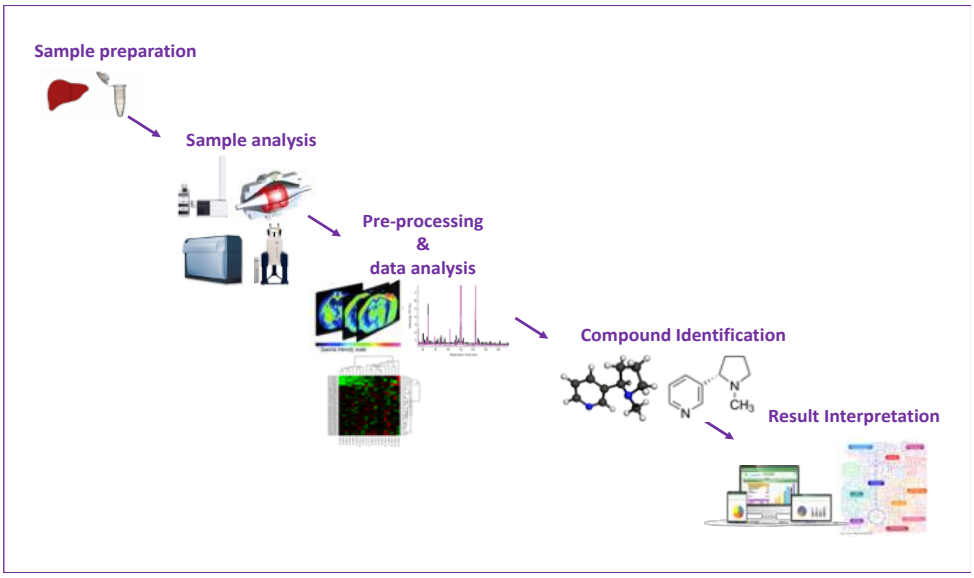

Figure 11. Untargeted workflow

1.5.1 LC-MS experiments

In untargeted approaches for LC-MS experiments sample preparation is extremely important because it affects both the observed compound content and the interpretation of the data [151]. Normally, regardless of the origin of the sample, an extraction method to isolate analytes from complex matrices is required. Due to the large chemical diversity of compounds and the different range of concentrations present in the environmental and biological samples, there is no universal extraction method for detecting all compounds. Generally, high throughput methods with a good compromise between extraction efficiency and time are preferred.

Compound extraction in untargeted methods aims to: (a) efficiently extract the largest number of compounds from the matrix; (b) be nonselective and not exclude compounds with particular physical or chemical properties; (c) remove interferences that hinder a proper analysis; (d) be reproducible; and (e) make the extract compatible with the chosen analytical technique[152].

However, in the case of biological samples an additional requirement must be considered. The use of biological samples makes sample manipulation and sample storage a very important step since metabolite stability needs to be preserve. Metabolite stability depends on its chemical nature and lability. The amount of enzymatic activity remaining in the sample during storage and/or preparation, and processes such as protein degradation, which can elevate levels of some metabolites, can disturb metabolite stability [152]. Thereby the extraction method chosen also has to be simple and fast to prevent metabolite loss and/or degradation during the preparation procedure. Moreover, reduced temperatures during sample preparation (4°C) and storage (-80°C) are commonly used.[153]

Therefore, most of the metabolomics protocols involve two major strategies: the stop of metabolic processes by protein precipitation and the extraction of metabolites from the studied samples.

Protein precipitation is performed prior to the extraction and its typically performed using cold solvents such as acetonitrile, ethanol or methanol in acidic or basic pH, in order to cause protein denaturation and reduce its solubility [154].

Generally, extraction protocols are classified depending on whether the metabolites to be extracted are hydrophilic or hydrophobic. For hydrophilic metabolites polar solvents such as methanol, methanol-water mixtures or ethanol are normally used [155–157]. Non-polar solvents like chloroform or hexane can be used to extract hydrophobic metabolites such as lipids. Metabolites can also be extracted at extreme pH (such as perchloric acid [157] or meta-phosphoric acid [155]) with the aim to extract acid-stable compounds. Usually after the extraction procedure a sample evaporation step is performed in order to concentrate the metabolites and redissolved them in a solvent compatible with the analytical technique selected for the sample analysis.

LC-MS is the preferred method for the untargeted analysis of trace organic contaminants in environmental samples and untargeted metabolomics of biological samples since it brings the widest chemical/metabolome coverage. UHPLC has become the gold standard for LC as it enables elution of sample components in much narrower, concentrated bands, resulting in better chromatographic resolution and increased peak capacity[158] while decreasing the risk of matrix effects [159]. Moreover, recent developments in column technology have greatly improved separation efficiency while expanding selectivity, yet chromatographic separations are not universal. Therefore,

different combinations of chromatography column and mobile phases setups must be used to increase the coverage of any LC-MS experiment. The most common chromatographic separation is RP, but lately interest in HILIC has grown given its complementarity to RP analysis. Therefore, many approaches include the analysis of the samples by using both RP and HILIC. HILIC provides good retention for polar and ionic compounds, and good ionization efficiency due to the use of mobile phase rich in organic solvents, however when using HILIC there are constrains such as allowing sufficient equilibration time to reach acceptable analytical repeatability. [112,160]

The mass spectrometers more used in untargeted approaches are high resolution instruments such as Orbitrap and qTOF which have demonstrated to be very suitable in the analysis of complex matrices. This is largely thanks to a combination of higher mass spectral resolving power, which reduces interferences, high mass accuracy which allows prediction of molecular formulas for the spectral peaks and sensitivity in full scan acquisition which allows the detection of compounds at femtogram levels [161]. However, datasets are exceedingly complex with file sizes on the order of gigabytes per sample for some new high-resolution MS instruments [162]. Typically, HRMS analysis involves acquisition of full scan MS data, resulting on data matrices containing thousands of variables (m/z, retention time, intensity), that have to be converted into more manageable information [163]. Thus, following data acquisition, pre-processing is extremely important to reduce data quantity and complexity.

Data pre-processing usually involves four basic steps: raw data conversion, peak detection, alignment, filtering and grouping and is a critical step for prioritizing the most relevant and interesting components in sample sets [164].

Raw data conversion relies on the transformation of specific data formats from instrument vendors into common, unique data. The transformation of vendor formats into mzML, previously mzXML[165] is a common first step in untargeted data processing, and can be performed by using free software (e.g., ProteoWizard[166]). Peak detection, alignment and correspondence can be performed using free packages within the R programming environment. The XCMS [167]software has been widely used in untargeted approaches including environmental and metabolomic studies. XCMS implements three main steps:

a) Peak detection: it is also known as peak picking or feature detection. A feature is known as all raw data points that originate from one particular ion. A feature is characterized by a retention time, an m/z value and an intensity (RT, mz, intensity). The purpose of the feature detection stage is to extract as many recorded signals caused by true molecular ions as possible. This step also aims to provide as accurate quantitative information about ion abundance as possible. Peak detection is usually performed using the centWave algorithm [168]. The two most critical parameters for centWave are the peak width (expected range of chromatographic peak widths) and ppm (maximum expected deviation of m/z values of centroids corresponding to one chromatographic peak), this is usually much larger than the ppm specified by the manufacturer parameters. Therefore, visual inspection of some peaks in each sample is vital in order to decide the parameters that the algorithm will apply across samples.

b) Alignment: the time at which analytes elute in the chromatography can vary between samples. The alignment step, also referred to as retention time correction, aims at adjusting this by shifting signals along the retention time axis to align the signals between different samples within an experiment. The

method to perform the alignment/retention time correction in XCMS is adjustRtime which uses different alignment algorithms depending on the provided parameter class. Also, here it is advisable to modify the settings for each experiment and evaluate if retention time correction did align internal controls or known compounds properly.

c) Feature correspondence: the final step in pre-processing is the correspondence that matches detected chromatographic peaks between samples (and depending on the settings, also within samples if they are adjacent). The method to perform the correspondence in XCMS is groupChromPeaks. This algorithm uses the peak density method to group chromatographic peaks. Users can choose the minFraction value, as an example a value of 0.4 for the minFraction parameter will only grouped into a feature chromatographic peaks present in at least 40% of the samples[167] .

After pre-processing, features defined by their m/z and retention time, and their intensities in different samples are evaluated using multivariate statistical models [169]. Statistical comparison of the groups can be calculated with classical tests and multivariate analysis can be performed using methods such as principal component analysis (PCA), clustering and regression analysis. Samples can be grouped and can be observed using score plots, heatmaps or hierarchical clustering. These data analysis is critical for maximizing differences between groups, to prioritize the most relevant and interesting components in sample sets and to highlight potential environmental and metabolic markers [170].

In LC-MS compound identification is performed by the comparison of exact mass or MS/MS spectra in online mass spectral libraries (e.g., MassBank, METLIN, mxCloud, NIST). Moreover other databases such as ChemSpider [171] or

the U.S. Environmental Protection Agency (U.S. EPA) CompTox Chemistry Dashboard [172] contain useful additional data to support identification, such as literature references, patent data, functional uses and toxicological/bioassay data. Moreover, the Suspect Exchange from the NORMAN Network, network of reference laboratories, and research centres for monitoring of emerging environmental substances [173], contains many different suspect lists that can be used in non-target screenings of environmental samples. In metabolomics the main online spectral databases are Metlin[174] and the Human Metabolome Database (HMDB)[175] which contains more than 114,222 metabolites entries including both water-soluble and lipid soluble metabolites.

In general, for untargeted approaches, an exact mass match is not sufficient for identification alone. For this reason, MS/MS acquisition is required in order to increase the identification confidence. The reporting of confidence in the annotation or identification should be reported in all studies. The first set of reporting standards were designed by Sumner et al. as part of the Metabolomics Standards Initiative (MSI) in 2007 with four different confidence levels. [176] More recently Schymanski et al. have reported a five-level confidence system. [177]Those levels correspond to:

- **Level 1**: *Confirmed structure*. The proposed structure has been confirmed via appropriate measurement of a reference standard with MS, MS/MS and retention time matching. If possible, an orthogonal method should also be used. Typically, the term identification is used when level 1 is reached and for the following levels it is accepted the term “annotation”. Most compounds are annotated (and should be reported as annotated) unless two complementary properties are matched to the same properties for a chemical standard analysed

applying identical analytical conditions for biological sample and chemical standard [178].

- **Level 2**. *Probable structure*: This differs from Level 1 in the fact that the reference standard is not analyzed under identical conditions. Putative (level 2 or 3) annotation is typically based on: one or two properties only and often relies on comparison to data collected in different laboratories and acquired with different analytical methods, instead of a direct comparison with an authentic chemical standard under identical analytical methods. We can differentiate between two levels, ***Level 2a: Library*** this is the case of comparing acquired MS/MS spectra against an equivalent found in spectral databases. This level at least confirms 2D structure. ***Level 2b: Diagnostic*** represents the case where no other structure fits the experimental information, but no standard or literature information is available for confirmation.

- **Level 3**: *Tentative candidate*: Identifications at this level are not confident enough to supply an identity but may supply information about the formula and compound subclass or family. This level has some certainty about compound formula and part of its structure.

- **Level 4:** *Unequivocal molecular formula*. This is possible when a formula can be unambiguously assigned using the spectral information (e.g., adduct, isotope, and/or fragment information), but insufficient evidence exists to propose possible structures. These arise when accurate mass and isotopic distribution patterns produce tentative structures from database searches. Note, a single molecular formula typically renders multiple candidate structures.

- **Level 5**: *Exact mass.* A feature (m/z) can be measured in a sample but the MS/MS spectra or formula are impossible to annotate.

The five identification levels proposed are summarized in Figure 12, from Schymanski, et.al.

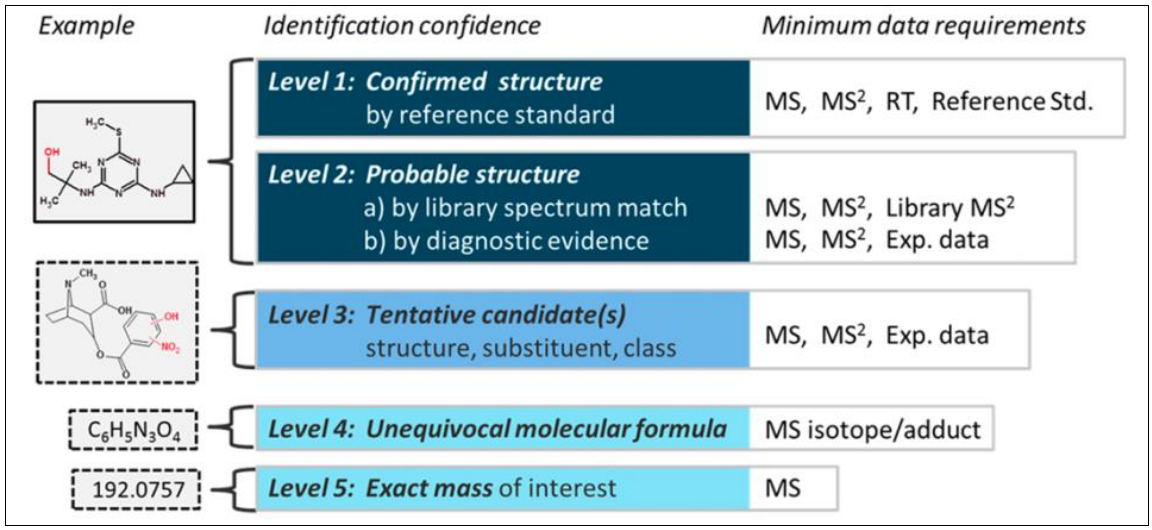

Figure 12. Proposed identification confidence levels in high resolution mass spectrometric analysis. Note: MS^2 is intended to also represent any form of MS fragmentation [177].

In most of the studies levels 2 and 3 are the most commonly reported since level 1 is out of financial reach for the majority of research groups. Consequently MS/MS match spectra of a reference spectrum found in compound spectral databases is the most conclusive evidence for validating the annotation of a feature. However, a few considerations including acquisition instrument type, mass accuracy, ionization mode, fragmentation method and energy used and precursor ion must be taken when checking the match with spectral libraries.

1.5.2 MSI experiments

For MSI analysis, sample preparation methods must use rapid and consistent protocols to prevent delocalization or degradation of metabolites. The most common method used for sample stabilization is to snap-freeze the tissue at the point of collection. Tissues are best frozen free-floating on liquid nitrogen to prevent them from deforming and taking the shape of a container and therefore presenting complications when sectioning[179].

In MALDI MSI applications, matrix deposition is a critical step that affects spatial resolution as well as the number of unique ions detected. The reproducibility of the signal intensities is also largely determined by the type of matrices used and sample preparation[180]. Many kinds of organic matrices such as α-cyano-4-hydroxycinnamic acid (CHCA) and 2,5-dihydroxybenzoic acid (DHB) have rarely been used for low-molecular-weight metabolite analysis because matrix and/or matrix-analyte cluster ion peaks are observed in the low-mass range ($m/z < 700$), thus interfering with the detection of the target compounds. Besides, the application step, which is typically performed by spraying coating or droplet printing deposition (wet deposition methods) promote the diffusion of metabolites within the tissue and the formation of heterogeneous size of crystal which limit the spatial resolution. Consequently, dry matrix application methods like sublimation have been reported for imaging small molecules in tissues. Sublimation minimize metabolite delocalization but show poor sensitivity due to the lack of incorporation of the analyte into the matrix [181]. Other matrix application methods such as dry vapor deposition followed by controlled recrystallization in a statured water atmosphere have been proposed achieving resolution of 2 µm [182]. As an alternative to typical organic matrices used 9-aminoacridine (9-AA)[183] and ionic

liquid matrices which not present crystals that limit the spatial resolution have been recently use [184,185].

Matrix-free methods are becoming the preferred method for MSI in metabolomics studies since they provide good lateral resolution and avoid wet matrix deposition processes. As an example, the deposition of metal nanoparticles is usually performed by sputtering which allows the deposition of nanolayers in an inert outer space thus avoiding sample contamination and metabolite delocalization. Common used materials are metals such as Au [122,186,187], Ag [188], Pt [189] and metal oxide nanolayers nanolayers (WO_3, TiO_2, Fe_3O_4, ZnO) [122,186,188,190]. In this context gold nanoparticles are likely the ideal substrate because they present high stability, have only one stable isotope, which reduces the number of interfering peaks facilitating the detection of trace compounds and are able to absorb the UV light emitted by the laser and effectively promote the ionization of low mass range metabolites with very low background signal [191–193]. Other nanomaterials including carbon nanotubes [194], carbon dots [195] and graphene oxide [196] have been extensively developed as effective matrices for the profiling of small molecules in biological tissues.

The main goal in MSI analysis is acquiring good quality images. The spatial resolution of the MS image is determined by the diameter of the laser beam of a specific instrument which needs to be optimized prior the acquisition.

At low spatial resolutions (small laser diameter), the acquisition time increases and the quality of the MSI worsens due to the abundance of lower MS peaks in the acquired spectra. Furthermore, lower resolutions generate higher volumes of data and, therefore, the need of sophisticated computational strategies.[121] Consequently, a good compromise between resolution and acquisition time must be reached.

TOF spectrometers operating in MS mode have been widely used in metabolomics studies, however working in the low mass range of the spectrum without previous separation techniques as in the case of LC-MS requires higher mass resolution. Thus the preferred MS spectrometers are, Fourier transform orbitrap (FT-orbitrap) and Fourier transform ion cyclotron resonance (FT-ICR) which facilitate the identification of metabolites by exact mass and mass fragmentation. [125]

The most important information obtained from an imaging experiment is a visualization of the distribution of various molecules throughout the tissue. As each pixel of an imaging experiment contains an entire mass spectrum, the bottleneck of MSI data processing is the large size of the data files and the high degree of dimensionality. This is becoming more problematic with the increase in spatial resolution causing an exponential growth in data file sizes. Consequently, key software developments have been made to address these challenges and ensure that effective analyses are being done without the loss of valuable information.

The pre-processing steps used in MSI include normalization, baseline correction, peak alignment, spectra recalibration, smoothing, and data compression (unsupervised and supervised). Normalization is used to remove systematic artifacts that can affect the mass spectra like sample preparation, ion suppression, and differential ionization efficiencies since can influence the intensity peaks of mass spectra [121,197].

Normalization to the total ion count (TIC) is the most commonly implemented method.[198]. Normalization to the TIC ensures that all spectra have the same integrated area and is based on the assumption that there is a comparable number of signals in each spectrum.[199]

Following normalization, baseline subtraction and spectral recalibration are usually performed. Smoothing it is especially important for imaging data as removes sudden fluctuations between pixels that do not necessarily represent the in vivo distributions. Pre-processing steps help to ensure accurate interpretation of the data.

Several compression strategies have been implemented to reduce the size of data while still retaining the important information. Binning mass spectra for each pixel of an imaged tissue and compression based on region of interest (ROI) are the most successful methods. However, for untargeted approaches unsupervised clustering of the data is performed in order to compress data into features. Unsupervised analysis can be divided into a) manual analysis b) component analysis and c) segmentation analysis.[197]

a) manual analysis: is carried out by selecting m/z values unique to the region of interest and generating an image for each m/z value.

b) Component analysis requires a statistical or machine learning algorithm to cluster the data. Typically, PCA is used to reduce the dimensionality of the data set by converting possibly correlated variables into a set of linearly uncorrelated values.

c) segmentation analysis: bins together similar spectra into regions of interests and identifies colocalized m/z values. This includes methods such as hierarchical clustering, a type of spatial segmentation, and K-means which is frequently used to rearrange multiple variables to visualize possible groups in the data.[200]

Because processing imaging data requires numerous different treatments compared to conventional LC-MS data, software with complete data analysis pipelines are required. While there are numerous open sources and freely available software packages for processing data, functionality tends to be restricted, and there are typically no export options for the data. Several software packages can be used including Spectral analysis[201] which incorporates all processing steps from preprocessing to multivariate analysis and MSiReader[202], which is an open-source package to view and analyze MS imaging files on MATLAB platform. It incorporates various aspects of data analysis, including visualization, quantitation, and annotation in a streamlined, easy-to-use platform. However, MATLAB platform is not free, and it is not the preferred environment in MSI metabolomics, in this sense a free package working in an R-based environment which is widely used in the community has been developed in our group. rMSI[203] and rMSIproc [204] are used for data handling, data visualization, and data processing respectively. rMSI directly imports data from vendors format and permit the visualization of the images of all the MS peaks in the spectra. rMSIproc provides a novel strategy for spectral alignment and recalibration, which allows to process multiple datasets simultaneously and to perform a confident statistical analysis with multiple datasets from one or several experiments. Another packages widely used that also permits the quantification of the compounds in MSI are msIQuant [205] and Cardinal [206].

Identification can be performed extracting a list of the metabolites of interest and using the same data bases used in LC-MS experiments. However, specific repositories for MSI images are being developed in order to allow researches access to imaging data for comparison of the results and for discovering new answers to biological questions. In this sense, Metaspace is an

online engine based on big-data technologies that automatically translates millions of ion images to molecular annotations.[207]

1.5.3 NMR experiments

Samples for NMR can be analysed without extraction of compounds provided that the active volume of the NMR probe is filled, typically with 500 µL of biofluid for 5 mm NMR tubes. However, the intrinsic low sensitivity of NMR greatly hinders accurate assignments and quantification of a large number of metabolites from biofluids [208,209] or intact tissues [210]. In this context, extraction of metabolites may reduce broad signals in the spectra arising from the high overlap of chemical shifts of proteins and generate narrower and better-resolved NMR resonances that allow reliable quantification of metabolites. In general, all the considerations taken for the development of an efficient extraction method for LC-MS can applied to NMR analysis [211]. However, a few some aspects related to the NMR technique must be considered. Typically, in ^{1}H-NMR experiments, extractions are performed using deuterated solvents in order to avoid a huge solvent signal that would dominate the ^{1}H-NMR spectrum. Moreover, for the removal of chemical shift between samples reference standards are added. The reference compound used in aqueous media is usually the sodium salt of 3-trimethylsilylpropionic acid (TSP) with the methylene groups deuterated to avoid giving rise to ^{1}H peaks in the NMR spectrum. Other reference standards are DSS [2,2-dimethyl-2-silapentane-5-sulfonate sodium salt], and tetramethylsilane (TMS) for organic solvents. If reference standards are added in a known concentration, peak integrals from the standard can be related to the concentrations of the substances in the sample [212]. Recently, a synthetic electronic reference signal

(ERETIC, Electronic reference to access in vivo concentrations) has been introduced for quantitation purposes, without the requirement of an internal standard[213].

The majority of environmental and biological applications employ ^{1}H One-dimensional (1D) NMR spectroscopy and carbon (^{13}C-NMR) spectroscopy. This is because ^{1}H and ^{13}C atoms are found in almost every organic compound and therefore, in almost every known metabolite. Although less frequently, other atoms such as phosphorus (^{31}P NMR) are also targeted by NMR, providing additional information on specific analyte types[214]. Initially, sensitivity depends on the natural abundance of the atom studied (100% of ^{1}H, ^{31}P and ^{19}F; 1.10% of ^{13}C; 0.37% of ^{15}N). Improvements in sensitivity can be obtained by longer analysis times or the application of higher magnetic fields[129]. The chemical information contained in a single 1D NMR spectrum of a biofluid or tissue extract is often sufficient to identify and quantify 50–100 metabolites at a time [215]. However, the analysis of complex matrices such as urine and plasma/serum are not trivial. In particular, the ^{1}H NMR spectra of samples such as urine are very complex, typically consisting of > 1000 detectable and often overlapping peaks. In these cases ^{1}H 1D spectra are acquired in conjunction with two-dimensional (2D) ones [216].

NMR data analysis is also divided in pre-processing or spectral processing and post processing or data processing. The pre-processing steps include; chemical shift referencing, phasing and baseline correction, which are critical for generating high quality NMR data. The post processing steps include: sub-spectral selection and filtering, spectral alignment, binning and peak picking, normalization, transformation and scaling. Their correct implementation is essential to successful statistical spectroscopy in the NMR analysis of complex biofluids such as urine and serum/plasma [216]. For data processing two different

approaches have emerged in the field of NMR-based metabolomics, (a) targeted profiling and (b) statistical spectroscopy.

a) Targeted profiling: uses spectral deconvolution software to identify and quantify compounds in individual NMR spectra. Each NMR spectrum is analysed individually and the resulting compound IDs and concentrations from multiple spectra are compiled to create a data matrix for statistical analysis[217]. A variety of software tools for NMR spectral deconvolution have been developed, those include commercial packages such as Chenomx NMR Suite [218], Bruker's AMIX [219], and non-commercial packages such as Batman [220], and Bayesil [221] and Dolphin [222]among others.

b) Statistical spectroscopy or spectral binning: uses statistical approaches to initially align multiple NMR spectra, to scale or normalize the aligned spectra, and then to identify interesting spectral regions (e.g. binning) or peaks that differentiate cases from controls [212,223]. This approach performs compound identification or quantification only after the most interesting peaks have been identified.

1.5.4 Result Interpretation

In untargeted approaches the final goal is the conversion of long lists of compounds into meaningful information. In this sense in environmental studies the contamination source, the toxicity of the compounds as well as the risk that this compound causes to health are valuable information. For this purpose, the EPA has developed guidance, handbooks, framework documents, standard operating procedures (SOPs) and other related material to conduct reliable risk assessment [224]. Risk assessments are used to characterize the nature and

magnitude of health risks to humans from chemical contaminants and other stressors, that may be present in the environment.

Biological interpretation is the final goal in metabolomics: long list of metabolites are reduced to meaningful biological terms, such as the pathways and biological routes involved. This information serves as a phenotypic readout that can be used effectively in clinical diagnostics, to identify therapeutic targets of disease, and to investigate the mechanisms of fundamental biological processes.

In this sense, several software tools have become available for the functional and biological interpretation of metabolomic experiments. They can be classified in two groups that allow complementary analysis. The first comprises tools that allow mappings and visualizations of a set of metabolites in graph representations of the metabolism (mainly metabolic pathways) and the second group comprises tools for the statistical analysis of metabolite annotations, commonly known as enrichment analysis [225].

The visualization of the identified metabolites and associated experimental measurements in the context of metabolic pathways and other general biological networks can provide a quick overview on the metabolic context of the metabolites showing up in the experiment. There are numerous computational tools to interpret alterations in metabolite abundances, including pathway-oriented databases such as KEGG [226], Cytoscape [227], and Reactome [228]. Additionally, the HMDB contains chemical, clinical and biochemical information (i.e., MetaboCards) for most of the endogenous metabolites.

In the enrichment analysis, an overrepresentation (enrichment) analysis of categorical annotations for a set of compounds of interest is performed. One of

the methods used in enrichment analysis is set enrichment analysis (SEA) which uses a collection of predefined metabolite pathways and disease states to identify and interpret patterns of metabolite concentration changes in a biologically meaningful way [229]. Typically, a list of compound names, a list of compound names with concentrations, or a concentration table should be provided. The general output is a list of annotations and their associated P-value. Some tools available for enrichment analysis are; MBRole [230], IMPaLA [231], MPEA [232] and MSEA [229]. The analysis is based on several libraries containing ~6300 groups of biologically meaningful metabolite sets collected primarily from human studies. MSEA is offered as a service both through a stand-alone web server [229] and as part of a larger metabolomics analysis suite called MetaboAnalyst.[233]

Besides these tools, generally, an effective approach to put metabolite changes into their appropriate biological context is to search thoroughly in the literature. However, the combination of both is usually the best option.

1.6 Thesis motivation and objectives

The work presented in this thesis was carried out at the Metabolomics Interdisciplinary Lab (MIL@b) research group at the Department of Electronic, Electrical and Automation Engineering (DEEEA) of the University Rovira i Virgili (URV), the Institut d'Investigació Sanitària Pere Virgili (IISPV) and CIBER of Diabetes and Metabolic Diseases (CIBERDEM).

This thesis is the first one of the research line of Toxicology and Environmental Metabolomics at the MIL@b group. It is the result of the research performed at the *THS Exposure Project* under the European Union's

Horizon 2020 research and innovation program (H2020-MSCA-IF-2014-660034). This project led by Dr. Noelia Ramirez is focused on the THS chemical characterization and human exposure to THS by using metabolomics approaches. This thesis is also part of the research project (TEC 2015-69076-P) under Prof. Xavier Correig research line which is based on the development of nanosurfaces and algorithms for the processing of images obtained by laser desorption ionization mass spectrometry.

The motivation of this thesis is to advance on the current knowledge of THS by using novel target and untargeted approaches, in this context the two main objectives have been: 1) to improve the chemical characterization of THS, and 2) to advance on the health effects derived from THS exposure.

To accomplish the first objective, we aimed to combined the most advanced analytical techniques used either in target and untargeted methods for the determination of known and unknown compounds related to THS in dust samples. Therefore, the secondary objectives have been;

i) the development of a targeted analytical method for the simultaneous analysis of nicotine, cotinine and TSNAs in indoor settled dust using UHPLC coupled to MS

ii) the development and testing of a new non-targeted screening workflow for THS exposed dust characterization using high resolution MS.

With this last purpose we've stablished a collaboration with Dr. Emma Schymanski, head of the Environmental Cheminformatics group at the Luxembourg Centre for Systems Biomedicine (LSCB). The Environmental Cheminformatics group, focuses on the comprehensive identification of known

and unknown chemicals in our environment to investigate their effects on health and disease. Dr Schymanski has specialized on processing high resolution mass spectrometry data to enhance the identification of molecules in complex samples.

To accomplish the second objective of this thesis, the characterization of THS health effects, the derived objective has been: iii) the application of a multiplatform metabolomics approach for a broad characterization of liver samples of mice exposed to THS.

For this work we stablished a collaboration with Prof. Manuela Martins-Green head of the Cell and Systems Biology Department of the University of California Riverside. They performed the characterization of THS-exposed animal models. The University of California Riverside is part of the California Consortium on Thirdhand Smoke and Human health effects, funded in 2011. Dr. Ramírez is also affiliated researcher of this consortium. The consortium is a multi-institutional and interdisciplinary effort, involving research groups from Lawrence Berkeley National Laboratory, San Diego State University, University of California Riverside, University of California San Francisco, and University of Southern California. Their main goal is to determine how much harm THS causes to human health and carry out robust risk assessments so the policy implications of THS become clear and compelling.

1.7 Organization of the document

This chapter has provided a general overview on the background of THS which is the thread that runs through the thesis, as well as the analytical

techniques used and the common strategies applied in environmental and metabolomic analysis.

Chapter 2 continues elaborating the state of the art of the determination of SHS and THS exposure biomarkers and the role of tobacco biomarkers in the characterization of the health effects related to this exposure. Chapter 2 is an already published review in the International Journal of Environmental Research and Public Health.

Chapter 3 and Chapter 4 contain the two scientific articles related to the second objective of this thesis, the chemical characterization of THS. Chapter 3 is a submitted article that focuses on the development of a novel analytical method for the simultaneous determination of nicotine, cotinine and four tobacco-specific nitrosamines (TSNAs) in household dust by using ultra high-performance liquid-chromatography (UHPLC) coupled to tandem mass spectrometry (LC-MS/MS) using a triple quadrupole (QQQ) mass spectrometer.

In Chapter 4, we present for the first time a combination of targeted and NTS strategies for the advance characterization of household dust from smokers' and non-smokers' homes. The untargeted workflow developed combines the acquisition by UHPLC coupled to high-resolution mass spectrometry (HR-MS) with the application of advanced data processing strategies, the statistical prioritization of relevant features and a novel strategy for compound annotation.

Chapter 5 is a published article in the Environment International journal which is based on the second objective of this thesis, the advance on the health effects derived from THS exposure. In this work a multiplatform untargeted metabolomics approach was implemented to unravel the molecular alterations of liver from mice exposed to THS. We used two analytical platforms (UHPLC-

HRMS and nuclear magnetic resonance, NMR) for a comprehensive determination of the altered metabolites in liver extracts, and mass spectrometry imaging (MSI) for the study of the differential spatial distribution of metabolites in the liver tissues.

Finally, Chapter 6 contains the general discussion and the conclusions of this thesis, respectively.

1.8 References

(1) Öberg, M.; Jaakkola, M. S.; Woodward, A.; Peruga, A.; Prüss-Ustün, A. Worldwide Burden of Disease from Exposure to Second-Hand Smoke: A Retrospective Analysis of Data from 192 Countries. *Lancet* **2011**, *377* (9760), 139–146. https://doi.org/10.1016/S0140-6736(10)61388-8.

(2) Talhout, R.; Schulz, T.; Florek, E.; van Benthem, J.; Wester, P.; Opperhuizen, A. Hazardous Compounds in Tobacco Smoke. *Int. J. Environ. Res. Public Health* **2011**. https://doi.org/10.3390/ijerph8020613.

(3) Thielen, A.; Klus, H.; Müller, L. Tobacco Smoke: Unraveling a Controversial Subject. *Exp. Toxicol. Pathol.* **2008**. https://doi.org/10.1016/j.etp.2008.01.014.

(4) IARC (International Agency for Reasearch on Cancer). IARC Monographs on Tobacco smoke and involuntary smoking, vol 83. Lyon, France; 2004. https://monographs.iarc.fr/wp-content/uploads/2018/06/mono83.pdf (accessed May 16, 2018). https://doi.org/10.1007/978-1-61737-995-6_3.

(5) Carreras, G.; Lugo, A.; Gallus, S.; Cortini, B.; Fernández, E.; López, M. J.; Soriano, J. B.; López-Nicolás, A.; Semple, S.; Gorini, G.; Castellano, Y.; Fu, M.; Ballbè, M.; Amalia, B.; Tigova, O.; Continente, X.; Arechavala, T.; Henderson, E.; Liu, X.; Bosetti, C.; Davoli, E.; Colombo, P.; O'Donnell, R.; Dobson, R.; Clancy, L.; Keogan, S.; Byrne, H.; Behrakis, P.; Tzortzi, A.; Vardavas, C.; Vyzikidou, V. K.; Bakellas, G.; Mattiampa, G.; Boffi, R.; Ruprecht, A.; De Marco, C.; Borgini, A.; Veronese, C.; Bertoldi, M.; Tittarelli, A.; Verdi, S.; Chellini, E.; Trapero-Bertran, M.; Guerrero, D. C.; Radu-Loghin, C.; Nguyen, D.; Starchenko, P.; Ancochea, J.; Alonso, T.; Pastor, M. T.; Erro, M.; Roca, A.; Pérez, P. Burden of Disease Attributable to Second-Hand Smoke Exposure: A Systematic Review. *Preventive Medicine*. 2019. https://doi.org/10.1016/j.ypmed.2019.105833.

(6) World Health Organization. Fact Sheet on Smoke Free Legislation. *Who* **2016**, 8–10.

(7) Daisey, J. M. Tracers for Assessing Exposure to Environmental Tobacco Smoke: What Are They Tracing? *Environ. Health Perspect.* **1999**, *107* (SUPPL. 2), 319–327. https://doi.org/10.2307/3434424.

(8) Singer, B. C.; Hodgson, A. T.; Nazaroff, W. W. Gas-Phase Organics in Environmental Tobacco Smoke: 2. Exposure-Relevant Emission Factors and Indirect Exposures from Habitual Smoking. In *Atmospheric Environment*; 2003. https://doi.org/10.1016/j.atmosenv.2003.07.015.

(9) Singer, B. C.; Hodgson, A. T.; Guevarra, K. S.; Hawley, E. L.; Nazaroff, W. W. Gas-Phase Organics in Environmental Tobacco Smoke. 1. Effects of Smoking Rate, Ventilation, and Furnishing Level on Emission Factors. *Environ. Sci. Technol.* **2002**. https://doi.org/10.1021/es011058w.

(10) Destaillats, H.; Singer, B. C.; Lee, S. K.; Gundel, L. A. Effect of Ozone on Nicotine Desorption from Model Surfaces: Evidence for Heterogeneous Chemistry. *Environ. Sci. Technol.* **2006**, *40* (6), 1799–1805. https://doi.org/10.1021/es050914r.

(11) Schick, S. F.; Farraro, K. F.; Perrino, C.; Sleiman, M.; van de Vossenberg, G.; Trinh, M. P.; Hammond, S. K.; Jenkins, B. M.; Balmes, J. Thirdhand Cigarette Smoke in an Experimental Chamber: Evidence of Surface Deposition of Nicotine, Nitrosamines and Polycyclic Aromatic Hydrocarbons and de Novo Formation of NNK. *Tob. Control* **2014**, *23* (2), 152

LP – 159. https://doi.org/10.1136/tobaccocontrol-2012-050915.

(12) Hoh, E.; Hunt, R. N.; Quintana, P. J. E.; Zakarian, J. M.; Chatfield, D. A.; Wittry, B. C.; Rodriguez, E.; Matt, G. E. Environmental Tobacco Smoke as a Source of Polycyclic Aromatic Hydrocarbons in Settled Household Dust. *Environ. Sci. Technol.* **2012**. https://doi.org/10.1021/es300267g.

(13) Sleiman, M.; Logue, J. M.; Luo, W.; Pankow, J. F.; Gundel, L. A.; Destaillats, H. Inhalable Constituents of Thirdhand Tobacco Smoke: Chemical Characterization and Health Impact Considerations. *Environ. Sci. Technol.* **2014**, *48* (22), 13093–13101. https://doi.org/10.1021/es5036333.

(14) Ramírez, N.; Vallecillos, L.; Lewis, A. C.; Borrull, F.; Marcé, R. M.; Hamilton, J. F. Comparative Study of Comprehensive Gas Chromatography-Nitrogen Chemiluminescence Detection and Gas Chromatography-Ion Trap-Tandem Mass Spectrometry for Determining Nicotine and Carcinogen Organic Nitrogen Compounds in Thirdhand Tobacco Smoke. *J. Chromatogr. A* **2015**. https://doi.org/10.1016/j.chroma.2015.11.035.

(15) Ramírez, N.; Özel, M. Z.; Lewis, A. C.; Marcé, R. M.; Borrull, F.; Hamilton, J. F. Exposure to Nitrosamines in Thirdhand Tobacco Smoke Increases Cancer Risk in Non-Smokers. *Environ. Int.* **2014**, *71*, 139–147. https://doi.org/10.1016/j.envint.2014.06.012.

(16) S. Torres, N. Ramirez, E. S. SMOKING|NORMAN: Thirdhand Smoke (THS) Compounds: Suspect List https://comptox.epa.gov/dashboard/chemical_lists/THSMOKE (accessed Jul 10, 2020).

(17) IARC. RISK OF CHEMICALS TO HUMANS. Tobacco Smoking. *38*.

(18) Hecht, S. S.; Hoffmann, D. In Tobacco and Tobacco Smoke. *Carcinogenesis* **1988**, *9* (6), 875–884.

(19) Sleiman, M.; Gundel, L. A.; Pankow, J. F.; Jacob, P.; Singer, B. C.; Destaillats, H. Formation of Carcinogens Indoors by Surface-Mediated Reactions of Nicotine with Nitrous Acid, Leading to Potential Thirdhand Smoke Hazards. *Proc. Natl. Acad. Sci.* **2010**. https://doi.org/10.1073/pnas.0912820107.

(20) Hecht, S. S. Tobacco Carcinogens, Their Biomarkers and Tobacco-Induced Cancer. *Nat. Rev. Cancer* **2003**, *3* (10), 733–744. https://doi.org/10.1038/nrc1190.

(21) Whitehead, T. P.; Havel, C.; Metayer, C.; Benowitz, N. L.; Jacob, P. Tobacco Alkaloids and Tobacco-Specific Nitrosamines in Dust from Homes of Smokeless Tobacco Users, Active Smokers, and Nontobacco Users. *Chem. Res. Toxicol.* **2015**, *28* (5), 1007–1014. https://doi.org/10.1021/acs.chemrestox.5b00040.

(22) Ramírez, N.; Özel, M. Z.; Lewis, A. C.; Marcé, R. M.; Borrull, F.; Hamilton, J. F. Determination of Nicotine and N-Nitrosamines in House Dust by Pressurized Liquid Extraction and Comprehensive Gas Chromatography-Nitrogen Chemiluminiscence Detection. *J. Chromatogr. A* **2012**, *1219*, 180–187. https://doi.org/10.1016/j.chroma.2011.11.017.

(23) Thomas, J. L.; Hecht, S. S.; Luo, X.; Ming, X.; Ahluwalia, J. S.; Carmella, S. G. Thirdhand Tobacco Smoke: A Tobacco-Specific Lung Carcinogen on Surfaces in Smokers' Homes. *Nicotine Tob. Res.* **2014**. https://doi.org/10.1093/ntr/ntt110.

(24) Northrup, T. F.; Matt, G. E.; Hovell, M. F.; Khan, A. M.; Stotts, A. L. Thirdhand Smoke in the Homes of Medically Fragile Children: Assessing the Impact of Indoor Smoking Levels

and Smoking Bans. *Nicotine Tob. Res.* **2016**. https://doi.org/10.1093/ntr/ntv174.

(25) Matt, G. E.; Fortmann, A. L.; Quintana, P. J. E.; Zakarian, J. M.; Romero, R. A.; Chatfield, D. A.; Hoh, E.; Hovell, M. F. Towards Smoke-Free Rental Cars: An Evaluation of Voluntary Smoking Restrictions in California. *Tob. Control* **2013**. https://doi.org/10.1136/tobaccocontrol-2011-050231.

(26) Matt, G. E.; Quintana, P. J. E.; Fortmann, A. L.; Zakarian, J. M.; Galaviz, V. E.; Chatfield, D. a; Hoh, E.; Hovell, M. F.; Winston, C. Thirdhand Smoke and Exposure in California Hotels: Non-Smoking Rooms Fail to Protect Non-Smoking Hotel Guests from Tobacco Smoke Exposure. *Tob. Control* **2014**, *23* (3), 264–272. https://doi.org/10.1136/tobaccocontrol-2012-050824.

(27) Lewinson, T.; Bryant, L. O. There's No Fresh Air There: Narratives of Smoke Exposure among Residents of Extended-Stay Hotels. *Heal. Soc. Work* **2015**. https://doi.org/10.1093/hsw/hlv016.

(28) Matt, G. E.; Quintana, P. J. E.; Hoh, E.; Zakarian, J. M.; Chowdhury, Z.; Hovell, M. F.; Jacob, P.; Watanabe, K.; Theweny, T. S.; Flores, V.; Nguyen, A.; Dhaliwal, N.; Hayward, G. A Casino Goes Smoke Free: A Longitudinal Study of Secondhand and Thirdhand Smoke Pollution and Exposure. *Tob. Control* **2018**. https://doi.org/10.1136/tobaccocontrol-2017-054052.

(29) Santos e Silva, S. I.; Bowdler, P.; Giltrow, D.; Riddell, S.; Honeychurch, K. C. A Simple and Rapid Method for the Determination of Nicotine in Third-Hand Smoke by Liquid Chromatography and Its Application for the Assessment of Contaminated Outdoor Communal Areas. *Drug Test. Anal.* **2016**. https://doi.org/10.1002/dta.1822.

(30) Bahl, V.; Jacob, P.; Havel, C.; Schick, S. F.; Talbot, P. Thirdhand Cigarette Smoke: Factors Affecting Exposure and Remediation. *PLoS One* **2014**, *9* (10), 1–10. https://doi.org/10.1371/journal.pone.0108258.

(31) Matt, G. E.; Quintana, P. J. E.; Zakarian, J. M.; Fortmann, A. L.; Chatfield, D. A.; Hoh, E.; Uribe, A. M.; Hovell, M. F. When Smokers Move out and Non-Smokers Move in: Residential Thirdhand Smoke Pollution and Exposure. *Tob. Control* **2011**, *20* (1), e1–e1. https://doi.org/10.1136/tc.2010.037382.

(32) Matt, G. E.; Quintana, P. J. E.; Hoh, E.; Zakarian, J. M.; Dodder, N. G.; Record, R. A.; Hovell, M. F.; Mahabee-Gittens, E. M.; Padilla, S.; Markman, L.; Watanabe, K.; Novotny, T. E. Persistent Tobacco Smoke Residue in Multiunit Housing: Legacy of Permissive Indoor Smoking Policies and Challenges in the Implementation of Smoking Bans. *Prev. Med. Reports* **2020**, *18* (March), 101088. https://doi.org/10.1016/j.pmedr.2020.101088.

(33) Matt, G. E.; Quintana, P. J. E.; Zakarian, J. M.; Hoh, E.; Hovell, M. F.; Mahabee-Gittens, M.; Watanabe, K.; Datuin, K.; Vue, C.; Chatfield, D. A. When Smokers Quit: Exposure to Nicotine and Carcinogens Persists from Thirdhand Smoke Pollution. *Tob. Control* **2017**, *26* (5), 548–556. https://doi.org/10.1136/tobaccocontrol-2016-053119.

(34) Matt, G. E.; Quintana, P. J. E.; Destaillats, H.; Gundel, L. A.; Sleiman, M.; Singer, B. C.; Jacob, P.; Benowitz, N.; Winickoff, J. P.; Rehan, V.; Talbot, P.; Schick, S.; Samet, J.; Wang, Y.; Hang, B.; Martins-Green, M.; Pankow, J. F.; Hovell, M. F. Thirdhand Tobacco Smoke: Emerging Evidence and Arguments for a Multidisciplinary Research Agenda. *Environ. Health Perspect.* **2011**, *119* (9), 1218–1226. https://doi.org/10.1289/ehp.1103500.

(35) Roberts, J. W.; Dickey, P. Exposure of Children to Pollutants in House Dust and Indoor Air. *Reviews of environmental contamination and toxicology*. 1995.

(36) Tulve, N. S.; Suggs, J. C.; McCurdy, T.; Cohen Hubal, E. A.; Moya, J. Frequency of Mouthing Behavior in Young Children. *J. Expo. Anal. Environ. Epidemiol.* **2002**. https://doi.org/10.1038/sj.jea.7500225.

(37) Jung, J. W.; Ju, Y. S.; Kang, H. R. Association between Parental Smoking Behavior and Children's Respiratory Morbidity: 5-Year Study in an Urban City of South Korea. *Pediatr. Pulmonol.* **2012**. https://doi.org/10.1002/ppul.21556.

(38) De La Riva-Velasco, E.; Krishnan, S.; Dozor, A. J. Relationship between Exhaled Nitric Oxide and Exposure to Low-Level Environmental Tobacco Smoke in Children with Asthma on Inhaled Corticosteroids. *J. Asthma* **2012**. https://doi.org/10.3109/02770903.2012.701363.

(39) Leung, L. T.; Ho, S. Y.; Wang, M. P.; Lam, T. H. Secondhand Smoke from Multiple Sources, Thirdhand Smoke and Respiratory Symptoms in Hong Kong Adolescents. *Nicotine Tob. Res.* **2018**. https://doi.org/10.1093/ntr/ntw302.

(40) Hang, B.; Wang, P.; Zhao, Y.; Sarker, A.; Chenna, A.; Xia, Y.; Snijders, A. M.; Mao, J. H. Adverse Health Effects of Thirdhand Smoke: From Cell to Animal Models. *Int. J. Mol. Sci.* **2017**, *18* (5). https://doi.org/10.3390/ijms18050932.

(41) Hammer, T. R.; Fischer, K.; Mueller, M.; Hoefer, D. Effects of Cigarette Smoke Residues from Textiles on Fibroblasts, Neurocytes and Zebrafish Embryos and Nicotine Permeation through Human Skin. *Int. J. Hyg. Environ. Health* **2011**. https://doi.org/10.1016/j.ijheh.2011.04.007.

(42) Bahl, V.; Weng, N. J. H.; Schick, S. F.; Sleiman, M.; Whitehead, J.; Ibarra, A.; Talbot, P. Cytotoxicity of Thirdhand Smoke and Identification of Acrolein as a Volatile Thirdhand Smoke Chemical That Inhibits Cell Proliferation. *Toxicol. Sci.* **2016**. https://doi.org/10.1093/toxsci/kfv327.

(43) Bahl, V.; Shim, H. J.; Jacob, P.; Dias, K.; Schick, S. F.; Talbot, P. Thirdhand Smoke: Chemical Dynamics, Cytotoxicity, and Genotoxicity in Outdoor and Indoor Environments. *Toxicol. Vitr.* **2016**. https://doi.org/10.1016/j.tiv.2015.12.007.

(44) Bahl, V.; Johnson, K.; Phandthong, R.; Zahedi, A.; Schick, S. F.; Talbot, P. Thirdhand Cigarette Smoke Causes Stress-Induced Mitochondrial Hyperfusion and Alters the Transcriptional Profile of Stem Cells. *Toxicol. Sci.* **2016**. https://doi.org/10.1093/toxsci/kfw102.

(45) Xu, B.; Chen, M.; Yao, M.; Ji, X.; Mao, Z.; Tang, W.; Qiao, S.; Schick, S. F.; Mao, J. H.; Hang, B.; Xia, Y. Metabolomics Reveals Metabolic Changes in Male Reproductive Cells Exposed to Thirdhand Smoke. *Sci. Rep.* **2015**. https://doi.org/10.1038/srep15512.

(46) Hang, B.; Sarker, A. H.; Havel, C.; Saha, S.; Hazra, T. K.; Schick, S.; Jacob, P.; Rehan, V. K.; Chenna, A.; Sharan, D.; Sleiman, M.; Destaillats, H.; Gundel, L. A. Thirdhand Smoke Causes DNA Damage in Human Cells. *Mutagenesis* **2013**. https://doi.org/10.1093/mutage/get013.

(47) Hang, B.; Wang, Y.; Huang, Y.; Wang, P.; Langley, S. A.; Bi, L.; Sarker, A. H.; Schick, S. F.; Havel, C.; Jacob, P.; Benowitz, N.; Destaillats, H.; Tang, X.; Xia, Y.; Jen, K. Y.; Gundel, L. A.; Mao, J. H.; Snijders, A. M. Short-Term Early Exposure to Thirdhand Cigarette Smoke Increases Lung Cancer Incidence in Mice. *Clin. Sci.* **2018**. https://doi.org/10.1042/CS20171521.

(48) Adhami, N.; Starck, S. R.; Flores, C.; Green, M. M. A Health Threat to Bystanders Living in the Homes of Smokers: How Smoke Toxins Deposited on Surfaces Can Cause Insulin

Resistance. *PLoS One* **2016**, *11* (3), 1–20. https://doi.org/10.1371/journal.pone.0149510.

(49) Martins-Green, M.; Adhami, N.; Frankos, M.; Valdez, M.; Goodwin, B.; Lyubovitsky, J.; Dhall, S.; Garcia, M.; Egiebor, I.; Martinez, B.; Green, H. W.; Havel, C.; Yu, L.; Liles, S.; Matt, G.; Destaillats, H.; Sleiman, M.; Gundel, L. A.; Benowitz, N.; Jacob, P.; Hovell, M.; Winickoff, J. P.; Curras-Collazo, M. Cigarette Smoke Toxins Deposited on Surfaces: Implications for Human Health. *PLoS One* **2014**, *9* (1), 1–12. https://doi.org/10.1371/journal.pone.0086391.

(50) Dhall, S.; Alamat, R.; Castro, A.; Sarker, A. H.; Mao, J. H.; Chan, A.; Hang, B.; Martins-Green, M. Tobacco Toxins Deposited on Surfaces (Third Hand Smoke) Impair Wound Healing. *Clin. Sci.* **2016**. https://doi.org/10.1042/CS20160236.

(51) Kind, T.; Tsugawa, H.; Cajka, T.; Ma, Y.; Lai, Z.; Mehta, S. S.; Wohlgemuth, G.; Barupal, D. K.; Showalter, M. R.; Arita, M.; Fiehn, O. Identification of Small Molecules Using Accurate Mass MS/MS Search. *Mass Spectrometry Reviews*. 2018. https://doi.org/10.1002/mas.21535.

(52) Holčapek, M.; Jirásko, R.; Lísa, M. Basic Rules for the Interpretation of Atmospheric Pressure Ionization Mass Spectra of Small Molecules. *Journal of Chromatography A*. 2010. https://doi.org/10.1016/j.chroma.2010.02.049.

(53) Holčapek, M.; Jirásko, R.; Lísa, M. Recent Developments in Liquid Chromatography-Mass Spectrometry and Related Techniques. *J. Chromatogr. A* **2012**, *1259*, 3–15. https://doi.org/10.1016/j.chroma.2012.08.072.

(54) Ho, C. S.; Lam, C. W. K.; Chan, M. H. M.; Cheung, R. C. K.; Law, L. K.; Lit, L. C. W.; Ng, K. F.; Suen, M. W. M.; Tai, H. L. Electrospray Ionisation Mass Spectrometry: Principles and Clinical Applications. *Clin. Biochem. Rev.* **2003**.

(55) Konermann, L.; Ahadi, E.; Rodriguez, A. D.; Vahidi, S. Unraveling the Mechanism of Electrospray Ionization. *Anal. Chem.* **2013**, *85* (1), 2–9. https://doi.org/10.1021/ac302789c.

(56) Forcisi, S.; Moritz, F.; Kanawati, B.; Tziotis, D.; Lehmann, R.; Schmitt-Kopplin, P. Liquid Chromatography-Mass Spectrometry in Metabolomics Research: Mass Analyzers in Ultra High Pressure Liquid Chromatography Coupling. *J. Chromatogr. A* **2013**, *1292*, 51–65. https://doi.org/10.1016/j.chroma.2013.04.017.

(57) Byrdwell, W. C. Atmospheric Pressure Chemical Ionization Mass Spectrometry for Analysis of Lipids. *Lipids*. 2001. https://doi.org/10.1007/s11745-001-0725-5.

(58) *Principles and Applications of Clinical Mass Spectrometry*; 2018. https://doi.org/10.1016/c2017-0-03476-6.

(59) Cottrell, J. S.; Greathead, R. J. Extending the Mass Range of a Sector Mass Spectrometer. *Mass Spectrom. Rev.* **1986**. https://doi.org/10.1002/mas.1280050302.

(60) Dubois, F.; Knochenmuss, R.; Zenobi, R.; Brunelle, A.; Deprun, C.; Le Beyec, Y. A Comparison between Ion-to-Photon and Microchannel Plate Detectors. *Rapid Commun. Mass Spectrom.* **1999**. https://doi.org/10.1002/(SICI)1097-0231(19990515)13:9<786::AID-RCM566>3.0.CO;2-3.

(61) Amorim Madeira, P. J.; Helena, M. Applications of Tandem Mass Spectrometry: From Structural Analysis to Fundamental Studies. In *Tandem Mass Spectrometry - Applications and Principles*; 2012. https://doi.org/10.5772/31736.

(62) Westman-Brinkmalm, A.; Brinkmalm, G. Tandem Mass Spectrometry. In *Mass Spectrometry: Instrumentation, Interpretation, and Applications*; 2008. https://doi.org/10.1002/9780470395813.ch3.

(63) Anderson, L.; Hunter, C. L. Quantitative Mass Spectrometric Multiple Reaction Monitoring Assays for Major Plasma Proteins. *Mol. Cell. Proteomics* **2006**. https://doi.org/10.1074/mcp.M500331-MCP200.

(64) Allen, D. R.; Mcwhinney, B. C. Quadrupole Time-of-Flight Mass Spectrometry: A Paradigm Shift in Toxicology Screening Applications. *Clin. Biochem. Rev.* **2019**, *40* (3), 135–146. https://doi.org/10.33176/aacb-19-00023.

(65) Díaz, R.; Ibáñez, M.; Sancho, J. V.; Hernández, F. Target and Non-Target Screening Strategies for Organic Contaminants, Residues and Illicit Substances in Food, Environmental and Human Biological Samples by UHPLC-QTOF-MS. *Anal. Methods* **2012**. https://doi.org/10.1039/c1ay05385j.

(66) Roemmelt, A. T.; Steuer, A. E.; Poetzsch, M.; Kraemer, T. Liquid Chromatography, in Combination with a Quadrupole Time-of-Flight Instrument (LC QTOF), with Sequential Window Acquisition of All Theoretical Fragment-Ion Spectra (SWATH) Acquisition: Systematic Studies on Its Use for Screenings in Clinical and Foren. *Anal. Chem.* **2014**. https://doi.org/10.1021/ac503144p.

(67) Zhang, Y.; Bilbao, A.; Bruderer, T.; Luban, J.; Strambio-De-Castillia, C.; Lisacek, F.; Hopfgartner, G.; Varesio, E. The Use of Variable Q1 Isolation Windows Improves Selectivity in LC-SWATH-MS Acquisition. *J. Proteome Res.* **2015**. https://doi.org/10.1021/acs.jproteome.5b00543.

(68) Sparkman, O. D.; Penton, Z.; Kitson, F. G. *Gas Chromatography and Mass Spectrometry: A Practical Guide*; 2011. https://doi.org/10.1016/C2009-0-17039-3.

(69) Teske, J.; Engewald, W. Methods for, and Applications of, Large-Volume Injection in Capillary Gas Chromatography. *TrAC - Trends Anal. Chem.* **2002**, *21* (9–10), 584–593. https://doi.org/10.1016/S0165-9936(02)00801-4.

(70) Cramers, C. A.; McNair, H. M. Gas Chromatography. *J. Chromatogr. Libr.* **1983**. https://doi.org/10.1016/S0301-4770(08)60867-2.

(71) Eiceman, G. A.; Gardea-Torresdey, J.; Dorman, F.; Overton, E.; Bhushan, A.; Dharmasena, H. P. Gas Chromatography. *Anal. Chem.* **2006**, *78* (12), 3985–3996. https://doi.org/10.1021/ac060638e.

(72) Pasikanti, K. K.; Ho, P. C.; Chan, E. C. Y. Gas Chromatography/Mass Spectrometry in Metabolic Profiling of Biological Fluids. *Journal of Chromatography B: Analytical Technologies in the Biomedical and Life Sciences*. 2008, pp 202–211. https://doi.org/10.1016/j.jchromb.2008.04.033.

(73) Korytár, P.; Janssen, H. G.; Matisová, E.; Brinkman, U. A. T. Practical Fast Gas Chromatography: Methods, Instrumentation and Applications. *TrAC - Trends Anal. Chem.* **2002**, *21* (9–10), 558–572. https://doi.org/10.1016/S0165-9936(02)00811-7.

(74) Rigano, F.; Tranchida, P. Q.; Dugo, P.; Mondello, L. High-Performance Liquid Chromatography Combined with Electron Ionization Mass Spectrometry: A Review. *TrAC - Trends Anal. Chem.* **2019**, *118*, 112–122. https://doi.org/10.1016/j.trac.2019.05.032.

(75) Niessen, W. M. A.; Tinke, A. P. Liquid Chromatography-Mass Spectrometry General Principles and Instrumentation. *Journal of Chromatography A*. 1995.

https://doi.org/10.1016/0021-9673(94)01198-N.

(76) Boersema, P. J.; Mohammed, S.; Heck, A. J. R. Hydrophilic Interaction Liquid Chromatography (HILIC) in Proteomics. *Anal. Bioanal. Chem.* **2008**, *391* (1), 151–159. https://doi.org/10.1007/s00216-008-1865-7.

(77) Contrepois, K.; Jiang, L.; Snyder, M. Optimized Analytical Procedures for the Untargeted Metabolomic Profiling of Human Urine and Plasma by Combining Hydrophilic Interaction (HILIC) and Reverse-Phase Liquid Chromatography (RPLC)-Mass Spectrometry. *Mol. Cell. Proteomics* **2015**. https://doi.org/10.1074/mcp.M114.046508.

(78) Buszewski, B.; Noga, S. Hydrophilic Interaction Liquid Chromatography (HILIC)-a Powerful Separation Technique. *Anal. Bioanal. Chem.* **2012**, *402* (1), 231–247. https://doi.org/10.1007/s00216-011-5308-5.

(79) Blue, L. E.; Franklin, E. G.; Godinho, J. M.; Grinias, J. P.; Grinias, K. M.; Lunn, D. B.; Moore, S. M. Recent Advances in Capillary Ultrahigh Pressure Liquid Chromatography. *J. Chromatogr. A* **2017**, *1523*, 17–39. https://doi.org/10.1016/j.chroma.2017.05.039.

(80) Guillarme, D.; Schappler, J.; Rudaz, S.; Veuthey, J. L. Coupling Ultra-High-Pressure Liquid Chromatography with Mass Spectrometry. *TrAC - Trends Anal. Chem.* **2010**, *29* (1), 15–27. https://doi.org/10.1016/j.trac.2009.09.008.

(81) Schwamborn, K.; Caprioli, R. M. Molecular Imaging by Mass Spectrometry-Looking beyond Classical Histology. *Nat. Rev. Cancer* **2010**, *10* (9), 639–646. https://doi.org/10.1038/nrc2917.

(82) Cornett, D. S.; Reyzer, M. L.; Chaurand, P.; Caprioli, R. M. MALDI Imaging Mass Spectrometry: Molecular Snapshots of Biochemical Systems. *Nat. Methods* **2007**, *4* (10), 828–833. https://doi.org/10.1038/nmeth1094.

(83) Bodzon-Kulakowska, A.; Suder, P. Imaging Mass Spectrometry: Instrumentation, Applications, and Combination with Other Visualization Techniques. *Mass Spectrom. Rev.* **2016**. https://doi.org/10.1002/mas.21468.

(84) Ràfols, P.; Vilalta, D.; Brezmes, J.; Cañellas, N.; del Castillo, E.; Yanes, O.; Ramírez, N.; Correig, X. Signal Preprocessing, Multivariate Analysis and Software Tools for MA(LDI)-TOF Mass Spectrometry Imaging for Biological Applications. *Mass Spectrometry Reviews*. 2018. https://doi.org/10.1002/mas.21527.

(85) Ràfols, P.; Vilalta, D.; Torres, S.; Calavia, R.; Heijs, B.; McDonnell, L. A.; Brezmes, J.; del Castillo, E.; Yanes, O.; Ramírez, N.; Correig, X. Assessing the Potential of Sputtered Gold Nanolayers in Mass Spectrometry Imaging for Metabolomics Applications. *PLoS One* **2018**, *13* (12), e0208908. https://doi.org/10.1371/journal.pone.0208908.

(86) Hölscher, D.; Fuchser, J.; Knop, K.; Menezes, R. C.; Buerkert, A.; Svatoš, A.; Schubert, U. S.; Schneider, B. High Resolution Mass Spectrometry Imaging Reveals the Occurrence of Phenylphenalenone-Type Compounds in Red Paracytic Stomata and Red Epidermis Tissue of Musa Acuminata Ssp. Zebrina Cv. "Rowe Red." *Phytochemistry* **2015**. https://doi.org/10.1016/j.phytochem.2015.04.010.

(87) Shah, N.; Sattar, A.; Benanti, M.; Hollander, S.; Cheuck, L. Magnetic Resonance Spectroscopy as an Imaging Tool for Cancer: A Review of the Literature. *Journal of the American Osteopathic Association*. 2006. https://doi.org/10.7556/jaoa.2006.106.1.23.

(88) Alonso, A.; Marsal, S.; Julià, A. Analytical Methods in Untargeted Metabolomics: State of the Art in 2015. *Frontiers in Bioengineering and Biotechnology*. 2015.

https://doi.org/10.3389/fbioe.2015.00023.

(89) Dunn, W. B.; Ellis, D. I. Metabolomics: Current Analytical Platforms and Methodologies. *TrAC - Trends Anal. Chem.* **2005**. https://doi.org/10.1016/j.trac.2004.11.021.

(90) Marion, D. An Introduction to Biological NMR Spectroscopy. *Mol. Cell. Proteomics* **2013**, *12* (11), 3006–3025. https://doi.org/10.1074/mcp.O113.030239.

(91) Emwas, A. H.; Roy, R.; McKay, R. T.; Tenori, L.; Saccenti, E.; Nagana Gowda, G. A.; Raftery, D.; Alahmari, F.; Jaremko, L.; Jaremko, M.; Wishart, D. S. Nmr Spectroscopy for Metabolomics Research. *Metabolites* **2019**, *9* (7). https://doi.org/10.3390/metabo9070123.

(92) Lankadurai, B. P.; Nagato, E. G.; Simpson, M. J. Environmental Metabolomics: An Emerging Approach to Study Organism Responses to Environmental Stressors. *Environ. Rev.* **2013**, *21* (3), 180–205. https://doi.org/10.1139/er-2013-0011.

(93) Viant, M. R. Recent Developments in Environmental Metabolomics. *Mol. Biosyst.* **2008**, *4* (10), 980–986. https://doi.org/10.1039/b805354e.

(94) Monteiro, M. S.; Carvalho, M.; Bastos, M. L.; Guedes de Pinho, P. Metabolomics Analysis for Biomarker Discovery: Advances and Challenges. *Curr. Med. Chem.* **2013**. https://doi.org/10.2174/092986713804806621.

(95) European Comission. Indoor Air Pollution: New EU Research Reveals Higher Risks than Previously Thought. *Eur. Com.* **2003**, No. September, IP/03/1278.

(96) Whitehead, T.; Metayer, C.; Buffler, P.; Rappaport, S. M. Estimating Exposures to Indoor Contaminants Using Residential Dust. *J. Expo. Sci. Environ. Epidemiol.* **2011**, *21* (6), 549–564. https://doi.org/10.1038/jes.2011.11.

(97) Lindon, J. C.; Nicholson, J. K.; Holmes, E. *The Handbook of Metabonomics and Metabolomics*; 2007. https://doi.org/10.1016/B978-0-444-52841-4.X5000-0.

(98) Nicholson, J. K.; Lindon, J. C.; Holmes, E. "Metabonomics": Understanding the Metabolic Responses of Living Systems to Pathophysiological Stimuli via Multivariate Statistical Analysis of Biological NMR Spectroscopic Data. *Xenobiotica*. 1999. https://doi.org/10.1080/004982599238047.

(99) Bundy, J. G.; Davey, M. P.; Viant, M. R. Environmental Metabolomics: A Critical Review and Future Perspectives. *Metabolomics* **2009**, *5* (1), 3–21. https://doi.org/10.1007/s11306-008-0152-0.

(100) Wishart, D. S. Emerging Applications of Metabolomics in Drug Discovery and Precision Medicine. *Nature Reviews Drug Discovery*. 2016. https://doi.org/10.1038/nrd.2016.32.

(101) Wishart, D. S. Metabolomics: Applications to Food Science and Nutrition Research. *Trends in Food Science and Technology*. 2008. https://doi.org/10.1016/j.tifs.2008.03.003.

(102) Miller, M. G. Environmental Metabolomics: A SWOT Analysis (Strengths, Weaknesses, Opportunities, and Threats). *J. Proteome Res.* **2007**, *6* (2), 540–545. https://doi.org/10.1021/pr060623x.

(103) Patti, G. J.; Yanes, O.; Siuzdak, G. Metabolomics: The Apogee of the Omic Triology NIH Public Access. *Nat Rev Mol Cell Biol* **2012**. https://doi.org/10.1038/nrm3314.

(104) Griffiths, W. J.; Koal, T.; Wang, Y.; Kohl, M.; Enot, D. P.; Deigner, H. P. Targeted

Metabolomics for Biomarker Discovery. *Angewandte Chemie - International Edition*. 2010. https://doi.org/10.1002/anie.200905579.

(105) Blaise, B. J.; Correia, G.; Tin, A.; Young, J. H.; Vergnaud, A. C.; Lewis, M.; Pearce, J. T. M.; Elliott, P.; Nicholson, J. K.; Holmes, E.; Ebbels, T. M. D. Power Analysis and Sample Size Determination in Metabolic Phenotyping. *Anal. Chem.* **2016**. https://doi.org/10.1021/acs.analchem.6b00188.

(106) Rager, J. E.; Strynar, M. J.; Liang, S.; McMahen, R. L.; Richard, A. M.; Grulke, C. M.; Wambaugh, J. F.; Isaacs, K. K.; Judson, R.; Williams, A. J.; Sobus, J. R. Linking High Resolution Mass Spectrometry Data with Exposure and Toxicity Forecasts to Advance High-Throughput Environmental Monitoring. *Environ. Int.* **2016**, *88*, 269–280. https://doi.org/10.1016/j.envint.2015.12.008.

(107) Špánik, I.; Machyňáková, A. Recent Applications of Gas Chromatography with High-Resolution Mass Spectrometry. *J. Sep. Sci.* **2018**, *41* (1), 163–179. https://doi.org/10.1002/jssc.201701016.

(108) Butte, W.; Heinzow, B. Pollutants in House Dust as Indicators of Indoor Contamination. *Rev. Environ. Contam. Toxicol.* **2002**.

(109) García, M.; Rodríguez, I.; Cela, R. Optimisation of a Matrix Solid-Phase Dispersion Method for the Determination of Organophosphate Compounds in Dust Samples. *Anal. Chim. Acta* **2007**. https://doi.org/10.1016/j.aca.2007.03.026.

(110) Regueiro, J.; Llompart, M.; García-Jares, C.; Cela, R. Determination of Polybrominated Diphenyl Ethers in Domestic Dust by Microwave-Assisted Solvent Extraction and Gas Chromatography-Tandem Mass Spectrometry. *J. Chromatogr. A* **2006**. https://doi.org/10.1016/j.chroma.2006.09.080.

(111) Mercier, F.; Glorennec, P.; Thomas, O.; Bot, B. Le. Organic Contamination of Settled House Dust, a Review for Exposure Assessment Purposes. *Environ. Sci. Technol.* **2011**, *45* (16), 6716–6727. https://doi.org/10.1021/es200925h.

(112) Maceira, A.; Marcé, R. M.; Borrull, F. Analytical Methods for Determining Organic Compounds Present in the Particulate Matter from Outdoor Air. *TrAC - Trends Anal. Chem.* **2020**, *122*. https://doi.org/10.1016/j.trac.2019.115707.

(113) Pérez, R. A.; Albero, B.; Tadeo, J. L. *Matrix Solid Phase Dispersion*; Elsevier Inc., 2019. https://doi.org/10.1016/B978-0-12-816906-3.00019-4.

(114) Elorduy, I.; Elcoroaristizabal, S.; Durana, N.; García, J. A.; Alonso, L. Diurnal Variation of Particle-Bound PAHs in an Urban Area of Spain Using TD-GC/MS: Influence of Meteorological Parameters and Emission Sources. *Atmos. Environ.* **2016**, *138*, 87–98. https://doi.org/10.1016/j.atmosenv.2016.05.012.

(115) Albinet, A.; Nalin, F.; Tomaz, S.; Beaumont, J.; Lestremau, F. A Simple QuEChERS-like Extraction Approach for Molecular Chemical Characterization of Organic Aerosols: Application to Nitrated and Oxygenated PAH Derivatives (NPAH and OPAH) Quantified by GC-NICIMS. *Anal. Bioanal. Chem.* **2014**, *406* (13), 3131–3148. https://doi.org/10.1007/s00216-014-7760-5.

(116) González-Curbelo, M.; Socas-Rodríguez, B.; Herrera-Herrera, A. V.; González-Sálamo, J.; Hernández-Borges, J.; Rodríguez-Delgado, M. Evolution and Applications of the QuEChERS Method. *TrAC - Trends Anal. Chem.* **2015**, *71*, 169–185. https://doi.org/10.1016/j.trac.2015.04.012.

(117) Hecht, S. S.; Spratt, T. E.; Trushin, N. Absolute Configuration of 4-(Methylnitrosamino)-1-(3-Pyridyl)-1-Butanol Formed Metabolically from 4-(Methylnitrosamino)-1-(3-Pyridyl)-1-Butanone. **2000**, *21* (4), 3605.

(118) Wu, W.; Ashley, D. L.; Watson, C. H. Simultaneous Determination of Five Tobacco-Specific Nitrosamines in Mainstream Cigarette Smoke by Isotope Dilution Liquid Chromatography/Electrospray Ionization Tandem Mass Spectrometry. *Anal. Chem.* **2003**. https://doi.org/10.1021/ac030135y.

(119) Li, C.; Chen, Z.; Wen, D.; Zhang, J.; Cong, W.; Yu, B.; Liao, Y.; Liu, H. Determination of Tobacco-Specific N-Nitrosamines in Rabbit Serum by Capillary Zone Electrophoresis and Capillary Electrophoresis-Electrospray Ionization-Mass Spectrometry with Solid-Phase Extraction. *Electrophoresis* **2006**. https://doi.org/10.1002/elps.200600009.

(120) Kim, S.; Aung, T.; Berkeley, E.; Diette, G. B.; Breysse, P. N. Measurement of Nicotine in Household Dust. *Environ. Res.* **2008**, *108* (3), 289–293. https://doi.org/10.1016/j.envres.2008.07.004.

(121) Whitehead, T. P.; Metayer, C.; Park, J. S.; Does, M.; Buffler, P. A.; Rappaport, S. M. Levels of Nicotine in Dust from Homes of Smokeless Tobacco Users. *Nicotine Tob. Res.* **2013**, *15* (12), 2045–2052. https://doi.org/10.1093/ntr/ntt096.

(122) Whitehead, T.; Metayer, C.; Ward, M. H.; Nishioka, M. G.; Gunier, R.; Colt, J. S.; Reynolds, P.; Selvin, S.; Buffler, P.; Rappaport, S. M. Is House-Dust Nicotine a Good Surrogate for Household Smoking? *Am. J. Epidemiol.* **2009**, *169* (9), 1113–1123. https://doi.org/10.1093/aje/kwp021.

(123) Matt, G. E.; Quintana, P. J. E.; Hovell, M. F.; Bernert, J. T.; Song, S.; Novianti, N.; Juarez, T.; Floro, J.; Gehrman, C.; Garcia, M.; Larson, S. Households Contaminated by Environmental Tobacco Smoke: Sources of Infant Exposures. *Tob. Control* **2004**, *13* (1), 29–37. https://doi.org/10.1136/tc.2003.003889.

(124) Matt, G. E.; Mahabee-Gittens, E. M.; Zakarian, J. M.; Quintana, P. J. E.; Hoh, E.; Myers, M. Nicotine in Thirdhand Smoke Residue Predicts Relapse from Smoking Cessation: A Pilot Study. *Addict. Behav.* **2019**, *98* (June), 106041. https://doi.org/10.1016/j.addbeh.2019.106041.

(125) Whitehead, T. P.; Havel, C.; Metayer, C.; Benowitz, N. L.; Jacob, P. Tobacco Alkaloids and Tobacco-Specific Nitrosamines in Dust from Homes of Smokeless Tobacco Users, Active Smokers, and Nontobacco Users. *Chem. Res. Toxicol.* **2015**, *28* (5), 1007–1014. https://doi.org/10.1021/acs.chemrestox.5b00040.

(126) Dunn, W. B.; Wilson, I. D.; Nicholls, A. W.; Broadhurst, D. The Importance of Experimental Design and QC Samples in Large-Scale and MS-Driven Untargeted Metabolomic Studies of Humans. *Bioanalysis* **2012**. https://doi.org/10.4155/bio.12.204.

(127) Schrimpe-Rutledge, A. C.; Codreanu, S. G.; Sherrod, S. D.; McLean, J. A. Untargeted Metabolomics Strategies—Challenges and Emerging Directions. *J. Am. Soc. Mass Spectrom.* **2016**, *27* (12), 1897–1905. https://doi.org/10.1007/s13361-016-1469-y.

(128) Moco, S.; Vervoort, J.; Moco, S.; Bino, R. J.; De Vos, R. C. H.; Bino, R. Metabolomics Technologies and Metabolite Identification. *TrAC - Trends Anal. Chem.* **2007**. https://doi.org/10.1016/j.trac.2007.08.003.

(129) Vuckovic, D. Current Trends and Challenges in Sample Preparation for Global Metabolomics Using Liquid Chromatography-Mass Spectrometry. *Analytical and Bioanalytical Chemistry*. 2012. https://doi.org/10.1007/s00216-012-6039-y.

(130) Maher, A. D.; Zirah, S. F. M.; Holmes, E.; Nicholson, J. K. Experimental and Analytical Variation in Human Urine in 1H NMR Spectroscopy-Based Metabolic Phenotyping Studies. *Anal. Chem.* **2007**. https://doi.org/10.1021/ac070212f.

(131) Zhou, J.; Yin, Y. Strategies for Large-Scale Targeted Metabolomics Quantification by Liquid Chromatography-Mass Spectrometry. *Analyst* **2016**, *141* (23), 6362–6373. https://doi.org/10.1039/c6an01753c.

(132) Yanes, O.; Tautenhahn, R.; Patti, G. J.; Siuzdak, G. Expanding Coverage of the Metabolome for Global Metabolite Profiling. *Anal. Chem.* **2011**. https://doi.org/10.1021/ac102981k.

(133) Prasad Maharjan, R.; Ferenci, T. Global Metabolite Analysis: The Influence of Extraction Methodology on Metabolome Profiles of Escherichia Coli. *Anal. Biochem.* **2003**. https://doi.org/10.1016/S0003-2697(02)00536-5.

(134) Rammouz, R. El; Létisse, F.; Durand, S.; Portais, J. C.; Moussa, Z. W.; Fernandez, X. Analysis of Skeletal Muscle Metabolome: Evaluation of Extraction Methods for Targeted Metabolite Quantification Using Liquid Chromatography Tandem Mass Spectrometry. *Anal. Biochem.* **2010**. https://doi.org/10.1016/j.ab.2009.12.006.

(135) Ahlf Wheatcraft, D. R.; Liu, X.; Hummon, A. B. Sample Preparation Strategies for Mass Spectrometry Imaging of 3D Cell Culture Models. *J. Vis. Exp.* **2014**, No. 94, 3–9. https://doi.org/10.3791/52313.

(136) Sleno, L.; Volmer, D. A. Some Fundamental and Technical Aspects of the Quantitative Analysis of Pharmaceutical Drugs by Matrix-Assisted Laser Desorption/Ionization Mass Spectrometry. *Rapid Commun. Mass Spectrom.* **2005**. https://doi.org/10.1002/rcm.2006.

(137) Hankin, J. A.; Barkley, R. M.; Murphy, R. C. Sublimation as a Method of Matrix Application for Mass Spectrometric Imaging. *J. Am. Soc. Mass Spectrom.* **2007**. https://doi.org/10.1016/j.jasms.2007.06.010.

(138) Bouschen, W.; Schulz, O.; Eikely, D.; Spengler, B. Matrix Vapor Deposition/Recrystallization and Dedicated Spray Preparation for High-Resolution Scanning Microprobe Matrix-Assisted Laser Desorption/Ionization Imaging Mass Spectrometry (SMALDI-MS) of Tissue and Single Cells. *Rapid Commun. Mass Spectrom.* **2010**. https://doi.org/10.1002/rcm.4401.

(139) Shroff, R.; Muck, A.; Svatoš, A. Analysis of Low Molecular Weight Acids by Negative Mode Matrix-Assisted Laser Desorption/Ionization Time-of-Flight Mass Spectrometry. *Rapid Commun. Mass Spectrom.* **2007**. https://doi.org/10.1002/rcm.3216.

(140) Meriaux, C.; Franck, J.; Wisztorski, M.; Salzet, M.; Fournier, I. Liquid Ionic Matrixes for MALDI Mass Spectrometry Imaging of Lipids. *J. Proteomics* **2010**. https://doi.org/10.1016/j.jprot.2010.02.010.

(141) Tholey, A.; Heinzle, E. Ionic (Liquid) Matrices for Matrix-Assisted Laser Desorption/Ionization Mass Spectrometry-Applications and Perspectives. In *Analytical and Bioanalytical Chemistry*; 2006. https://doi.org/10.1007/s00216-006-0600-5.

(142) Sekuła, J.; Nizioł, J.; Rode, W.; Ruman, T. Gold Nanoparticle-Enhanced Target (AuNPET) as Universal Solution for Laser Desorption/Ionization Mass Spectrometry Analysis and Imaging of Low Molecular Weight Compounds. *Anal. Chim. Acta* **2015**. https://doi.org/10.1016/j.aca.2015.01.046.

(143) Dufresne, M.; Masson, J. F.; Chaurand, P. Sodium-Doped Gold-Assisted Laser Desorption

Ionization for Enhanced Imaging Mass Spectrometry of Triacylglycerols from Thin Tissue Sections. *Anal. Chem.* **2016**. https://doi.org/10.1021/acs.analchem.6b01141.

(144) Dufresne, M.; Thomas, A.; Breault-Turcot, J.; Masson, J. F.; Chaurand, P. Silver-Assisted Laser Desorption Ionization for High Spatial Resolution Imaging Mass Spectrometry of Olefins from Thin Tissue Sections. *Anal. Chem.* **2013**. https://doi.org/10.1021/ac3037415.

(145) Ozawa, T.; Osaka, I.; Ihozaki, T.; Hamada, S.; Kuroda, Y.; Murakami, T.; Miyazato, A.; Kawasaki, H.; Arakawa, R. Simultaneous Detection of Phosphatidylcholines and Glycerolipids Using Matrix-Enhanced Surface-Assisted Laser Desorption/Ionization-Mass Spectrometry with Sputter-Deposited Platinum Film. *J. Mass Spectrom.* **2015**, *50* (11), 1264–1269. https://doi.org/10.1002/jms.3700.

(146) Basu, S. S.; McMinn, M. H.; Giménez-Cassina Lopéz, B.; Regan, M. S.; Randall, E. C.; Clark, A. R.; Cox, C. R.; Agar, N. Y. R. Metal Oxide Laser Ionization Mass Spectrometry Imaging (MOLI MSI) Using Cerium(IV) Oxide. *Anal. Chem.* **2019**. https://doi.org/10.1021/acs.analchem.9b00894.

(147) Xu, S.; Li, Y.; Zou, H.; Qiu, J.; Guo, Z.; Guo, B. Carbon Nanotubes as Assisted Matrix for Laser Desorption/Ionization Time-of-Flight Mass Spectrometry. *Anal. Chem.* **2003**. https://doi.org/10.1021/ac0345695.

(148) Baker, S. N.; Baker, G. A. Luminescent Carbon Nanodots: Emergent Nanolights. *Angewandte Chemie - International Edition*. 2010. https://doi.org/10.1002/anie.200906623.

(149) Kim, Y. K.; Min, D. H. Mechanistic Study of Laser Desorption/Ionization of Small Molecules on Graphene Oxide Multilayer Films. *Langmuir* **2014**, *30* (42), 12675–12683. https://doi.org/10.1021/la5027653.

(150) Vinaixa, M.; Rodriguez, M. A.; Samino, S.; Díaz, M.; Beltran, A.; Mallol, R.; Bladé, C.; Ibañez, L.; Correig, X.; Yanes, O. Metabolomics Reveals Reduction of Metabolic Oxidation in Women with Polycystic Ovary Syndrome after Pioglitazone-Flutamide-Metformin Polytherapy. *PLoS One* **2011**. https://doi.org/10.1371/journal.pone.0029052.

(151) Verwaest, K. A.; Vu, T. N.; Laukens, K.; Clemens, L. E.; Nguyen, H. P.; Van Gasse, B.; Martins, J. C.; Van Der Linden, A.; Dommisse, R. 1H NMR Based Metabolomics of CSF and Blood Serum: A Metabolic Profile for a Transgenic Rat Model of Huntington Disease. *Biochim. Biophys. Acta - Mol. Basis Dis.* **2011**. https://doi.org/10.1016/j.bbadis.2011.08.001.

(152) Beckonert, O.; Coen, M.; Keun, H. C.; Wang, Y.; Ebbels, T. M. D.; Holmes, E.; Lindon, J. C.; Nicholson, J. K. High-Resolution Magic-Angle-Spinning NMR Spectroscopy for Metabolic Profiling of Intact Tissues. *Nat. Protoc.* **2010**. https://doi.org/10.1038/nprot.2010.45.

(153) Beltran, A.; Suarez, M.; Rodríguez, M. A.; Vinaixa, M.; Samino, S.; Arola, L.; Correig, X.; Yanes, O. Assessment of Compatibility between Extraction Methods for NMR- and LC/MS-Based Metabolomics. *Anal. Chem.* **2012**. https://doi.org/10.1021/ac3005567.

(154) Chiaia-Hernandez, A. C.; Schymanski, E. L.; Kumar, P.; Singer, H. P.; Hollender, J. Suspect and Nontarget Screening Approaches to Identify Organic Contaminant Records in Lake Sediments. *Anal. Bioanal. Chem.* **2014**, 7323–7335. https://doi.org/10.1007/s00216-014-8166-0.

(155) Nguyen, D. T. T.; Guillarme, D.; Rudaz, S.; Veuthey, J. L. Fast Analysis in Liquid Chromatography Using Small Particle Size and High Pressure. *Journal of Separation*

Science. 2006. https://doi.org/10.1002/jssc.200600189.

(156) Churchwell, M. I.; Twaddle, N. C.; Meeker, L. R.; Doerge, D. R. Improving LC-MS Sensitivity through Increases in Chromatographic Performance: Comparisons of UPLC-ES/MS/MS to HPLC-ES/MS/MS. *J. Chromatogr. B Anal. Technol. Biomed. Life Sci.* **2005**. https://doi.org/10.1016/j.jchromb.2005.05.037.

(157) Fukuhara, K.; Ohno, A.; Ota, Y.; Senoo, Y.; Maekawa, K.; Okuda, H.; Kurihara, M.; Okuno, A.; Niida, S.; Saito, Y.; Takikawa, O. NMR-Based Metabolomics of Urine in a Mouse Model of Alzheimer's Disease: Identification of Oxidative Stress Biomarkers. *J. Clin. Biochem. Nutr.* **2013**. https://doi.org/10.3164/jcbn.12-118.

(158) Giraudeau, P. NMR-Based Metabolomics and Fluxomics: Developments and Future Prospects. *Analyst* **2020**, *145* (7), 2457–2472. https://doi.org/10.1039/d0an00142b.

(159) Lindon, J. C.; Nicholson, J. K.; Holmes, E.; Everett, J. R. Metabonomics: Metabolic Processes Studied by NMR Spectroscopy of Biofluids. *Concepts Magn. Reson.* **2000**. https://doi.org/10.1002/1099-0534(2000)12:5<289::AID-CMR3>3.0.CO;2-W.

(160) Emwas, A. H.; Saccenti, E.; Gao, X.; McKay, R. T.; dos Santos, V. A. P. M.; Roy, R.; Wishart, D. S. Recommended Strategies for Spectral Processing and Post-Processing of 1D 1 H-NMR Data of Biofluids with a Particular Focus on Urine. *Metabolomics* **2018**, *14* (3). https://doi.org/10.1007/s11306-018-1321-4.

(161) Ernst, R. R.; Bodenhausen, G.; Wokaun, A.; Redfield, A. G. Principles of Nuclear Magnetic Resonance in One and Two Dimensions . *Phys. Today* **1989**. https://doi.org/10.1063/1.2811094.

(162) Dettmer, K.; Aronov, P. A.; Hammock, B. D. Mass Spectrometry-Based Metabolomics. *Mass Spectrometry Reviews*. 2007. https://doi.org/10.1002/mas.20108.

(163) Bevilacqua, M.; Bro, R.; Marini, F.; Rinnan, Å.; Rasmussen, M. A.; Skov, T. Recent Chemometrics Advances for Foodomics. *TrAC - Trends in Analytical Chemistry*. 2017. https://doi.org/10.1016/j.trac.2017.08.011.

(164) Hollender, J.; Schymanski, E. L.; Singer, H. P.; Ferguson, P. L. Nontarget Screening with High Resolution Mass Spectrometry in the Environment: Ready to Go? *Environ. Sci. Technol.* **2017**, *51* (20), 11505–11512. https://doi.org/10.1021/acs.est.7b02184.

(165) Martens, L.; Chambers, M.; Sturm, M.; Kessner, D.; Levander, F.; Shofstahl, J.; Tang, W. H.; Römpp, A.; Neumann, S.; Pizarro, A. D.; Montecchi-Palazzi, L.; Tasman, N.; Coleman, M.; Reisinger, F.; Souda, P.; Hermjakob, H.; Binz, P. A.; Deutschh, E. W. MzML - A Community Standard for Mass Spectrometry Data. *Molecular and Cellular Proteomics*. 2011. https://doi.org/10.1074/mcp.R110.000133.

(166) Chambers, M. C.; MacLean, B.; Burke, R.; Amodei, D.; Ruderman, D. L.; Neumann, S.; Gatto, L.; Fischer, B.; Pratt, B.; Egertson, J.; Hoff, K.; Kessner, D.; Tasman, N.; Shulman, N.; Frewen, B.; Baker, T. A.; Brusniak, M. Y.; Paulse, C.; Creasy, D.; Flashner, L.; Kani, K.; Moulding, C.; Seymour, S. L.; Nuwaysir, L. M.; Lefebvre, B.; Kuhlmann, F.; Roark, J.; Rainer, P.; Detlev, S.; Hemenway, T.; Huhmer, A.; Langridge, J.; Connolly, B.; Chadick, T.; Holly, K.; Eckels, J.; Deutsch, E. W.; Moritz, R. L.; Katz, J. E.; Agus, D. B.; MacCoss, M.; Tabb, D. L.; Mallick, P. A Cross-Platform Toolkit for Mass Spectrometry and Proteomics. *Nature Biotechnology*. 2012. https://doi.org/10.1038/nbt.2377.

(167) Smith, C. A.; Want, E. J.; O'Maille, G.; Abagyan, R.; Siuzdak, G. XCMS: Processing Mass Spectrometry Data for Metabolite Profiling Using Nonlinear Peak Alignment, Matching, and Identification. *Anal. Chem.* **2006**. https://doi.org/10.1021/ac051437y.

(168) Tautenhahn, R.; Bottcher, C.; Neumann, S. Highly Sensitive Feature Detection for High Resolution LC/MS. *BMC Bioinformatics* **2008**. https://doi.org/10.1186/1471-2105-9-504.

(169) Riedl, J.; Esslinger, S.; Fauhl-Hassek, C. Review of Validation and Reporting of Non-Targeted Fingerprinting Approaches for Food Authentication. *Analytica Chimica Acta*. 2015. https://doi.org/10.1016/j.aca.2015.06.003.

(170) Cavanna, D.; Righetti, L.; Elliott, C.; Suman, M. The Scientific Challenges in Moving from Targeted to Non-Targeted Mass Spectrometric Methods for Food Fraud Analysis: A Proposed Validation Workflow to Bring about a Harmonized Approach. *Trends Food Sci. Technol.* **2018**, *80* (August), 223–241. https://doi.org/10.1016/j.tifs.2018.08.007.

(171) ChemSpider. *Choice Rev. Online* **2008**. https://doi.org/10.5860/choice.46-1485.

(172) Williams, A. J.; Grulke, C. M.; Edwards, J.; McEachran, A. D.; Mansouri, K.; Baker, N. C.; Patlewicz, G.; Shah, I.; Wambaugh, J. F.; Judson, R. S.; Richard, A. M. The CompTox Chemistry Dashboard: A Community Data Resource for Environmental Chemistry. *J. Cheminform.* **2017**. https://doi.org/10.1186/s13321-017-0247-6.

(173) Dulio, V.; Slobodnik, J. NORMAN-Network of Reference Laboratories, Research Centres and Related Organisations for Monitoring of Emerging Substances. *Environ. Sci. Pollut. Res.* **2009**. https://doi.org/10.1007/s11356-009-0129-1.

(174) Smith, C. A.; O'Maille, G.; Want, E. J.; Qin, C.; Trauger, S. A.; Brandon, T. R.; Custodio, D. E.; Abagyan, R.; Siuzdak, G. METLIN: A Metabolite Mass Spectral Database. In *Therapeutic Drug Monitoring*; 2005. https://doi.org/10.1097/01.ftd.0000179845.53213.39.

(175) Wishart, D. S.; Feunang, Y. D.; Marcu, A.; Guo, A. C.; Liang, K.; Vázquez-Fresno, R.; Sajed, T.; Johnson, D.; Li, C.; Karu, N.; Sayeeda, Z.; Lo, E.; Assempour, N.; Berjanskii, M.; Singhal, S.; Arndt, D.; Liang, Y.; Badran, H.; Grant, J.; Serra-Cayuela, A.; Liu, Y.; Mandal, R.; Neveu, V.; Pon, A.; Knox, C.; Wilson, M.; Manach, C.; Scalbert, A. HMDB 4.0: The Human Metabolome Database for 2018. *Nucleic Acids Res.* **2018**. https://doi.org/10.1093/nar/gkx1089.

(176) Sumner, L. W.; Amberg, A.; Barrett, D.; Beale, M. H.; Beger, R.; Daykin, C. A.; Fan, T. W. M.; Fiehn, O.; Goodacre, R.; Griffin, J. L.; Hankemeier, T.; Hardy, N.; Harnly, J.; Higashi, R.; Kopka, J.; Lane, A. N.; Lindon, J. C.; Marriott, P.; Nicholls, A. W.; Reily, M. D.; Thaden, J. J.; Viant, M. R. Proposed Minimum Reporting Standards for Chemical Analysis: Chemical Analysis Working Group (CAWG) Metabolomics Standards Initiative (MSI). *Metabolomics* **2007**. https://doi.org/10.1007/s11306-007-0082-2.

(177) Buchberger, A. R.; DeLaney, K.; Johnson, J.; Li, L. Mass Spectrometry Imaging: A Review of Emerging Advancements and Future Insights. *Anal. Chem.* **2018**, *90* (1), 240–265. https://doi.org/10.1021/acs.analchem.7b04733.

(178) Deininger, S. O.; Cornett, D. S.; Paape, R.; Becker, M.; Pineau, C.; Rauser, S.; Walch, A.; Wolski, E. Normalization in MALDI-TOF Imaging Datasets of Proteins: Practical Considerations. *Anal. Bioanal. Chem.* **2011**. https://doi.org/10.1007/s00216-011-4929-z.

(179) Fonville, J. M.; Carter, C.; Cloarec, O.; Nicholson, J. K.; Lindon, J. C.; Bunch, J.; Holmes, E. Robust Data Processing and Normalization Strategy for MALDI Mass Spectrometric Imaging. *Anal. Chem.* **2012**. https://doi.org/10.1021/ac201767g.

(180) Deininger, S. O.; Ebert, M. P.; Fütterer, A.; Gerhard, M.; Röcken, C. MALDI Imaging Combined with Hierarchical Clustering as a New Tool for the Interpretation of Complex Human Cancers. *J. Proteome Res.* **2008**. https://doi.org/10.1021/pr8005777.

(181) Race, A. M.; Palmer, A. D.; Dexter, A.; Steven, R. T.; Styles, I. B.; Bunch, J. SpectralAnalysis: Software for the Masses. *Anal. Chem.* **2016**. https://doi.org/10.1021/acs.analchem.6b01643.

(182) Robichaud, G.; Garrard, K. P.; Barry, J. A.; Muddiman, D. C. MSiReader: An Open-Source Interface to View and Analyze High Resolving Power MS Imaging Files on Matlab Platform. *J. Am. Soc. Mass Spectrom.* **2013**. https://doi.org/10.1007/s13361-013-0607-z.

(183) Ràfols, P.; Torres, S.; Ramírez, N.; Del Castillo, E.; Yanes, O.; Brezmes, J.; Correig, X. RMSI: An R Package for MS Imaging Data Handling and Visualization. *Bioinformatics* **2017**, *33* (15), 2427–2428. https://doi.org/10.1093/bioinformatics/btx182.

(184) Källback, P.; Nilsson, A.; Shariatgorji, M.; Andrén, P. E. MsIQuant - Quantitation Software for Mass Spectrometry Imaging Enabling Fast Access, Visualization, and Analysis of Large Data Sets. *Anal. Chem.* **2016**. https://doi.org/10.1021/acs.analchem.5b04603.

(185) Alexandrov, T. Metaspace.

(186) Brennan, L. NMR-Based Metabolomics: From Sample Preparation to Applications in Nutrition Research. *Prog. Nucl. Magn. Reson. Spectrosc.* **2014**, *83*, 42–49. https://doi.org/10.1016/j.pnmrs.2014.09.001.

(187) Mercier, P.; Lewis, M. J.; Chang, D.; Baker, D.; Wishart, D. S. Towards Automatic Metabolomic Profiling of High-Resolution One-Dimensional Proton NMR Spectra. *J. Biomol. NMR* **2011**. https://doi.org/10.1007/s10858-011-9480-x.

(188) Czaplicki, J.; Ponthus, C. A Specialized Database Manager for Interpretation of NMR Spectra of Synthetic Glucides: JPD. *J. Chim. Phys. Physico-Chimie Biol.* **1998**. https://doi.org/10.1051/jcp:1998124.

(189) Hao, J.; Liebeke, M.; Astle, W.; De Iorio, M.; Bundy, J. G.; Ebbels, T. M. D. Bayesian Deconvolution and Quantification of Metabolites in Complex 1D NMR Spectra Using BATMAN. *Nat. Protoc.* **2014**. https://doi.org/10.1038/nprot.2014.090.

(190) Ravanbakhsh, S.; Liu, P.; Bjordahl, T. C.; Mandal, R.; Grant, J. R.; Wilson, M.; Eisner, R.; Sinelnikov, I.; Hu, X.; Luchinat, C.; Greiner, R.; Wishart, D. S. Accurate, Fully-Automated NMR Spectral Profiling for Metabolomics. *PLoS One* **2015**. https://doi.org/10.1371/journal.pone.0124219.

(191) Gómez, J.; Brezmes, J.; Mallol, R.; Rodríguez, M. A.; Vinaixa, M.; Salek, R. M.; Correig, X.; Cañellas, N. Dolphin: A Tool for Automatic Targeted Metabolite Profiling Using 1D and 2D 1 H-NMR Data. *Anal. Bioanal. Chem.* **2014**. https://doi.org/10.1007/s00216-014-8225-6.

(192) Barton, R. H.; Nicholson, J. K.; Elliott, P.; Holmes, E. High-Throughput 1H NMR-Based Metabolic Analysis of Human Serum and Urine for Large-Scale Epidemiological Studies: Validation Study. *Int. J. Epidemiol.* **2008**. https://doi.org/10.1093/ije/dym284.

(193) Beckonert, O.; Keun, H. C.; Ebbels, T. M. D.; Bundy, J.; Holmes, E.; Lindon, J. C.; Nicholson, J. K. Metabolic Profiling, Metabolomic and Metabonomic Procedures for NMR Spectroscopy of Urine, Plasma, Serum and Tissue Extracts. *Nat. Protoc.* **2007**. https://doi.org/10.1038/nprot.2007.376.

(194) Chagoyen, M.; Pazos, F. Tools for the Functional Interpretation Ofmetabolomic Experiments. *Brief. Bioinform.* **2013**. https://doi.org/10.1093/bib/bbs055.

(195) Kanehisa, M.; Goto, S. KEGG: Kyoto Encyclopedia of Genes and Genomes. *Nucleic Acids*

Research. 2000. https://doi.org/10.1093/nar/28.1.27.

(196) Shannon, P.; Markiel, A.; Ozier, O.; Baliga, N. S.; Wang, J. T.; Ramage, D.; Amin, N.; Schwikowski, B.; Ideker, T. Cytoscape: A Software Environment for Integrated Models of Biomolecular Interaction Networks. *Genome Res.* **2003**. https://doi.org/10.1101/gr.1239303.

(197) Sidiropoulos, K.; Viteri, G.; Sevilla, C.; Jupe, S.; Webber, M.; Orlic-Milacic, M.; Jassal, B.; May, B.; Shamovsky, V.; Duenas, C.; Rothfels, K.; Matthews, L.; Song, H.; Stein, L.; Haw, R.; D'Eustachio, P.; Ping, P.; Hermjakob, H.; Fabregat, A. Reactome Enhanced Pathway Visualization. *Bioinformatics* **2017**. https://doi.org/10.1093/bioinformatics/btx441.

(198) Xia, J.; Wishart, D. S. MSEA: A Web-Based Tool to Identify Biologically Meaningful Patterns in Quantitative Metabolomic Data. *Nucleic Acids Res.* **2010**. https://doi.org/10.1093/nar/gkq329.

(199) López-Ibáñez, J.; Pazos, F.; Chagoyen, M. MBROLE 2.0-Functional Enrichment of Chemical Compounds. *Nucleic Acids Res.* **2016**. https://doi.org/10.1093/nar/gkw253.

(200) Kamburov, A.; Cavill, R.; Ebbels, T. M. D.; Herwig, R.; Keun, H. C. Integrated Pathway-Level Analysis of Transcriptomics and Metabolomics Data with IMPaLA. *Bioinformatics* **2011**. https://doi.org/10.1093/bioinformatics/btr499.

(201) Kankainen, M.; Gopalacharyulu, P.; Holm, L.; Orešič, M. MPEA-Metabolite Pathway Enrichment Analysis. *Bioinformatics* **2011**. https://doi.org/10.1093/bioinformatics/btr278.

(202) Pang, Z.; Chong, J.; Li, S.; Xia, J. Metaboanalystr 3.0: Toward an Optimized Workflow for Global Metabolomics. *Metabolites* **2020**. https://doi.org/10.3390/metabo10050186.

2. Biomarkers of Exposure to Secondhand and Thirdhand Tobacco Smoke: Recent Advances and Future Perspectives

UNIVERSITAT ROVIRA I VIRGILI
ADVANCES ON THIRDHAND SMOKE USING TARGETED AND UNTARGETED APPROACHES
Sònia Torres Gené

2.1 Abstract

Smoking is the leading preventable disease worldwide and passive smoking is estimated to be the cause of about 1.0% of worldwide mortality. The determination of tobacco smoke biomarkers in human biological matrices is key to assess the health effects related to the exposure to environmental tobacco smoke. The biomonitoring of cotinine, the main nicotine metabolite, in human biofluids—including urine, serum or saliva—has been extensively used to assess this exposure. However, the simultaneous determination of cotinine together with other tobacco biomarkers and the selection of alternative biological matrices, such as hair, skin or exhaled breath, would enable a better characterization of the kind and extent of tobacco exposure. This review aims to perform a critical analysis of the up-to-date literature focused on the simultaneous determination of multiple tobacco smoke biomarkers studied in different biological matrices, due to the exposure to secondhand smoke (SHS) and thirdhand smoke (THS). Target biomarkers included both tobacco-specific biomarkers—nicotine and tobacco specific nitrosamine biomarkers—and tobacco-related biomarkers, such as those from polycyclic aromatic hydrocarbons, volatile organic compounds, metals and carbon monoxide. To conclude, we discuss the suitability of determining multiple biomarkers through several relevant examples of SHS and THS exposure.

2.2 Introduction

Passive smoking is estimated to be the cause of about 1.0% of worldwide mortality, responsible for approximately 603,000 deaths each year among children and adults, a number which has been increasing over the years [1].

Environmental tobacco smoke (ETS), most commonly called secondhand smoke (SHS), is a complex and reactive mixture made up of the mainstream smoke exhaled by the smokers and sidestream smoke emitted from the burning tobacco diluted with ambient air. This mixture contains over 4700 chemicals including hazardous amines, carbonyls, hydrocarbons or metals among others [2–4]. SHS exposure can cause several illnesses in nonsmokers including ischaemic heart diseases in adults and lower respiratory infections and asthma in adults and children, among other adverse health effects [1]. Moreover, the International Agency for Research on Cancer (IARC) classifies 63 chemicals reported in mainstream tobacco smoke as carcinogenic, 11 of them are known as human carcinogens with a proven role on the development of different types of cancer including lung and bladder cancer [2].

Nevertheless, SHS is not the only source of exposure for nonsmokers to tobacco smoke components. Most of the smoke gases and particles of SHS deposit, age and remain for long periods of time in fabrics, surfaces and dust forming the so-called thirdhand smoke (THS), a less studied source of exposure to tobacco smoke toxicants [5,6]. THS components not only remain on surfaces and in settled dust, they can also be re-emitted into the gas phase or even react with oxidants and other atmospheric compounds to yield secondary contaminants, some of them with increased toxicity. This is the case of nicotine, which deposits almost entirely on indoor surfaces, where it can react with ozone, nitrous acid and other atmospheric oxidants producing carcinogenic tobacco-specific nitrosamines (TSNAs) [7]. To date, dozens of toxicants have been identified in THS including tobacco specific toxicants—such as nicotine, and TSNAs—as well as tobacco related toxicants including volatile N-nitrosamines, aromatic amides, polycyclic aromatic hydrocarbons (PAHs) and volatile carbonyls [8–12]. Exposure to THS causes numerous alterations in organ and cellular

systems of mouse models, including lung and liver damage, several metabolic effects and signs of hyperactivity [13–15]. THS extracts also inhibit cell proliferation and cause DNA strand breaks and oxidative damage in DNA and mitochondria [16]. Pathways of exposure to THS are mainly non-dietary ingestion and dermal absorption, although inhalation of resuspended particles may also occur. Consequently, THS could be one of the major pathways of children exposure to tobacco smoke toxicants. Despite these emerging evidences on THS toxicity and carcinogenicity, this way of exposure to tobacco smoke contaminants is still unrecognized by most of the population and it has been omitted in public health and environmental policies.

The determination of biomarkers of tobacco chemicals is key to assess the health effects related to SHS and THS exposure. The biomonitoring of cotinine, the main nicotine biomarker, in urine, blood and saliva has been the preferred option to assess the kind, extent and frequency of tobacco smoke exposure. However, SHS and THS exposure results in the uptake of complex mixtures of toxicants, therefore, a wide range of tobacco specific and related biomarkers could be assessed. Tobacco exposure biomarker concentrations can vary depending on which source of exposure, SHS or THS, is predominant. Many other factors can induce variation, such as the life-stage of the target population or their race, among others that will be discussed below. Therefore, the simultaneous study of multiple tobacco smoke biomarkers and the analysis of different biological matrices would provide a wider assessment of the extent of tobacco smoke exposure that may help to better understand its implications in human health.

Hence, this review aims to provide a critical overview on the assessment of exposure to tobacco smoke in nonsmokers, including both SHS and THS exposures, through the determination of cotinine, as the most renowned

tobacco-specific biomarker, together with other specific and related tobacco biomarkers. In recent years, an acceptable number of studies have focused on this multiple approach to assess both SHS and THS exposure. In 2013, a former publication reviewed the use of tobacco-specific biomarkers to study SHS exposure [17]. In the present paper we aimed to establish for the first time a joint discussion on the convenience of this multiple biomarkers approach to assess both, SHS and THS exposures, through the review of the most up-to-date bibliography in this respect. To that end, this report includes those studies published from 2012 to March 2018 that focus on tobacco smoke biomarkers from conventional tobacco smoke and waterpipe smoke. Here, different aspects are covered, from the advantages and disadvantages of the different biological matrices, to a general introduction about the biomarkers studied in this period of time, metabolism, general toxicity of their precursors and main ranges of concentrations. To conclude, we discuss the suitability of the determination of multiple biomarkers for assessing the kind and extent of SHS and THS exposure through several relevant examples of applications.

2.3 Selection of Papers

For the purpose of this review, we have selected original research publications published from 2012 to March 2018 with content based on the exposure to SHS and THS from tobacco combustion, in order to cover the recent trends in this topic. Reviews and articles exclusively based on the analysis of previous survey data were excluded and also those from e-cigarettes. Various searches were combined to identify relevant literature in the Web of Science (using the Web of Science® Core Collection WoS, Thomson Reuters; http://webofscience.com) using the keyword “cotinine” AND multiple

combinations of the following keywords: “environmental”, “secondhand” OR “second-hand”, “thirdhand” OR “third-hand”, “tobacco”, “smoke” and “cigarette”. The papers obtained in this search were then individually revised to meet the inclusion criteria. To be included in this review, articles had to: (A) Provide original data from observational or experimental studies in human nonsmokers exposed to SHS and/or THS; (B) provide levels of other tobacco smoke biomarkers besides cotinine, including either specific and non-specific biomarkers of SHS and THS exposure. A further revision of the preselected papers was performed to assess the quality of the studies, excluding those based on isolated observations, and those not addressing quality parameters of the reported concentrations.

Table S1 in the Supplementary Information summarizes the 44 papers included in this review, as well as their most relevant information, including the number and main characteristics of the target population, the biological matrices analyzed, the determined biomarkers and the ranges of the reported concentrations in nonsmokers exposed to SHS and/or THS. To complete the discussion, biomarker concentrations of smokers have been included, when available.

2.4 Biological Matrices

Biological matrix selection is one of the key points for a rigorous characterization of the kind and extent of the exposure. The selected matrix or matrices will depend on the aim and nature of the study, the life stage of the target population, the type of exposure and also the availability of robust analytical methods that allow a reliable determination of the biomarkers of interest in a concrete matrix. Commonly, the reasonable choice is to analyze the

least-invasive matrix in which the target biomarkers are more easily determined with the available analytical methods and to choose a matrix that will provide a broader assessment of the exposure. In the papers reviewed here, urine, saliva and blood have been the preferred matrices for SHS and THS human biomonitoring, but there is an increasing interest in alternative matrices, such as hair, skin and, to a lesser extent, exhaled breath.

Urine has been the most widely used biological matrix to asses tobacco smoke exposure, since it is a non-invasive biofluid which can be easily obtained. Besides, it accumulates higher concentrations of some biomarkers in comparison with other biofluids, making urine the most sensitive matrix for the assessment of both SHS and THS exposure. The main disadvantages are that renal diseases or the use of certain prescription drugs may interfere with the clearance of urinary biomarkers and that urine dilution adjustments, such as creatinine or specific gravity adjustments, are needed prior to biomarker concentration comparison across samples [17]. Most of the urinary biomarkers are also excreted as glucuronide conjugates. The deglucuronization to the original form prior to the analysis would depend on the application and aim of the study. As an example, the concentration of free urinary cotinine correlates better with serum cotinine than with total cotinine concentration (including both free cotinine and cotinine glucuronide measured after deglucuronization) [18], whilst the evaluation of total 4-(methylnitrosamino)-1-(3-pyridyl)-1-butanol (NNAL) concentration in low SHS and THS exposures is preferred because NNAL glucuronide is excreted in higher concentrations (by a factor of about two, ethnicity dependent) than urinary free NNAL [19].

Blood does not require dilution adjustments, but its collection is more invasive and tobacco biomarkers are less concentrated than in urine (i.e., cotinine concentrations in serum are about four-fold to six-fold lower than in

urine) making blood less suitable for the assessment of THS exposure and low and intermittent SHS exposure [17]. Blood biomonitoring can be performed in different formats: Whereas plasma and serum are the most commonly used formats, whole blood is appropriate for the evaluation of metals because they are distributed between non-cellular and intra-cellular compartments [20]. Furthermore, dried blood spots (DBS) and cord blood are becoming popular for the screening of early-life exposure to tobacco smoke toxicants [21,22].

Saliva is a valuable alternative matrix to determine SHS and THS biomarkers, as it is non-invasive and easy to obtain. For smokers and nonsmokers recently exposed, salivary cotinine values correlate well with blood cotinine and, therefore, saliva collection is a feasible alternative when collecting blood samples is not a viable option, or when multiple measurements are required in a limited period of time [17].

Hair is the most likely used matrix to determine long-term SHS and THS exposure. Compared to other biological matrices, it is less affected by daily exposure and metabolism variability than other biological matrices allowing a more robust comparison [23]. The main advantages of hair are that it is a non-invasive matrix, easy to collect and can be stored at room temperature up to five years [24]. There seems to be a significant role played by hair melanin with basic and less polar compounds being selectively enriched, which embeds them in hair as it grows [25].

Although the major intake of tobacco smoke toxicants is through the inhalation of SHS, the biomonitoring of toxicants accumulated in the skin is especially relevant in the case of THS exposure where nonsmokers are exposed to smoke toxicants bound to fabrics, clothing, settle dust and surfaces. Even

though the skin performs an effective barrier function [26], nicotine can be dermally absorbed and transported to the dermal blood supply [27].

Finally, exhaled breath condensate is a biological matrix of increased interest in epidemiology because it provides an immediate, non-invasive method of assessing smoking status. In the context of tobacco smoke exposure, the determination of CO in exhaled breath could be used as a short-term SHS biomarker, though, other sources of pollution including exhaust gases may cause elevations in the fractional concentrations of CO in expired air [28].

In Figure 1, the summary of the reviewed biological matrices analyzed in the papers and the tobacco smoke biomarkers determined in each matrix are shown.

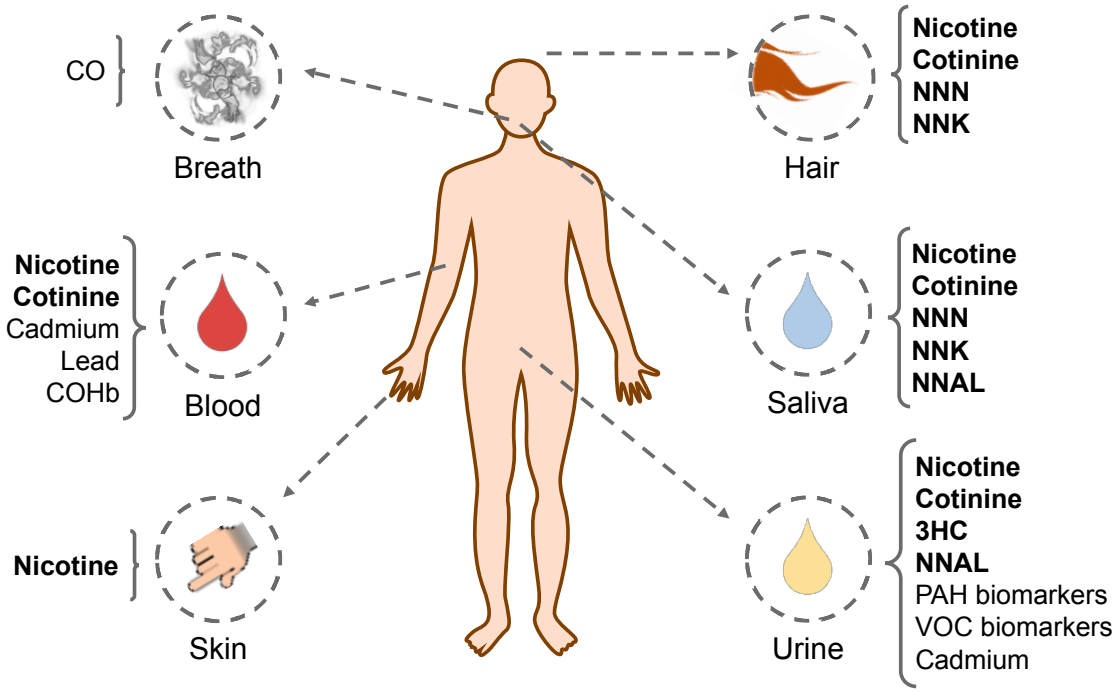

Figure 1. Summary of the biological matrices studied in this review and the tobacco smoke biomarkers determined in each matrix. Tobacco specific biomarkers are indicated in bold. CO: carbon monoxide; NNN: N'-nitrosonornicotine; NNK: 4-(methylnitrosoamino)-1-(3-pyridyl)-1-butanone; COHb: Carboxyhemoglobin; 3HC: trans-3'-hydroxycotinine; NNAL: 4-(methylnitrosamino)-1-(3-pyridyl)-1-butanol; PAH: polycyclic aromatic hydrocarbon; VOC: volatile organic compounds.

2.5 Tobacco-Specific Biomarkers

Tobacco-specific biomarkers are those derived from chemicals exclusively from tobacco smoke: Nicotine and tobacco specific nitrosamines. This section describes the specific tobacco smoke biomarkers that have been determined in the research papers reviewed here, their mechanism of formation, as well as the toxicity of their precursors, with the aim of highlighting their toxicological relevance. Table 1 shows the biomarkers reviewed here, their half-life times and also the main toxicological information of the biomarker precursors, including the either carcinogenic and non-carcinogenic data. Table 2 summarizes the most common ranges of concentrations of the studied biomarkers in each biological matrix in accordance with the reviewed references. These concentrations have been classified regarding the type of tobacco smoke exposure: Smokers, SHS exposure and THS exposure. The column “No exposure”, includes the biomarkers found in a non-exposed population. This table only includes those biomarkers with information in more than one type of tobacco exposure.

Table 1. Biomarkers of tobacco smoke exposure studied in the reviewed papers, their half-life time, precursor toxicant and main toxicological characteristics including: The International Agency for Research on Cancer (IARC) classification; cancer inhalation unit risk, expressed in (µg/m3)−1; inhalation and oral cancer slope factors, in (mg/kg-day)−1; non-cancer chronic inhalation reference exposure level (REL), in µg/m3; and other relevant toxicological information. Risk values are from the Office of Environmental Health Hazard Assessment at the California Environmental Protection Agency (OEHHA-CalEPA) Chemical Database [29]. Different sources of information are indicated.

Biomarker	Half-Life Time ($t_{1/2}$) [a]	Toxicant Precursor	IARC Classification [b]	Cancer		Non-Cancer	Other
				Inhalation Unit Risk	Slope Factor	Chronic Inhalation REL	
Tobacco smoke specific biomarkers							
Nicotine	Blood ($t_{1/2}$): 2 h Urine ($t_{1/2}$): 11 h	Nicotine	NA	NA	NA	NA	Reproductive toxicity
Cotinine	Saliva ($t_{1/2}$): 15 h Blood ($t_{1/2}$): 16 h Urine ($t_{1/2}$): 3–4 days						
trans-3′-hydroxycotinine (3HC)	Blood ($t_{1/2}$): 6.6 h Urine ($t_{1/2}$): 6.4 h						
N′-nitrosonornicotine (NNN)	NA	NNN	1	4.0×10^{-4}	1.4	NA	NSRL: 0.5 µg/day
4-(methylnitrosoamino)-1-(3-pyridyl)-1-butanone (NNK)	Urine ($t_{1/2}$): 2.6 h	NNK	1	5.2×10^{-3} [c]	49 (oral)	NA	NSRL: 0.014 µg/day
4-(methylnitrosoamino)-1-(3-pyridyl)-1-butanol (NNAL)	Urine ($t_{1/2}$): 40–45 days						
Tobacco smoke related biomarkers							
Polycyclic aromatic hydrocarbon biomarkers							
1-hydroxy naphthalene (1-OHNap)	NA	Naphthalene	2B	3.4×10^{-5}	0.12	9	NSRL: 5.8 µg/day
2-hydroxy naphthalene (2-OHNap)	Urine ($t_{1/2}$): 9.4 h						
2-hydroxy fluorene (2-OHFlu)	Urine ($t_{1/2}$): 4.1 h	Fluorene	3	NA	NA	NA	NA
3-hydroxy fluorene (3-OHFlu)	NA						
9-hydroxy fluorene (9-OHFlu)	NA						
1-hydroxy phenanthrene (1-OHPA)	NA	Phenanthrene	3	NA	NA	NA	NA
2-hydroxy phenanthrene (2-OHPA)	NA						
3-hydroxy phenanthrene (3-OHPA)	NA						
1-hydroxy-pyrene (1-OHPyr)	Urine ($t_{1/2}$): 6 h	Pyrene	3	NA	NA	NA	NA
1-hydroxy-pyrene glucuronide (1-OHPyrG)	NA						
Volatile organic compounds biomarkers							
Benzene	NA	Benzene	1	2.9×10^{-5}	0.1	3	Reproductive toxicity NSRL: 13 (inhalation) 6.4 (oral) µg/day

N-acetyl-S-(3-hydroxypropyl-1-methyl)-L-cysteine (HPMM)	Urine ($t_{1/2}$): 5–9 h	Crotonaldehyde	3	NA	1.9 (oral) [d]	NA	NA
3-hydroxypropyl mercapturic acid (HPMA)	Urine ($t_{1/2}$): 5–9 h	Acrolein	3	NA	NA	0.35	NA
Metals							
Cadmium	Blood and urine ($t_{1/2}$): 1–2 decades	Cadmium	1	4.2×10^{-3}	15	0.02	Reproductive toxicity NSRL (inhalation): 0.05 µg/day
Lead	Blood ($t_{1/2}$): 36 days	Lead	2B	1.2×10^{-5}	0.042 (inhalation) 8.5×10^{-3} (oral)	NA	Reproductive toxicity NSRL (oral): 15 µg/day
Other							
Carbon monoxide (CO) Carboxyhemoglobin (COHb)	Exhaled ($t_{1/2}$): 2–6 h Blood ($t_{1/2}$): 4–6 h	CO	NA	NA	NA	23,000 (acute REL)	Reproductive toxicity

[a]Half-life time references of each metabolite are described in Sections 4 and 5. [b] IARC classification: 1—carcinogenic to humans—; 2B—possibly carcinogenic to humans—; 3—not classifiable as to its carcinogenicity to humans [30]. [c] Information from Naufal et al. [31]. [d] Data from the Risk Assessment Information System (RAIS) [32]. Glossary*:* NSRL (No significant risk level): Daily intake level posing a 10^{-5} lifetime risk of cancer [29]; Chronic Inhalation non-cancer REL (Reference exposure level): Concentration level at or below which no adverse health effects are anticipated for a specified exposure duration [33]; Cancer slope factor: Toxicity value for evaluating the probability of an individual developing cancer from exposure to contaminant levels over a lifetime [32]; Unit risk (UR): Estimation of the increased cancer risk from the exposure to a concentration of 1 µg/m^3 for a lifetime [34]. NA: Not available.

Table 2. Summary of the most common concentration ranges of the studied biomarkers in nonsmokers, accordingly with the reviewed references. Concentration ranges have been classified regarding the type of tobacco smoke exposure of the target population: "Smokers" for the smoker population and "SHS exposure", "THS exposure" or "No exposure", for non-exposed population.

Biomarker	Matrix	Smokers	SHS Exposure	THS Exposure	No Exposure	References
Nicotine	Hair	2.01–79.30 ng/mg (min–max)	0.08–5.02 ng/mg (IQR)	NA	NA	[23,35–40]
	Skin	44–1160 ng/wipe (min–max)	25.6 (13.2–48.9) ng/wipe (GM (95% CI))	2.9 (<LOD–46.1) ng/wipe (GM (95% CI)	2.5 (<LOD–17.7) ng/wipe (GM (min–max))	[41–43]
Cotinine	Urine	34.5–489.15 ng/mL (GM range)	0.25–30 ng/mL (min–cutoff point)	0.05–5 ng/mL (Cutoff range)	0.88 ng/mL (max value)	[22,36,41–50]
	Serum/Plasma	>10–499 ng/mL (cutoff–max)	0.015–14.6 ng/mL (Cutoff range)	NA	<LOD (<0.05) ng/mL	[49,51–58]
	Saliva	>13–653 ng/mL (cutoff–IQR)	0.04–14.9 ng/mL (min–max)	NA	NA	[36,38–40,59–63]
	Hair (min–max)	0.08–2.49 ng/mg	0.05–1.57 ng/mg	NA	NA	[23,35,64]
3HC	Urine (Mean (SD))	653.81 (62.30) µg/g cr	60.79 (46.70) µg/g cr	NA	NA	[65]
NNN	Saliva (Mean (IQR))	118 (3.9–91) pg/mL	5.3 (1.2–2.9) pg/mL [a]	NA	NA	[60]
NNK	Saliva (Mean (IQR))	6.6 (2.8–7.1) pg/mL	4.5 (2.4–5.2) pg/mL [a]	NA	NA	[60]
NNAL	Urine	80.9–405.5 pg/mL (Median range)	Low: 0.95–2.21 pg/mL (GM Range) High: 5.9–20.1 pg/mL (*CI*)	2.7–6.7 pg/mL (GM range)	0.86 pg/mg cr (CI)	[36,42–44,48,50,51,54,58,61,66]
	Saliva (Mean (IQR))	3.2 (0.98–3.5) pg/mL	1.3 (0.83–1.8) pg/mL [a]	NA	NA	[60]
1-OHNap, 2-OHNap	Urine	NA	4587.6–6045.6 ng/L [b]	NA	4466.1 ng/L (GM)	[57]
2-OHFLu, 3-OHFlu, 9-OHFlu	Urine	NA	571.0–824.8 ng/L [b]	NA	439.9 ng/L (GM)	[57]
1-OHPA, 2-OHPA, 3-OHPA	Urine	NA	288.1–351.2 ng/L [b]	NA	241.2 ng/L (GM)	[57]
1-OHPyr	Urine	NA	118.1–165.1 ng/L [b]	NA	95.7 ng/L (GM)	[57]
Benzene	Urine (Median ± IQR)	NA	596 ± 548 ng/L	Low: 282 ± 131 ng/L High: 314.5 ± 177 ng/L	92.5 ± 90 ng/L	[67]
HPMM	Urine (Median (IQR))	1.63 (0.680–3.29) mg/g cr	NA	NA	0.313 (0.231–0.451) mg/g	[55]
HMPA	Urine (IQR)	1203–4898 pmol/mg cr	1580–3964 pmol/mg cr	NA	NA	[68]
Cadmium	Urine (CI)	NA	0.11–0.29 µg/L	NA	0.097–0.12 µg/L	[46]
	Whole blood [c]	NA	1.07 µg/L	NA	1.02 µg/L	[69]
CO	Exhaled breath	>6–22.81 ppm (cutoff–mean)	1.9–5.9 ppm (min–max)	NA	NA	[47,59]
COHb	Plasma (Mean (SD))	17.57% (8.79)	1.2% (0.8)	NA	NA	[70]

a: Tobacco smoke exposure not specified; b: GM range between low and high SHS exposure; c: Age adjusted blood cadmium level. CI: Confidence interval; GM: Geometric mean; IQR: Interquartile range; LOD: Limit of detection; SD: Standard deviation. NA: Not available.

3HC: *trans*-3'-hydroxycotinine; NNN: N' -nitrosonornicotine; NNK: 4-(methylnitrosoamino)-1-(3-pyridyl)-1-butanone; NNAL: 4-(methylnitrosoamino)-1-(3-pyridyl)-1-butanol; 1-OHNap: 1-hydroxy naphthalene; 2-OHNap: 2-hydroxy naphthalene; 2-OHFLu: 2-hydroxy fluorene; 3-OHFlu: 3-hydroxy fluorene; 9-OHFlu: 9-hydroxy fluorene; 1-OHPA: 1-hydroxy phenanthrene; 2-OHPA: 2-hydroxy phenanthrene; 3-OHPA: 3-hydroxy phenanthrene; 1-OHPyr: 1-hydroxy-pyrene; HPMM: N-acetyl-S-(3-hydroxypropyl-1-methyl)-L-cysteine; HMPA: 3-hydroxypropyl mercapturic acid; CO: carbon monoxide; COHb: carboxyhemoglobin.

2.5.1 Nicotine

Nicotine is the main alkaloid found in tobacco leaves and an exclusive marker of tobacco smoke exposure. During smoking, nicotine is emitted in both gas and particulate phases and rapidly absorbed into the bloodstream. It is then distributed along body tissues and organs, such as the liver which metabolizes nicotine into other compounds. Although nicotine is not considered to be a carcinogen by the International Agency for Research on Cancer (IARC), it can participate in carcinogenesis through inhibition of apoptosis and cell proliferation [71]. Moreover, nicotine is involved in tobacco addiction, promotion of inflammation, adverse effects in the vascular system, reproductive toxicity and alterations in fetus brain development [24,72].

Few studies have focused on the determination of nicotine in human biofluids, mainly because of the low nicotine half-life times (t1/2) (11 h and 2 h in urine and blood, respectively) [73]. However, nicotine is a useful biomarker for long-term tobacco smoke exposure in hair, where it remains unmetabolized and, consequently, as hair grows over the months, tobacco exposure is “recorded” over long periods of time [74]. As shown in Table 2, nicotine in hair can be found in 10 to 100 times higher concentrations than cotinine typically ranging from 2.01 to 79.3 ng/mg in smokers [35] and from 0.08 to 5.02 ng/mg [23,35–40] in a SHS-exposed population. Hair nicotine concentrations also highly correlated with airborne nicotine and cotinine in urine, thus confirming its suitability as an alternative tobacco smoke exposure biomarker. Furthermore, since nicotine in hair is less affected by daily variability, possible cutoff values have been proposed to distinguish active smokers from SHS-exposed nonsmokers, such as 5.68 ng/mg (sensitivity, 94.2%; specificity, 87.0%) [64].

Besides, the determination of nicotine in skin, especially in hands and fingers, could be also an excellent indicator of the kind and extent of tobacco smoke exposure. Skin nicotine concentrations reached values up to 1160 ng/wipe in smokers [41] and up to 48.9, 46.1 and 17.7 ng/wipe in nonsmokers exposed to SHS, THS and non-exposed, respectively [42,43]. Similarly to hair, the accumulation of nicotine in the hands of nonsmokers also correlated with airborne nicotine and urinary cotinine, making skin nicotine a feasible biomarker to monitor low SHS and THS exposure.

2.5.2 Nicotine Metabolites

Nicotine metabolism, summarized in Figure 2A, depends on several factors including ethnicity, gender, age, genetics, pregnancy or several diseases, such as liver or kidney disease [24]. Around 70% to 80% of nicotine is transformed into its main metabolite, cotinine, by two enzymatic reactions [75] carried out by cytochrome P450 2A6 (CYP2A6) in combination with a cytoplasmic aldehyde oxidase [76,77]. The higher persistence of cotinine (t1/2 of 15 h in saliva, 16 h in blood and 3–4 days in urine, shown in Table 1), together with the wide range of available analytical methods, makes it the most widely used biomarker to assess tobacco smoke exposure [75,78]. However, it is estimated that only around 10% to 15% of cotinine is found in smokers' urine because most of cotinine is converted into other metabolites [75], mainly trans-3'-hydroxycotinine (3HC), also through a CYP2A6 mediated reaction [79]. The occurrence of 3HC in urine is 33% to 40% and the average half-life of 3HC is similar in both plasma and urine (an average of 6.6 h and 6.4 h, respectively) [80]. Nicotine and its metabolites could also be transformed into N-quaternary glucuronides by the uridine diphosphate-glucuronosyltransferase (UGT). These glucuronides are present in

urine with occurrences of 3% to 5%, 12% to 17% and 7% to 9% for nicotine, cotinine and 3HC glucuronides, respectively [73], but may be partially hydrolyzed after sample collection [81]. Hence, the enzymatic hydrolyzation of the glucuronides conjugates is the common procedure prior to the samples analysis.

Cotinine concentrations have been mainly monitored in biofluids. Urine, blood and saliva cotinine concentrations have been used to both establish cutoff values to distinguish active smokers from nonsmokers and characterize the type and extent of the exposure. The typical urinary cotinine cutoff value is 30 ng/mL. Urinary cotinine concentrations usually range from 34.5 to 489 ng/mL for smokers [46,47], from 0.25 to 30 ng/mL for SHS exposed nonsmokers [22,36,42,45,46,48–50], up to 5 ng/mL for THS exposed nonsmokers [41,43,44] and around 0.88 ng/mL in non-exposed nonsmokers [43]. Nevertheless, acute exposure to SHS can raise urinary cotinine concentrations to levels similar to those reported in smokers' concentrations. This is for instance the case of nonsmoker workers of bars and restaurants without smoking bans that presented mean urinary cotinine concentrations in the range of 35.9 to 61.2 ng/mL [44,47].

In serum and plasma, cotinine cutoff values are typically 10 or 15 ng/mL [51,53–55,57,58]. Common cotinine levels ranged from 0.015 to 14.6 ng/mL for SHS exposed nonsmokers [49,53–58], whereas cotinine levels in smokers can be more than one order of magnitude higher [51–55,57,58]. Non-exposed nonsmokers did not present quantifiable cotinine values. The incidence of several illnesses may affect serum cotinine levels of nonsmokers. For instance, nonsmoker adults with self-reported asthma from the 2007–2008 US National Health and Nutrition Examination Survey (NHANES) presented serum cotinine concentrations reaching up to 57 ng/mL [51].

Salivary cotinine is an alternative to blood worth considering: Concentration in saliva is usually between 15% and 40% higher than in blood because cotinine molecules are small, relatively water soluble and present minimal protein binding in the blood [82]. The interpretation of saliva cotinine can be limited by variability across individuals caused by the effect of age, gender, race, oral pH, type of diet, dehydration or drug treatment [17]. The usual salivary cotinine cutoff value was 13 ng/mL to distinguish between active smokers from nonsmokers, whilst 10 ng/mL was useful to distinguish low and high SHS exposure [39]. More recently, Lam et al. examined the associations between measured SHS exposure and mental health. Salivary cotinine levels were used to categorize the studied population into different groups according to the level of exposure: Low SHS exposure (0.1–0.3 ng/mL), moderate SHS exposure (0.4–0.7 ng/mL) and high SHS (0.8–14.9 ng/mL) [59]. As shown in Table 2, salivary cotinine concentration ranged between 0.04 and 14.9 ng/mL in nonsmokers exposed to SHS [36,38–40,59,61–63], and reached up to 653 ng/mL in active smokers [38,39,59,60]. Salivary cotinine concentrations increase even after a short time of SHS exposure, thus demonstrating the suitability of salivary cotinine as a short-term SHS exposure biomarker [61].

3HC urinary concentration values are usually three-to four-fold higher than those found for urinary cotinine and, therefore, the determination of urinary 3HC would provide a more sensitive measurement of tobacco smoke exposure [73,83]. Nevertheless, the study of 3HC is mainly used in smoker cohorts and only one of the studies that met our selection criteria have focused on the determination of this biomarker in nonsmokers. Mean 3HC concentrations were ca. 10 fold-higher in smokers than in SHS exposed nonsmokers (654 vs. 60.8 µg per g of creatinine (µg/g cr), respectively) [65].

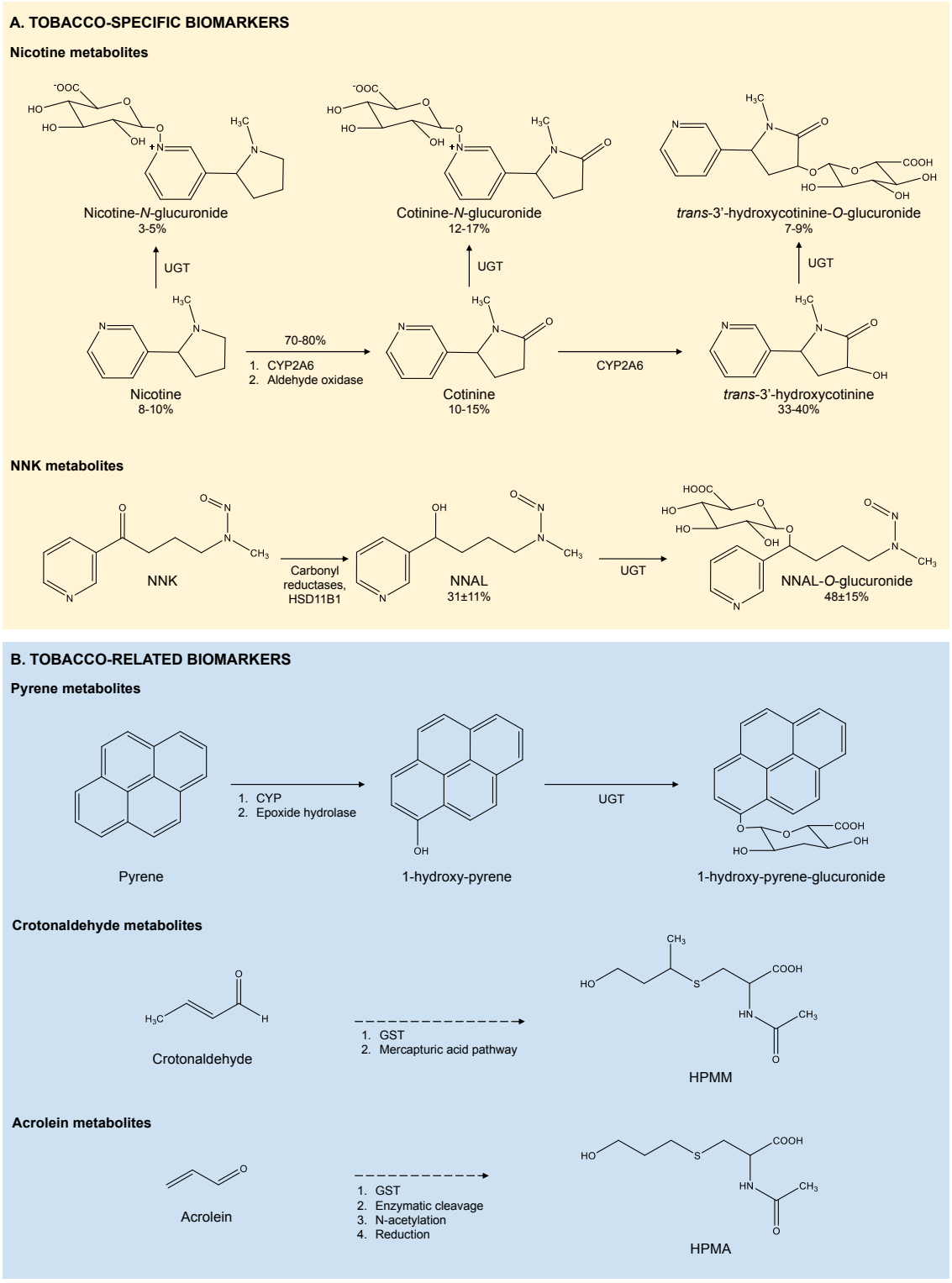

Figure 2. (A) Mechanisms of formation of the tobacco smoke specific biomarkers studied in this review, including the main ranges of transformation, expressed in percentage (%) [24,84]. (B) Mechanisms of formation of some tobacco smoke-related biomarkers reviewed here [85–87].

2.5.3 Tobacco Specific Nitrosamines

During tobacco curing and burning, nicotine reacts to form tobacco-specific nitrosamines (TSNAs), a leading class of carcinogens in tobacco products. TSNAs can also be formed by the oxidation of residual nicotine deposited in dust particles and surfaces through the reaction with ozone, nitrous acid and other atmospheric oxidants [7]. Therefore, the determination of TSNAs biomarkers is especially relevant to evaluate THS exposure. As shown in Table 1, N'-nitrosonornicotine (NNN) and 4-(methylnitrosoamino)-1-(3-pyridyl)-1-butanone (NNK) are considered carcinogenic for humans (Group 1) by the IARC [88] with an inhalation unit risk of 4.0 × 10−4 (μg/m3)−1 and 5.2 × 10−3 (μg/m3)−1, respectively. Carcinogenesis of NNN and NNK comes through their metabolic activation mainly conducted by cytochrome P450, generating reactive species that form adducts with DNA [89]. Studies performed in small rodents showed that NNK induced tumors in the lungs, nasal cavities, trachea and liver, while NNN produced tumors in esophagus as well as in lungs, nasal cavities and trachea [90,91]. After absorption, carbonyl reductases and 11β-hydroxysteroid dehydrogenase type 1 (HSD11B1) rapidly convert NNK to its main metabolite 4-(methylnitrosamino)-1-(3-pyridyl)-1-butanol (NNAL), shown in Figure 2A, which is considered to have similar adverse health effects as its precursor [92]. Urinary levels of total NNAL and total NNN have been linked with lung and esophageal cancer risk, respectively [93,94]. NNAL can be transformed to NNAL-glucuronide by UGT enzymes prior to body detoxification [84], mainly into NNAL-O-glucuronide in urine [95]. The higher occurrence of NNAL in urine (i.e., urinary NNAL levels are about 30-fold higher than urinary NNN levels) and its higher half-life time (40–45 days against 2.6 h for NNAL and NNK, respectively, shown in Table 1), makes urinary NNAL a good biomarker of long-term and intermittent exposure to tobacco smoke [84,88]. Besides, as SHS ages, nicotine levels rapidly

decline but NNK levels increase confirming the suitability of urinary NNAL as a more reliable biomarker of THS exposure than nicotine metabolites. Mean urinary NNAL concentrations were 80.9–405.5 pg/mL in active smokers [50,51,58], 5.9–20.1 pg/mL for high SHS exposure [44,48,58,66], 0.95–2.21 pg/mL for low SHS exposure [36,50,51,54,61], 2.7–6.7 pg/mL for THS exposure [42] and 0.81 pg/mL for no exposure [43]. Recently, Benowitz et al. estimated a urinary NNAL cutoff value to distinguish between active smokers and nonsmokers exposed to SHS. For a cotinine cutoff of 30 mg/L, the estimated NNAL was 14.4 pg/mL (10.2 pg/mg creatinine), with 94.6% sensitivity and 93.4% specificity [50].

Data from the 2011–2012 NHANES showed that urinary NNAL was over 20 times higher for nonsmokers exposed to SHS at home compared to those non-exposed. Moreover, irrespective of smoking status, non-Hispanic Asian American presented lower biomarkers concentrations compared to both non-Hispanic whites and non-Hispanic blacks thus corroborating differences in the elimination kinetics of nicotine/cotinine and NNAL [58]. Data from NHANES 2011–2012 was also used to assess NNK exposure by age group and ethnicity by measuring urinary NNAL in 4831 nonsmokers. Among all non-tobacco users, significantly higher geometric means and 95th percentiles of urinary total NNAL were observed among children aged 6 to 19 years old (2.43 (1.96–3.02) pg/mL) vs. adults aged >20 years (1.38 (1.21–1.57) pg/mL). Among these nonsmokers, non-Hispanic Blacks had higher urinary levels of NNAL (volume-base and creatinine corrected) than other ethnicity groups [54].

Nevertheless, non-metabolized TSNAs could be the preferable choice in other biological matrices. In this sense, a recent study performed by Perez-Ortuño et al. showed that NNK was the most concentrated TSNA in hair of nonsmokers exposed to SHS, with a mean concentration of 2.1 pg/mg,

correlating well with nicotine and cotinine. Consequently, NNK could be the most suitable hair biomarker of cumulative exposure to TSNAs [23]. Conversely, the same group of researchers found that NNN was the most prevalent TSNAs in nonsmokers' saliva samples, with a mean concentration of 5.3 pg/mL. The salivary NNN/cotinine ratio confirmed the relative NNN increase in SHS exposure. Considering that NNN is associated with esophageal and oral cavity cancers, the authors proposed the monitoring of salivary NNN to assess the cancer risk associated with exposure to tobacco smoke.

2.6 Tobacco-Related Biomarkers

SHS and THS exposure results in the uptake of a wide range of toxicants apart from those specific to tobacco smoke. These tobacco-related toxicants may come from other sources of exposure besides tobacco smoke. However, their high toxicity makes them worthy of study in different tobacco smoke exposure scenarios in combination with cotinine and other tobacco-specific biomarkers, thus providing a broader perception of the health harms derived from tobacco smoke exposure. The non-specific biomarkers analyzed in the papers reviewed here included polycyclic aromatic hydrocarbons, several kinds of volatile organic compounds, metals and carbon monoxide.

2.6.1 Policiclic Aromatic Hydrocarbons

Although polycyclic aromatic hydrocarbons (PAHs) are not tobacco smoke-specific markers, they are present in higher concentrations in smoking environments [96]. PAHs are metabolized in the liver by cytochrome P450

generating reactive epoxy intermediates which are converted to its non-reactive hydroxylated forms by epoxide hydrolase. Figure 2B shows the pyrene metabolism as an example of PAH metabolism. To perform body detoxification, PAH intermediaries are conjugated with glucuronide acid or glutathione by UGTs or glutathione S-transferases (GSTs), respectively, and excreted [85,97,98]. As shown in Table 1, half-life time of some common PAH biomarkers vary from 4.1 to 9.4 h [99]. The main health effects of PAHs have been related with immunotoxicity, genotoxicity, cytotoxicity, mutagenicity and carcinogenicity in humans [100]. Short-term exposure to PAHs may also result in several non-carcinogenic effects, such as eye and skin irritation, nausea, vomiting and inflammation. Long-term exposure to PAHs has been related with cataracts, kidney and liver damage, break-down of red blood cells and several types of cancer, such as skin, lung, bladder and gastrointestinal cancer [101]. As an example of the occurrence of PAH biomarkers in relation with tobacco smoke exposure, Kim et al. performed cross-sectional analyses of 1985 children aged 6 to 18 years using data from the 2003–2008 US NHANES survey. SHS exposure, measured as serum cotinine, was strongly associated with urinary concentrations of nine PAH biomarkers, with concentrations in SHS exposed nonsmokers ranging from 118 ng/mL for 1-OHPyr and up to 6046 ng/mL for naphthalene metabolites. PAH biomarkers of non-exposed children were generally lower, as seen in Table 2 [57].

2.6.2 Volatile Organic Compounds (VOCs)

Tobacco smoke also contains a wide range of VOCs, including several carbonyl compounds, such as crotonaldehyde and acrolein, and aromatic compounds like benzene, among others [2]. Exposure to these VOCs is associated

with many adverse health effects including irritations, tissue damage, DNA-adducts formation, mutagenicity and even strong carcinogenic effects in the case of benzene [102–104]. Following exposure, body detoxification from crotonaldehyde and acrolein mostly begins with the conjugation of glutathione by GSTs in the liver and ends with the production of their main metabolites N-acetyl-S-(3-hydroxypropyl-1-methyl)-L-cysteine (HPMM) and 3-hydroxypropyl mercapturic acid (HPMA), respectively, which are excreted through urine, as shown in Figure 2B [86,87]. Urinary half-life of HPMM and HPMA is 5–9 h [105]. Waterpipe smoke exposure is a source of acrolein. In waterpipe venues urinary 3-HPMA and cotinine were positively correlated among smokers and nonsmokers with values up to 3686 pmoL/mg cr in daily waterpipe smokers and 2498 pmoL/mg cr in nonsmokers attending a waterpipe social event [68].

Bagchi et al. examined the influence of tobacco exposure and crotonaldehyde in 4692 participants of the 2005–2006 and 2011–2012 NHANES surveys, with mean (IQR) values of 1.63 (068–3.29) in smokers and 0.313 (0.231–0.451) in nonsmokers. Urinary HPMM levels were positively associated with serum cotinine and even though demographic variables, such as age, gender and race, showed distinct effects on crotonaldehyde exposure, authors concluded that tobacco smoke is a major source of crotonaldehyde exposure [55].

An average of 17% of the inhaled benzene is exhaled and the remaining part is metabolized and excreted through urine as unmodified benzene and as other metabolites such as S-phenyl-mercapturic acid (SPMA) or trans,trans-muconic acid (ttMA) [103,106]. The association between urinary benzene and SHS exposure was measured by Protano et al. in 122 children from an Italian rural area [67]. Benzene median concentrations and IQR for children with smoking parents were 359.5 ± 362 ng/L, whereas non-exposed children's were 92.5 ± 90 ng/L. For children with smoking parents who did not smoke inside the homes,

benzene concentrations were 282 ± 131 ng/L and 314.5 ± 177 ng/L for children whose parents smoked inside the house when children were out, thus indicating the relevance of THS exposure in children. If parents smoked inside when children were in, children's benzene concentrations were 596 ± 548 ng/L. Urinary cotinine concentrations varied similarly. In a latter study, urinary cotinine was positively correlated with urinary benzene ($r = 0.164$, $p < 0.05$) and its metabolite SPMA ($r = 0.190$, $p < 0.01$) in morning urine samples [107]. Although benzene may occur from different emission sources, the relationship of benzene with SHS and THS was proved in the studied children.

2.6.3 Metals

A numerous amount of toxic metals, such as cadmium and lead, are transferred to tobacco smoke during cigarette burning and absorbed by humans through inhalation. Tobacco smoke is considered to be one of the main source of cadmium and lead intake by humans [108,109]. After absorption, cadmium and lead are transported through the blood to several tissues, such as lungs, kidneys or bones, where they can be accumulated [110,111]. These toxicants are mainly eliminated through urine but their clearance is quite slow (i.e., 0.001% per day of Cd) [108]. As shown in Table 1, half-life time of lead in blood averages 36 days while half-life time of cadmium in urine and blood can be up to one or two decades [110,112]. Both cadmium and lead can produce tubular dysfunction and renal failure in the kidney [113], hence lead is classified as a possible human carcinogen and cadmium as carcinogenic to humans [30].

The presence of heavy metals in combination with cotinine has been assessed in sensible populations. For instance, Polanska et al. reported a mean

lead concentration of 1.1 µg/dL with a range from 0.4 to 5.7 µg/dL in cord blood of SHS-exposed newborn babies. Prenatal lead exposure together with a long-term exposure to SHS resulted in a negative effect on the development of motor abilities for children tested in 2-year-olds [22]. In pregnant women at delivery time, Jedrychowski et al. found a low lead concentration of 1.63 µg/dL in whole blood, which might be associated with hypertension during pregnancy. Nevertheless, the occurrence of lead was not clearly correlated with cotinine levels [56]. However, there were small but significant correlations between cotinine and lead in newborns and children DBS [52,114].

The role of SHS exposure in urinary cadmium levels was also not conclusive. As an example, similar cadmium concentrations were found in children exposed and non-exposed to SHS, without clear correlations with urinary cotinine [46,115]. Conversely, Sánchez-Rodríguez et al. found that urinary cadmium levels slightly decreased in 83 adults after the implementation of a restrictive anti-smoking legislation, ranging from 0.17 (0.11–0.29) µg/g cr before the smoking ban to 0.10 (0.06–0.22) µg/g cr one year after the law implementation. The reduction of urinary cotinine was lower than urinary Cd, thus the authors concluded that further monitoring is necessary as Cd variations could be also due to atmospheric Cd exposure and may be influenced by differences in body mass indexes [116]. Nevertheless, a possible correlation of whole blood cadmium concentrations with SHS exposure was studied in 1398 adults participating in the 2007–2012 Korean National Health and Nutrition Examination Survey (KNHANES) that self-reported SHS exposure. Age adjusted blood cadmium levels in adults were higher in nonsmokers exposed to SHS than in non-exposed ones (1.07 µg/L vs. 1.02 µg/L). In addition, blood cadmium levels of both adults and adolescents correlated positively with levels of urinary cotinine [69].

2.6.4 Carbon Monoxide

SHS is considered an important source of exposure to CO in nonsmokers [117]. CO levels in mainstream smoke average 5 to 22 mg/cigarette (approximately 4.5% of tobacco smoke [118]) and are on the level of 9 to 35 mg/cigarette for sidestream smoke [119]. Once released in the atmosphere, CO rapidly diffuses into the body through alveolar, capillary and placental membranes during inhalation. Since CO has 200 to 250 times more affinity to haemoglobin than oxygen, 80% to 90% of CO successfully binds to haemoglobin, forming its main blood metabolite, carboxyhaemoglobin (COHb). As shown in Table 1, half-life time of exhaled CO and blood COHb average 2–6 h and 4–6 h, respectively and therefore they can be used as short-term SHS exposure biomarkers [24]. Cigarette consumption and high concentrations of exhaled CO could be related to low birth weight [120]. However, further research is needed to determine the toxicological importance of CO in SHS exposure. As seen in Table 2, CO concentration ranges between 1.9 and 5.9 ppm in nonsmokers exposed to SHS, whereas in smokers commonly range from 6 ppm (common cutoff value) to 22.81 ppm [47,59]. Exhaled carbon monoxide (CO) from workers who are exposed to SHS in public venues could be measured to investigate indoor air quality [121]. Whole blood COHb correlates with the smoking status, with mean concentrations of 17.57% in smokers and 1.2% in nonsmokers exposed to SHS [70]. Among nonsmokers, 30 min of exposure to waterpipe smoke increased the COHb levels, which correlated with serum cotinine, corroborating the relevance of CO emissions, even in short-time SHS exposure.

2.7 Determination of Multiple Specific Biomarkers. Examples of Applicaitons

In the previous sections we have already commented the suitability of each studied biomarker and their association with cotinine concentrations and the type of tobacco smoke exposure. The aim of this section is to comment some selected examples to further discuss the usefulness of the simultaneous determination of multiple biomarkers for the characterization of either SHS or THS exposure.

2.7.1 Evaluation of SHS Exposure

The intrinsic characteristics of the studied populations have a key role not only in the selection of the biological matrix, but also in the election of biomarkers. For instance, the determination of nicotine in biofluids does not provide very valuable information, the simultaneous analysis of urinary nicotine and cotinine can be suitable in individuals with a decreased ability to metabolize nicotine due to a reduced CYP2A6 activity. In this sense, Matsumoto et al. studied the total nicotine and cotinine urinary concentrations of 117 Japanese nonsmokers, concluding that 54% of these nonsmokers presented higher nicotine concentrations than those found for cotinine [45] and, therefore, the simultaneous determination of both biomarkers provided a better characterization of SHS exposure for that population group.

Although the study of cotinine and 3HC has been extensively used in cohorts of smokers, the simultaneous determination of urinary NNAL and urinary or serum cotinine is usually the preferred approach for characterizing long term

SHS. As TSNAs are formed while SHS ages, urinary NNAL/cotinine ratio is 10 times higher in SHS exposure compared to active smoking, without gender, race/ethnicity or age differences [50], and it is estimated to be even higher in young children exposed to THS. Therefore this ratio could be used as a biomarker to distinguish between SHS and THS exposure [6]. The NNAL/cotinine ratio was also higher among pregnant women who did not smoke (0.0076) in comparison to those who smoke (0.0013) [48]. Nevertheless, Benowitz et al. recently suggested that by comparing sensitivity and specificity, the single determination of NNAL has a better performance than the NNAL/cotinine ratio in discriminating smokers from nonsmokers [50].

Since urinary cotinine and NNAL have different metabolic clearances, the joint study of both biomarkers could be useful to evaluate changes in SHS exposure. For instance, the role of SHS exposure in cars was evaluated by exposing eight nonsmoker volunteers to SHS for one hour (3 cigarettes). After this exposure, urinary cotinine increased 6-fold whilst the increase of NNAL was ca. 27-fold in comparison with baseline biomarker levels. In the same study plasma nicotine did not change after SHS exposure [49]. In another example, the application of the smoking ban reduced urinary cotinine and NNAL from mean values of 35.9 ng/mL and 18.2 pg/mL, respectively, to values below the detection limit (<5 ng/mL) for cotinine and 7.3 pg/mL for NNAL, two months after implementing the law [44]. Urinary cotinine and NNAL concentrations also correlate with airborne particulate matter (PM2.5) [37,122,123].

Finally, another example of the determination of multiple tobacco smoke biomarkers is the evaluation of SHS exposure in waterpipe venues, which exposure to smoke toxicants may differ from conventional cigarette smoke exposure. For instance, Moon et al. recently investigated the possible correlations of four tobacco specific biomarkers (urinary and salivary cotinine,

urinary NNAL and hair cotinine) with two related biomarkers (urinary 1-OHPyrG and CO in breath). In nonsmoking employees, they found moderate correlations among the tobacco-specific biomarkers, urinary cotinine and 1-OHPG. However, in this study CO concentrations were not associated with any of the tobacco-specific biomarkers studied (salivary cotinine, hair nicotine, urinary NNAL, and exhaled CO) which could be due to the short half-life of CO or the sampling process when business activity was low [36].

2.7.2 Evaluation of THS Exposure

When designing studies to evaluate THS exposure, it is necessary to take into consideration three main characteristics that make THS different from SHS exposure [6]. The first one is that the concentration of TSNAs increases as SHS ages, therefore, the TSNAs/cotinine ratio in nonsmokers exposed to THS is usually higher than in non-exposed ones. The second consideration is that 4-(methylnitrosamino)-4-(3-pyridyl)butanal (NNA) is a TSNA that is specific to THS, and the evaluation of its possible main metabolites—4-(methylnitrosamino)-4-(3-pyridyl)-1-butanol (iso-NNAL) and 4-(methylnitrosamino)-4-(3-pyridyl)butyric acid (iso-NNAC)—would enable the distinction between SHS and THS exposure. However, to date, there is a lack of biomonitoring studies of these specific NNA biomarkers. The third consideration is that unlike SHS, the main pathways of exposure to THS are nondietary ingestion and dermal absorption. Dermal absorption is usually overlooked as a possible pathway of exposure, but it is especially relevant in the case of THS contamination where nonsmokers are exposed to smoke toxicants bound to fabrics, clothing, settle dust and surfaces. Different studies demonstrated that nicotine has a large dermal permeability coefficient (kp_g—from air through skin to blood—4.4 m/h) [27], that dermal

uptake of nicotine can occur directly from air, which is comparable to the estimated inhalation uptake of nicotine [124] and lastly, that a substantial fraction of tobacco smoke exposure is through dermal absorption [125].

The accumulation of nicotine in the hands of nonsmokers has been proved in several studies. Different research groups of the University of California in San Diego leaded by Matt el al., have measured finger nicotine as a biomarker of THS exposure [42,43]. The main aim of these studies was to examine whether THS persists during long periods of time in different indoor environments. For instance, finger nicotine concentrations of nonsmokers who stayed overnight in guest rooms were up to 17.7 ng/wipe in hotels with complete smoking bans, up to 226.9 ng/wipe in non-smoking rooms in hotels without complete smoking bans and up to 1713.5 ng/wipe in smoking rooms, correlating with the nicotine found on guestroom surfaces and urinary cotinine. Urinary cotinine GM levels were five to six times higher for volunteers staying in smoking rooms. Mean cotinine levels were similar between those volunteers staying in non-smoking rooms of smoke-free and smoking hotels, suggesting that the single study of cotinine did not provide an accurate measure of THS exposure. NNAL was measured only in guests staying in the most polluted smoking rooms. For these guests NNAL's GM increased from 0.86 pg/mg cr to 1.24 pg/mg cr after staying overnight [43].

In a study published in 2017, homes of former smokers were examined until 6 months after quitting [42]. In the first week after quitting, they observed a significant reduction of nicotine in fingers of non-smoking residents (from 29.1 to 9.1 ng/wipe) without any significant changes thereafter, matching with nicotine levels in surfaces. These findings indicated that surfaces may be the main source of finger nicotine and also that homes of smokers remained polluted with THS for up to 6 months after cessation. Levels of cotinine declined from the

first week after quitting, decreasing from a baseline GM concentration of 9.9 to 1.5 ng/mL 1 month after quitting, and remaining stable after that time point. However, NNK exposure declined more gradually since it was not until 3 months after quitting that NNAL levels decreased significantly (11.0 pg/mL at basal level to 3.2 pg/mL 3 months post quitting). After this initial decline, both urinary cotinine and NNAL levels remained stable and above levels found in nonsmokers without exposure to SHS or THS. Authors concluded that smoking cessation did not immediately and completely eliminate exposure risk since homes of smokers remained polluted with nicotine and TSNAs in dust and on surfaces, and residents continued to be exposed for at least 6 months after smoking cessation.

Recently, the relationship between tobacco smoke exposure and hand nicotine was studied in 25 children with potentially tobacco related illnesses [63]. All children had detectable hand nicotine in the range of 18.3 to 690.94 ng/wipe (GM 86.4 ng/wipe) confirming the relevance of THS exposure in young children. Furthermore, hand nicotine levels presented a significant positive association with salivary cotinine, therefore, hand wipes could be useful as a proxy for exposure and to determine overall tobacco smoke pollution. These findings corroborated that tobacco exposure is produced via multiple pathways and, therefore, a comprehensive assessment of tobacco exposure must include both SHS and THS.

Nicotine in fingers has also been used for the assessment of THS transportation, thus Northrup et al. evaluated THS exposure in infants of smoking mothers, admitted to the neonatal intensive care unit on their date of birth [41]. Nicotine in mother's fingers highly correlated with tobacco biomarkers in infant urine. Levels of urinary NNAL in the newborn were comparable to those levels found in nonsmokers exposed to SHS and to the urinary NNAL

concentrations in former smokers just 1 week after quitting [42], thus corroborating the role of THS transportation in tobacco smoke exposure.

Besides, four studies have focused on the suitability of urinary cotinine and NNAL to assess THS exposure. Urinary cotinine values for THS exposure ranged between 0.05 to 5 ng/mL for most of the studies [41,43,44] and were up to 6 ng/mL in one case [42]. These levels exceeded the range proposed by Benowitz et al. of 0.05–0.25 ng/mL for low-level SHS exposure or THS exposure [50]. These values also include cotinine levels of bar employees after a smoking ban implementation and hence, exposed to THS in an environment where smoking was previously permitted [44]. NNAL levels were between 2.7 and 6.7 pg/mL for nonsmokers exposed to THS at home [42] and were up to 7.3 for bar employees exposed to THS at work [123]. These levels have been exceeded in the case of infants admitted in intensive care unit who have smoking mothers (12.4 pg/mL) [41].

2.8 Conclusions

The determination of biomarkers of tobacco smoke exposure plays a key role in the characterization of the health effects related to this exposure. In this review we have discussed the suitability of the determination of multiple biomarkers to assess SHS and THS exposure. The selected biological matrices will determine the kind of information obtained in a concrete study. Urine was the most widely used biological matrix in the studies summarized here, suitable for the assessment of SHS and THS. Nevertheless, depending on the nature of the study, it can be useful to complement the information provided by the urinary biomarkers with the analysis of other biological matrices, such as blood. For short-term exposure, saliva and exhaled breath are commonly studied, whilst

hair enables the assessment of long-term exposure. Dermal absorption is usually overlooked as a pathway of exposure to tobacco toxicants, however, several studies have demonstrated the relevance of skin in the transport and accumulation of tobacco smoke toxicants. In the characterization of THS exposure, nicotine in hands and fingers correlated with urinary cotinine and NNAL.

The selection of the appropriate target biomarkers will depend on the available biological matrices (that influence on biomarker availability and half-life time), source of exposure (i.e., cigarettes or waterpipe), objectives of the study (i.e., short term, long-term or intermittent SHS exposure or THS exposure) and the characteristics of the target population (i.e., age, race, specific diseases, etc.). Cotinine is the gold standard biomarker of tobacco exposure. Nevertheless, an approach worthy of further investigation could be the simultaneous determination of urinary cotinine and NNAL that enables a better characterization of low SHS and THS exposure. Besides, NNK and NNN were the most concentrated TSNAs in saliva and hair, respectively, and the identification of these biomarkers in these biomatrices must be considered in future works. The assessment of non-specific biomarkers provided a broader knowledge about the health effects associated with tobacco smoke exposure. Nevertheless, exposure to these biomarkers can also occur from other sources and, therefore, their concentrations are not always clearly linked with tobacco exposure.

Finally, although few studies have focused on determining THS exposure, the data reviewed here confirms the risks of this poorly described tobacco smoke exposure pathway. Consequently, future research must include the assessment of both SHS and THS exposure, especially in the most vulnerable population to THS: Children.

2.9 Supplementary Information

Table S1. Summary of the results obtained in the papers included in this review. The data presented in this table corresponds to the biomarker concentrations from the nonsmokers studied that were exposed to sencondhand (SHS) or thirdhand smoke (THS), including the main characteristics of the target population, the analyzed biomatrix and the biomarker concentration, expressed as reported in the original paper. The smokers (S) concentrations are also summarized, if available.

Reference	Target population	Biological matrix	Biomarkers	Concentrations
[1]	Pregnant women: n= 431, age: 18-35 years Low SHS: Low exposure to $PM_{2.5}$ High SHS: High exposure to $PM_{2.5}$ (Poland)	Serum	Cotinine *Not specified*	*Low SHS:* 0.16 ng/mL *High SHS:* 0.33 ng/mL
		Whole blood	Lead *GM (95% CI)*	*SHS:* 1.63 (1.63-1.75) µg/dL
[2]	Children: n= 122, age: 5-11 years, male and female Exposure to SHS and THS at home Low THS: If the cohabitants smoke outside the house High THS: If the cohabitants smoke inside the house when children are out (Italy)	Urine	Cotinine *Median ± IQR*	*Low THS:* 3.04 ± 4.19 µg/g cr *High THS:* 3.61 ± 21.92 µg/g cr *SHS:* 5.95 ± 51.23 µg/g cr
			Benzene *Median ± IQR*	*Low THS:* 282 ± 131 ng/L *High THS:* 314.5 ± 177 ng/L *SHS:* 596 ± 548 ng/L
[3]	Adults: n= 27-23, age: 21-37 years, male and female 3 hours of controlled SHS exposure in a terrace of a bar or a restaurant (Rest.) (USA)	Urine	NNAL *GM (min-max)*	*Bar (SHS):* 0.109 (0-3.60) pg/mL *Rest. (SHS):* 0.008 (0-2.1) pg/mL
		Saliva	Cotinine *GM (min-max)*	*Bar (SHS):* 0.161 (0.094-0.407) ng/mL *Rest. (SHS):* 0.075 (0.036-0.188) ng/mL
[4]	Adults (A): Smokers n = 25, SHS exposed n = 19 Children (C) exposed to SHS: n = 18, age: ≤ 2years (Greece)	Hair	Cotinine *A: Mean (min-max)* *C: Min-max*	*A (S):* 1.16 (0.08-2.49) ng/mg *A (SHS):* 0.13 (0.05-0.32) ng/mg *C (SHS):* 0.13-1.57 ng/mg
			Nicotine *A: Mean (min-max)* *C: min-max*	*A (S):* 27.97 (2.01-79.30) ng/mg *A (SHS):* 1.49 (0.12-2.58) ng/mg *C (SHS):* 0.69-28.71 ng/mg
[5]	Bar employees: n= 40, age: 21-73 years, 70% female Exposure before smoking ban (Bef.) and after ban (Aft.) (USA)	Urine	Cotinine *Mean (SD)*	*Bef. (SHS):* 35.9 (17.4) ng/mL *Aft.:* Non-quantifiable (<5 ng/mL)
			NNAL *Mean (SD)*	*Bef. (SHS):* 0.087 (0.065) pmol/mL *Aft.:* 0.035 (0.033) pmol/mL
[6]	Bar and restaurant employees: Smokers n = 21, SHS exposed n = 17, age: <25-≥35 years, male and female. Before smoking ban (Bef.) and after ban (Aft.) (Ankara, Turkey)	Urine	Cotinine *Mean (SD)*	*Bef. (S):* 67.26 (0.86) ng/mL *Aft. (S):* 63.16 (10.81) ng/mL
				Bef. (SHS): 61.24 (4.66) ng/mL *Aft. :* 56.26 (7.66) ng/mL
		Breath	CO *Mean (SD)*	*Bef. (S):* 22.81 (12.23) ppm *Aft. (S):* 14.29 (7.41) ppm

				Bef. (SHS): 3.94 (5.26) ppm *Aft.:* 1.82 (1.98) ppm
[7]	Adults with self-reported asthma: Smokers and Nonsmokers with possible SHS exposure (NS) n = 456, age: 20->65 years, male and female. NHANES (USA)	Serum	Cotinine *Median (min-max)*	*S:* 265.5 (87-499) ng/mL
				NS: 0.048 (0.01-57) ng/mL
		Urine	NNAL *Median (min-max*)	*S:* 405.5 (49.6-1770) pg/mL
				NS: 0.55 (0.4-223) pg/mL
[8]	Children: n= 1541, age: 7-48 months, male and female. Assessment of SHS in DBS collected from children for lead screening. (USA)	Dried blood spots (DBS)	Cotinine *Median range*	*NS:* <0.3-5.06 ng/g
			Lead *Min-max*	*NS:* <1-9 µg/dL
[9]	Adults: Smokers n = 815-2146, SHS exposed n = 1651-1891 age: 18-99 years, male and female (UK)	Saliva	Cotinine *S: cutoff* *SHS: Min-max*	*S:* > 15 ng/mL
				SHS: 0.1-14.9 ng/mL
		Breath	CO *S: cutoff* *SHS: Min-max*	*S:* > 6 ppm
				SHS: 1.9-5.9 ppm
[10]	Preschool children: n= 329, age: 2-7 years, 45.9% female (China)	Urine	Cotinine *Mean (SD)*	*SHS:* 1.02 (0.56) log-transformed urinary cotinine-to-cr ratio
			Cadmium *Median (IQR)*	*SHS:* 0.28 (0.21-0.37) nmol/mmol Cd-to-cr
[11]	Adults (A): Smokers n = 83, SHS exposed n = 99, age: 18-80 years Children (C): 283, age: ≤4-10 years, male and female (USA) **Subjects with a mean plasma cotinine > 10 ng/mL (n=81).*	Dried blood spots (DBS) or plasma	Cotinine *A: min-max* *C: Median (min-max)*	*A (S):* 0.9-443 ng/mL *(plasma)*
				A (SHS): <0.02-56 ng/mL *(plasma)* *C (NS):* 0.42 (<0.3-55) ng/g *(DBS)*
			3HC *min-max*	*A (S)*:* 0.2-183 ng/mL *(plasma)* *A (S)*:* 0.4-42 ng/g *(DBS)*
			Lead *min-max*	*C (NS):* <2-9 µg/dL *(DBS)*
[12]	Pregnant women (A)*: n= 55–384, mean age= 29.8 years Children (C): n= 116-233, age = birth, 1 and 2 years, 52.7 % female Polish Mother and Child Cohort Study	Urine	Cotinine *Mean (min-max)*	*C (NS)* *1 year:* 7.1 (<LOD-66.7) ng/mL *2 years:* 8.1 (<LOD-32.3) ng/mL
			1-OHPyr	*A*:* 0.5 (0.01-8.5) µg/g cr

	(Poland) **Possible smokers*		*Mean (min-max)*	
		Cord blood	Lead *Mean (min-max)*	C *(NS)* *Birth:* 1.1 (0.4-5.7) µg/dL
		Hair	Mercury *Mean (min-max)*	*A*:* 0.3 (0.02-1.5) µg/g
		Saliva	Cotinine *Min-max*	*A*:* <LOD – 400 ng/mL
[13]	Hospitality venue employees: n = 35-44, age: 18-65 years Before smoking ban (Bef.) and after ban (Aft.) (Switzerland)	Saliva	Cotinine *Mean (95% CI)*	*Bef. (SHS):* 0.67 (0.04-1.30) ng/mL *Aft. 3-6 months:* 2.75 (0.32-5.17) ng/mL *Aft. 9-12 months:* 0.81 (0.00-1.61) ng/mL
			Nicotine *Mean (95% CI)*	*Bef. (SHS):* 1.99 (0.98-3.00) ng/mL *Aft. 3-6 months:* 2.42 (0.01-4.86) ng/mL *Aft. 9-12 months A:* 2.81 (0.12-5.75) ng/mL
[14]	Adults: n = 26, age: 18-50 years, 15 female 30 min exposure to tobacco smoke. AE: After exposure BB: Before bed 1stAM: 1st moorning 22H: 22hours after exposure (USA)	Urine	Cotinine *Median (IQR)*	*AE (SHS):* 0.98 (0.37-1.48) ng/mg cr *BB:* 2.13 (1.55-3.35) ng/mg cr *1st AM:* 1.80 (1.26-3.29) ng/mg cr *22H:* 1.26 (1.10-1.87) ng/mg cr
			3HC *Median (IQR)*	*AE (SHS):* 1.34 (0.85-2.05) ng/mg cr *BB:* 6.29 (4.58-9.36) ng/mg cr *1stAM:* 7.55 (5.13-10.37) ng/mg cr *22H:* 7.74 (5.41-12.99) ng/mg cr
			NNAL *Median (IQR)*	*AE (SHS):* 4.45 (2.70-6.75) pg/mg cr *BB:* 3.99 (2.54-5.53) pg/mg cr *1stAM:* 2.73 (2.08-3.87) pg/mg cr *22H:* 2.44 (1.60 -3.52) pg/mg cr
[15]	Adults: Smokers n = 40, SHS exposed n = 25, mean age: 20.6 years, male and female Silesian Medical University (Poland)	Urine	Cotinine *Mean (SD)*	*S:* 523.10 (68.10) µg/g cr
				SHS: 40.89 (24.80) µg/g cr
			OH-Cot *Mean (SD)*	*S:* 653.81 (62.30) µg/g cr
				SHS: 60.79 (46.70) µg/g cr
[16]	Pregnant women: Smokers n = 57, SHS exposed n = 60-367 Low SHS: ≤2 sources of exposure High SHS: >2 sources of exposure Rhea, Mother Childbirth Cohort	Urine	Cotinine (n=367) *GM (95% CI)*	*Low SHS:* 7.6 (6.45-8.76) ng/mL *High SHS:* 15.61 (13.03-18.2) ng/mL
			NNAL (n=60) *GM (95% CI)*	*S:* 0.612 (0.365-0.860) pmol/mL
				Low SHS: 0.049 (0.038-0.060) pmol/mL

	(Greece)			*High SHS:* 0.072 (0.055-0.089) pmol/mL
[17]	Adults: Smokers n = 102, Nonsmokers with possible SHS exposure (NS) n = 117, age: 18-60 years, male and female (Japan)	Urine	Nicotine *Median (IQ)*	*S*: 1635.2 (2222.2) ng/mL
				NS: 3.5 (5.3) ng/mL
			Cotinine *Median (IQ)*	*S:* 3948.1 (3512.2) ng/mL
				NS: 2.8 (4.2) ng/mL
[18]	Adults: Smokers n = 107 (BL) and n = 18 (Follow), SHS exposed n = 105 (BL) and n = 34 (Follow), age: 27-52 years, male and female BL: Baseline Follow: After 2 months follow-up (USA)	Saliva	Cotinine *Median (IQR)*	*BL (S):* 181.0 (76.3-290.2) ng/mL *Follow (S):* 135.1 (62.2-228.6) ng/mL
				BL (SHS): 0.27 (0.04-0.80) ng/mL (26% < LOD) *Follow (SHS):* 0.41(0.035-1.08) ng/mL (27% < LOD)
		Hair	Nicotine *Median (IQR)*	*BL (S):* 16.2 (4.0-40.6) ng/mg *Follow (S):* 16.4 (3.3-27.3) ng/mg
				BL (SHS): 0.36 (0.17-3.03) ng/mg (52% < LOD) *Follow (SHS):* 0.29 (0.20-3.30) ng/mg (59% < LOD)
[19]	Adults: n = 8, age: 18-34 years, 4 females Before (BE) and after (AE) exposure to 1h of SHS exposure in a vehicle (USA)	Plasma	Cotinine *Average (SD)*	*BE:* 0.04 (0.03) ng/mL *AE (SHS):* 0.17 (0.05) ng/mL
		Urine	Cotinine *Average (SD)*	*BE:* 0.38 (0.25) ng/mg cr *AE (SHS):* 2.41 (1.79) ng/mg cr
			Oh-Cot + Cotinine *Average (SD)*	*BE:* 0.006 (0.005) nmol/mg cr *AE (SHS):* 0.025 (0.020) nmol/mg cr
			NNAL *Average (SD)*	*BE:* 0.10 (0.19) pg/mg cr *AE (SHS):* 2.68 (1.36) pg/mg cr
[20]	Adults: Smokers n = 47, SHS exposed n = 15, mean age: 24.9 years, male and female Before (BE) and after (AE) smoking or 30 min of being exposed to water pipe smoke (Israel)	Plasma	Nicotine *Mean (SD)*	*BE (S):* 1.1 (4.1) ng/mL *AE (S):* 19.1 (13.9) ng/mL
				BE (SHS): 0.44 (1.7) ng/mL *AE (SHS):* 0.4 (1.4) ng/mL
			Cotinine *Mean (SD)*	*BE (S):* 61.2 (96.7) ng/mL *AE (S):* 78.2 (93.7) ng/mL
				BE (SHS): 9.2 (25) ng/mL *AE (SHS):* 13.9 (46) ng/mL
		Urine	Nicotine	*BE (S):* 70.4 (232.2) ng/mL

			Mean (SD)	*AE (S):* 290.8 (319.6) ng/mL
			Cotinine *Mean (SD)*	*BE (S):* 146.2 (232.2) ng/mL *AE (S):* 165.3 (243.6) ng/mL
		Whole blood	COHb *Mean (SD)*	*BE (S):* 2.02% (2.89) *AE (S):* 17.57% (8.79)
				BE (SHS): 0.8% (0.2) *AE (SHS):* 1.2% (0.8)
[21]	Children: n = 1985, age: 6-18 years, 49.4% female. NHANES (USA)	Serum	Cotinine *Cut-off range*	*Low SHS*: 0.015-0.1 ng/mL *Medium SHS*: 0.1-1.0 ng/mL *High SHS*: 1.0-10.0 ng/mL
		Urine	1-OHNap, 2-OHNap *GM*	*Low SHS*: 4587.6 ng/L *Medium SHS*: 5439.8 ng/L *High SHS*: 6045.6 ng/L
			2-OHFLu, 3-OHFlu, 9-OHFlu *GM*	*Low SHS*: 571.0 ng/L *Medium SHS*: 677.2 ng/L *High SHS*: 824.8 ng/L
			1-OHPA,2-OHPA, 3-OHPA *GM*	*Low SHS*: 288.1 ng/L *Medium SHS*: 352.4 ng/L *High SHS*: 351.2 ng/L
			1-OHPyr *GM*	*Low SHS*: 118.1 ng/L *Medium SHS*: 139.6 ng/L *High SHS*: 165.1 ng/L
[22]	Adults: n = 10 – 30 rooms Low THS: Overnight in nonsmoking rooms of hotels without smoking ban n = 30 High THS: Overnight in smoking rooms of hotels without smoking ban n = 29 NE: Not exposure - Overnight in hotels with complete smoking ban n = 9 BE: Before overnight exposure AE: After overnight exposure (USA)	Finger	Nicotine *Median (min-max)*	*Low THS:* 13.6 (0-226.9) ng/wipe *High THS:* 93.7 (0-1713.5) ng/wipe *NE*: 2.5 (0-17.7) ng/wipe
		Urine	Cotinine *Median (min-max)*	*Low THS:* 0.10 (0-0.41) ng/mL *High THS:* 0.64 (0-2.64) ng/mL *NE:* 0.05 (0-0.88) ng/mL
			NNAL *GM* (10 most polluted smoking rooms)	*BE*: 0.86 pg/mg cr *AE (THS)*: 1.24 pg/mg cr
[23]	Adults: n = 83, age: 25-62 years, 59 female	Urine	Cotinine *Median (p25,p50)*	*Bef. (S):* 839.8 (318.0-1167.2) µg/g cr *Aft. (S):* 865.7 (443.2-1262.2) µg/g cr

	Before smoking ban (Bef.) in 2010 and after ban (Aft.) in 2011 (Spain)			*Bef. (SHS)*: 0.8 (0.5-1.2) µg/g cr *Aft.:* 0.7 (0.4-1.0) µg/g cr
			Cadmium *Median (p25,p50)*	*Bef. (S):* 0.25 (0.17-0.43) µg/g cr *Aft. (S):* 0.24 (0.17-0.38) µg/g cr
				Bef. (SHS): 0.17 (0.11-0.29) µg/g cr *Aft.:* 0.10 (0.06-0.22) µg/g cr
[24]	Adults: Smokers n = 404-420, SHS exposed n = 116-118, age: >20 years, male and female NHANES (USA)	Serum	Cotinine *GM (95%CI)*	*S*: 149.205 (133.602-166.63) ng/mL
				SHS: 0.717 (0.254-2.022) ng/mL
		Urine	NNAL *GM (95%CI)*	*S*: 0.212 (0.184-0.246) ng/mL
				SHS: 0.0109 (0.0059-0.0201) ng/mL
[25]	Staff in pub and restaurants (Rest.): n = 101, mean age: 47.4 years, 69% female Sampling based on the type (Rest. and Pubs) and size (<150 m^2 and ≥150 m^2) of facilities Before smoking ban (Bef.) and after ban (Aft.) (Korea)	Urine	Cotinine *GM (GSD)*	Rest. < 150 m^2 *Bef. (SHS)*: 1.5 (2.0) ng/mg cr *Aft.*: 1.9 (2.4) ng/mg cr Rest. ≥ 150 m^2 *Bef. (SHS)*: 1.3 (1.9) ng/mg cr *Aft.:* 1.4 (2.4) ng/mg cr Pub < 150 m^2 *Bef. (SHS)*: 2.6 (3.1) ng/mg cr *Aft.:* 3.5 (3.1) ng/mg cr Pub ≥ 150 m^2 *Bef. (SHS)*: 1.9 (2.9) ng/mg cr *Aft.:* 3.0 (4.1) ng/mg cr
			NNAL *GM (GSD)*	Rest. < 150 m^2 *Bef. (SHS)*: 6.4 (1.9) pg/mg cr *Aft.:* 6.2 (2.1) pg/mg cr Rest. ≥ 150 m^2 *Bef. (SHS)*:4.3 (2.3) pg/mg cr *Aft.:* 4.9 (2.1) pg/mg cr Pub <150 m^2 *Bef. (SHS)*: 9.8 (2.3) pg/mg cr *Aft.:* 10.4 (2.3) pg/mg cr Pub ≥ 150 m^2 *Bef. (SHS)*: 12.1 (2.0) pg/mg cr *Aft.:* 7.3 (1.7) pg/mg cr
[26]		Oral Fluid	Cotinine	*S*: 358 (74-653) ng/mL

	Adults: Smokers n = 166 (quantificable: 70-163), Nonsmokers with possible SHS exposure (NS) n = 529 (quantificable: 8-81), female median age: 58 years, male median age: 55 years, 54% female (Spain)		*Median (IQR)*	*NS*: 0.17 (0.13-0.31) ng/mL
			NNN *Median (IQR)*	*S*: 17 (3.9-91) pg/mL
				NS: 1.6 (1.2-2.9) pg/mL
			NNK *Median (IQR)*	*S*: 4.0 (2.8-7.1) pg/mL
				NS: 3.0 (2.4-5.2) pg/mL
			NNAL *Median (IQR)*	*S*: 1.7 (0.98-3.5) pg/mL
				NS: 1.2 (0.83-1.8) pg/mL
[27]	Newborns (C) in ICU with smoker mothers (A) n = 5 (USA)	Finger	Nicotine *min-max*	*A (S)*: 44-1160 ng/wipe
		Urine	Cotinine *min-max*	*C (THS)*: 0.17-5.01 ng/mL
			OH-Cot *min-max*	*C (THS)*: 0.63-31.58 ng/mL
			NNAL *min-max*	*C (THS)*: 0.47-12.38 pg/mL
[28]	Employees exposed to SHS in public places: GB: Government buildings n = 10 LB: Large Buildings n = 11 N: Nurseries n = 6 EI: Private educational institutions n=8 (Korea)	Urine	Cotinine *GM*	*GB (SHS):* 4.99 µg/g cr *LB (SHS):* 1.00 µg/g cr *N (SHS):* 0.78 µg/g cr *EI (SHS):* 5.28 µg/g cr
		Hair	Nicotine *GM*	*GB (SHS):* 0.86 ng/mg *LB (SHS):* 0.47 ng/mg *N (SHS):* 0.14 ng/mg *EI (SHS):* 1.62 ng/mg
		Urine	NNAL *GM*	*GB (SHS):* 2.93 µg/g cr *LB (SHS):* 0.84 µg/g cr *N (SHS):* 0.34 µg/g cr *EI (SHS):* 1.84 µg/g cr
[29]	Adults: n = 20, age: >18 years, 9 female SHS exposed at home and/or hopatility venues (USA)	Hair	Nicotine *Median (min-max)*	*SHS:* 0.1 (0-5.5) ng/mg
		Saliva	Cotinine *Min-max* *Cut-off value*	*SHS:* 0 - 11 ng/mL *Cutoff low SHS:* < 10 ng/mL *Cutoff high SHS:* > 10 ng/mL - 13 ng/mL

[30]	Adults: SHS exposed at home n = 24, Non-exposed at home (NE) n = 24, male and female (Spain)	Hair	Nicotine *Median (IQR)*	*SHS*: 2040 (1200-4650) pg/mg *NE*: 623 (221-1160) pg/mg
			Cotinine *Median (IQR)*	*SHS*: 49 (26-106) pg/mg *NE*: 26 (16-43) pg/mg
			NNN *Median (IQR)*	*SHS*: 0.54 (0.29-0.60) pg/mg *NE*: 0.41 (NO IQR) pg/mg
			NNK *Median (IQR)*	*SHS*: 1.3 (0.92-2.7) pg/mg *NE*: 0.74 (0.31-1.1) pg/mg
			NNAL	*SHS*: Not quantified *NE*: Not quantified
[31]	Children: n = 559, age : 12-19 years old, 48.2% female NHANES (USA)	Serum	Cotinine *Cutoff range*	*Low SHS*: 0.05-0.268 ng/mL *High SHS*: 0.268-14.6 ng/mL
		Urine	NNAL *Cutoff range*	*Low SHS* : 0.001-0.005 ng/mL cr *High SHS*: ≥0.005-≤0.082 ng/mL cr
[32]	Adults: n = 6-25, mean age: 49 years, 51% female Non smokers living with former smokers BL: Baseline n = 9-25 W1: Week 1 postquit n = 9-17 M1: Month 1 postquit n = 9 M3: Month 3 postquit n = 8 M6: Month 6 postquit n = 6 (USA)	Finger	Nicotine *GM (95% CI)*	*BL (SHS):* 25.6 (13.2-48.9) ng/wipe *W1 (THS):* 9.1 (3.8-20.2)ng/wipe *M1 (THS):* 10.2 (4.7-21.2) ng/wipe *M3 (THS):* 5.2 (0.9-19.9)ng/wipe *M6 (THS):* 2.9 (0-46.1) ng/wipe
		Urine	Cotinine *GM (95% CI)*	*BL (SHS):* 9.9 (2.6-32.5) ng/mL *W1 (THS):* 6.0 (1.2-20.8) ng/mL *M1 (THS):* 1.5 (0.5-3.4) ng/mL *M3 (THS):* 1.7 (0.4-4.2)ng/mL *M6 (THS):* 2.7 (0-6.3) ng/mL
			NNAL *GM (95% CI)*	*BL (SHS):* 10.7 (4.7-24.2) pg/mL *W1 (THS):* 6.7 (2.5-15.9) pg/mL *M1 (THS):* 6.7 (3.5-12.2) pg/mL *M3 (THS):* 3.2 (1.1-7.4)pg/mL *M6 (THS):* 2.7 (0.5-8.1) pg/mL
[33]	Adults and children: Smokers and Nonsmokers with possible SHS exposure (NS) n = 5792, age: 6 - >60 years, 2964 female	Serum	Cotinine *Cut-off value*	*SHS:* <10 ng/mL

	06-11 years (NS n = 769) 12-19 (S n = 66, NS n=824) 20-59 (S n= 703, NS n=2123) >60 (S n= 192, NS n=1115) NHANES (USA)	Urine	NNAL *GM(95% CI)*	*S (12-19 years):* 60.5 (46.2-79) pg/ mg cr *S (20-59 years):* 209 (171-256) pg/ mg cr *S (>60 years):* 365 (328-405) pg/ mg cr
				NS (6-11 years): 2.43 (1.96-3.02) pg/mg cr *NS (12-19 years):* 1.38 (1.21-1.57) pg/mg cr *NS (20-59 years):* 1.09 (1.00-1.19) pg/ mg cr *NS (>60 years):* NA
[34]	Staff working in smoking hospitality venues: n= 62, 44 female (Korea)	Urine	Cotinine *GM (SD)*	*SHS:* 1.8 (2.8) ng/mg cr
			NNAL *GM (SD)*	*SHS:* 7.3 (2.5) pg/mg cr
[35]	Adults: Smokers n = 69, SHS exposed n = 123, mean age: 56.7 years, men (Japan)	Hair	Cotinine *Mean (SD)*	*S*: 1.9 (2.1) ng/mg
				SHS: 0.2 (0.6) ng/mg
			Nicotine *Mean (SD)*	*S*: 26.6 (24.7) ng/mg
				SHS: 3.6 (8.4) ng/mg
[36]	Adults: n = 10, mean age: 24.6 years, 20% female Before exposure (BE) and after exposure (AE) during the work shift in waterpipe smoking bars (USA)	Saliva	Cotinine *Mean*	*BE (SHS):* 23.8 ng/mL *AE(SHS):* 27.9 ng/mL
		Breath	CO *Mean (SD)*	*BE (SHS):* 8.3 (6.9) ppm *AE (SHS):* 49.4 (32.7) ppm
[37]	Mothers (A): Smokers n = 41, Nonsmokers n = 76 Daily S: Daily smokers n = 12 Oc. S: Ocassional smokers n = 11 Former S: Former smokers n = 18 NE: Not exposed - Nonsmoker n = 76 Children (C): n = 120, age: 6-11 years Low SHS: less than daily exposure to SHS n = 6 High SHS: Daily exposure to SHS n = 6 NE: Not exposed n = 108	Urine	Cotinine *GM (95%CI)*	*A (Daily S)*: 489.15 (127.78-1872.44) µg/L *A (Oc. S)*: 34.50 (6.35-187.55) µg/L
				A (Former S): 2.58 (1.51-4-39) µg/L *A (NE)*: 1.41 (1.23-1.61) µg/L *C (High SHS):* 10.77 (3.27-35.45) µg/L *C (Low SHS):* 2.44 (1.26-4.71) µg/L *C (NE)*: 1.39 (1.25-1.55) µg/L
			Cadmium *GM (95%CI)*	*A (Daily S)*: 0.36 (0.30-0.44) µg/L *A (Oc. S)*: 0.22 (0.15-0.33) µg/L

	COPHES/DEMOCOPHES Projects (Czech Republic)			*A (Former S):* 0.21 (0.16-0.28) µg/L *A (NE)*: 0.21 (0.18-0.25) µg/L *C (High SHS):* 0.180 (0.110-0.294) µg/L *C (Low SHS):* 0.061 (0.028-0.131) µg/L *C (NE)*: 0.110 (0.097-0.124) µg/L
[38]	Adults: n = 1398, age: 19-65 years, male and female KNHANES (Korea)	Urine	Cotinine *Cut-off value*	*SHS:* < 550 µg/L
		Whole blood	Cadmium *Age adjusted blood cadmium level*	*SHS*: 1.07 µg/L
[39]	Adolescents: n = 338, mean age: 12.9 years, 53% female AdoQuest II longitudinal cohort (Canada)	Saliva	Cotinine *Mean (SD)*	*SHS*: 0.48 (1.21) ng/mL
		Hair	Nicotine *Mean (SD)*	*SHS*: 0.38 (1.40) ng/mg
[40]	Children: n = 25, mean age: 5.4 years, male and female Children with a potentially SHS-related illness with smoker parents (USA)	Saliva	Cotinine *Median (IQR)*	*SHS*: 5.3 (2.3-9.1) ng/mL
		Hand (wipes)	Nicotine *Median (IQR)*	*SHS*: 91.6 (57.2-121.6) ng/wipe
[41]	Adults: Smokers n = 90/105, SHS exposed n = 91/103, S median age: 22 years, SHS meadian age: 27 years, male and female Daily S: Daily smokers n= 17/20 Oc. S: Ocassional smokers n = 73/85 Before exposure (BE) and after exposure (AE) to waterpipe smoke in a waterpipe social event (USA)	Saliva	Cotinine *Cut-off value*	*SHS:* ≤ 10 ng/mL
		Urine	HPMA *Median (IQR)*	*BE (Daily S):* 1443 (1131-3639) pmol/mg cr *AE (Daily S)*: 3686 (2502-4046) pmol/mg cr *BE (Oc. S):* 1660 (940-2890) pmol/mg cr *AE (Oc. S)*: 2039 (1203-4898) pmol/mg cr
				BE: 1770 (1001-2787) pmol/mg cr *AE (SHS):* 2498 (1580-3964) pmol/mg cr
[42]	Adolescents: Smokers n = 55, SHS exposed n = 410, age: 13-19 years, male and female (USA)	Urine	Cotinine *Median (IQR)*	*S:* > 30 ng/ mL
				Low SHS: 0.05-0.25 ng/mL *High SHS:* 0.25-30 ng/ mL
			NNAL	*S*: 80.9 (42.6-151.3) pg/mL

			Median (IQR)	*SHS*: 1.2 (0.5-3.2) pg/mL
[43]	Adults and children: Smokers n = 867, Nonsmokers with possible SHS exposure (NS) n = 3825, age: 6->60 years, 53.4% female NHANES (USA)	Serum	Cotinine *Cut-off range*	*SHS:* 0.05-10 ng/mL
		Urine	HPMM *Median (IQR)*	*S*: 1.63 (0.680-3.29) mg/g cr
				NS: 0.313 (0.231-0.451) mg/g cr
[44]	Adults: n = 52-73, age: 24-40 years, male and female Waterpipe Tobacco employees (Turkey, Russia, Egipt)	Urine	Cotinine *Median (IQR)*	*SHS*: 1.1 (0.2-40.9) µg/g cr
			NNAL *Median (IQR)*	*SHS*: 1.48 (0.98-3.97) pg/mg cr
			1-OHPG (1-hydroxy-pyrene glucuronide) *Median (IQR)*	*SHS*: 0.54 (0.25-0.97) pmol/mg cr
		Saliva	Cotinine *Median (IQR)*	*SHS*: 5.5 (2.0-15.0) ng/mL
		Hair	Nicotine *Median (IQR)*	*SHS*: 0.95 (0.36-5.02) ng/mg
		Breath	CO *Median (IQR)*	*SHS*: 1.67 (1.33-2.33) ppm

Abbreviations:

A: Adults; C: Children; NE: Nonsmokers not exposed to tobacco smoke; NS: Nonsmokers whose tobacco smoke exposure was not specified in the study; S: Smokers; SHS: Nonsmokers exposed to SHS; THS: Nonsmokers exposed to THS; AE: After exposure; Aft.: After smoking ban; BE: Before exposure; Bef.: Before smoking ban; BL: Baseline; Rest.: Restaurant; CI: Confidence interval; GM: Geometric mean; GSD: Geometric standard deviation; IQR: Interquartile range; LOD: Limit of detection; SD: Standard deviation; cr: Creatinine

2.10 References

1. Oberg, M.; Jaakkola, M. S.; Woodward, A.; Peruga, A.; Pruss-Ustun, A. Worldwide burden of disease from exposure to second-hand smoke: A retrospective analysis of data from 192 countries. *Lancet* **2011**, *377*, 139–146, doi:10.1016/S0140-6736(10)61388-8.

2. IARC (International Agency for Reasearch on Cancer). IARC Monographs on Tobacco smoke and involuntary smoking, vol 83. Lyon, France; 2004. Available online: https://monographs.iarc.fr/wp-content/uploads/2018/06/mono83.pdf (accessed on May 16, 2018).

3. Thielen, A.; Klus, H.; Müller, L. Tobacco smoke: Unraveling a controversial subject. *Exp. Toxicol. Pathol.* **2008**, *60*, 141–156, doi:10.1016/j.etp.2008.01.014.

4. Talhout, R.; Schulz, T.; Florek, E.; van Benthem, J.; Wester, P.; Opperhuizen, A. Hazardous compounds in tobacco smoke. *Int. J. Environ. Res. Public Health* **2011**, *8*, 613–628, doi:10.3390/ijerph8020613.

5. Matt, G. E.; Quintana, P. J. E.; Destaillats, H.; Gundel, L. a.; Sleiman, M.; Singer, B. C.; Jacob, P.; Benowitz, N.; Winickoff, J. P.; Rehan, V.; Talbot, P.; Schick, S.; Samet, J.; Wang, Y.; Hang, B.; Martins-Green, M.; Pankow, J. F.; Hovell, M. F. Thirdhand Tobacco Smoke: Emerging Evidence and Arguments for a Multidisciplinary Research Agenda. *Environ. Health Perspect.* **2011**, *119*, 1218–1226, doi:10.1289/ehp.1103500.

6. Jacob, P.; Benowitz, N. L.; Destaillats, H.; Gundel, L.; Hang, B.; Martins-Green, M.; Matt, G. E.; Quintana, P. J. E.; Samet, J. M.; Schick, S. F.; Talbot, P.; Aquilina, N. J.; Hovell, M. F.; Mao, J. H.; Whitehead, T. P. Thirdhand Smoke: New Evidence, Challenges, and Future Directions. *Chem. Res. Toxicol.* **2017**, *30*, 270–294, doi:10.1021/acs.chemrestox.6b00343.

7. Sleiman, M.; Gundel, L. A.; Pankow, J. F.; Jacob, P.; Singer, B. C.; Destaillats, H. Formation of carcinogens indoors by surface-mediated reactions of nicotine with nitrous acid, leading to potential thirdhand smoke hazards. *Proc. Natl. Acad. Sci.* **2010**, *107*, 6576–6581, doi:10.1073/pnas.0912820107.

8. Hoh, E.; Hunt, R. N.; Quintana, P. J. E.; Zakarian, J. M.; Chatfield, D. A.; Wittry, B. C.; Rodriguez, E.; Matt, G. E. Environmental Tobacco Smoke as a Source of Polycyclic Aromatic Hydrocarbons in Settled Household Dust.pdf. **2012**.

9. Schick, S. F.; Farraro, K. F.; Perrino, C.; Sleiman, M.; van de Vossenberg, G.; Trinh, M. P.; Katharine Hammond, S.; Jenkins, B. M.; Balmes, J. Thirdhand cigarette smoke in an experimental chamber: Evidence of surface deposition of nicotine, nitrosamines and polycyclic aromatic hydrocarbons and de novo formation of NNK. *Tob. Control* **2014**, *23*, 152–159, doi:10.1136/tobaccocontrol-2012-050915.

10. Sleiman, M.; Logue, J. M.; Luo, W.; Pankow, J. F.; Gundel, L. A.; Destaillats, H. Inhalable Constituents of Thirdhand Tobacco Smoke: Chemical Characterization and Health Impact Considerations. *Environ. Sci. Technol.* **2014**, *48*, 13093–13101, doi:10.1021/es5036333.

11. Ramírez, N.; Özel, M. Z.; Lewis, A. C.; Marcé, R. M.; Borrull, F.; Hamilton, J. F. Exposure to nitrosamines in thirdhand tobacco smoke increases cancer risk in non-smokers. *Environ. Int.* **2014**, *71*, 139–147, doi:10.1016/j.envint.2014.06.012.

12. Ramírez, N.; Vallecillos, L.; Lewis, A. C.; Borrull, F.; Marcé, R. M.; Hamilton, J. F. Comparative study of comprehensive gas chromatography-nitrogen chemiluminescence detection and gas chromatography-ion trap-tandem mass spectrometry for determining

nicotine and carcinogen organic nitrogen compounds in thirdhand tobacco smoke. *J. Chromatogr. A* **2015**, *1426*, 191–200, doi:10.1016/j.chroma.2015.11.035.

13. Adhami, N.; Starck, S. R.; Flores, C.; Green, M. M. A health threat to bystanders living in the homes of smokers: How smoke toxins deposited on surfaces can cause insulin resistance. *PLoS One* **2016**, *11*, 1–19, doi:10.1371/journal.pone.0149510.

14. Adhami, N.; Chen, Y.; Martins-Green, M. Biomarkers of disease can be detected in mice as early as 4 weeks after initiation of exposure to third-hand smoke levels equivalent to those found in homes of smokers. *Clin. Sci.* **2017**, *131*, 2409–2426, doi:10.1042/CS20171053.

15. Martins-Green, M.; Adhami, N.; Frankos, M.; Valdez, M.; Goodwin, B.; Lyubovitsky, J.; Dhall, S.; Garcia, M.; Egiebor, I.; Martinez, B.; Green, H. W.; Havel, C.; Yu, L.; Liles, S.; Matt, G.; Destaillats, H.; Sleiman, M.; Gundel, L. a.; Benowitz, N.; Jacob, P.; Hovell, M.; Winickoff, J. P.; Curras-Collazo, M. Cigarette smoke toxins deposited on surfaces: Implications for human health. *PLoS One* **2014**, *9*, 1–12, doi:10.1371/journal.pone.0086391.

16. Hang, B.; Sarker, A. H.; Havel, C.; Saha, S.; Hazra, T. K.; Schick, S.; Jacob, P.; Rehan, V. K.; Chenna, A.; Sharan, D.; Sleiman, M.; Destaillats, H.; Gundel, L. A. Thirdhand smoke causes DNA damage in human cells. *Mutagenesis* **2013**, *28*, 381–391, doi:10.1093/mutage/get013.

17. Avila-Tang, E.; Al-Delaimy, W. K.; Ashley, D. L.; Benowitz, N.; Bernert, J. T.; Kim, S.; Samet, J. M.; Hecht, S. S. Assessing secondhand smoke using biological markers. *Tob. Control* **2013**, *22*, 164–171, doi:10.1136/tobaccocontrol-2011-050298.

18. Benowitz, N. I.; Dains, K. M.; Dempsey, D.; Herrera, B.; Yu, L.; Jacob, P. Urine nicotine metabolite concentrations in relation to plasma cotinine during low-level nicotine exposure. *Nicotine Tob. Res.* **2009**, *11*, 954–960, doi:10.1093/ntr/ntp092.

19. Wassenaar, C. A.; Conti, D. V.; Das, S.; Chen, P.; Cook, E. H.; Ratain, M. J.; Benowitz, N. L.; Tyndale, R. F. UGT1A and UGT2B Genetic Variation Alters Nicotine and Nitrosamine Glucuronidation in European and African American Smokers. *Cancer Epidemiol. Biomarkers Prev.* **2015**, *24*, 94–104, doi:10.1158/1055-9965.EPI-14-0804.

20. Schultze, B.; Lind, P. M.; Larsson, A.; Lind, L. Whole blood and serum concentrations of metals in a Swedish population-based sample. *Scand. J. Clin. Lab. Invest.* **2014**, *74*, 143–148, doi:10.3109/00365513.2013.864785.

21. Yang, J.; Pearl, M.; Jacob, P.; DeLorenze, G. N.; Benowitz, N. L.; Yu, L.; Havel, C.; Kharrazi, M. Levels of cotinine in dried blood specimens from newborns as a biomarker of maternal smoking close to the time of delivery. *Am. J. Epidemiol.* **2013**, *178*, 1648–1654, doi:10.1093/aje/kwt182.

22. Polanska, K.; Hanke, W.; Sobala, W.; Trzcinka-Ochocka, M.; Ligocka, D.; Brzeznicki, S.; Strugala-Stawik, H.; Magnus, P. Developmental Effects of Exposures to Environmental Factors: The Polish Mother and Child Cohort Study. *Biomed Res. Int.* **2013**, *ID 629716*, doi:10.1155/2013/629716.

23. Pérez-Ortuño, R.; Martínez-Sánchez, J. M.; Fu, M.; Fernández, E.; Pascual, J. A. Evaluation of tobacco specific nitrosamines exposure by quantification of 4-(methylnitrosamino)-1-(3-pyridyl)-1-butanone (NNK) in human hair of non-smokers. *Sci. Rep.* **2016**, *6*, 1–8, doi:10.1038/srep25043.

24. Benowitz, N. L.; Hukkanen, J.; Jacob, P. Nicotine chemistry, Metabolism, Kinetics and Biomarkers. *Handb. Exp. Pharmacol.* **2009**, *192*, 29–60, doi:10.1007/978-3-540-69248-5_2.

25. Al-Delaimy, W. K. Hair as a biomarker for exposure to tobacco smoke. *Tob. Control* **2002**, *11*, 176–182, doi:10.1136/TC.11.3.176.

26. U.S. EPA (U.S. Environmental Protection Agency). Dermal exposure assessment: A summary of epa approaches. U.S. Environmental Protection Agency, Washington, DC, EPA/600/R-07/040F; 2007. Available online: https://cfpub.epa.gov/ncea/risk/recordisplay.cfm?deid=183584 (accessed on Jul 2, 2018).

27. Weschler, C. J.; Nazaroff, W. W. Dermal Uptake of Organic Vapors Commonly Found in Indoor Air. *Environ. Sci. Technol.* **2014**, *48*, 1230–1237, doi:10.1021/es405490a.

28. Deveci, S. E.; Deveci, F.; Açik, Y.; Ozan, A. T. The measurement of exhaled carbon monoxide in healthy smokers and non-smokers. *Respir. Med.* **2004**, *98*, 551–556, doi:10.1016/j.rmed.2003.11.018.

29. OEHHA-CalEPA Chemical Database CalEPA, 2018b. Toxicity Criteria on Chemicals Evaluated by OEHHA. California Environmental Protection Agency. Available online: https://oehha.ca.gov/chemicals (accessed on Jun 4, 2018).

30. IARC (International Agency for Research on Cancer). List of classifications by alphabetical order; 2013. Available online: https://monographs.iarc.fr/wp-content/uploads/2018/07/ClassificationsAlphaOrder.pdf (accessed on May 15, 2018).

31. Naufal, Z.; Kathman, S.; Wilson, C. Bayesian derivation of an oral cancer slope factor distribution for 4-(methylnitrosamino)-1-(3-pyridyl)-1-butanone (NNK). *Regul. Toxicol. Pharmacol.* **2009**, *55*, 69–75, doi:10.1016/J.YRTPH.2009.06.002.

32. RAIS: RAIS (The Risk Assessment Information System); 2009. Available online: https://rais.ornl.gov/tools/tox_profiles.html (accessed on Jun 7, 2018).

33. OEHHA-CalEPA. Air Toxics Hot Spots Program Risk Assessment Guidelines. Part I: The Determination of Acute Reference Exposure Levels for Airborne Toxicants; 1999. Available online: https://oehha.ca.gov/media/downloads/crnr/acuterel.pdf (accessed on Jun 11, 2018).

34. EPA (United States Environmental Protection Agency). Basic Information about the Integrated Risk Information System Available online: https://www.epa.gov/iris/basic-information-about-integrated-risk-information-system (accessed on Jun 3, 2018).

35. Tzatzarakis, M. N.; Vardavas, C. I.; Terzi, I.; Kavalakis, M.; Kokkinakis, M.; Liesivuori, J.; Tsatsakis, A. M. Hair nicotine/cotinine concentrations as a method of monitoring exposure to tobacco smoke among infants and adults. *Hum. Exp. Toxicol.* **2012**, *31*, 258–265, doi:10.1177/0960327111422401.

36. Moon, K. A.; Rule, A. M.; Magid, H. S.; Ferguson, J. M.; Susan, J.; Sun, Z.; Torrey, C.; Abubaker, S.; Levshin, V.; Çarkoglu, A.; Radwan, G. N.; El-Rabbat, M.; Cohen, J. E.; Strickland, P.; Breysse, P. N.; Navas-Acien, A. Biomarkers of secondhand smoke exposure in waterpipe tobacco venue employees in Istanbul, Moscow, and Cairo. *Nicotine Tob. Res.* **2018**, *20*, 482–491, doi:10.1093/ntr/ntx125.

37. Park, E. Y.; Yun, E. H.; Lim, M. K.; Lee, D.-H.; Yang, W.; Jeong, B. Y.; Hwang, S.-H. Consequences of incomplete smoke-free legislation in the Republic of Korea: Results from environmental and biochemical monitoring: Community based study. *Cancer Res. Treat.* **2016**, *48*, 376–383, doi:10.4143/crt.2014.269.

38. Kim, S.; Apelberg, B. J.; Avila-Tang, E.; Hepp, L.; Yun, D.; Samet, J. M.; Breysse, P. N. Utility

and Cutoff Value of Hair Nicotine as a Biomarker of Long-Term Tobacco Smoke Exposure, Compared to Salivary Cotinine. *Int. J. Environ. Res. Public Health* **2014**, *11*, 8368–8382, doi:10.3390/ijerph110808368.

39. Okoli, C. A Comparison of Survey Measures and Biomarkers of Secondhand Tobacco Smoke Exposure among Nonsmokers. *Public Health Nurs.* **2016**, *33*, 82–89, doi:10.1111/phn.12207.

40. McGrath, J. J.; Racicot, S.; Okoli, C. T. C.; Hammond, S. K.; O'Loughlin, J. Airborne Nicotine, Secondhand Smoke, and Precursors to Adolescent Smoking. *Pediatrics* **2018**, *141*, S63–S74, doi:10.1542/peds.2017-1026J.

41. Northrup, T. F.; Khan, A. M.; Jacob, P.; Benowitz, N. L.; Hoh, E.; Hovell, M. F.; Matt, G. E.; Stotts, A. L. Thirdhand smoke contamination in hospital settings: Assessing exposure risk for vulnerable paediatric patients. *Tob. Control* **2016**, *25*, 619–623, doi:10.1136/tobaccocontrol-2015-052506.

42. Matt, G. E.; Quintana, P. J. E.; Zakarian, J. M.; Hoh, E.; Hovell, M. F.; Mahabee-Gittens, M.; Watanabe, K.; Datuin, K.; Vue, C.; Chatfield, D. A. When smokers quit: exposure to nicotine and carcinogens persists from thirdhand smoke pollution. *Tob. Control* **2017**, *26*, 548–556, doi:10.1136/tobaccocontrol-2016-053119.

43. Matt, G. E.; Quintana, P. J. E.; Fortmann, A. L.; Zakarian, J. M.; Galaviz, V. E.; Chatfield, D. a; Hoh, E.; Hovell, M. F.; Winston, C. Thirdhand smoke and exposure in California hotels: non-smoking rooms fail to protect non-smoking hotel guests from tobacco smoke exposure. *Tob. Control* **2014**, *23*, 264–272, doi:10.1136/tobaccocontrol-2012-050824.

44. Wilson, T.; Shamo, F.; Boynton, K.; Kiley, J. The impact of Michigan's Dr Ron Davis smoke-free air law on levels of cotinine, tobacco-specific lung carcinogen and severity of self-reported respiratory symptoms among non-smoking bar employees. *Tob. Control* **2012**, *21*, 593–595, doi:10.1136/tobaccocontrol-2011-050328.

45. Matsumoto, A.; Matsumoto, A.; Ichiba, M.; Payton, N. M.; Oishi, H.; Hara, M. Simultaneous measurement of urinary total nicotine and cotinine as biomarkers of active and passive smoking among Japanese individuals. *Environ. Health Prev. Med.* **2013**, *18*, 244–250, doi:10.1007/s12199-012-0307-5.

46. Forysová, K.; Pinkr-Grafnetterová, A.; Malý, M.; Krsková, A.; Mráz, J.; Kašparová, L.; Čejchanová, M.; Sochorová, L.; Rödlová, S.; Černá, M. Urinary Cadmium and Cotinine Levels and Hair Mercury Levels in Czech Children and Their Mothers Within the Framework of the COPHES/DEMOCOPHES Projects. *Arch. Environ. Contam. Toxicol.* **2017**, *73*, 421–430, doi:10.1007/s00244-017-0412-y.

47. Caman, O. K.; Erguder, B. I.; Ozcebe, H.; Bilir, N. Urinary Cotinine and Breath Carbon Monoxide Levels Among Bar and Restaurant Employees in Ankara. *Nicotine Tob. Res.* **2013**, *15*, 1446–1452, doi:10.1093/ntr/nts345.

48. Vardavas, C. I.; Fthenou, E.; Patelarou, E.; Bagkeris, E.; Murphy, S.; Hecht, S. S.; Connolly, G. N.; Chatzi, L.; Kogevinas, M. Exposure to different sources of secondhand smoke during pregnancy and its effect on urinary cotinine and tobacco-specific nitrosamine (NNAL) concentrations. *Tob. Control* **2013**, *22*, 194–200, doi:10.1136/tobaccocontrol-2011-050144.

49. Jones, I. A.; St Helen, G.; Meyers, M. J.; Dempsey, D. A.; Havel, C.; Jacob, P.; Northcross, A.; Hammond, S. K.; Benowitz, N. L. Biomarkers of secondhand smoke exposure in automobiles. *Tob. Control* **2014**, *23*, 51–57, doi:10.1136/tobaccocontrol-2012-050724.

50. Benowitz, N. L.; Nardone, N.; Jain, S.; Dempsey, D. A.; Addo, N.; St. Helen, G.; Jacob, P. Comparison of Urine 4-(Methylnitrosamino)-1-(3)Pyridyl-1-Butanol and Cotinine for Assessment of Active and Passive Smoke Exposure in Urban Adolescents. *Cancer Epidemiol. Biomarkers Prev.* **2018**, *27*, 254–261, doi:10.1158/1055-9965.EPI-17-0671.

51. Ho, G.; Tang, H.; Robbins, J. A.; Tong, E. K. Biomarkers of Tobacco Smoke Exposure and Asthma Severity in Adults. *Am. J. Prev. Med.* **2013**, *45*, 703–709, doi:10.1016/j.amepre.2013.09.002.

52. Murphy, S. E.; Wickham, K. M.; Lindgren, B. R.; Spector, L. G.; Joseph, A. Cotinine and trans 3'-hydroxycotinine in dried blood spots as biomarkers of tobacco exposure and nicotine metabolism. *J. Expo. Sci. Environ. Epidemiol.* **2013**, *23*, 513–518, doi:10.1038/jes.2013.7.

53. Moore, B. F.; Clark, M. L.; Bachand, A.; Reynolds, S. J.; Nelson, T. L.; Peel, J. L. Interactions Between Diet and Exposure to Secondhand Smoke on Metabolic Syndrome Among Children: NHANES 2007-2010. *J. Clin. Endocrinol. Metab.* **2016**, *101*, 52–58, doi:10.1210/jc.2015-2477.

54. Wei, B.; Blount, B. C.; Xia, B.; Wang, L. Assessing exposure to tobacco-specific carcinogen NNK using its urinary metabolite NNAL measured in US population: 2011-2012. *J. Expo. Sci. Environ. Epidemiol.* **2016**, *26*, 249–256, doi:10.1038/jes.2014.88.

55. Bagchi, P.; Geldner, N.; DeCastro, B. R.; De Jesús, V. R.; Park, S. K.; Blount, B. C. Crotonaldehyde exposure in U.S. tobacco smokers and nonsmokers: NHANES 2005–2006 and 2011–2012. *Environ. Res.* **2018**, *163*, 1–9, doi:10.1016/j.envres.2018.01.033.

56. Jedrychowski, W. A.; Perera, F. P.; Maugeri, U.; Spengler, J.; Mroz, E.; Flak, E.; Stigter, L.; Majewska, R.; Kaim, I.; Sowa, A.; Jacek, R. Prohypertensive Effect of Gestational Personal Exposure to Fine Particulate Matter. Prospective Cohort Study in Non-smoking and Non-obese Pregnant Women. *Cardiovasc. Toxicol.* **2012**, *12*, 216–225, doi:10.1007/s12012-012-9157-z.

57. Kim, H.-W.; Kam, S.; Lee, D.-H. Synergistic interaction between polycyclic aromatic hydrocarbons and environmental tobacco smoke on the risk of obesity in children and adolescents: The U.S. National Health and Nutrition Examination Survey 2003–2008. *Environ. Res.* **2014**, *135*, 354–360, doi:10.1016/j.envres.2014.08.032.

58. Jain, R. B. Serum cotinine and urinary 4-(methylnitrosamino)-1-(3-pyridyl)-1-butanonol levels among non-Hispanic Asian American smokers and nonsmokers as compared to other race/ethnicities: Data from NHANES 2011-2012. *Chemosphere* **2015**, *120*, 584–591, doi:10.1016/j.chemosphere.2014.09.069.

59. Lam, E.; Kvaavik, E.; Hamer, M.; Batty, G. D. Association of secondhand smoke exposure with mental health in men and women: Cross-sectional and prospective analyses using the UK Health and Lifestyle Survey. *Eur. Psychiatry* **2013**, *28*, 276–281, doi:10.1016/j.eurpsy.2012.04.001.

60. Pérez-Ortuño, R.; Martínez-Sánchez, J. M.; Fu, M.; Ballbè, M.; Quirós, N.; Fernández, E.; Pascual, J. A. Assessment of tobacco specific nitrosamines (TSNAs) in oral fluid as biomarkers of cancer risk: A population-based study. *Environ. Res.* **2016**, *151*, 635–641, doi:10.1016/j.envres.2016.08.036.

61. St.Helen, G.; Thomas Bernert, J.; Hall, D. B.; Sosnoff, C. S.; Xia, Y.; Balmes, J. R.; Vena, J. E.; Wang, J.-S.; Holland, N. T.; Naeher, L. P. Exposure to Secondhand Smoke Outside of a Bar and a Restaurant and Tobacco Exposure Biomarkers in Nonsmokers. *Environ. Health Perspect.* **2012**, *120*, 1010–1016, doi:10.1289/ehp.1104413.

62. Rajkumar, S.; Huynh, C. K.; Bauer, G. F.; Hoffmann, S.; Röösli, M. Impact of a smoking ban in hospitality venues on second hand smoke exposure: a comparison of exposure assessment methods. *BMC Public Health* **2013**, *13*, 536, doi:10.1186/1471-2458-13-536.

63. Mahabee-Gittens, E. M.; Merianos, A. L.; Matt, G. E. Preliminary evidence that high levels of nicotine on children's hands may contribute to overall tobacco smoke exposure. *Tob. Control* **2018**, *27*, 217–219, doi:10.1136/tobaccocontrol-2016-053602.

64. Tsuji, M.; Kanda, H.; Hayakawa, T.; Mori, Y.; Ito, T.; Hidaka, T.; Kakamu, T.; Kumagai, T.; Osaki, Y.; Kawazoe, M.; Sato, S.; Fukushima, T. Nicotine cut-off value in human hair as a tool to distinguish active from passive smokers: A cross-sectional study in Japanese men. *Cancer Biomarkers* **2017**, *20*, 41–48, doi:10.3233/CBM-170004.

65. Szumska, M.; Tyrpień, K.; Kowalska, M.; Wielkoszyński, T.; Dobosz, C. Medicine students and exposure to environmental tobacco smoke. *Int. J. Occup. Med. Environ. Health* **2013**, *26*, 313–320, doi:10.2478/s13382-013-0100-8.

66. Schick, S. F.; Van Den Vossenberg, G.; Luo, A.; Whitlatch, A.; Jacob, P.; Balmes, J.; Shusterman, D. Thirty minute-exposure to aged cigarette smoke increases nasal congestion in nonsmokers. *J. Toxicol. Environ. Heal. - Part A Curr. Issues* **2013**, *76*, 601–613, doi:10.1080/15287394.2013.800811.

67. Protano, C.; Andreoli, R.; Manini, P.; Guidotti, M.; Vitali, M. A tobacco-related carcinogen: assessing the impact of smoking behaviours of cohabitants on benzene exposure in children. *Tob. Control* **2012**, *21*, 325–329, doi:10.1136/tc.2010.039255.

68. Kassem, N. O. F.; Kassem, N. O.; Liles, S.; Zarth, A. T.; Jackson, S. R.; Daffa, R. M.; Chatfield, D. A.; Carmella, S. G.; Hecht, S. S.; Hovell, M. F. Acrolein Exposure in Hookah Smokers and Non-Smokers Exposed to Hookah Tobacco Secondhand Smoke: Implications for Regulating Hookah Tobacco Products. *Nicotine Tob. Res.* **2018**, *20*, 492–501, doi:10.1093/ntr/ntx133.

69. Lee, W.; Lee, S.; Roh, J.; Won, J. U.; Yoon, J. H. The Association between Involuntary Smoking Exposure with Urine Cotinine Level and Blood Cadmium Level in General Non-Smoking Populations. *J. Korean Med. Sci.* **2017**, *32*, 568–575, doi:10.3346/jkms.2017.32.4.568.

70. Bentur, L.; Hellou, E.; Goldbart, A.; Pillar, G.; Monovich, E.; Salameh, M.; Scherb, I.; Bentur, Y. Laboratory and Clinical Acute Effects of Active and Passive Indoor Group Water-Pipe (Narghile) Smoking. *Chest* **2014**, *145*, 803–809, doi:10.1378/chest.13-0960.

71. Catassi, A.; Servent, D.; Paleari, L.; Cesario, A.; Russo, P. Multiple roles of nicotine on cell proliferation and inhibition of apoptosis: Implications on lung carcinogenesis. *Mutat. Res. - Rev. Mutat. Res.* **2008**, *659*, 221–231, doi:10.1016/j.mrrev.2008.04.002.

72. Benowitz, N. L. Nicotine Addiction. *N Engl J Med* **2010**, *362*, 2295–2303, doi:10.1056/NEJMra0809890.

73. Hukkanen, J.; Jacob, P.; Benowitz, N. L.; Jacob, P. Metabolism and Disposition Kinetics of Nicotine. *Pharmacol. Rev.* **2005**, *57*, 79–115, doi:10.1124/pr.57.1.3.79.

74. Uematsu, T.; Mizuno, A.; Nagashima, S.; Oshima, A.; Nakamura, M. The axial distribution of nicotine content along hair shaft as an indicator of changes in smoking behaviour: evaluation in a smoking- cessation programme with or without the aid of nicotine chewing gum. *Br. J. Clin. Pharmacol.* **1995**, *39*, 665–669, doi:10.1111/j.1365-2125.1995.tb05726.x.

75. Benowitz, N. L.; Jacob, P. Metabolism of nicotine to cotinine studied by a dual stable

isotope method. *Clin. Pharmacol. Ther.* **1994**, *56*, 483–493, doi:10.1038/clpt.1994.169.

76. Murphy, P. J. Enzymatic oxidation of nicotine to nicotine 1'(5') iminium ion. A newly discovered intermediate in the metabolism of nicotine. *J. Biol. Chem.* **1973**, *248*, 2796–2800.

77. Brandänge, S.; Lindblom, L. The enzyme "aldehyde oxidase" is an iminium oxidase. Reaction with nicotine Δ1'(5') iminium ion. *Biochem. Biophys. Res. Commun.* **1979**, *91*, 991–996, doi:10.1016/0006-291X(79)91977-6.

78. Benowitz, N. L.; Jacob, P. Nicotine and cotinine elimination pharmacokinetics in smokers and nonsmokers. *Clin. Pharmacol. Ther.* **1993**, *53*, 316–323, doi:10.1038/clpt.1993.27.

79. Murphy, S. E.; Johnson, L. M.; Pullo, D. A. Characterization of multiple products of cytochrome P450 2A6-catalyzed cotinine metabolism. *Chem. Res. Toxicol.* **1999**, *12*, 639–645, doi:10.1021/tx990015e.

80. Benowitz, N. L.; Jacob, P. Trans-3'-hydroxycotinine: Disposition kinetics, effects and plasma levels during cigarette smoking. *Br. J. Clin. Pharmacol.* **2008**, *51*, 53–59, doi:10.1046/j.1365-2125.2001.01309.x.

81. Hagan, R. L.; Ramos, J. M.; Jacob, P. M. Increasing urinary cotinine concentrations at elevated temperatures: the role of conjugated metabolites. *J. Pharm. Biomed. Anal.* **1997**, *16*, 191–197.

82. Benowitz, N. L.; Kuyt, F.; Jacob, P.; Jones, R. T.; Osman, A.-L. Cotinine disposition and effects. *Clin. Pharmacol. Ther.* **1983**, *34*, 604–611, doi:10.1038/clpt.1983.222.

83. Benowitz, N. L.; Jacob, P.; Fong, I.; Gupta, S. Nicotine metabolic profile in man: comparison of cigarette smoking and transdermal nicotine. *J. Pharmacol. Exp. Ther.* **1994**, *268*, 296–303.

84. Hecht, S. S.; Stepanov, I.; Carmella, S. G. Exposure and Metabolic Activation Biomarkers of Carcinogenic Tobacco-Specific Nitrosamines. *Acc. Chem. Res.* **2016**, *49*, 106–114, doi:10.1021/acs.accounts.5b00472.

85. Luukkanen, L.; Mikkola, J.; Forsman, T.; Taavitsainen, P.; Taskinen, J.; Elovaara, E. Glucuronidation of 1-Hydroxypyrene by Human Liver Microsomes and Human UDP-Glucuronosyltransferases UGT1A6, UGT1A7, and UGT1A9: Development of a High-Sensitivity Glucuronidation Assay for Human Tissue. *Drug Metab. Dispos.* **2001**, *29*, 1096–1101.

86. CDC (Centers for Disease Control). Urinary Volatile Organic Compound Metabolites: Reference Ranges, Chemical Structures and Parent Compounds Volatile Organic Compounds Laboratory, CDC/DLS/Tobacco and Volatiles Branch; 2017. Available online: https://biomonitoring.ca.gov/sites/default/files/downloads/CDC_VOCMetaboliteTable_July2017.pdf (accessed on Jun 18, 2018).

87. Stevens, J. F.; Maier, C. S. Acrolein: sources, metabolism, and biomolecular interactions relevant to human health and disease. *Mol. Nutr. Food Res.* **2008**, *52*, 7–25, doi:10.1002/mnfr.200700412.

88. IARC (International Agency for Research on Cancer). IARC Monographs on the Evaluation of Carcinogenic Risks to Humans Smokeless Tobacco and Some Tobacco-specific Nitrosamines, vol. 89. Lyon, France: WHO; 2007. Available online: https://monographs.iarc.fr/wp-content/uploads/2018/06/mono89.pdf (accessed on May 30, 2018).

89. Hecht, S. S. Tobacco Smoke Carcinogens and Lung Cancer. *J. Natl. Cancer Inst.* **1999**, *91*, 1194–1210, doi:10.1093/jnci/91.14.1194.

90. Hoffmann, D.; Hecht, S. S. Nicotine-derived N-Nitrosamines and Tobacco-related Cancer: Current Status and Future Directions. *Cancer Res.* **1985**, *45*, 935–944.

91. Hecht, S. S. Biochemistry, Biology, and Carcinogenicity of Tobacco-Specific N-Nitrosamines. *Chem. Res. Toxicol.* **1998**, *11*, 559–603, doi:10.1021/TX980005Y.

92. Breyer-Pfaff, U.; Martin, H.-J.; Ernst, M.; Maser, E. Enantioselectivity of carbonyl reduction of 4-methylnitrosamino-1-(3-pyridyl)-1-butanone by tissue fractions from human and rat and by enzymes isolated from human liver. *Drug Metab. Dispos.* **2004**, *32*, 915–922.

93. Yuan, J.-M.; Koh, W.-P.; Murphy, S. E.; Fan, Y.; Wang, R.; Carmella, S. G.; Han, S.; Wickham, K.; Gao, Y.-T.; Yu, M. C.; Hecht, S. S. Urinary levels of tobacco-specific nitrosamine metabolites in relation to lung cancer development in two prospective cohorts of cigarette smokers. *Cancer Res.* **2009**, *69*, 2990–2995, doi:10.1158/0008-5472.CAN-08-4330.

94. Yuan, J.-M.; Knezevich, A. D.; Wang, R.; Gao, Y.-T.; Hecht, S. S.; Stepanov, I. Urinary levels of the tobacco-specific carcinogen N'-nitrosonornicotine and its glucuronide are strongly associated with esophageal cancer risk in smokers. *Carcinogenesis* **2011**, *32*, 1366–1371, doi:10.1093/carcin/bgr125.

95. Carmella, S. G.; Ming, X.; Olvera, N.; Brookmeyer, C.; Yoder, A.; Hecht, S. S. High throughput liquid and gas chromatography-tandem mass spectrometry assays for tobacco-specific nitrosamine and polycyclic aromatic hydrocarbon metabolites associated with lung cancer in smokers. *Chem. Res. Toxicol.* **2013**, *26*, 1209–17, doi:10.1021/tx400121n.

96. Castro, D.; Slezakova, K.; Delerue-Matos, C.; Alvim-Ferraz, M. da C.; Morais, S.; Pereira, M. do C. Polycyclic aromatic hydrocarbons in gas and particulate phases of indoor environments influenced by tobacco smoke: Levels, phase distributions, and health risks. *Atmos. Environ.* **2011**, *45*, 1799–1808, doi:10.1016/J.ATMOSENV.2011.01.018.

97. Ewa, B.; Danuta, M.-Š. Polycyclic aromatic hydrocarbons and PAH-related DNA adducts. *J. Appl. Genet.* **2017**, *58*, 321–330, doi:10.1007/s13353-016-0380-3.

98. Gil, L.; Adonis, M. Genomics and proteomics offers new hopes towards a personalized approach to lung cancer prevention and treatment. *Electron. J. Biotechnol.* **2003**, *6*, doi:10.2225/vol6-issue3-fulltext-i01.

99. St Helen, G.; Goniewicz, M. L.; Dempsey, D.; Wilson, M.; Jacob, P.; Benowitz, N. L. Exposure and Kinetics of Polycyclic Aromatic Hydrocarbons (PAHs) in Cigarette Smokers. *Chem. Res. Toxicol.* **2012**, *25*, 952–964, doi:10.1021/tx300043k.

100. WHO (World Health Organization). Air Quality Guidelines for Europe. Second Edition; 2000. Available online: http://www.euro.who.int/__data/assets/pdf_file/0005/74732/E71922.pdf (accessed on Jul 15, 2018).

101. Kim, K.-H.; Jahan, S. A.; Kabir, E.; Brown, R. J. C. A review of airborne polycyclic aromatic hydrocarbons (PAHs) and their human health effects. *Environ. Int.* **2013**, *60*, 71–80, doi:10.1016/J.ENVINT.2013.07.019.

102. Wilson, V. L.; Foiles, P. G.; Chung, F.-L.; Povey, A. C.; Frank, A. A.; Harris, C. C. Detection of acrolein and crotonaldehyde DNA adducts in cultured human cells and canine peripheral

blood lymphocytes by 32P-postlabeling and nucleotide chromatography. *Carcinogenesis* **1991**, *12*, 1483–1490, doi:10.1093/carcin/12.8.1483.

103. Snyder, R.; Hedli, C. C. An overview of benzene metabolism. *Environ. Health Perspect.* **1996**, *104*, 1165–1171.

104. Snyder, R. Leukemia and benzene. *Int. J. Environ. Res. Public Health* **2012**, *9*, 2875–2893, doi:10.3390/ijerph9082875.

105. Gregg, E. O.; Minet, E.; McEwan, M. Urinary biomarkers of smokers' exposure to tobacco smoke constituents in tobacco products assessment: a fit for purpose approach. *Biomarkers* **2013**, *18*, 467–486, doi:10.3109/1354750X.2013.821523.

106. Waidyanatha, S.; Rothman, N.; Fustinoni, S.; Smith, M. T.; Hayes, R. B.; Bechtold, W.; Dosemeci, M.; Guilan, L.; Yin, S.; Rappaport, S. M. Urinary benzene as a biomarker of exposure among occupationally exposed and unexposed subjects. *Carcinogenesis* **2001**, *22*, 279–286, doi:10.1093/carcin/22.2.279.

107. Andreoli, R.; Spatari, G.; Pigini, D.; Poli, D.; Banda, I.; Goldoni, M.; Riccelli, M. G.; Petyx, M.; Protano, C.; Vitali, M.; Barbaro, M.; Mutti, A. Urinary biomarkers of exposure and of oxidative damage in children exposed to low airborne concentrations of benzene. *Environ. Res.* **2015**, *142*, 264–272, doi:10.1016/j.envres.2015.07.003.

108. Bernhard, D.; Rossmann, A.; Wick, G. Metals in cigarette smoke. *IUBMB Life (International Union Biochem. Mol. Biol. Life)* **2005**, *57*, 805–809, doi:10.1080/15216540500459667.

109. Järup, L. Hazards of heavy metal contamination. *Br. Med. Bull.* **2003**, *68*, 167–182, doi:10.1093/bmb/ldg032.

110. Rabinowitz, M. B.; Wetherill, G. W.; Kopple, J. D. Kinetic analysis of lead metabolism in healthy humans. *J. Clin. Invest.* **1976**, *58*, 260–270, doi:10.1172/JCI108467.

111. WHO (World Health Organization) Task Group on Environmental Health Criteria for Cadmium.; Friberg, L.; Elinder, C.-G.; Kjellström, T.; United Nations Environment Programme.; International Labour Organisation.; World Health Organization.; International Program on Chemical Safety. Cadmium. Geneva, Switzerland; 1992. Available online: http://www.inchem.org/documents/ehc/ehc/ehc134.htm (accessed on Jul 3, 2018).

112. Richter, P.; Faroon, O.; Pappas, R. S. Cadmium and Cadmium/Zinc Ratios and Tobacco-Related Morbidities. *Int. J. Environ. Res. Public Health* **2017**, *14*, doi:10.3390/ijerph14101154.

113. Satarug, S.; Ujjin, P.; Vanavanitkun, Y.; Nishijo, M.; Baker, J. R.; Moore, M. R. Effects of cigarette smoking and exposure to cadmium and lead on phenotypic variability of hepatic CYP2A6 and renal function biomarkers in men. *Toxicology* **2004**, *204*, 161–73, doi:10.1016/j.tox.2004.06.022.

114. Joseph, A.; Spector, L.; Wickham, K.; Janis, G.; Winickoff, J.; Lindgren, B.; Murphy, S. Biomarker evidence of tobacco smoke exposure in children participating in lead screening. *Am. J. Public Health* **2013**, *103*, e54–e59, doi:10.2105/AJPH.2013.301315.

115. Leung, T. F.; Chan, I. H. S.; Liu, T. C.; Lam, C. W. K.; Wong, G. W. K. Relationship Between Passive Smoking Exposure and Urinary Heavy Metals and Lung Functions in Preschool Children. *Pediatr. Pulmonol.* **2013**, *48*, 1089–1097, doi:10.1002/ppul.22801.

116. Sánchez-Rodríguez, J. E.; Bartolomé, M.; Cañas, A. I.; Huetos, O.; Navarro, C.; Rodríguez,

A. C.; Arribas, M.; Esteban, M.; López, A.; Castaño, A. Anti-smoking legislation and its effects on urinary cotinine and cadmium levels. *Environ. Res.* **2015**, *136*, 227–233, doi:10.1016/j.envres.2014.09.033.

117. Czogala, J.; Goniewicz, M. L. The Complex Analytical Method for Assessment of Passive Smokers' Exposure to Carbon Monoxide. *J. Anal. Toxicol.* **2005**, *29*, 830–834, doi:10.1093/jat/29.8.830.

118. Raub, J. A.; Mathieu-Nolf, M.; Hampson, N. B.; Thom, S. R. Carbon monoxide poisoning — a public health perspective. *Toxicology* **2000**, *145*, 1–14, doi:10.1016/S0300-483X(99)00217-6.

119. Czogala, J.; Goniewicz, M. L. Carbon monoxide levels in main- and sidestream smoke from cigarettes of selected brands and estimation of active and passive smokers exposure to this compound. *Ann Pol Chem Soc.* **2003**, *2*, 316–320.

120. Secker-Walker, R.; Vacek, P.; Flynn, B.; Mead, P. Smoking in Pregnancy, Exhaled Carbon Monoxide, and Birth Weight. *Obstet. Gynecol.* **1997**, *89*, 648–653, doi:10.1016/S0029-7844(97)00103-8.

121. Zhou, S.; Behrooz, L.; Weitzman, M.; Pan, G.; Vilcassim, R.; Mirowsky, J. E.; Breysee, P.; Rule, A.; Gordon, T. Secondhand hookah smoke: An occupational hazard for hookah bar employees. *Tob. Control* **2017**, *26*, 40–45, doi:10.1136/tobaccocontrol-2015-052505.

122. Kim, J.; Lee, K.; Kwon, H.-J.; Lee, D. H.; Kim, K. Association between Secondhand Smoke in Hospitality Venues and Urinary 4-(methylnitrosamino)-1-(3-pyridyl)-1-butanol Concentrations in Non-Smoking Staff. *Int. J. Environ. Res. Public Health* **2016**, *13*, doi:10.3390/ijerph13111101.

123. Kim, J.; Kwon, H.-J.; Lee, K.; Lee, D.-H.; Paek, Y.; Kim, S.-S.; Hong, S.; Lim, W.; Heo, J.-H.; Kim, K. Air Quality, Biomarker Levels, and Health Effects on Staff in Korean Restaurants and Pubs Before and After a Smoking Ban. *Nicotine Tob. Res.* **2015**, *17*, 1337–1346, doi:10.1093/ntr/ntv012.

124. Bekö, G.; Morrison, G.; Weschler, C.; Koch, H.; Palmke, C.; Salthammer, T.; Schripp, T.; Toftum, J.; Clausen, G. Measurements of dermal update of nicotine directly from air and clothing. *Indoor Air* **2017**, *27*, 427–433, doi:10.1111/ina.12327.

125. Bekö, G.; Morrison, G.; Weschler, C. J.; Koch, H. M.; Pälmke, C.; Salthammer, T.; Schripp, T.; Eftekhari, A.; Toftum, J.; Clausen, G. Dermal uptake of nicotine from air and clothing: Experimental verification. *Indoor Air* **2018**, *28*, 247–257, doi:10.1111/ina.12437.

3. Development of a quick and cost-effective method for determining tobacco-specific toxicants in indoor dust

UNIVERSITAT ROVIRA I VIRGILI
ADVANCES ON THIRDHAND SMOKE USING TARGETED AND UNTARGETED APPROACHES
Sònia Torres Gené

3.1 Abstract

Thirdhand smoke (THS) is a new term given to the tobacco smoke particles and toxicants that remain on surfaces and in dust long after active smoking has ceased. A main characteristic of THS is the fact that it becomes increasingly toxic with age, reemitting back into the gas phase and/or reacting with environmental chemicals producing secondary toxicants, like carcinogens. THS remains in indoor environments long after smokers move out which makes it a serious public health concern. The aim of this study is the development of a high-throughput method to determine six tobacco specific toxicants in house dust, including nicotine, cotinine and four tobacco-specific nitrosamines. Two extraction approaches have been tested: a quick, easy, cheap, effective, rugged and safe (QuEChERS) extraction method and ultra-sound assisted solvent extraction. Different extraction solvents, solvent combinations, solvent ratios and clean-up sorbents were compared. The best performance was obtained with a QuEChERS based method, using basic water to hydrate the dust samples and acetonitrile as the extraction solvent, together with the European Committee for Standardization salt mixture followed by a clean-up step using a Z-sep+ sorbent. The extracts were analysed by liquid chromatography-tandem mass spectrometry in multiple reaction monitoring mode. The repeatability of all the method optimization stages was between 3-9%. To our knowledge, this is the first time that a QuEChERS method has been developed for the extraction of tobacco-specific nitrosamines and for the extraction of house dust. The developed method was used in smokers' and non-smokers´ house dust samples from the Tarragona area.

3.2 Introduction

Indoor dust is rising attention as a key environmental matrix to assess human exposure. Indoor dust particles act as a sink and a repository of both outdoor and indoor contaminants that could enter the human body through ingestion, skin absorption and in less extent, by inhalation of re-suspended particles [1]. Therefore, indoor dust constitutes an important route of toxicant exposure, often overlooked, that especially affects young children, because of their hand-to-mouth behaviours and the fact that they spend over 90% of their time indoors [2]. Characterization of the toxicants present in indoor dust are not only a measure of indoor and outdoor contamination, but also provides valuable information for the assessment of children indoor exposure [3].

Recent studies revealed the ubiquitous presence of tobacco smoke toxicants in outdoor airborne particles and settled dust from cars and homes, including those with strict smoking bans [3–5]. Secondhand smoke (SHS), considered carcinogen to humans by the International Agency for Research on Cancer (IARC 2004), is formed by a mixture of gases and particles from the burning of tobacco and the smoke exhaled by smokers ref. IARC. Exposure to SHS is estimated to be the cause of about 1.0% of worldwide mortality, approximately 600,000 deaths each year [6]. However, the risks of tobacco exposure do not end when a cigarette is extinguished, as most SHS particles and toxicants that remain on surfaces and in dust long after active smoking has ceased forming the so-called thirdhand smoke (THS) [7]. THS is a new term given to the tobacco smoke particles and toxicants that remain on surfaces and in dust long after active smoking has ceased. A main characteristic of THS is the fact that it becomes increasingly toxic with age, reemitting back into the gas phase and/or reacting with environmental chemicals producing secondary toxicants, like carcinogens[7]. Exposure to THS can occur through inhalation,

ingestion and dermal contact, making children with smoking parents the most vulnerable population to THS [8].

The analysis of contaminants in dust requires the use of exhaustive extraction techniques due to the complexity of dust composition and the high adsorption capacity of dust particles. The most widely extraction techniques used in the analysis of dust are Soxhlet extraction, pressurized liquid extraction (PLE), pressurized solvent extraction (PSE), accelerated solvent extraction (ASE) and extraction assisted by sonication or mechanical agitation [9]. As innovation the QuEChERS method has been recently applied in the analysis of urban dust [10].

For the characterization of indoor smokers' environments, several studies have determined nicotine in house dust, using different methods like solid phase extraction (SPE) [11–13], sonication or mechanical agitation followed by a evaporation step [8,14–16]. Liquid-liquid extraction followed by sonication and PLE have been successfully applied for the simultaneous determination of nicotine and TSNAs in dust [17,18]. However, PLE is a high time and solvent consuming method and the temperature applied can lead to degradation of TSNAs since they are thermally unstable. For the determination of nicotine, cotinine and TSNAs the most common analytical technique used is gas chromatography (GC) [17]. GC has been coupled with different detectors such as, mass spectrometry (MS) [14], especially ion trap MSMS [19]; thermal energy analysis [20]; and nitrogen chemiluminescence detector (NCD) [21]. Comprehensive gas chromatography (GC×GC) has also been used in combination with NCD [17]. Whereas GC is usually the preferred method for determining nicotine, liquid chromatography (LC) coupled to tandem mass spectrometry is commonly used for the analysis of TSNAs. [11–13,22–24].

Hence, the main objective of this study is to develop a quick, efficient and robust analytical method for determining specific THS toxicants in dust samples. The selected toxicants are nicotine —the most abundant compound emitted during smoking [25]—, cotinine — the predominant nicotine metabolite—, the two carcinogenic TSNAs — N'-nitrosonornicotine (NNN), 4-(methylnitrosoamino)-1-(3-pyridyl)-1-butanone (NNK) —, 4-(methylnitrosoamino)-1-(3-pyridyl)-1-butanol (NNAL) —the main NNK degradation product—, and 4-(methylnitrosamino)-4-(3-pyridyl)-butanal (NNA), which has been proposed as specific marker for THS formation [25]. We have compared two different extraction procedures: QuEChERS and sonication and the performance of several variables such as extraction solvent, pH and solvent ratio have been tested. We have also studied the adequacy of a clean-up step prior to analysis based on dispersive solid phase extraction and the efficiency of different types and sorbent ratio. The applicability of the method has been tested by the analysis of a subset of indoor dust samples from smokers' and from non-smokers homes.

3.3 Experimental

3.3.1 Reagents and standards

The individual standards of nicotine and cotinine and their internal standards were supplied by Sigma Aldrich (St. Louis, USA). The rest of the standards were supplied by Toronto Research Chemicals (North York, Canada), including the four target TSNAs N-nitrosonornicotine (NNN), 4-(methylnitrosoamino)-1-(3-pyridyl)-1-butanone (NNK), 4-(methylnitrosamino)-4-(3-pyridyl)-butanal (NNA) and 4-(methylnitrosamino)-1-(3-pyridyl)-1-butanol

(NNAL) and the internal standards nicotine-d3, cotinine-d3, 5-(1-Nitroso-2-pyrrolidinyl)pyridine-2,3,4,6-d4 (NNN-d4), 4-[(methyl-d3)nitrosoamino]-1-(3-pyridyl)-1-butanone (NNK), 4-[(methyl-d3)nitrosamino]-4-(3-pyridyl)butanal (NNA-d3) and 4-(methyl-d3-nitrosamino)-1-(3-pyridyl)-1-butanol (NNAL-d3). The main physicochemical characteristics of the target compounds as well as the concentration range in which these compounds have been previously found in dust are listed in Table 1.

The European Committee for Standardization (CEN) extraction salts were from Scharlab, (Sentmenat, Spain). All solvents tested were LC-MS grade, including acetonitrile (from Scharlab), isopropanol, methanol and ethyl acetate (supplied by ChemLab, Zedelgem, Belgium). We tested performance of different clean-up sorbents including primary/secondary amines (PSA, supplied by Agilent), C18, graphitized carbon black (GCB) and Z-sep+ (from Sigma Aldrich).

The concentrated standard solutions of the target compounds were prepared in methanol and stored in small aliquots at -80°C. The diluted mixtures were daily prepared in the different tested solvents.

Table 1. Chemical structures, molecular weight (MW), acid strength (pKa), partition coefficient (logP) and concentration ranges in smokers' and non-smokers' house dust of each compound of interest. Concentration ranges correspond to median/geometric mean values collected in [26]. *Minimum and median values from [3].

Compound	Chemical Name	pKa [a] (strongest basic)	log K_{ow} [b]	Concentration ranges in house dust	
				Smokers (ng/g)	Non-smokers (ng/g)
Nicotine	3-(1-methylpyrrolidin-2-yl)pyridine	8.6	0.87	$7x10^3$-$26x10^3$	510-2.310^3
Cotinine	1-methyl-5-(pyridin-3-yl)pyrrolidin-2-one	4.8	0.39	430-460	26-54
NNN	N'-Nitrosonornicotine	4.8	0.71	1.6 - 20	1.3 - 4
NNK	4-(N-Methyl-N-nitrosamino)-1-(3-pyridyl)-1-butanone	3.8	0.33	3.7 - 540	0.45 -20
NNA	4-(methylnitrosamino)-4-(3-pyridyl)butanal	-	0.04	0.46 - 0.6	<0. 45
NNAL	4-(methylnitrosamino)-1-(3-pyridyl)-1-butanol	4.7	0.48	n.d-460*	n.d-30*

[a] Predicted with ChemAxon, HMDB

[b] Predicted median [CompTox database]

3.3.2 Sample collection and pretreatment

Indoor house dust was collected from non-smokers' and smokers' private homes in the area of Tarragona (north-eastern Spain), using vacuum cleaners in regular use in households. In this study we considered smokers' homes, those in which at least one of the regular occupants was a conventional tobacco smoker, even if they only smoke outside the home (i.e. balcony or terrace). Non-smoking homes were those where residents have never smoked or who have quit smoking at least one year before sampling, and in which no visitor has smoked in the last 30 days. The collected dust was sieved using a stainless-

steel sieve with a 100 μm mesh size and stored at -20°C in pre-weighted amber glass vials.

Method optimization and validation was performed using a pool of non-smokers' house dust from suburban areas (likely less polluted with THS toxicants)[3]. Spiked samples were prepared by adding different volumes of standard solution of the target compounds and the internal standards in acetone, adding enough volume to soak the dust. The mixtures were homogenized and kept in a cupboard funnel at room temperature until the complete evaporation of the solvent. The dried spiked dust samples were stored at -20°C in pre-weighted amber glass vials and extracted within 2 days..

3.3.3 Extraction

Indoor dust samples were extracted using a QhEChERS extraction method. Under the optimized conditions, we placed 300 mg of dust sample, spiked with a mixture of the labelled surrogate standards at a concentration of 0.5 $\mu g\ g^{-1}$, into 15 mL centrifuge tubes and added 665 mL of KOH 0.1 M in ultrapure water. After shaking the tube vigorously for 1 min, we added 2 mL of ACN followed by 0.5 g of the European Committee for Standardization (CEN) extraction method salt mixture [27], which consisted of 307 mg of anhydrous magnesium sulphate, 77 mg of sodium chloride, 38 mg of sodium citrate dibasic sesquihydrate and 77 mg of sodium citrate tribasic dihydrate. We vigorously shook the sample tube followed by vortex mixing for 1 min and further centrifugation at 4°C and 4000 rpm for 5 min. We transfered a 1.6 mL aliquot of the supernatant phase (ACN layer) to a 2 mL tube containing 50 mg of clean-up sorbent mixture (42.9 mg $MgSO_4$ and 7.1 mg Supel Que Z-sep$^+$). The tube was next vortex mixed for 1 min and centrifuged under the above described conditions. A 1.4 mL aliquot of the supernatant phase was filtered with a 0.22 μm Nylon syringe filter into a 2 mL

amber glass autosampler vial, ready to be analysed by UPLC-MS/MS.

Efficiency of the QuEChERS extraction was tested using different organic solvents (including acetonitrile, isopropanol, ethyl acetate and methanol and mixtures of them), solvent ratio, pH and different clean-up sorbents (including PSA, C_{18}, GCB and Supel Que Z-sep^{+}). We also compared the performance of the QuEChERS extraction against ultrasound-assisted extraction (sonication for 15 min at room temperature) using ACN and MeOH. Discussion of these tests can be found in section 3.4.2.

3.3.4 UHPLC-MS/MS analysis

Determination of the target compounds was performed by the direct injection of 1 µL of the dust extracts on the chromatographic system, consisting on a UHPLC 1290 Infinity II Series instrument coupled to a 6490 iFunnel triple quadrupole mass spectrometer, both from Agilent (Agilent Technologies, Sta. Clara, CA, USA). Chromatographic separation was achieved on a Kinetex® EVO C18 column (100×21mm i.d., 1.7 µm particle size, 100 Å pore size), kept at 30°C, at a flow of 0.45 mL min-1. The mobile phase consisted on 0.1 mM of ammonium acetate in ultrapure water (solvent A) and methanol with 0.1% of formic acid (solvent B). The solvent gradient was programmed as follows: initially 1% of solvent B changed to 100% of solvent B in 8 min, kept at 100% of solvent B for 2 min, returned to the initial conditions in 1 min and kept for 5 min to allow column re-equilibration.

The targeted compounds were ionized in an electrospray source in positive mode (ESI +). The mass spectrometer was operated at a nitrogen gas flow of 14 L min-1, gas temperature at 240 °C, ion spray voltage at 3,500 V, and nebulizer gas pressure at 50 psi. The product ion spectra of the target compounds were measured in multiple reaction monitoring (MRM) scan mode at scan range of

m/z 40-400 and fragmentor voltage of 380 V. Identification of the target compounds was performed using one quantifier transition and one qualifier transition. Collision energy for each transition was selected using the Mass Hunter Optimizer Software (Agilent Technologies, Sta. Clara, USA). Compounds were quantified by internal calibration.

3.4 Results and discussion

3.4.1 UHPLC-MS/MS

In this study, we have tested different mobile phases, being the combination of ammonium acetate and formic acid the one that provided a better peak shape and resolution of the target compounds in less than 4 min.

Since the samples were dissolved in acetonitrile, we tested acetonitrile with 0.1% of formic acid as solvent B and kept the same solvent A. It was observed that methanol provided better compound separation and peak intensities for nicotine, cotinine, NNAL, NNN, NNA and NNK were 53%, 12%, 10%, 40%, 92% and 40% were higher when using methanol, hence it was chosen as the organic solvent for the mobile phase.

MS/MS parameters were optimized by the consecutive injection of 1 µL of the individual standards at 1 mg L-1 of a mixture of the standards in a mobile phase composition of 30:70 of solvent A and B. The best parameters for each transition are described in section 3.3.3. For most of the target compounds the precursor ion with higher abundance was the molecular protonated ion $[M-H]^+$ except for NNA and its labelled standard (NNA-d3), which the most abundant precursor ion was [M+40]+, probably corresponding to the formation of the

[M+CH3OH+H]+ adduct. The collision energies (0-50 eV) for the fragmentation of the precursor ions of these compounds were also automatically optimized. The chosen collision energies showed partially fragmented precursor ions and larger product ions the MRM conditions for all compounds are listed in Table 2.

Table 2. Target compounds in elution order, their retention time (t_R) expressed in min, precursor ion, quantitative* and qualitative product ions, and each collision energy used for compound quantification in dust samples.

Compound	t_R (min)	Precursor Ion (m/z)	Product Ion*(m/z), CE (eV)	Product Ion (m/z), CE (eV)
Nicotine	1.96	163	132 (5)	84 (5)
Nicotine-d_3	1.97	166	130 (20)	87 (20)
NNAL	2.88	210	93 (10)	180 (5)
NNAL-d_3	2.88	213	183 (5)	93 (10)
Cotinine	2.93	177	80 (5)	98 (5)
Cotinine-d_3	2.92	180	101 (20)	80 (25)
NNN	3.11	178	148 (5)	120 (10)
NNN-d_4	3.12	182	152 (8)	124 (8)
NNA	3.26	240	106 (10)	179 (5)
NNA-d_3	3.25	243	106 (8)	179 (5)
NNK	3.57	208	122 (5)	106 (10)
NNK-d_4	3.57	212	126 (8)	83 (52)

3.4.2 Indoor dust extraction

3.4.2.1 Extraction technique and solvent selection

Initial experiments were carried out to select extraction technique and solvent. For the QuEChERS extraction, we choose the CEN salt mixture for the salting-out step as it has been successfully used in environmental matrices and it has demonstrated less interferences when a further PSA clean-up is required, compared to the AOAC Method [28]. The initial QuEChERS extraction conditions

were adapted from the official CEN method [27], using 2 mL of water to hydrate the dust prior to the addition of 2 mL of the tested organic solvent.

Despite acetonitrile is the ultimate extraction solvent used in the regular methodology, several solvents were tested in the present study in order to compare their extraction efficiencies, including isopropanol, acetonitrile, acetonitrile: ethyl acetate 80:20 (v/v), acetonitrile: methanol 80:20 (v/v) and methanol: H2O 90:10 (v/v). Acetonitrile and methanol were the solvents used to test the performance of sonication. A matrix-matched calibration curve was used to calculate absolute recoveries. Specifically, in LC-MS, ion suppression/enhancement effects due to matrix can significantly reduce or enhance the analyte response [29], hence the matrix matching approach was used. In order to obtain a matrix-matched calibration curve, non-spiked samples were extracted following the established procedure and spiked at different concentrations (from 0.2 to 0.6 μg/mL) before the filtering step and following analysis. The coefficient of determination (R^2) for all matrix-matched calibration curves was higher than 0.991 for all compounds. The obtained recoveries were absolute recoveries because they do not take into account the differences caused by the matrix effect, only the extraction yield. The absolute recoveries obtained with the different extraction solvents and methods are shown in Figure 2.

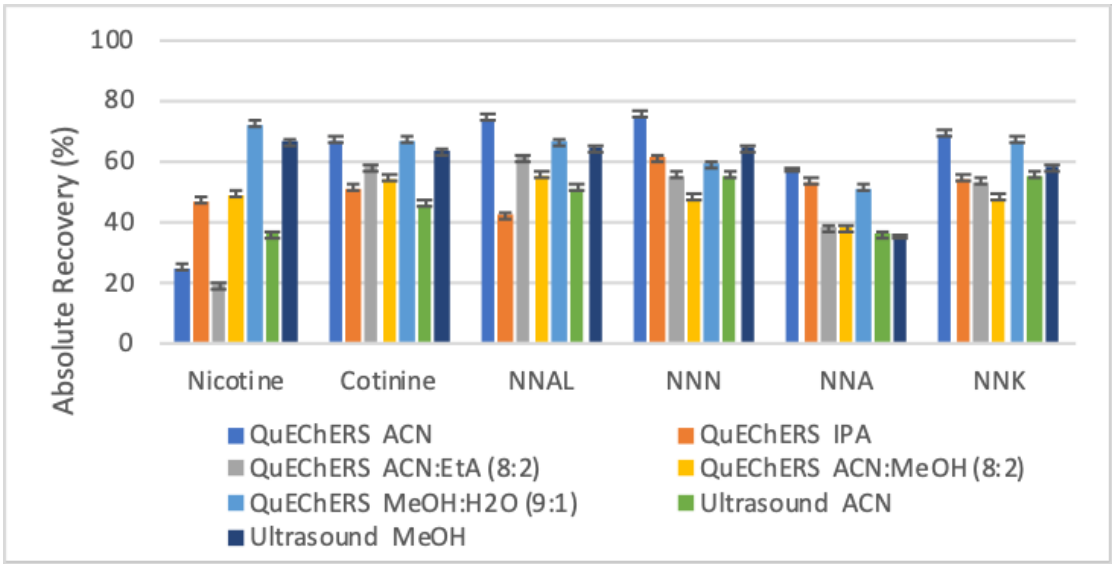

Figure 2. Absolute recoveries (expressed in %) and their relative standard deviation (%RSD, in error bars) obtained with different extraction solvents for the QuEChERS extraction and the ultrasound-assisted extraction methods, using a matrix-matched calibration curve.

Acetonitrile was the first solvent tested, as it is the most commonly used extraction solvent for a QuEChERS extraction method [17]. The obtained recoveries ranged between 67 and 75% for cotinine and the TSNAs, but were around 25% for nicotine, which was considered too low. A more polar solvent than acetonitrile, isopropanol was next tested in order to improve the nicotine recovery. The recovery for nicotine was 47% and the rest ranged between 42-61%. Several combinations of acetonitrile with ethyl acetate and methanol were separately tested. The combination with a less polar solvent than acetonitrile, ethyl acetate, resulted in lower recoveries (between 19 and 61%) compared to the combination with a more polar solvent than acetonitrile, methanol (recoveries ranged between 38-55%). In order to improve the nicotine recovery, a mixture of methanol and H_2O (90:10 v/v) was also tested as organic solvent as a previous study showed it was the best solvent to extract red beetroot betalains [30]. Although that study was considered a QuEChERS extraction, no salting-out effect occurred and only one mixed phase was

obtained after the addition of the extraction salts. Nevertheless, nicotine recoveries were the highest (72%) and the recoveries of the rest of the target compounds ranged between 51-72%. These higher recoveries are understandable because no compounds were lost as they were all present in the mixed phase. However, peak areas were between 10-20% smaller compared to those obtained with the previously mentioned extraction solvents, concluding that the methanol/water mixture induced to a higher matrix effect. Recoveries of sonication tests were between 36-55% when using acetonitrile and between 36-66% with methanol.

Even though a low nicotine recovery (25%) was obtained with acetonitrile as the QuEChERS extraction solvent, the recoveries for cotinine and TSNAs were the best ones out of all the solvents tested so far. Moreover, nicotine is the major compound present in dust samples, found always at higher concentrations than cotinine and TSNAs (as shown in Table 1). Taking this into consideration, a solvent with high recoveries for cotinine and TSNAs was prioritized.

In order to enhance nicotine recovery a pH modification was tested. As seen in Table 4, recoveries for acetonitrile with 0.1% of acetic acid were generally lower (between 19% and 75%) than the ones obtained with acetonitrile (between 25% and 74%). All of these compounds of interest are protonated in an acidic solution and some of them will mainly stay in the aqueous phase, and therefore discarded. Conversely, a basic solution has the opposite effect, in which the compounds of interest will remain in the organic phase, which is the relevant phase that is kept. This phenomenon is reflected in the obtained recoveries. The recovery of nicotine and cotinine obtained with the acidified solution ranged from 19-28% versus the 60-70% obtained with the basified solution (0.1M KOH).

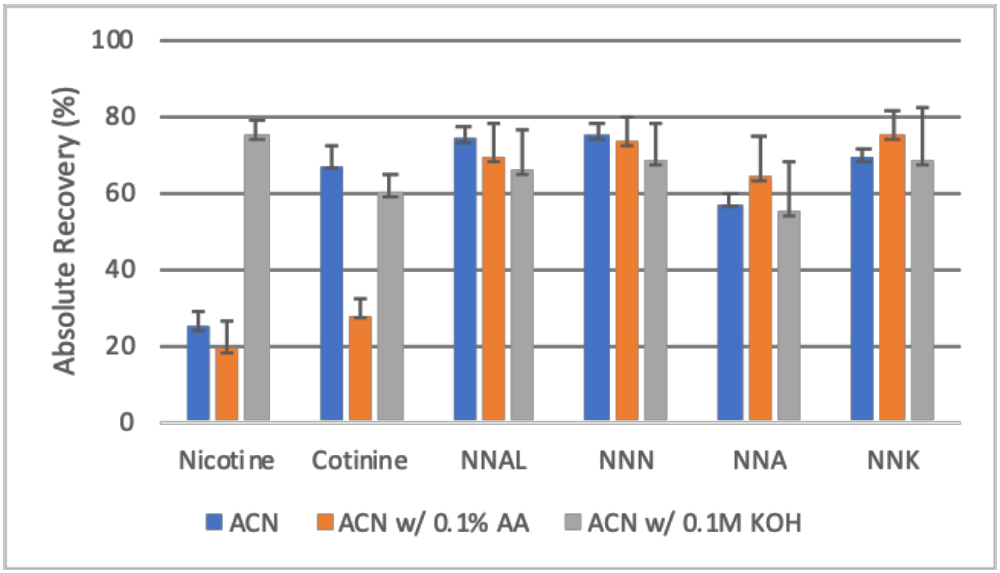

Figure 3. Absolute recoveries (expressed in %) and their relative standard deviation (%RSD, in error bars) obtained in the pH modification tests for the QuEChERS extraction method, using a matrix-matched calibration curve.

Considering all the results, acetonitrile with 0.1M KOH aqueous solution was selected for subsequent optimization steps. Even though TSNAs recoveries were between 1-8% lower than those obtained in neutral conditions, the nicotine recovery was 50% higher. RSDs ranged between 2-14% for all the solvent tests, showing a great repeatability.

Extraction time, centrifugation time, speed and the type of extraction salts were not optimized any further because their optimization was considered to be well established by already published literature [28,31].

3.4.2.2 Solvent ratio

The QuEChERS method is usually applied to samples with a high water content (for example, fruit and vegetables) but it can be applied to dried samples if the sample weight is reduced and water is added up to the sample

weight proposed by the official methods [27,32]. 300 mg of dust (spiked at 5 μg/g for nicotine and 1 μg/g for cotinine and the TSNAs) was weighed into a 15 mL centrifuge tube and 2 mL of 0.1M KOH aqueous solution was added prior to the extraction procedure. Moreover, in order to optimize the solvent ratio, 2 mL, 1 mL and 0.6 mL of KOH aqueous solution were added to different samples. The volume of acetonitrile was fixed at 2 mL, in order to be able to compare the solvent ratio optimization results with the extraction solvent optimization results.

Matrix-matched calibration curves was used to calculate these absolute recoveries. As nicotine is always found at higher concentrations in dust samples compared to cotinine and TSNAs, the matrix-matched calibration curve was prepared from 0.3 to 0.6 μg/mL for nicotine and from 0.05 to 0.5 μg/mL for cotinine and TSNAs. Coefficients of determination (r^2) were higher than 0.994 for all compounds. Figure 3 shows the absolute recoveries obtained with the different solvent ratios.

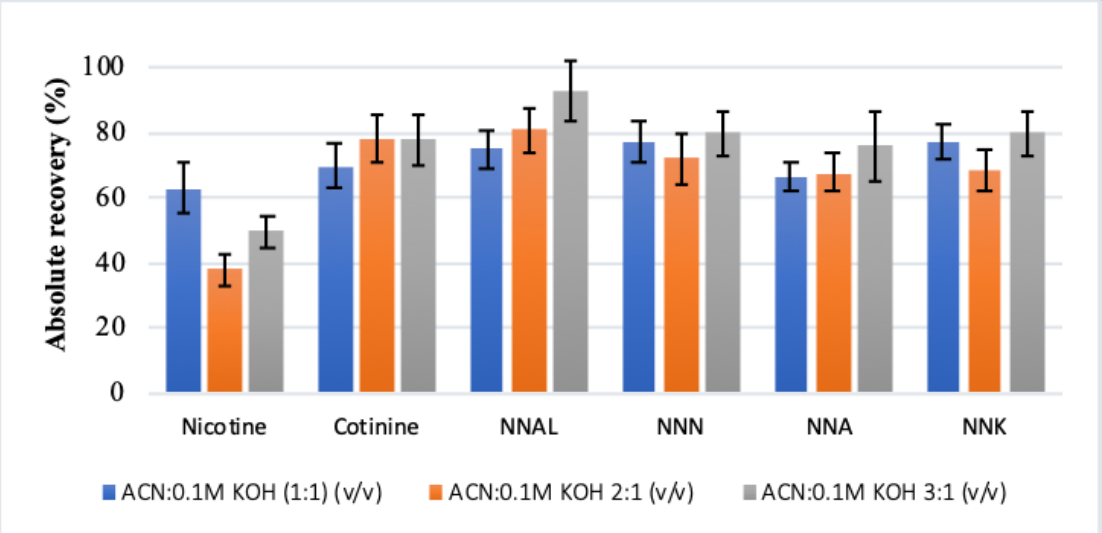

Figure 4. Absolute recoveries (%) with their relative standard deviation (%RSD, in error bars) obtained with different solvent ratios for the salting-out liquid-liquid extraction, using a matrix-matched calibration curve.

The best cotinine and TSNAs recoveries were obtained with 2 mL of ACN and 0.665 mL of 0.1M KOH aqueous solution (3:1 ratio), ranging between 76-93%. Even though the best nicotine recovery was obtained using a 1:1 ratio (recovery of 63%) versus the 50% recovery obtained with the 3:1 ratio, this last approach was selected for subsequent optimization steps. All RSDs ranged between 7-14%, showing a good repeatability.

3.4.2.3 dSPE sorbent selection

A sample clean-up step was next optimized in order to reduce matrix interferences. The QuEChERS extraction was combined with a dSPE to remove matrix constituents. Several bulk sorbents were tested, combined with anhydrous $MgSO_4$. They were added to the 1.6 mL aliquots from the organic layer obtained after the salting-out liquid-liquid extraction.

To date, the most common dSPE sorbents used in QuEChERS have been primary-secondary amine (PSA) for the removal of acids, polar pigments and sugars, graphitized carbon black (GCB) for the removal of color pigments and C18 for the removal of lipid and non-polar components. More recently, a Z-sep$^+$ dSPE sorbent has been commercialized. This sorbent is based on the interaction of fats by a Lewis acid-base mechanism with a zirconium (Zr) atom attached to silica solid particle [33]. In a previous study in which nicotine and N-nitrosamines were extracted from house dust by a pressurized liquid extraction method, diatomaceous earth, florisil, C_{18}, silica and alumina were tested. Florisil was in general the most retentive sorbent, C_{18} did not lead to any significant reduction of interferences and silica was chosen as the clean-up sorbent as it was the least retentive one [17]. Taking this into account, PSA/$MgSO_4$, z-sep$^+$/MgSO4, GCB/$MgSO_4$ and C_{18}/$MgSO_4$ were tested as dSPE strategies for reducing the

matrix.

A standard calibration curve of the target compounds prepared in acetonitrile was used to calculate the recoveries obtained in the dSPE optimization. A series of standards across a range of concentrations near the expected concentration of the analytes were prepared. The calibration curve was prepared from 0.01 to 0.6 μg mL^{-1} for nicotine and from 0.002 to 0.15 μg/mL for cotinine and TSNAs. The R^2 was higher than 0.993 for all compounds.

Table 5 shows the apparent recoveries obtained with the different sorbents. These recoveries take into account the differences caused by the matrix effect.

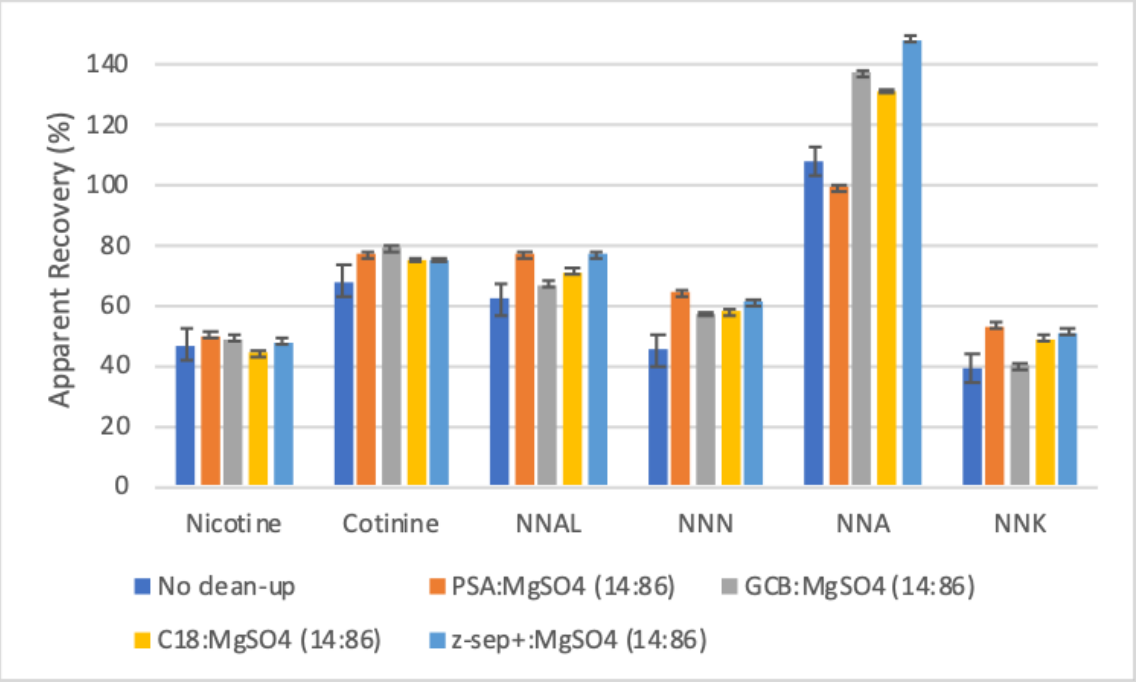

Figure 5. Apparent recoveries (%) with their relative standard deviation (%RSD, in error bars) obtained with different solvent ratios for the salting-out liquid-liquid extraction, using a matrix-matched calibration curve.

For each dSPE test, 14% of sorbent and 86% of $MgSO_4$ was added. These proportions correspond to the commercially available dSPE kits, which are

widely used [28]. The least retentive sorbents were PSA and z-sep$^+$ (14:86). The main difference between them was the recovery of NNA (99% with PSA and 148% for z-sep$^+$). Using the rest of the sorbents, the recovery for NNA was over 100%, showing how, in this case, the matrix effect increases the signal (signal enhancement). Z-sep$^+$ was the selected sorbent hereafter. A larger proportion of z-sep$^+$ (25%) was tested in order to find out if the recoveries improved. The recovery for nicotine decreased (37%) compared to the recovery of 48% obtained with a smaller proportion of z-sep$^+$ (14%). The recoveries for cotinine and TSNAs decreased slightly (between 2-15% lower) proving how this increase in the amount of z-sep$^+$ induced the retention of the compounds. All RSDs ranged between 2-14%, showing a great repeatability. On the basis of these results, z-sep$^+$:$MgSO_4$ (14:86) was the chosen sorbent for the dSPE stage.

Method validation was performed using a calibration curve prepared in acetonitrile using internal standards (IS). The IS were isotopically labelled nicotine-d_3, cotinine-d_3, NNAL-d_3, NNN-d_4, NNA-d_3 and NNK-d_4. Both the matrix-matched calibration and the IS calibration were optimum. However, using matrix-matched calibration curves entails having to create a new calibration curve for every type of matrix. Applied to this study, different matrix-matched calibration curves would have to be created for dust collected from rural areas, urban areas, different geographical areas, cars, etc. Therefore, as IS were available for those compounds, external calibration was chosen for the quantification method.

3.5 Method validaiton

In order to validate the method, we calculated the linear range, the limits of quantification and detection, recovery, repeatability (intra-day) and

reproducibility (day-to-day) by applying the developed method and analysing 5 non-spiked and 5 spiked samples at 100 ng mL^{-1} for nicotine and cotinine and at 10 ng mL^{-1} for the four TSNAs, the results are displayed in Table 3.

Linear range was evaluated by constructing calibration curves in a range of different concentrations (10 calibration points) from 3 ng mL^{-1} to 0.05 ng mL^{-1} for nicotine, 0.015 ng mL^{-1} to 0.05 ng mL^{-1} for cotinine and for the case of TSNAs the lower point of calibration curve corresponded a concentration of 0.015 ng mL^{-1} for NNAL and NNK, 0.05 ng mL^{-1} for NNN and 0.1 ng mL^{-1} for NNA, and the last point of the calibration curve was 1000 ng mL^{-1} for all the TSNAs. Internal standard was spiked at 50 ng mL^{-1}. The linear range was good for all the target compounds with coefficient of determination (r^2) values higher than 0.997.

Repeatability and reproducibility expressed as % Relative Standard Deviation (%RSD) were also calculated using the spiked samples. As can be seen in Table 3, repeatability and reproducibility were below 9%. Recoveries were higher than 74%, except for NNA (55%). Recoveries were comparable to those obtained using more time and solvent consuming analytical methods [17].

The LODs of those compounds that were present in the non-spiked samples (nicotine and cotinine), were calculated using the standard deviation of 5 non-spiked samples extracted and analysed following the developed method. LODs was the concentration of three times the sd and LOQs of ten times the sd. For those compounds not present in the non-spiked samples LODs were established as the concentrations corresponding to a signal/noise ratio of 3 and LOQs were defined as the lowest point of the calibration curve. Thus, instrumental LODs ranged between 5 to 15 pg ml^{-1} and LOQs between 15 to 100 pg ml^{-1}. Method detection limits (MDLs) ranged between 0.03 - 0.40 ng g^{-1}

dust and 0.11 - 2.66 ng g^{-1} dust respectively being cotinine the compound with better performance and NNA the compound with higher values due to its peak shape. NNA is the most polar compound in the mixture making its extraction and analysis with LC-MS more difficult than the others. However, the results in this study show that either the extraction and chromatographic analysis are consistent and reproducible. Other authors converse NNA to its pentafluoro phenylhydrazone derivative to have a satisfactory LC-MS/MS performance [18].

The limits of quantification obtained in this work are two orders of magnitude lower when comparing nicotine quantification with a frequently used method where the LOQ was 10 ng g^{-1} [13]. Comparing with a method developed for the simultaneous quantification of nicotine and TSNAs, LOD was higher 15.6 ng g^{-1} compared to ours 0.2 ng g^{-1} for nicotine quantification. TSNAs presented LODs between 2.5-15 ng g^{-1} which is also higher than the range presented here 0.12-2.66 ng g^{-1} [17].

Table 3. Method parameters: method detection limit (MDL) and method quantification limit (MQL), expressed in ngg^{-1}. Recoveries, repeatability and reproducibility of pooled spiked house dust samples spiked at 100ng/mL of nicotine and cotinine and 10ng/mL of the four TSNAs, method detection limit (MDL) and method quantification limit (MQL), expressed in ngg^{-1}

Compound	LOD ng/g	LOQ ng/g	Recovery (%)		Repeatability (%RSD, n=5)	Reproducibility (%RSD, n=5)
			Low conc.	High conc.		
Nicotine	0.06	0.21	90	89	6.7	8.6
NNAL	0.3	0.92	95	92	2.6	6.9
Cotinine	0.04	0.12	98	94	5.7	7.2
NNN	0.17	0.56	89	85	5.1	8.0
NNK	0.08	0.24	92	88	3.4	5.6
NNA	0.26	0.86	75	74	9.1	10.2

3.6 Application to indoor samples

The optimized method was applied for the determination of nicotine, cotinine and the four TSNAs in settled dust samples from 20 homes, 10 of them from smokers' and 10 of them from non-smokers' homes. Prior to extraction, the sieved house dust samples were spiked with the internal standard mixture at a concentration of 0.5 μg g-1 and were extracted using the developed QuEChERS method. The presence of the compounds detected was confirmed with the quantification and qualitative transition (Table 2) and the matching of the internal standard retention times. A chromatogram of a standard mixture at 0.3 ng mL-1 of nicotine and 0.075 ng mL-1 of cotinine and TSNAs of the calibration curve used for the quantification is presented in Figure 6 shows the extracted ion chromatogram of the two transitions for each compound in a smokers' dust extract.

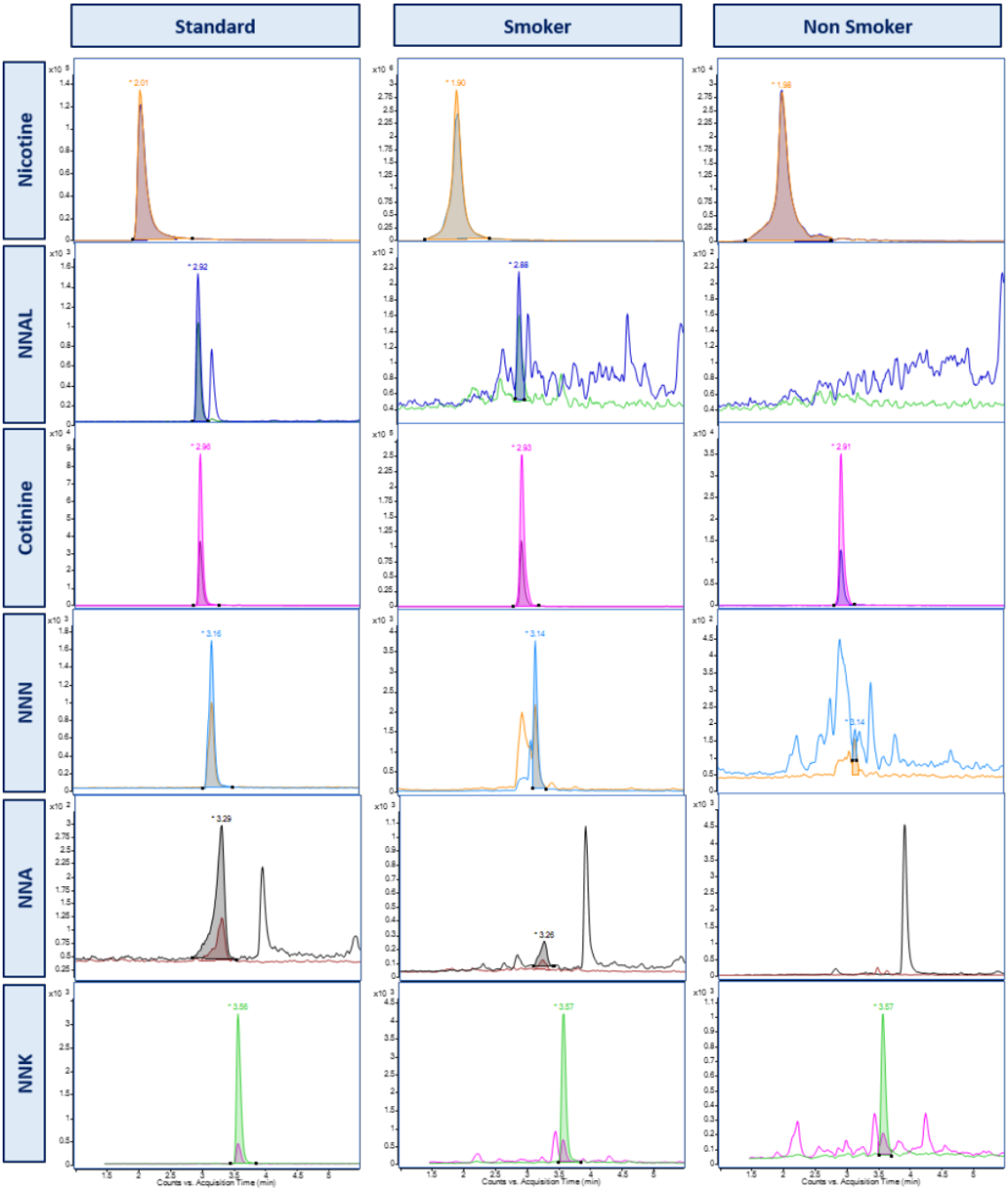

Figure 6. a) Extracted chromatogram of the quantitative and qualitative transitions of the targeted compounds in a calibration standard prepared in acetonitrile at 0.35 $\mu g \cdot mL^{-1}$ of nicotine and cotinine and $2 \cdot 10^{-4}$ $\mu g \cdot mL^{-1}$ of NNAL, NNN, NNA and NNK, in a smokers' dust extract (Smoker 2, table 7) and in a non-smokers' dust extract (Non-Smoker4, table 7).

A summary of the concentrations of the 6 target compounds and their occurrence in the samples is presented in Table 4. As expected, compound concentrations in house dust were higher in smokers' homes than in the non-smokers' ones. Nicotine concentration is a thousand-fold higher in smokers' samples. Nicotine concentration found in this study agree with concentration ranges found in a previous study performed in the same area [3] and in studies performed in other countries [11–13].

NNK and NNN were found in all the smokers' samples and in the 80% and 60% of the non-smoker's samples respectively. NNAL and NNA were not detected in non-smokers' samples and only quantified in the 60% and 20% of the smoker's samples, respectively. Concentration of NNK and NNN are approximately 6 times higher in smokers' dust in both cases. Our results for NNK and NNN are also in agreement with previous studies performed in the US [11,18], this validating the capability of the developed method to determining tobacco-specific toxicants in dust samples.

Table 4. Mean, median minimum and maximum concentration in ng/g of dust, of Nicotine, Cotinine and the four TSNAs found in 10 smokers' and 10 non-smokers' dust samples. (n.d: values under the limit of detection; n.q: values under the limit of quantification)

	Smokers				Non-Smokers			
Compound	**Mean**	**Median**	**Min**	**Max**	**Mean**	**Median**	**Min**	**Max**
Nicotine	$9.6x10^4$	$3.0x10^4$	$8.7x10^3$	$4.7x10^5$	$3.0x10^3$	$2.7x10^3$	$7.6x10^2$	$5.5x10^3$
Cotinine	$8.1x10^3$	$4.8x10^3$	$2.2x10^3$	$3.1x10^4$	$2.1x10^3$	$1.9x10^3$	$1.8x10^3$	$3.3x10^3$
NNK	25.1	7.1	0.2	175.9	4	2.4	0.4	11.6
NNN	15.2	5.3	0.9	77.7	2.4	1.6	0.6	6.9
NNAL	2.7	2	0.4	5.8	n.d	n.d	n.d	n.q
NNA	12.8	12.8	n.d	15.6	n.d	n.d	n.d	n.d

3.7 Conclusions

An efficient method based on a QuECHERS extraction followed by LC-MS for simultaneously determining nicotine, cotinine and four TSNAs in smokers and non-smokers house dust was developed. To the best of our knowledge this is the first time that the QuEChERS extraction method has been applied for the determination of these compounds in dust.

The method consisted on a salting-out liquid-liquid extraction using acetonitrile and a 0.1M KOH aqueous solution (3:1 ratio). Acetonitrile enhanced the extraction of the TSNAs and the basic solution improved nicotine's recovery. The second stage of the method consisted of a dSPE with z-sep+: $MgSO_4$ (14:86 ratio) as the chosen sorbent. The recoveries of the developed method were between 54,9-92.8%. The repeatability (intra-day) and reproducibility (day-to-day) of the method was less than 9.2% and 8.6% (%RSD,n=5) respectively. Limits of detection and quantification were between 0.03 - 0.40 ng/g and 0.11 - 2.66 ng/g respectively. Recoveries are comparable to those obtained using more time and solvent consuming analytical methods. Moreover, the limits of detection and quantification obtained in this work are lower, indicating that this method is more sensitive.

The reliability of the method was demonstrated through the determination of the compounds in smoking and non-smoking dust samples. All compounds were determined in smoker's homes. Nicotine was 1000 times higher in smokers' homes than in non-smokers. Surprisingly cotinine was the compound with the concertation more similar between groups, only 3 times higher in smokers' homes. The carcinogenic compounds NNK and NNN were found in the 80 and 60% of the non-smoker's samples with a concentration 6 times lower than smokers in both cases, demonstrating that non-smokers are exposed to carcinogenic compounds not in such a different way than smokers. This also

demonstrates that THS contamination due to the ubiquitous presence of nicotine in the environmental air affects not only smokers but also non-smokers.

3.8 References

(1) Butte, W.; Heinzow, B. Pollutants in House Dust as Indicators of Indoor Contamination. *Rev. Environ. Contam. Toxicol.* **2002**.

(2) Klepeis, N. E.; Nelson, W. C.; Ott, W. R.; Robinson, J. P.; Tsang, A. M.; Switzer, P.; Behar, J. V.; Hern, S. C.; Engelmann, W. H. The National Human Activity Pattern Survey (NHAPS): A Resource for Assessing Exposure to Environmental Pollutants. *J. Expo. Anal. Environ. Epidemiol.* **2001**. https://doi.org/10.1038/sj.jea.7500165.

(3) Ramírez, N.; Özel, M. Z.; Lewis, A. C.; Marcé, R. M.; Borrull, F.; Hamilton, J. F. Exposure to Nitrosamines in Thirdhand Tobacco Smoke Increases Cancer Risk in Non-Smokers. *Environ. Int.* **2014**, *71*, 139–147. https://doi.org/10.1016/j.envint.2014.06.012.

(4) Farren, N. J.; Ramírez, N.; Lee, J. D.; Finessi, E.; Lewis, A. C.; Hamilton, J. F. Estimated Exposure Risks from Carcinogenic Nitrosamines in Urban Airborne Particulate Matter. *Environ. Sci. Technol.* **2015**. https://doi.org/10.1021/acs.est.5b01620.

(5) Fortmann, A. L.; Romero, R. A.; Sklar, M.; Pham, V.; Zakarian, J.; Quintana, P. J. E.; Chatfield, D.; Matt, G. E. Residual Tobacco Smoke in Used Cars: Futile Efforts and Persistent Pollutants. *Nicotine Tob. Res.* **2010**. https://doi.org/10.1093/ntr/ntq144.

(6) Öberg, M.; Jaakkola, M. S.; Woodward, A.; Peruga, A.; Prüss-Ustün, A. Worldwide Burden of Disease from Exposure to Second-Hand Smoke: A Retrospective Analysis of Data from 192 Countries. *Lancet* **2011**. https://doi.org/10.1016/S0140-6736(10)61388-8.

(7) Matt, G. E.; Quintana, P. J. E.; Destaillats, H.; Gundel, L. a.; Sleiman, M.; Singer, B. C.; Jacob, P.; Benowitz, N.; Winickoff, J. P.; Rehan, V.; Talbot, P.; Schick, S.; Samet, J.; Wang, Y.; Hang, B.; Martins-Green, M.; Pankow, J. F.; Hovell, M. F. Thirdhand Tobacco Smoke: Emerging Evidence and Arguments for a Multidisciplinary Research Agenda. *Environ. Health Perspect.* **2011**, *119* (9), 1218–1226. https://doi.org/10.1289/ehp.1103500.

(8) Matt, G. E.; Quintana, P. J. E.; Hovell, M. F.; Bernert, J. T.; Song, S.; Novianti, N.; Juarez, T.; Floro, J.; Gehrman, C.; Garcia, M.; Larson, S. Households Contaminated by Environmental Tobacco Smoke: Sources of Infant Exposures. *Tob. Control* **2004**, *13* (1), 29–37. https://doi.org/10.1136/tc.2003.003889.

(9) Mercier, F.; Glorennec, P.; Thomas, O.; Bot, B. Le. Organic Contamination of Settled House Dust, a Review for Exposure Assessment Purposes. *Environ. Sci. Technol.* **2011**, *45* (16), 6716–6727. https://doi.org/10.1021/es200925h.

(10) Albinet, A.; Nalin, F.; Tomaz, S.; Beaumont, J.; Lestremau, F. A Simple QuEChERS-like Extraction Approach for Molecular Chemical Characterization of Organic Aerosols: Application to Nitrated and Oxygenated PAH Derivatives (NPAH and OPAH) Quantified by GC-NICIMS. *Anal. Bioanal. Chem.* **2014**, *406* (13), 3131–3148. https://doi.org/10.1007/s00216-014-7760-5.

(11) Matt, G. E.; Quintana, P. J. E.; Zakarian, J. M.; Hoh, E.; Hovell, M. F.; Mahabee-Gittens, M.; Watanabe, K.; Datuin, K.; Vue, C.; Chatfield, D. A. When Smokers Quit: Exposure to Nicotine and Carcinogens Persists from Thirdhand Smoke Pollution. *Tob. Control* **2017**, *26* (5), 548–556. https://doi.org/10.1136/tobaccocontrol-2016-053119.

(12) Matt, G. E.; Quintana, P. J. E.; Zakarian, J. M.; Fortmann, A. L.; Chatfield, D. A.; Hoh, E.; Uribe, A. M.; Hovell, M. F. When Smokers Move out and Non-Smokers Move in: Residential Thirdhand Smoke Pollution and Exposure. *Tob. Control* **2011**, *20* (1), e1–e1.

https://doi.org/10.1136/tc.2010.037382.

(13) Matt, G. E.; Mahabee-Gittens, E. M.; Zakarian, J. M.; Quintana, P. J. E.; Hoh, E.; Myers, M. Nicotine in Thirdhand Smoke Residue Predicts Relapse from Smoking Cessation: A Pilot Study. *Addict. Behav.* **2019**, *98* (June), 106041. https://doi.org/10.1016/j.addbeh.2019.106041.

(14) Kim, S.; Aung, T.; Berkeley, E.; Diette, G. B.; Breysse, P. N. Measurement of Nicotine in Household Dust. *Environ. Res.* **2008**, *108* (3), 289–293. https://doi.org/10.1016/j.envres.2008.07.004.

(15) Whitehead, T.; Metayer, C.; Ward, M. H.; Nishioka, M. G.; Gunier, R.; Colt, J. S.; Reynolds, P.; Selvin, S.; Buffler, P.; Rappaport, S. M. Is House-Dust Nicotine a Good Surrogate for Household Smoking? *Am. J. Epidemiol.* **2009**, *169* (9), 1113–1123. https://doi.org/10.1093/aje/kwp021.

(16) Whitehead, T. P.; Metayer, C.; Park, J. S.; Does, M.; Buffler, P. A.; Rappaport, S. M. Levels of Nicotine in Dust from Homes of Smokeless Tobacco Users. *Nicotine Tob. Res.* **2013**, *15* (12), 2045–2052. https://doi.org/10.1093/ntr/ntt096.

(17) Ramírez, N.; Özel, M. Z.; Lewis, A. C.; Marcé, R. M.; Borrull, F.; Hamilton, J. F. Determination of Nicotine and N-Nitrosamines in House Dust by Pressurized Liquid Extraction and Comprehensive Gas Chromatography-Nitrogen Chemiluminiscence Detection. *J. Chromatogr. A* **2012**, *1219*, 180–187. https://doi.org/10.1016/j.chroma.2011.11.017.

(18) Whitehead, T. P.; Havel, C.; Metayer, C.; Benowitz, N. L.; Jacob, P. Tobacco Alkaloids and Tobacco-Specific Nitrosamines in Dust from Homes of Smokeless Tobacco Users, Active Smokers, and Nontobacco Users. *Chem. Res. Toxicol.* **2015**, *28* (5), 1007–1014. https://doi.org/10.1021/acs.chemrestox.5b00040.

(19) Llop, A.; Borrull, F.; Pocurull, E. Fully Automated Determination of N-Nitrosamines in Environmental Waters by Headspace Solid-Phase Microextraction Followed by GC-MS-MS. *J. Sep. Sci.* **2010**, *33* (23–24), 3692–3700. https://doi.org/10.1002/jssc.201000527.

(20) Shah, K. A.; Karnes, H. T. A Review of the Analysis of Tobacco-Specific Nitrosamines in Biological Matrices. *Crit. Rev. Toxicol.* **2010**, *40* (4), 305–327. https://doi.org/10.3109/10408440903394435.

(21) Grebel, J. E.; (Mel) Suffet, I. H. Nitrogen-Phosphorus Detection and Nitrogen Chemiluminescence Detection of Volatile Nitrosamines in Water Matrices: Optimization and Performance Comparison. *J. Chromatogr. A* **2007**, *1175* (1), 141–144. https://doi.org/10.1016/j.chroma.2007.09.073.

(22) Wu, W.; Ashley, D. L.; Watson, C. H. Simultaneous Determination of Five Tobacco-Specific Nitrosamines in Mainstream Cigarette Smoke by Isotope Dilution Liquid Chromatography/Electrospray Ionization Tandem Mass Spectrometry. *Anal. Chem.* **2003**, *75* (18), 4827–4832. https://doi.org/10.1021/ac030135y.

(23) Kim, H. J.; Shin, H. S. Determination of Tobacco-Specific Nitrosamines in Replacement Liquids of Electronic Cigarettes by Liquid Chromatography-Tandem Mass Spectrometry. *J. Chromatogr. A* **2013**, *1291*, 48–55. https://doi.org/10.1016/j.chroma.2013.03.035.

(24) Al-Mukhaini, N.; Ba-Omar, T.; Eltayeb, E. A.; Al-Shehi, A. A. Analysis of Tobacco-Specific Nitrosamines in the Common Smokeless Tobacco Afzal in Oman. *Sultan Qaboos Univ. Med. J.* **2016**, *16* (1), e20–e26. https://doi.org/10.18295/squmj.2016.16.01.005.

(25) Sleiman, M.; Gundel, L. a; Pankow, J. F.; Jacob, P.; Singer, B. C.; Destaillats, H. Formation of Carcinogens Indoors by Surface-Mediated Reactions of Nicotine with Nitrous Acid, Leading to Potential Thirdhand Smoke Hazards. *Proc. Natl. Acad. Sci. U. S. A.* **2010**, *107* (15), 6576–6581. https://doi.org/10.1073/pnas.0912820107.

(26) Jacob, P.; Benowitz, N. L.; Destaillats, H.; Gundel, L.; Hang, B.; Martins-Green, M.; Matt, G. E.; Quintana, P. J. E.; Samet, J. M.; Schick, S. F.; Talbot, P.; Aquilina, N. J.; Hovell, M. F.; Mao, J. H.; Whitehead, T. P. Thirdhand Smoke: New Evidence, Challenges, and Future Directions. *Chem. Res. Toxicol.* **2017**, *30* (1), 270–294. https://doi.org/10.1021/acs.chemrestox.6b00343.

(27) European Committee for Stantarization. Foods of Plant Origin — Determination of Pesticide Residues Using GC-MS and / or LC-MS / MS Following Acetonitrile Extraction / Partitioning and Cleanup by Dispersive SPE — QuEChERS-Method. *Br. Stand.* **2008**, 1–83.

(28) Socas-Rodríguez, B.; González-Sálamo, J.; Herrera-Herrera, A. V.; Hernández-Borges, J.; Rodríguez-Delgado, M. Recent Advances and Developments in the QuEChERS Method. *Compr. Anal. Chem.* **2017**. https://doi.org/10.1016/bs.coac.2017.01.008.

(29) Hewavitharana, A. K. Matrix Matching in Liquid Chromatography-Mass Spectrometry with Stable Isotope Labelled Internal Standards-Is It Necessary? *J. Chromatogr. A* **2011**, *1218* (2), 359–361. https://doi.org/10.1016/j.chroma.2010.11.047.

(30) Sawicki, T.; Surma, M.; Zieliński, H.; Wiczkowski, W. Development of a New Analytical Method for the Determination of Red Beetroot Betalains Using Dispersive Solid-Phase Extraction. *J. Sep. Sci.* **2016**. https://doi.org/10.1002/jssc.201600196.

(31) González-Curbelo, M.; Socas-Rodríguez, B.; Herrera-Herrera, A. V.; González-Sálamo, J.; Hernández-Borges, J.; Rodríguez-Delgado, M. Evolution and Applications of the QuEChERS Method. *TrAC - Trends Anal. Chem.* **2015**, *71*, 169–185. https://doi.org/10.1016/j.trac.2015.04.012.

(32) AOAC. AOAC Official Method 2007 . 01 Pesticide Residues in Foods by Acetonitrile Extraction and Partitioning with Magnesium Sulfate [Applicable for the Following Pesticides in Grapes , Lettuces , and Oranges : Atrazine , Azoxystrobin , Bifenthrin , Carbaryl ,. *Aoac Ter Na Tional* **2007**, 1–9.

(33) Lehotay, S. J.; Son, K. A.; Kwon, H.; Koesukwiwat, U.; Fu, W.; Mastovska, K.; Hoh, E.; Leepipatpiboon, N. Comparison of QuEChERS Sample Preparation Methods for the Analysis of Pesticide Residues in Fruits and Vegetables. *J. Chromatogr. A* **2010**, *1217* (16), 2548–2560. https://doi.org/10.1016/j.chroma.2010.01.044.

4. Combination of Target and Non-target methods to advance on the chemical composition of Thirdhand Smoke in Household Dust

UNIVERSITAT ROVIRA I VIRGILI
ADVANCES ON THIRDHAND SMOKE USING TARGETED AND UNTARGETED APPROACHES
Sònia Torres Gené

4.1 Abstract

Thirdhand smoke (THS) is a novel pathway of exposure to tobacco smoke toxicants that consists on the deposit and ageing of secondhand smoke (SHS) gases and particles in dust and surfaces. In contrast SHS, which generally contains more volatile components, THS is of particular interest as it is the less volatile portion of cigarette smoke that remains in upholstery, carpets, clothes and airborne particles and has been associated with a higher health risk. Current chemical characterization of THS is limited to the targeted determination of specific compounds and compound families, representing only a small part of THS complexity. Here, we present the combination of target and non-target methods to enhance the chemical characterization of THS toxicants in 75 house dust samples from smokers' and non-smokers' homes. We selected six tobacco-specific toxicants, including nicotine, the main marker of tobacco, and carcinogen tobacco-specific nitrosamines, for targeted analysis by ultra high-resolution liquid chromatography (UPLC) tandem mass spectrometry. Non-targeted screening of the dust extracts was carried out by UPLC coupled to high-resolution mass spectrometry (HR-MS). For the interpretation of non-target screening data, we applied a combination of suspect screening for documented THS components and metabolomics-style non-target identification to identify masses with significant difference between the sample groups, followed by annotation using the in silico fragmenter MetFrag coupled to the CompTox Chemicals Dashboard and PubChem. Althoguh this work is still in progress, preliminary results show that the novel annotation strategy presented here and validated with the targeted results would imply a giant step forward, not only on THS chemical characterization, but also in exposure science.

4.2 Introduction

Thirdhand smoke (THS) is a novel way of exposure to tobacco toxicants formed by the accumulation of tobacco smoke compounds and particles that remain in the environment and deposit on surfaces for long periods of time [1]. The aging and the ability of these compounds to react with environmental gases to form secondary pollutants make THS a different way of exposure to tobacco contaminants that has been poorly studied to date. Thirdhand smoke is rarely considered as a route of tobacco smoke exposure, and the population is not commonly aware that THS entails a risk of exposure to carcinogenic contaminants, even in non-smoking environments [2]. Authorities treat tobacco smoke as a contaminant occurring only on places where people are actually smoking. Nevertheless, tobacco smoke toxicants are present in outdoor and indoor environments and, therefore, they must be considered ubiquitous environmental contaminants. In fact, nicotine and tobacco-specific nitrosamines (TSNAs) have been found in outdoor airborne particles of several cities including London [3], eight big cities in Italy [4] and San Francisco [5]. This ubiquitous presence of tobacco related compounds is a source of pollution often overlook that not only affects smokers' homes but non-smokers [6]. A previous study revealed the ubiquitous presence of nicotine and TSNAs in house dust, even in homes with strict non-smoking bans. The same study indicated that the estimated lifetime cancer risk through non-dietary exposure to carcinogenic TSNAs and volatile N-nitrosamines bound to dust particles at an early life stage (1 to 6 years old) exceeded the upper-bound risk recommended by the US EPA in 77% of smokers' and 64% of non-smokers' homes [6]. These results highlighted the potentially severe long-term consequences of early life THS exposure, and presented strong evidence of its potential health risk. Several studies have already documented the occurrence of dozens of toxicants

in THS [6–10]. Considering that SHS is formed by thousands of chemical compounds, the toxicants characterized to date in THS can only explain a small part of the potential risks associated to the exposure to THS.

Non-target screening (NTS) analytical approaches in combination high resolution mass spectrometry (HRMS) are arising as key methodologies for the characterization of the chemical complexity of the environmental matrices in the era of the exposome. HRMS allows the identification of a broad range of toxicants, and unknowns [11], and it has been applied for the NTS of a diversity of environmental samples [12]. Regarding the chemical characterization of dust, few studies have been performed using LC-HRMS [13,14], although a collaborative trial in non-target screening was performed by 26 different organisations worldwide by using GC-MS and LC-MS [15]. Typically, in environmental studies, the same kind of samples are analyzed in order to find common peaks, fragments and masses to help with the identification. In contrast in other fields such as metabolomics the case/control approach applied to different sampkle groups is frequently used. Therefore, applying different strategies in the experimental design and data analysis curation could enhance the identification of the relevant compounds in environmental studies.

The aim of this study is to advance on the characterization of THS contamination in household dust, by combing targeted and untargeted approaches and the development of a new methodology for conducting NTS studies with case/control approaches using HR-MS. To this end, we combined highly developed techniques used in NTS with an advanced annotation workflow. Dust samples of smokers and non-smokers homes in the area of Tarragona were analyzed for the screening of new THS toxicants in dust by using HRMS. Samples were also analyzed with a target approach for the

quantification of nicotine, cotinine and four TSNAs including NNK, NNN, NNAL and NNA.

4.3 Materials and Methods

4.3.1 Sample collection and preparation

Sample collection was carried out between January to October 2017 in the area of Tarragona (north-eastern Spain). We collected a total of 75 dust samples from private homes using conventional vacuum cleaners in regular use in households, including 42 and 33 samples from non-smokers' and smokers' homes, respectively. In this study we considered smokers' homes those with at least one adult resident that smokes conventional tobacco products every day, and at least 10 cigarettes per week during the last three months. Smokers have lived in their current home at least 5 days per week during the past year. We classified as non-smokers' homes whose residents are non-smokers or have quit smoking at least one year prior to sample collection and where anybody has smoked in the past 30 days (including visitors).

Dust samples were delivered by the households in hermetic plastic bags provided by the researchers. The collected dust was sieved using a stainless-steel sieve with a 100 μm mesh size and stored at -20°C in pre-weighted amber glass. Participants were requested to sign an informed consent and complete a questionnaire to collect information about the house and any activity that might affect chemical loading (Supplementary Information, Section 4.5). This study has been approved by the ethic committee of the clinical Research Hospital Sant Joan of Reus, in Catalonia, Spain (Ref. approbation: 15-05-

28/5proj4). Relevant information about the participants for this study is shown in Table 1.

Table 1. Summary of the characteristics of the homes and the participants included in this study.

Characteristics	Smokers' homes (n=33)	Non-smokers' homes (n=42)
Home Location	Rural: 4%	Rural: 3%
	Suburban: 33%	Suburban: 26%
	Urban: 67%	Urban: 71%
	Medium-high traffic: 68%	Medium-High traffic: 53%
Building information	Flat: 79%	Flat: 63%
	House:21%	House:37%
	Fireplace: 4%	Fireplace: 19%
	Carpets: 29%	Carpets: 40%
Household Residents	No. Adults	No. Adults
	One: 4%	One: 8%
	Two: 41%	Two: 68%
	Three: 8%	Three: 13%
	Four: 16%	Four: 10%
	Homes with children: 63%	Homes with children: 72%
	No. Children	No. Children
	One: 21%	One: 29%
	Two: 29%	Two: 45%
	Three: 12%	Three: 3%
	Ages[a]: 9 (<1, 5,75,12,17)	Ages[a]: 7 (1, 4.5,9,17)
Pets (dog or cat)	50%	29%
Smokers per home	One smoker: 67%	-
	Two smokers 33%	-
	Three smokers: 0%	-
	Smoking Indoor: 50%	-
	Outdoor smoking: 95 %	
	Indoor smoked cigarettes [a,b]: 0 (0, 0, 5, 40)	
	Total smoked cigarettes [a,c]: 20 (1, 11.5, 25, 45)	-
Cleaning information	Once a week: 33%	Once a week: 45%
Vacuum frequency	Twice a week: 29%	Twice a week: 26%
	3 to 5 times a week: 20%	3 to 5 times a week: 16%
	Every day: 8%	Every day: 13%
	Once a week: 4%	Once a week: 5%
Ventilation frequency	Twice a week: 4%	Twice a week: 0 %
	3 to 5 times a week: 8%	3 to 5 times a week: 24%
	Every day: 87%	Every day: 71%

[a] Median value (min, 0.25, 0.75, max)

[b] Cigarettes smoked inside the home per day

[c] Total number of cigarettes smoked by all the smoker households, including those cigarettes smoked in other locations

As seen in Table 1, most of the samples were from flats in urban areas, with medium-high traffic intensity for more than a half of the flats. Around half (44%) of the samples were characterized as from smokers' homes, where at least one occupant was a tobacco smoker, including those whose occupants do not smoke inside the home. The mean number of cigarettes smoked per day in this group was 20, including cigarettes smoked both inside the home and at other locations. In 63% of the smokers' homes lived at least 1 child.

4.3.2 Dust extraction and analysis

Dust samples were prepared as previously described by Torres et al. based on a QuEChERS extraction followed by dispersive solid extraction clean-up using Z-Sep$^+$ [16]. Briefly summarized, 300 mg of dust spiked with 0.05 µg/mL of internal standards (nicotine-d_3, cotininine-d_3, NNN-d_4, NNA-d_3 and NNAL-d_3) were extracted with 2 mL of acetonitrile (LC-MS grade). We used 0.5 g of CEN QuEChERS salts for the salting-out. This mixture was vortexed for 1 min and centrifuged for 5 min at 4000 rpm. The supernatant was cleaned-up and stored at -80°C until analysis.

For the targeted analysis the concentration of the six tobacco specific toxicants including nicotine, cotinine, NNK, NNN, NNAL and NNA was determined by injecting 1 µl of dust extract into an UHPLC chromatograph coupled to a triple quadrupole mass analyser, both from Agilent Technologies (Sta. Clara, CA, USA). Method details and key parameters used are detailed elsewhere [16]. Concentrations of the two carcinogenic nitrosamines NNN and NNK were used to estimate the human exposure to THS through the main pathways of THS exposure, non-dietary ingestion and dermal absorption.

Calculations were performed following the equations used for risk assessment described in the US EPA guidelines [6].

For the non-targeted analysis, 2 µl of dust extracts were injected into a Dionex Ultimate 3000 coupled to a Q-Exactive Plus HRMS equipped with electrospray ionization source, both from Thermo Scientific (Bremen, Germany). Chromatographic separation was performed in reverse phase mode using a Kinetex EVO C_{18} column (150 × 2.1mm i.d, 2.6 µm) kept at 25 °C during all the analysis time. The gradient elution procedure was set at 0.3 mL/min with a mixture of H2O containing 10 mM ammonium acetate (A) and MeOH containing 0.1% formic acid (B) as mobile phase (0-2min, 5% B; 2-25 min, 5-100% B; 25-30 min, 100% B; 30-31, 5% B; 31-35 min, 5% B). The electrospray ionization source was operated in the positive ionization mode under the following specific conditions: source temperature 275 °C, capillary temperature 275 °C, spray voltage 3.50 kV; sheath and auxiliary gas 50 and 10 arbitrary units, respectively. The untargeted analysis was performed in full scan mode, followed by data-dependent MS/MS scans (ddMS2). Full scan conditions were: scan range m/z = 50-750; mass resolution R=140,000; and automatic gain control (AGC) target and maximum injection time (IT) were set at 3×10^6 and 200 ms, respectively. For the $ddMS^2$, a top 5 experiment (the 5 highest ions of each scan were selected for MS/MS) was performed with the parameters set as follows: R=35,000; AGC target: 2×10^5; maximum IT = 5 ms; Loop count: 5; MSX count: 1; 1.2 Da isolation window; and nominal collision energy 20 eV.

In order to asses analytical variability throughout both analysis, quality control (QC) samples consisting of pooled dust samples from smokers' and non-smokers' homes were injected after every ten samples. The order of the dust samples during analysis was entirely randomized, to reduce the systematic error associated with instrumental drift. Additionally, in the untargeted analysis

pooled dust extracts from non-smokers' and smokers' homes were also analysed using an inclusion list in order to increase the chances of finding dust-related toxicants. The inclusion list consisted on a manual elaborated list containing the exact mass of the 95 compounds previously reported in THS samples. Those masses were searched in MS mode, isolated and fragmented to obtain the MS/MS spectra. The curated and compiled list used is available on NORMAN Suspect List Exchange and the CompTox Chemicals Dashboard [17–19].

4.3.3 Untargeted data analysis

LC/MS raw data files were converted from the vendor format into mzXML and mzML formats using Proteowizard software [20] using the vendor peak picking option to perform centroiding. The converted files were processed using the XCMS R package software (version 3.0.2) [21–24] to detect and align features. The parameters used in the XCMS workflow were: xcmsSet (method = "centWave", peakwidth = *c*(15,80)); retention correlation function retcor (method = "obiwarp", profStep = 0.1); and the grouping function group (minfrac = 0.8, bw = 5). The intensity of the features was normalized by performing a probabilistic quotient normalization (PQN) in order to correct instrumental drift along the sequence then features with peak height greater than 100,000 counts in at least one of the groups were kept for further processing. Quality control samples formed by a pool of all sample extracts, were used to reduce the number of features by filtering by analytical variation as previously described [25]. Following T-test analysis and fold change calculations were performed and statistically different features between smokers' and non-smokers' homes showing a FDR corrected p value < 0.05, and fold change > 1.2 were selected for annotation.

Non-target annotation was performed using the MetFrag [26] Command Line Tool (v 2.4.5) using either PubChem database [27] or a local CSV copy of the CompTox Chemicals Dashboard (created May 1st, 2018) [28]. A smoking-specific copy of the CompTox Dashboard CSV was created for the purposes of this study [29], designed on the basis of the MS-ready [30] export file created by the CompTox Dashboard team [31]. This file contains structural information linking mixtures to the individual components (as described in McEachran et al. 2018)[30], as well as several metadata fields. These include data sources, number of PubMed articles, number of PubChem data sources, predicted exposure values from EXPOCAST [3233], TOXCAST [34] % active bioassays and presence in the US EPA's Chemical and Products Database CPDat [35] and the NORMAN SusDat suspect screening list [36].

For the smoking-specific file used here, additional terms considered relevant for THS, dust, and smoking in general, were added. The column "PubMedNeuro" contains a list of potential neurotoxicants extracted from PubMed as described by Schymanski et al [37] with the total PubMed reference counts as a scoring term (and 0 for all other entries). A further 5 columns were added as suspect lists (1=present, 0=absent) including the one developed in this study ("THSMOKE") and the other lists CIGARETTES[38], INDOORCT16 [15,39], SRM2585DUST[40] and SLTCHEMDB[38] from the CompTox Dashboard. All entries were mapped using the CompTox chemical substance identifier DTXSID included in each list.

The MetFragConfig function of the ReSOLUTION package (v 0.1.8) [41]was used to prepare the configuration files using either the MS/MS extracted by RMassBank, or a "dummy" MS/MS spectrum (*m/z*=999, I=100, one entry only, which will never be scored) as the peak list. The MetFrag scoring terms

FragmenterScore, OfflineMetFusionScore and OfflineIndividualMoNAScore were used in both cases, weighted to 1.

For CompTox calculations, the additional terms "Number of PubMed articles", EXPOCAST, TOXCAST and CPDat, were used weighted to 1, while the two data sources terms (data sources, PubChem data sources) were weighted at 0.5 each to avoid the number of data sources dominating the score too much. This yields a maximum score of 8. For compounds without MS/MS, the maximum score will be 5. For PubChem calculations, the default built into MetFragConfig for the "PubChemExtended" database was used, i.e. the three spectral scores outlined above, plus the patents and references scores were added with default weight 0.5 each, to yield a maximum score of 4. A summary file was created automatically from the results files exported after the MetFrag calculations.

4.4 Results and discussion

4.4.1 Targeted results

The quantification of tobacco toxicants in house dust samples confirm the ubiquitous presence of tobacco related toxicants in the environment since both smokers' and non-smokers' homes dust contained the studied contaminants. Nicotine and cotinine were found in all homes (see Table 2) with a median level of 39.4 μg g^{-1} and 5.3 μg g^{-1} in smokers' homes and 2.5 μg g^{-1} and 1.9 μg g^{-1} in the non-smokers'. These results are in accordance with the nicotine levels found in a study performed in the same area in 2013 [6] and with several studies performed in the US [42–44]. In smokers' homes NNK was detected in all samples, NNN in the 96.9%, NNAL in 57.5 % and NNA in 6.0 % of the samples. NNK and

NNN median values are also in accordance with those found in a study performed in California [45]. In non-smokers' homes NNK and NNN were detected in the 88 and 64% of the non-smoker's samples, respectively, but NNA and NNAL were not detected. NNA mean and maximum levels found are similar to those estimated by Sleiman et al. in environmental chamber experiments [46], but NNK concentrations were higher in all cases and NNA in our smokers' house dust, and we could only detect it 6% of the samples.

Table 2. nicotine, cotinine and TSNAs concentration found in smokers' and non-smokers' homes expressed in ng/g of dust. Not detected and not quantified compounds are expressed as n.d and n.q respectively.

	Smoker Homes							Non-Smoker Homes						
Compound	Min	1st Qu.	Median	Mean	3rd Qu.	Max	% Quantified	Min	1st Qu.	Median	Mean	3rd Qu.	Max	%Quantified
Nicotine	1×10^3	1.8×10^4	3.9×10^4	1.0×10^5	9.3×10^4	5.5×10^5	100	7.6×10^2	1.5×10^3	2.5×10^3	3.2×10^3	4.0×10^3	1.1×10^4	100
Cotinine	1.7×10^3	3.2×10^3	5.3×10^3	8.9×10^3	1.0×10^4	5.7×10^4	100	1.7×10^3	1.8×10^3	1.9×10^3	2.4×10^3	2.4×10^3	1.4×10^4	100
NNK	0.2	2.9	8.6	27	17	237	100	n.q	0.3	0.6	2.2	2.7	19	88
NNN	n.q	2.7	8.1	15	13	153	97	n.q	0	0.2	1.5	2	13	64
NNAL	n.q	0	0.7	1.7	2.1	11	57	n.d	n.d	n.d	n.d	n.d	n.d	0
NNA	n.d	0	0	0.8	0	16	6	n.d	n.d	n.d	n.d	n.d	n.d	0

We calculated the ratio NNK/Nicotine which average was higher in non-smoker homes' (0.64) than in the smokers' one (0.29), in accordance with results previously reported by Jacob et al.[5] Analogously, the NNN/Nicotine ratio was also higher in non-smokers' homes (0.59 vs. 0.17) indicating that the NNN/Nicotine ratio would also serve as THS exposure indicator. The higher ratio NNK-NNN/Nicotine can be explained considering two factors: first that as THS ages, TSNAs concentrations increase, and second that nicotine can be removed by ventilation at a greater rate than TSNAs [47].

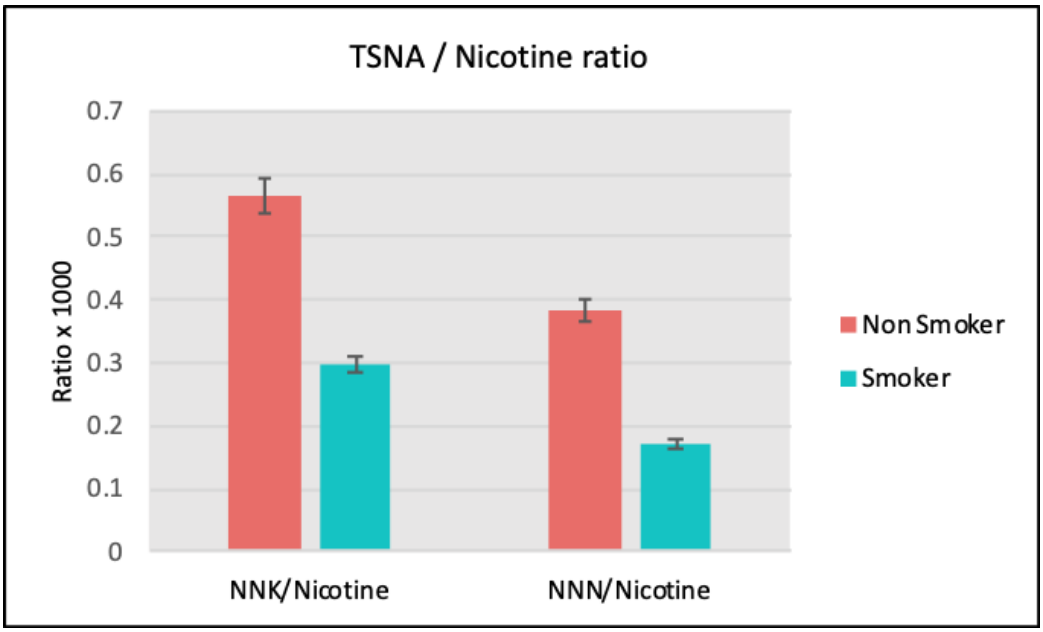

Figure 1. NNK/Nicotine and NNN/Nicotine ratios in smokers' and non-smokers' homes

The concentration of the carcinogenic nitrosamines NNK and NNN found in the samples were used for the estimation of cumulative cancer risk by dermal absorption and non-dietary ingestion by age group [6] (see Tables 2 and 3). As can be seen in the tables the cancer risk associated with dermal absorption was lower since this way of exposure is secondary in comparison with non-dietary ingestion. Moreover, the threshold of 1 excess cancer cases per 1 million population stablished by the US EPA guideline[48] is never excedded by this

exposure way. Nonetheless, median risk was higher in infants between 1-6 years in both smokers and non-smokers homes compared to the other groups being 1.7 x 10^{-12} in smokers and 1.3 x10^{-13} respectively (Table 2).

Table 3. Total Cancer Risk by dermal absorption of the carcinogenic compounds NNK and NNN, by age group, expressed in number of calculated excess cancer cases per exposed population.

	Smokers' homes					**Non-Smokers' homes**				
Age Range (years)	Min	0.25	Median	0.75	Max	Min	25%	Media	75%	Max
1 <	3.1×10^{-14}	1.2×10^{-13}	4.8×10^{-13}	1.1×10^{-12}	1.5×10^{-11}	1.3×10^{-15}	2.1×10^{-14}	3.8×10^{-14}	1.3×10^{-13}	1.1×10^{-12}
1-6	1.1×10^{-13}	4.1×10^{-13}	1.7×10^{-12}	3.7×10^{-12}	5.1×10^{-11}	4.4×10^{-15}	7.2×10^{-14}	1.3×10^{-13}	4.6×10^{-13}	3.8×10^{-12}
6-21	1.7×10^{-13}	6.4×10^{-13}	2.6×10^{-12}	5.8×10^{-12}	8.0×10^{-11}	6.9×10^{-15}	1.1×10^{-13}	2.1×10^{-13}	7.3×10^{-13}	5.9×10^{-12}
21-70	3.5×10^{-13}	1.3×10^{-12}	5.3×10^{-12}	1.2×10^{-11}	1.6×10^{-10}	1.4×10^{-14}	2.3×10^{-13}	4.2×10^{-13}	1.5×10^{-12}	1.2×10^{-11}

Table 4. Total Cancer Risk by non-dietary Ingestion of the carcinogenic compounds NNK and NNN, by age group, expressed in number of calculated excess cancer cases per exposed population.

	Smokers homes					**Non-Smokers' homes**				
Age range (years)	Min	25%	Median	75%	Max	Min	25%	Median	75%	Max
1<	1.5×10^{-08}	1.0×10^{-07}	3.1×10^{-07}	6.0×10^{-06}	8.0×10^{-06}	1.3×10^{-09}	8.3×10^{-09}	2.3×10^{-08}	7.9×10^{-08}	5.1×10^{-07}
1-6	3.6×10^{-08}	2.5×10^{-07}	7.4×10^{-07}	1.4×10^{-06}	1.9×10^{-05}	3.2×10^{-09}	2.0×10^{-08}	5.6×10^{-08}	1.9×10^{-07}	1.2×10^{-06}
6-21	1.2×10^{-08}	8.3×10^{-08}	2.5×10^{-07}	4.8×10^{-07}	6.4×10^{-06}	1.1×10^{-09}	6.6×10^{-09}	1.8×10^{-08}	6.3×10^{-08}	4.1×10^{-07}
21-70	7.0×10^{-09}	4.9×10^{-08}	1.4×10^{-07}	2.8×10^{-07}	3.8×10^{-06}	6.3×10^{-10}	3.9×10^{-09}	1.1×10^{-08}	3.7×10^{-08}	2.4×10^{-07}

The calculated risk estimates, based on a lifetime exposure (0–70 years) to the individual carcinogen nitrosamines in house dust for a non-dietary ingestion pathway, are shown in Figure 2. As can be seen children from 1 to 6-year-old living in smoker's homes are the population with highest cancer risk, exceeding 1 excess cancer cases per 1 million population exposed in 42% of the samples. This is due to habits associated to this age group since toddlers, spend relatively more time indoors, they engage in activities close to the floor and have hand-to-mouth behaviours.

For children from 0 to 1 the median is below that limit, but 15% of the samples were over that threshold. For population between 6 to 21 and 21-70 the calculated risk was over 10^{-6} in 21% and 9% of the cases respectively. In the case of non-smokers' homes although the median is below the threshold in all group age for children from 1 to 6 years, 2.6% of the samples were above the recommended level.

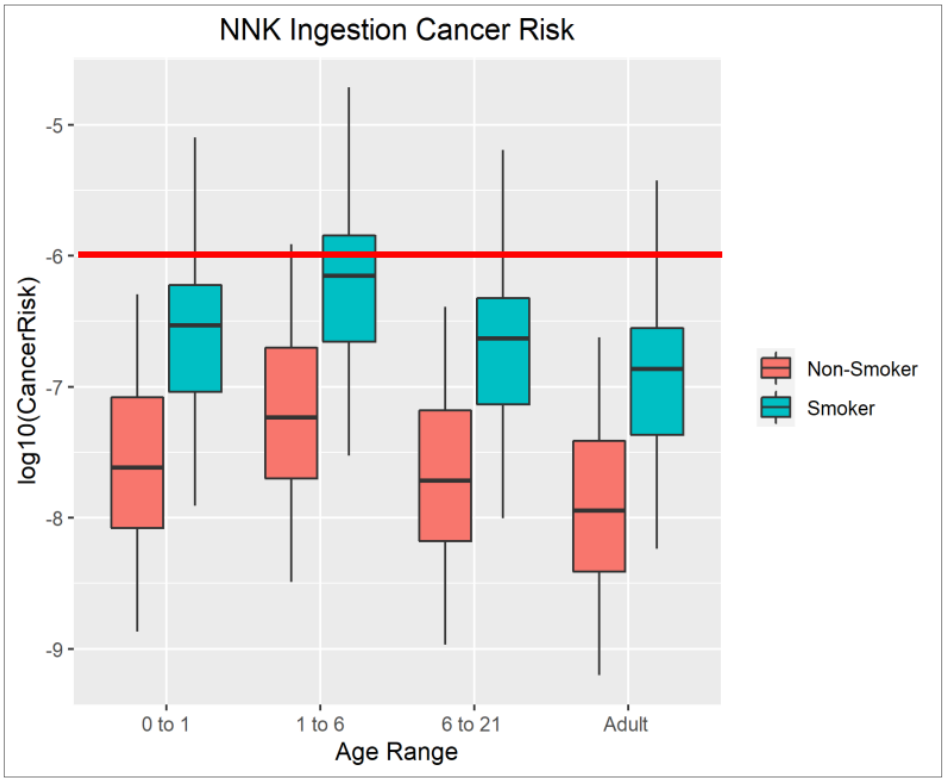

Figure 2. Boxplot of the logarithm (log10) of the estimated cancer risk by non-dietary ingestion of the compounds NNK and NNN found in the smokers and non-smokers homes, by age group. The red line indicates the limit stablished by the EPA.

4.4.2 Non-target results

A summary of the features and records obtained after each workflow step is represented in Figure 3. As can be seen in the figure the pre-procesign of the raw data provided a matrix containing the retention time, m/z value and peak height of 8012 features. Those features were normalized, and filtered by peak height and analytical variation resulting in a matrix of 4228 features. T-test analysis and fold change calculations were performed in order to reduce the matrix into those relevant features between sample groups. A total of 509 features presented statistical relevance (pvalue < 0.05, FC > 1.2) between smokers and non-smokers samples. MSMS was available for 251 of these features and 205 presented a match candidate in the search against PubChem and the CompTox Chemicals Dashboard.

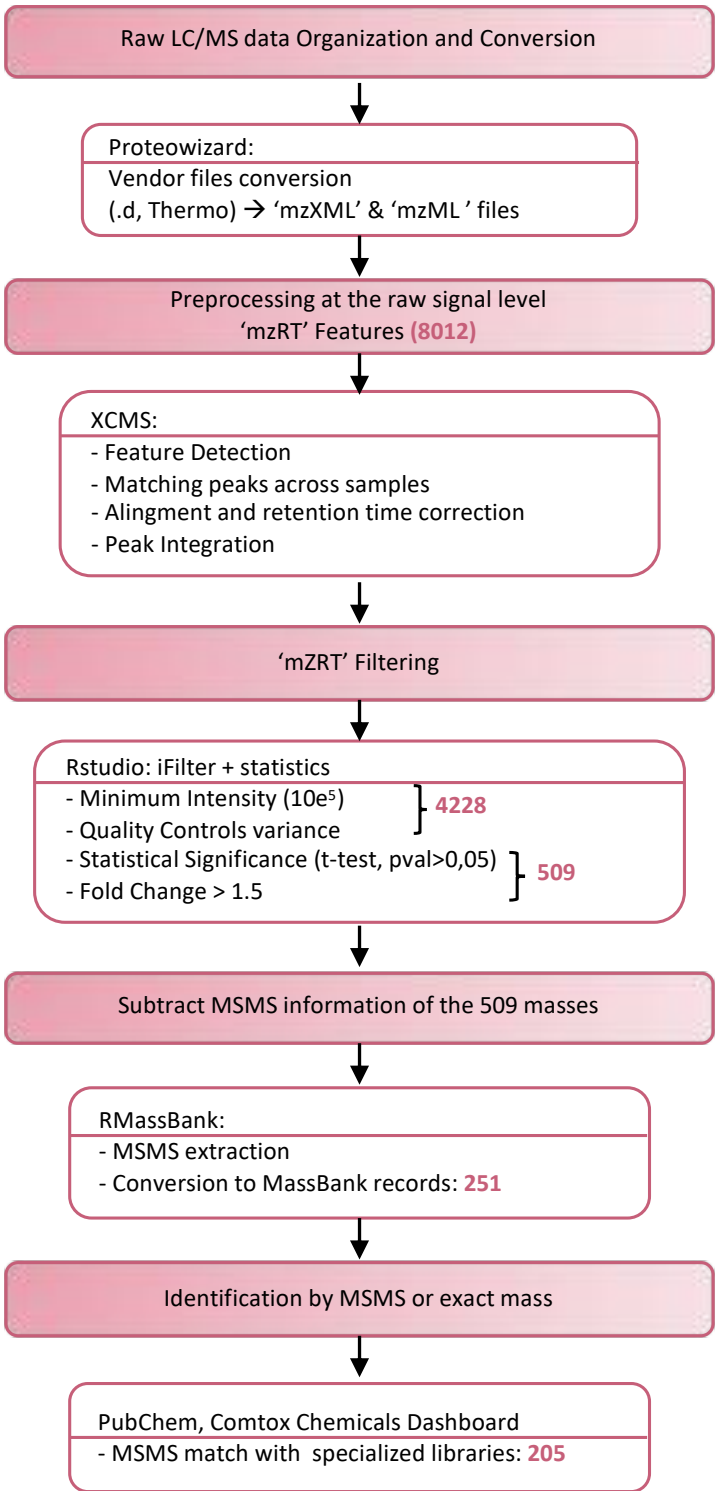

Figure 3. Non-targeted Screening workflow used for the data analysis of the dust samples analyzed by LC-HRMS. Red numbers indicate the number of features/putative compounds after each step of the process.

Table 5 show the compound putative identified with a total score > 5, including the feature retention time, m/z, pvalue, FC and the name of the candidate with maximum score for each feature. As can be seen we putatively annotated nicotine with a score of 7.2 out of 8, beeing the feature with the highest score. Nicotine also was the feature with lowest p value found in the analysis and the biggest fold change, thus indicating that this was the compound that clearly differed between samples.

In addition, by using this strategy we also annotated known tobacco related compounds such as N-N-Diethylnicotinamide, scopoletin an active principle of tobacco tree and cotinine. Moreover, the stastical results also support these annotations since in all cases the fold change is positive meaning that those compounds are found in higher concentration in the smokers' group.

Table 5. Summary of the parameters of the statistical analysis performed between smokers and non-smokers samples and some of the columns obtained in the file automatically created from the results files exported after the MetFrag calculations.

Name	*Rt*	*m/z*	*P value*	*FC*	*Max Score*	*Name maxScore*
FT0541	**1.07**	**163.122**	**4.60E-04**	**30.2**	**7.2**	**Nicotine**
FT0196	1.03	114.066	4.80E-02	1.7	7.229	Creatinine
FT0070	9.59	77.071	1.00E-02	1.5	7.000	2-Hydroxyethylhydrazine
FT3014	23.52	336.167	5.10E-03	3.1	6.977	Riboprine
FT2321	19.53	297.183	4.40E-02	2.3	6.685	17alpha-Ethinylestradiol
FT3332	24.74	355.108	3.00E-03	2.2	6.479	Flumioxazin
FT2924	14.26	331.207	4.50E-03	1.9	6.456	2,4-Bis(1-methyl-1-phenylethyl)phenol
FT2922	23.66	331.189	4.90E-03	1.4	6.417	Dicyclohexyl phthalate
FT0352	21.40	143.070	4.40E-02	2.3	6.346	Glycidyl methacrylate
FT0480	11.88	157.075	9.90E-04	3.1	6.305	2,2'-Bipyridine
FT0192	16.37	113.060	5.50E-04	3	6.211	2E,4E-Hexadienoic acid
FT4846	26.23	447.345	1.40E-03	2.4	6.093	Didecyl phthalate
FT7753	24.05	697.447	3.50E-03	-2.6	6.000	2,2'-Oxamidodiethyl bis[3-(3,5-di-tert-butyl-4hydroxy phenyl)propionate

FT3193	21.08	346.110	3.30E-02	21.5	5.973	Nitralin
FT2912	22.59	330.335	4.10E-02	1.8	5.973	N-Hexadecyl diethanolamine
FT0312	1.07	135.101	5.40E-03	1.6	5.966	2-(2-Ethoxyethoxy) ethanol
FT0689	**1.07**	**179.117**	**3.40E-02**	**2.3**	**5.960**	**N, N-Diethylnicotinamide**
FT0166	1.07	107.070	4.50E-02	1.2	5.943	Diethylene glycol
FT2652	20.83	315.176	1.40E-02	1.6	5.940	Ethidium bromide
FT2937	22.50	332.184	3.80E-02	6.7	5.885	Tetramethrin
FT2553	24.66	311.163	4.90E-03	2.4	5.848	1-(4-tert-Butylphenyl)-3-(4-methoxyphenyl) propane-1,3-dione
FT1092	14.43	211.108	8.00E-05	2.2	5.838	Phosphoric acid, dibutyl ester
FT1548	16.37	243.121	1.30E-02	1.5	5.820	Di (ethylene glycol) dimethacrylate
FT2098	25.21	282.278	1.50E-10	1.7	5.805	(9Z)-Octadec-9-enamide
FT3387	25.04	358.239	7.20E-02	2.3	5.758	Oxybutynin chloride
FT0858	**11.27**	**193.049**	**3.00E-03**	**2.2**	**5.713**	**Scopoletin**
FT0741	24.77	183.080	4.50E-03	1.9	5.690	Benzophenone
FT2433	21.12	302.304	4.90E-03	1.4	5.686	2,2'-(Tetradecylimino)diethanol
FT1543	22.46	243.137	3.30E-02	2.3	5.676	Bisphenol B
FT0898	1.18	195.122	9.60E-04	3.1	5.647	Tetraethylene glycol
FT2436	25.19	303.230	9.40E-03	1.4	5.636	Eicosapentaenoic acid
FT2226	24.77	291.195	1.70E-03	2.4	5.575	Octinoxate
FT4659	18.25	207.101	3.50E-03	-2.6	5.513	Ethyl methylphenylglycidate
FT0833	8.51	191.117	6.10E-02	1.8	5.478	5-Methoxytryptamine
FT0659	**7.68**	**177.101**	**5.40E-03**	**7.3**	**5.468**	**Cotinine**
FT0658	7.68	177.101	3.50E-02	1.5	5.354	4-Methyl-1-phenylpyrazolidin-3-one
FT0508	10.12	161.080	4.90E-03	2.4	5.143	Heptanedioic acid
FT4233	25.15	411.111	1.70E-02	1.5	5.075	Nicosulfuron
FT4217	25.15	410.108	7.70E-10	1.7	5.069	Sitafloxacin
FT3004	12.69	335.220	2.70E-03	2.1	5.020	Dihexyl phthalate

4.5 Conclusions

In this study we have determined nicotine, cotinine and 4 TSNAs with a targeted approach which confirms the ubicutious presence of tobacco related contaminants in smoke-free homes. We have also determined the for the first time the nicotine/NNN ratio which can serve as THS exposure indicator. Moreover, the cancer risk assessment performed highliths the risk of THS exposure to infants from 1 to 6 years old living with smokers.

The untargerted approach presented here by using metabolomics strategies such as the case/control approach with the score system for compound annotation demonstrates that combinig different results such as pvalue, fold change and the score helps to rely on the automated annotations performed. We have demonstrated that score system works since it has given maximum score to nicotine. Moreover, with the data dependent acquisition (DDA) performed here we have been able to obtain 251 MS/MS spectra statistically different between smokers and non-smokers samples. However, further research must be done in order to improve the selection of the peaks to performe the MS/MS analysis since using an intensity threshold value exclude compounds that are present in samples at lower concentrations, which is usually the case of environmental contaminants.

4.6 Supplementary Information

SURVEY OF THIRDHAND SMOKE EXPOSURE PROJECT

Name and surname:	Sample code	Dust:
Adress:		
Email:		
Phone:		
Date:		

A series of **questions** will be shown below about **the characteristics of your home, the people who live in it** and **other personal information about you, relevant to the study**. Please, **take the time to read each of the questions and answer them as honestly as possible**. These answers will help the research team to better understand the data obtained from the dust sample that you are going to provide. We appreciate the time spent in answering this survey and we assure you the maximum confidentiality of the data that you are going to provide us.

CHARACTERISTICS OF YOUR HOME

Specify the location of your home. **Location:** Urban / Suburban / Rural **Type of road:** Main road / Secondary road **Traffic intensity:** Low / Medium / High
When did you start living in your home? Date: ____ / _____ / _____ (Day / Month / Year) Approximately

What is the approximate age of your home? **Age:** Less than 1 year / 1 - 5 years / 6 - 10 years / 11 - 20 years / 21 - 50 years / 51 - 100 years / More than 100 years
What is the surface area of your home? Area (m^2):
Is it a flat or a house? Flat / House **If it is a flat, does any exterior window or door on your flat face the main street?** Yes / No **If the answer is yes, how many windows or exterior doors of your flat face the main street?** 1 / 2 / 3 / 4 / 5 / More than 5
Does your home have a fireplace? Yes / No **If the answer is yes, what type of fireplace do you have?** Open fireplace / Close fireplace **If you have a fireplace, have you used it during the dust collection period?** Yes / No **If you have used it in dust collection, how often per week?** 1 - 7 Hours/Week / 8 - 24 Hours/Week / 25 - 48 Hours/Week / 49 - 100 Hours/Week / More than 100 Hours/Week
What type of heating does your home have? (Several options can be selected) Radiators / Electric stoves / Convection systems / Combustion stoves / Gas stoves / Pellet stoves / Others: **Did you use the heater during the dust collection period?** Yes / No **If you have used it in dust collection, how often per week?** 1 - 7 Hours/Week / 8 - 24 Hours/Week / 25 - 48 Hours/Week / 49 - 100

Hours/Week / More than 100 Hours/Week
Does your home have rugs or carpeting? Yes / No **If the answer is affirmative, what area do they occupy?** Area (m2):
Have any renovations recently complete inside or outside your home? or are these being carried out now? Yes / No **If yes, what is the approximate completion date?** Date: ____ / _____ / _____ (Day / Month / Year)
Do you usually burn incense or candles inside your home? Yes / No **If the answer is yes, how often per week do you do it?** 1 - 7 Hours/Week / 8 - 24 Hours/Week / 25 - 48 Hours/Week / 49 - 100 Hours/Week / More than 100 Hours/Week
How often per week do you vacuum your home? 0 / 1 / 2 / 3 / 4 / 5 / 6 / 7 / More than 7 times
How often per week do you ventilate your home? 0 / 1 / 2 / 3 / 4 / 5 / 6 / 7 / More than 7 times **If you ventilate your home, how long do you do it each time?** 0 - 10 min / 11 - 30 min / 31 min - 1 hour / More than 1 hour

HOUSEHOLD'S INFORMATION

How many adults live in your household? 1 / 2 / 3 / 4 / 5 / 6 / 7 **How many children live in your home?** 0 / 1 / 2 / 3 / 4 / 5 / 6 / 7 **In the case of children in your home, how old are they? Age:**

How many pets live in your home? 0 / 1 / 2 / 3 / 4 / 5 / 6 / 7 **In the case of pets, what type are they?** (Multiple options can be selected) Dog / Cat / Rodents / Fish / Reptiles / Others:
Does anyone in your household smoke? Yes / No **If yes, how many smokers are?** 1 / 2 / 3 / 4 / 5 / 6 / 7
In the case of smokers, how many cigarettes per day are smoked inside the home? No. cigarettes: (Total sum of all smokers. Specify per day, per week or per month).
In the case of smokers, how many cigarettes per day are smoked outdoors? No. cigarettes: (Total sum of all smokers. Specify per day, per week or per month).
Do former smokers live in your home? Yes / No **If yes, how long has it been since they quit smoking?** Answer: (Specify by months or by years, for each person who has quit smoking).
Has it smoked inside your home for social reasons in the last few weeks? Yes / No (Meetings, dinners or meals with friends, among others).
Do smokers often enter your home, including those who do not smoke indoors? Yes / No

Do you notice tobacco smoke odour in your home when no one is smoking? Yes / No
Do you consider that inhalation of second-hand smoke is harmful to health? Yes / No / I don't know **Do you consider that thirdhand smoke is harmful to health?** Yes / No / I don't know (Thirdhand smoke consists of the remains of smoke that remain on surfaces and dust, and is perceived as the characteristic tobacco smoke odour).

4.7 References

(1) Matt, G. E.; Quintana, P. J. E.; Destaillats, H.; Gundel, L. A.; Sleiman, M.; Singer, B. C.; Jacob, P.; Benowitz, N.; Winickoff, J. P.; Rehan, V.; Talbot, P.; Schick, S.; Samet, J.; Wang, Y.; Hang, B.; Martins-Green, M.; Pankow, J. F.; Hovell, M. F. Thirdhand Tobacco Smoke: Emerging Evidence and Arguments for a Multidisciplinary Research Agenda. *Environ. Health Perspect.* **2011**, *119* (9), 1218–1226. https://doi.org/10.1289/ehp.1103500.

(2) WHO. *Tobacco and Its Environmental Impact: An Overview*; 2017. https://doi.org/ISBN 978-92-4-151249-7.

(3) Farren, N. J.; Ramírez, N.; Lee, J. D.; Finessi, E.; Lewis, A. C.; Hamilton, J. F. Estimated Exposure Risks from Carcinogenic Nitrosamines in Urban Airborne Particulate Matter. *Environ. Sci. Technol.* **2015**, *49* (16), 9648–9656. https://doi.org/10.1021/acs.est.5b01620.

(4) Cecinato, A.; Balducci, C.; Romagnoli, P.; Perilli, M. Airborne Psychotropic Substances in Eight Italian Big Cities: Burdens and Behaviours. *Environ. Pollut.* **2012**, *171*, 140–147. https://doi.org/10.1016/j.envpol.2012.07.033.

(5) Jacob, P.; Benowitz, N. L.; Destaillats, H.; Gundel, L.; Hang, B.; Martins-Green, M.; Matt, G. E.; Quintana, P. J. E.; Samet, J. M.; Schick, S. F.; Talbot, P.; Aquilina, N. J.; Hovell, M. F.; Mao, J. H.; Whitehead, T. P. Thirdhand Smoke: New Evidence, Challenges, and Future Directions. *Chem. Res. Toxicol.* **2017**, *30* (1), 270–294. https://doi.org/10.1021/acs.chemrestox.6b00343.

(6) Ramírez, N.; Özel, M. Z.; Lewis, A. C.; Marcé, R. M.; Borrull, F.; Hamilton, J. F. Exposure to Nitrosamines in Thirdhand Tobacco Smoke Increases Cancer Risk in Non-Smokers. *Environ. Int.* **2014**, *71*, 139–147. https://doi.org/10.1016/j.envint.2014.06.012.

(7) Ramírez, N.; Vallecillos, L.; Lewis, A. C.; Borrull, F.; Marcé, R. M.; Hamilton, J. F. Comparative Study of Comprehensive Gas Chromatography-Nitrogen Chemiluminescence Detection and Gas Chromatography-Ion Trap-Tandem Mass Spectrometry for Determining Nicotine and Carcinogen Organic Nitrogen Compounds in Thirdhand Tobacco Smoke. *J. Chromatogr. A* **2015**. https://doi.org/10.1016/j.chroma.2015.11.035.

(8) Hoh, E.; Hunt, R. N.; Quintana, P. J. E.; Zakarian, J. M.; Chatfield, D. A.; Wittry, B. C.; Rodriguez, E.; Matt, G. E. Environmental Tobacco Smoke as a Source of Polycyclic Aromatic Hydrocarbons in Settled Household Dust. *Environ. Sci. Technol.* **2012**, *46* (7), 4174–4183. https://doi.org/10.1021/es300267g.

(9) Schick, S. F.; Farraro, K. F.; Perrino, C.; Sleiman, M.; van de Vossenberg, G.; Trinh, M. P.; Katharine Hammond, S.; Jenkins, B. M.; Balmes, J. Thirdhand Cigarette Smoke in an Experimental Chamber: Evidence of Surface Deposition of Nicotine, Nitrosamines and Polycyclic Aromatic Hydrocarbons and de Novo Formation of NNK. *Tob. Control* **2014**, *23* (2), 152–159. https://doi.org/10.1136/tobaccocontrol-2012-050915.

(10) Sleiman, M.; Logue, J. M.; Luo, W.; Pankow, J. F.; Gundel, L. A.; Destaillats, H. Inhalable Constituents of Thirdhand Tobacco Smoke: Chemical Characterization and Health Impact Considerations. *Environ. Sci. Technol.* **2014**, *48* (22), 13093–13101.

https://doi.org/10.1021/es5036333.

(11) Hollender, J.; Schymanski, E. L.; Singer, H. P.; Ferguson, P. L. Nontarget Screening with High Resolution Mass Spectrometry in the Environment: Ready to Go? *Environ. Sci. Technol.* **2017**, *51* (20), 11505–11512. https://doi.org/10.1021/acs.est.7b02184.

(12) Chiaia-Hernandez, A. C.; Schymanski, E. L.; Kumar, P.; Singer, H. P.; Hollender, J. Suspect and Nontarget Screening Approaches to Identify Organic Contaminant Records in Lake Sediments. *Anal. Bioanal. Chem.* **2014**, 7323–7335. https://doi.org/10.1007/s00216-014-8166-0.

(13) Moschet, C.; Anumol, T.; Lew, B. M.; Bennett, D. H.; Young, T. M. Household Dust as a Repository of Chemical Accumulation: New Insights from a Comprehensive High-Resolution Mass Spectrometric Study. *Environ. Sci. Technol.* **2018**, *52* (5), 2878–2887. https://doi.org/10.1021/acs.est.7b05767.

(14) Rager, J. E.; Strynar, M. J.; Liang, S.; McMahen, R. L.; Richard, A. M.; Grulke, C. M.; Wambaugh, J. F.; Isaacs, K. K.; Judson, R.; Williams, A. J.; Sobus, J. R. Linking High Resolution Mass Spectrometry Data with Exposure and Toxicity Forecasts to Advance High-Throughput Environmental Monitoring. *Environ. Int.* **2016**, *88*, 269–280. https://doi.org/10.1016/j.envint.2015.12.008.

(15) Rostkowski, P.; Haglund, P.; Aalizadeh, R.; Alygizakis, N.; Thomaidis, N.; Arandes, J. B.; Nizzetto, P. B.; Booij, P.; Budzinski, H.; Brunswick, P.; Covaci, A.; Gallampois, C.; Grosse, S.; Hindle, R.; Ipolyi, I.; Jobst, K.; Kaserzon, S. L.; Leonards, P.; Lestremau, F.; Letzel, T.; Magnér, J.; Matsukami, H.; Moschet, C.; Oswald, P.; Plassmann, M.; Slobodnik, J.; Yang, C. The Strength in Numbers: Comprehensive Characterization of House Dust Using Complementary Mass Spectrometric Techniques. *Anal. Bioanal. Chem.* **2019**, *411* (10), 1957–1977. https://doi.org/10.1007/s00216-019-01615-6.

(16) Torres, S; Paton, B; Marcé, RM; Borull, F; Correig, X; Ramírez, N. Development of a Quick and Cost-Effective Method for Determining Tobacco-Specific Toxicants in Indoor Dust. *J. Chromatogr. A* **2020**.

(17) Torres, Sònia; Schymanski, Emma; Ramirez, N. Zenodo website. https://doi.org/http://doi.org/10.5281/zenodo.2669467.

(18) Torres, Sònia; Schymanski, Emma; Ramirez, N. Environmental Protection Agency website https://comptox.epa.gov/dashboard/chemical_lists/thsmoke.

(19) Torres, Sònia; Schymanski, Emma; Ramirez, N. NORMAN website. https://doi.org/10.5281/zenodo.2669466.

(20) Kessner, D.; Chambers, M.; Burke, R.; Agus, D.; Mallick, P. ProteoWizard: Open Source Software for Rapid Proteomics Tools Development. *Bioinformatics* **2008**, *24* (21), 2534–2536. https://doi.org/10.1093/bioinformatics/btn323.

(21) Tautenhahn, R.; Bottcher, C.; Neumann, S. Highly Sensitive Feature Detection for High Resolution LC/MS. *BMC Bioinformatics* **2008**, *9*, 1–16. https://doi.org/10.1186/1471-2105-9-504.

(22) Benton, H. P.; Want, E. J.; Ebbels, T. M. D. Correction of Mass Calibration Gaps in Liquid

Chromatography-Mass Spectrometry Metabolomics Data. *Bioinformatics* **2010**, *26* (19), 2488–2489. https://doi.org/10.1093/bioinformatics/btq441.

(23) Smith, C. A.; Want, E. J.; O'Maille, G.; Abagyan, R.; Siuzdak, G. XCMS: Processing Mass Spectrometry Data for Metabolite Profiling Using Nonlinear Peak Alignment, Matching, and Identification. *Anal. Chem.* **2006**, *78* (3), 779–787. https://doi.org/10.1021/ac051437y.

(24) Tautenhahn, R.; Patti, G. J.; Rinehart, D.; Siuzdak, G. XCMS Online: A Web-Based Platform to Process Untargeted Metabolomic Data. *Anal. Chem.* **2012**, *84* (11), 5035–5039. https://doi.org/10.1021/ac300698c.

(25) Vinaixa, M.; Samino, S.; Saez, I.; Duran, J.; Guinovart, J. J.; Yanes, O. A Guideline to Univariate Statistical Analysis for LC/MS-Based Untargeted Metabolomics-Derived Data. *Metabolites* **2012**, *2* (4), 775–795. https://doi.org/10.3390/metabo2040775.

(26) Ruttkies, C.; Schymanski, E. L.; Wolf, S.; Hollender, J.; Neumann, S. MetFrag Relaunched: Incorporating Strategies beyond in Silico Fragmentation. *J. Cheminform.* **2016**, *8* (1), 1–16. https://doi.org/10.1186/s13321-016-0115-9.

(27) Kim, S.; Thiessen, P. A.; Bolton, E. E.; Chen, J.; Fu, G.; Gindulyte, A.; Han, L.; He, J.; He, S.; Shoemaker, B. A.; Wang, J.; Yu, B.; Zhang, J.; Bryant, S. H. PubChem Substance and Compound Databases. *Nucleic Acids Res.* **2016**. https://doi.org/10.1093/nar/gkv951.

(28) Williams, A. J.; Grulke, C. M.; Edwards, J.; McEachran, A. D.; Mansouri, K.; Baker, N. C.; Patlewicz, G.; Shah, I.; Wambaugh, J. F.; Judson, R. S.; Richard, A. M. The CompTox Chemistry Dashboard: A Community Data Resource for Environmental Chemistry. *J. Cheminform.* **2017**, *9* (1), 1–27. https://doi.org/10.1186/s13321-017-0247-6.

(29) Schymanski, E. MetFrag Local CSV: CompTox (7 March 2019 Release) Smoking MetaData File. **2019**. https://doi.org/10.5281/ZENODO.3364464.

(30) McEachran, A. D.; Mansouri, K.; Grulke, C.; Schymanski, E. L.; Ruttkies, C.; Williams, A. J. "MS-Ready" Structures for Non-Targeted High-Resolution Mass Spectrometry Screening Studies. *J. Cheminform.* **2018**. https://doi.org/10.1186/s13321-018-0299-2.

(31) No Title. https://doi.org/10.23645/epacomptox.7525199.v2.

(32) Williams, A. J.; Grulke, C. M.; Edwards, J.; McEachran, A. D.; Mansouri, K.; Baker, N. C.; Patlewicz, G.; Shah, I.; Wambaugh, J. F.; Judson, R. S.; Richard, A. M. The CompTox Chemistry Dashboard: A Community Data Resource for Environmental Chemistry. *J. Cheminform.* **2017**. https://doi.org/10.1186/s13321-017-0247-6.

(33) Rager, J. E.; Strynar, M. J.; Liang, S.; McMahen, R. L.; Richard, A. M.; Grulke, C. M.; Wambaugh, J. F.; Isaacs, K. K.; Judson, R.; Williams, A. J.; Sobus, J. R. Linking High Resolution Mass Spectrometry Data with Exposure and Toxicity Forecasts to Advance High-Throughput Environmental Monitoring. *Environ. Int.* **2016**, *88*, 269–280. https://doi.org/10.1016/j.envint.2015.12.008.

(34) Richard, A. M.; Judson, R. S.; Houck, K. A.; Grulke, C. M.; Volarath, P.; Thillainadarajah, I.; Yang, C.; Rathman, J.; Martin, M. T.; Wambaugh, J. F.; Knudsen, T. B.; Kancherla, J.; Mansouri, K.; Patlewicz, G.; Williams, A. J.; Little, S. B.; Crofton, K. M.; Thomas, R. S.

ToxCast Chemical Landscape: Paving the Road to 21st Century Toxicology. *Chemical Research in Toxicology*. 2016. https://doi.org/10.1021/acs.chemrestox.6b00135.

(35) Dionisio, K. L.; Phillips, K.; Price, P. S.; Grulke, C. M.; Williams, A.; Biryol, D.; Hong, T.; Isaacs, K. K. Data Descriptor: The Chemical and Products Database, a Resource for Exposure-Relevant Data on Chemicals in Consumer Products. *Sci. Data* **2018**. https://doi.org/10.1038/sdata.2018.125.

(36) Aalizadeh, Reza; Alygizakis, Nikiforos; Schymanski, Emma; Slobodnik, J. Zenodo Website. https://doi.org/10.5281/zenodo.2664078.

(37) Schymanski, E. L.; Baker, N. C.; Williams, A. J.; Singh, R. R.; Trezzi, J. P.; Wilmes, P.; Kolber, P. L.; Kruger, R.; Paczia, N.; Linster, C. L.; Balling, R. Connecting Environmental Exposure and Neurodegeneration Using Cheminformatics and High Resolution Mass Spectrometry: Potential and Challenges. *Environ. Sci. Process. Impacts* **2019**, *21* (9), 1426–1445. https://doi.org/10.1039/c9em00068b.

(38) TOBACCO|SMOKING: Database of chemical compounds present in Smokeless tobacco products (SLTChemDB) https://comptox.epa.gov/dashboard/chemical_lists/SLTCHEMDB (accessed Oct 21, 2020).

(39) WIKILIST: Additives in cigarettes.

(40) Schymanski, E. S35 | INDOORCT16 | Indoor Environment Substances from 2016 Collaborative Trial https://zenodo.org/record/3653164#.X5AF2S8lPm0 (accessed Oct 21, 2020). https://doi.org/10.5281/zenodo.3653164.

(41) Schymanski, E. schymane/ReSOLUTION https://github.com/schymane/ReSOLUTION (accessed Sep 15, 2020).

(42) Matt, G. E.; Quintana, P. J. E.; Zakarian, J. M.; Fortmann, A. L.; Chatfield, D. A.; Hoh, E.; Uribe, A. M.; Hovell, M. F. When Smokers Move out and Non-Smokers Move in: Residential Thirdhand Smoke Pollution and Exposure. *Tob. Control* **2011**, *20* (1), e1–e1. https://doi.org/10.1136/tc.2010.037382.

(43) Matt, G. E.; Quintana, P. J. E.; Zakarian, J. M.; Hoh, E.; Hovell, M. F.; Mahabee-Gittens, M.; Watanabe, K.; Datuin, K.; Vue, C.; Chatfield, D. A. When Smokers Quit: Exposure to Nicotine and Carcinogens Persists from Thirdhand Smoke Pollution. *Tob. Control* **2017**, *26* (5), 548–556. https://doi.org/10.1136/tobaccocontrol-2016-053119.

(44) Matt, G. E.; Mahabee-Gittens, E. M.; Zakarian, J. M.; Quintana, P. J. E.; Hoh, E.; Myers, M. Nicotine in Thirdhand Smoke Residue Predicts Relapse from Smoking Cessation: A Pilot Study. *Addict. Behav.* **2019**, *98* (June), 106041. https://doi.org/10.1016/j.addbeh.2019.106041.

(45) Whitehead, T. P.; Havel, C.; Metayer, C.; Benowitz, N. L.; Jacob, P. Tobacco Alkaloids and Tobacco-Specific Nitrosamines in Dust from Homes of Smokeless Tobacco Users, Active Smokers, and Nontobacco Users. *Chem. Res. Toxicol.* **2015**, *28* (5), 1007–1014. https://doi.org/10.1021/acs.chemrestox.5b00040.

(46) Sleiman, M.; Gundel, L. a; Pankow, J. F.; Jacob, P.; Singer, B. C.; Destaillats, H. Formation of Carcinogens Indoors by Surface-Mediated Reactions of Nicotine with Nitrous Acid,

Leading to Potential Thirdhand Smoke Hazards. *Proc. Natl. Acad. Sci. U. S. A.* **2010**, *107* (15), 6576–6581. https://doi.org/10.1073/pnas.0912820107.

(47) Schick, S. F.; Glantz, S. Concentrations of the Carcinogen 4-(Methylnitrosamino)-1-(3-Pyridyl)-1- Butanone in Sidestream Cigarette Smoke Increase after Release into Indoor Air: Results from Unpublished Tobacco Industry Research. *Cancer Epidemiol. Biomarkers Prev.* **2007**. https://doi.org/10.1158/1055-9965.EPI-07-0210.

(48) US Environmental Protection Agency. Exposure Factors Handbook: 2011 Edition. *U.S. Environ. Prot. Agency* **2011**. https://doi.org/EPA/600/R-090/052F.

5. Unravelling the metabolic alterations of liver damage induced by Thirdhand Smoke

UNIVERSITAT ROVIRA I VIRGILI
ADVANCES ON THIRDHAND SMOKE USING TARGETED AND UNTARGETED APPROACHES
Sònia Torres Gené

5.1 Abstract

Background: Thirdhand smoke (THS) is the accumulation of tobacco smoke gases and particles that become embedded in materials. Previous studies concluded that THS exposure induces oxidative stress and hepatic steatosis in liver. Despite the knowledge of the increasing danger of THS exposure, the metabolic disorders caused in liver are still not well defined.

Objectives: The aim of this study is to investigate the metabolic disorders caused by THS exposure in liver of male mice and to evaluate the effects of an antioxidant treatment in the exposed mice.

Methods: We investigated liver from three mice groups: non-exposed mice, exposed to THS in conditions that mimic human exposure and THS-exposed treated with antioxidants. Liver samples were analyzed using a multiplatform untargeted metabolomics approach including nuclear magnetic resonance (NMR), liquid chromatography coupled to high-resolution mass spectrometry (LC-MS) and laser desorption/ionization mass spectrometry imaging (MSI), able to map lipids in liver tissues.

Results: Our multiplatform approach allowed the annotation of eighty-eight metabolites altered by THS exposure, including amino acids, nucleotides and several types of lipids. The main dysregulated pathways by THS exposure were D-glutamine and D-glutamate metabolism, glycerophospholipid metabolism and oxidative phosphorylation and glutathione metabolism, being the last two related to oxidative stress. THS-exposed mice also presented higher lipid accumulation and decrease of metabolites involved in the phosphocholine synthesis, as well as choline deficiency, which is related to Non-Alcoholic Fatty Liver Disease and steatohepatitis. Interestingly, the antioxidant treatment of THS-exposed mice reduced the accumulation of some lipids, but could not

revert all the metabolic alterations, including some related to the impairment of the mitochondrial function.

Conclusions: THS alters liver function at a molecular level, dysregulating many metabolic pathways. The molecular evidences provided here confirm that THS is a new factor for liver steatosis and provide the basis for future research in this respect.

5.2 Introduction

Non-Alcoholic Fatty Liver Disease (NAFLD) is becoming the most common chronic liver disorder in the western countries affecting both adults and children. The prevalence of NAFLD in Europe has reached very high levels (20-30%) (European Liver Patient's Association (ELPA), 2017) and it is expected to grow across many countries in the years to come. NAFLD comprises different stages starting with non-alcoholic fatty liver (NAFL) and non-alcoholic steatohepatitis (NASH) which can progress to more severe and irreversible stages of the disease such as fibrosis, cirrhosis and hepatocellular carcinoma (HCC) (Haas et al., 2016). As a result, NAFLD is becoming a leading indication for liver transplantation and cause of hepatocellular carcinoma (Adam et al., 2012; Bertuccio et al., 2017). Due to the importance on the early detection at previous stages with non-invasive techniques, current research focuses on finding reliable biomarkers to predict disease stages and development (Pirola and Sookoian, 2018). Since NAFLD is seen as a lifestyle condition, it is vital to determine all the risk factors associated on its prevalence. Previous research demonstrated that tobacco consumption is a risk factor in NAFLD development (Akhavan Rezayat et al., 2018; Hamabe et al., 2011; Kim et al., 2018; PeiYi et al.,

2017), and that the exposure to secondhand smoke (SHS) also increases this risk (Liu et al. 2013; Yuan et al. 2009) .

Nevertheless, exposure to tobacco smoke toxicants goes beyond SHS exposure. A less studied path of exposure is the so-called thirdhand smoke (THS) that is formed by the accumulation of tobacco smoke toxicants that settle on furniture, fabrics and surfaces in places where SHS was present (Jacob et al., 2017; Matt et al., 2011). These toxicants can also react with atmospheric oxidants to form secondary pollutants that could have increased toxicity (Sleiman et al., 2010), such as tobacco-specific nitrosamines, a leading class of carcinogens that affect humans (IARC, 2004). Recently, several studies have presented undeniable evidences of THS health hazards, including liver damage in in vitro and in vivo models (Flores et al., 2017, 2016; Hang et al., 2017; Jacob et al., 2017). THS exposure of mice caused abnormal lipid metabolism in liver, enhancing the accumulation of lipids in larger lipid droplets in the hepatocytes with higher concentrations of triglycerides that is mediated by oxidative stress. This accumulation of lipids can result in the development of NAFLD (Adhami et al., 2016; Flores et al., 2016; Martins-Green et al., 2014). After four weeks of THS exposure, male mice presented an increase of the liver damage biomarker aspartate aminotransferase (AST), and from two months there were signs of molecular damage induced by oxidative stress, including an increase of hydrogen peroxide (H_2O_2) and superoxide dismutase (SOD) (Adhami et al., 2017). The decrease of the oxidative stress with antioxidants ameliorated the THS-induced damage (Adhami et al., 2016; Chen et al., 2018; Flores et al., 2016). Moreover, acute and chronic exposure to THS of human liver cancer cells (HepG2) significantly increased DNA strand breaks (Hang et al., 2013). In view of these results, THS exposure could be a new risk factor for the

development of hepatic steatosis. Nevertheless, the extent of the molecular alterations in liver induced by THS exposure remains to be fully elucidated.

Here we present a novel approach for the comprehensive molecular characterization of THS-induced liver damage based on multiplatform untargeted metabolomics of liver samples from male mice exposed to THS in conditions that mimic exposure of humans in the homes of smokers. In order to determine if antioxidants could completely revert THS-induced molecular damage, some of the THS-exposed mice were treated with antioxidants. Untargeted metabolomics is a powerful tool that allows the simultaneous determination of hundreds of metabolites in biological samples and, therefore, is key to elucidate metabolic changes and disorders (Siuzdak et al., 2012). We have performed untargeted analysis of aqueous and lipidic liver extracts using two complementary analytical platforms to cover a wider range of metabolites: proton nuclear magnetic resonance (^{1}H NMR) and liquid chromatography coupled to high resolution mass spectrometry (LC-MS). Furthermore, we have also explored the spatial distribution of lipids in the liver samples by acquiring mass spectrometry images of liver sections using an innovative methodology based on sputtered gold nanolayers and laser desorption ionization mass spectrometry (LDI-MS). To our knowledge, this is the first study that assess the potential of a multiplatform metabolomics approach to unravel the molecular alterations of THS-induced liver damage.

5.3 Materials and mehtods

5.3.1 Animal Models

Animal models were developed at the Molecular, Cell and Systems Biology Department at the University of California Riverside. Male C57BL/6 mice model and THS exposure methodology was described by Martins-Green et al. (Flores et al., 2016; Martins-Green et al., 2014). Briefly, different household materials were exposed to secondhand smoke (SHS) from a smoking machine. Total particulate matter was 30 +/- 5 µg/m3, which is within the range detected by the Environmental Protection Agency (EPA) in the homes of smokers (15-35 µg/m3) (EPA, 2004; Ott et al., 2008). For this study, male mice were randomly divided into three experimental groups (5 mice for each group): control (CTRL), which was never exposed to THS; THS-exposed (THS) that were placed in the exposed cages from weaning (three weeks of age) to 24 weeks; and a third group of mice exposed to THS and then treated intraperitoneally with the antioxidant alpha-tocopherol (alpha-toc) and N-acetylcysteine (NAC) for 20 weeks while the mice still continued to be exposed to THS (THS-AO). THS and THS-AO groups were never exposed to SHS, and all groups were fed a standard chow diet (percent calories: 58% carbohydrates, 28.5% protein, and 13.5% fat). In order to assure the reliability of the THS exposure model, we measured the concentration of 4-(methylnitrosoamino)-1-(3-pyridyl)-1-butanol (NNAL) in the urine of mice that is the main metabolite of the tobacco-specific nitrosamine 4-(methylnitrosoamino)-1-(3-pyridyl)-1-butanone (NNK), a well-accepted biomarker of exposure to tobacco toxicants (Torres et al., 2018). Median urine concentration of NNAL of THS-exposed mice was 35 pg ml-1, 20% less than NNAL levels in urine of SHS-exposed infants/toddlers, confirming the suitability of our THS exposure model (Martins-Green et al., 2014).

Animal experimental protocols were approved by the University of California, Riverside, Institutional Animal Care and Use Committee (IACUC). Mice were euthanized with Carbon dioxide (CO_2) inhalation which is the most common method of euthanasia used by NIH for mice. The levels and time for CO2 exposure were approved by the University of California, Riverside IACUC, death was induced quickly and without pain. Liver samples were snap frozen and kept at -80 °C until analysis.

5.3.2 Untargeted metabolomic analysis

To cover a wider range of metabolites, we performed untargeted metabolomics analysis using two complementary analytical platforms: 1H NMR and LC-MS.

For 1H NMR analysis, five liver samples of each experimental group were lyophilized overnight and mechanically pulverized. Twenty mg of dried liver powder of each sample were extracted twice with 1.5 and 0.5 mL of a precooled acetonitrile–water mixture (1:1) by vigorous vortexing for 30 s, followed by the extraction of the hydrophilic metabolites in an ultrasound ice bath for 5 min. After centrifugation at 15000 rpm for 15 min at 4°C, the combined supernatants from both extractions were dried and redissolved with 700 µL of phosphate buffer (Na_2HPO_4/NaH_2PO_4, 0.2 M, in D_2O) containing 0.7 mM NaN_3 and 2.3 mM of 3-(trimethylsilyl)propionic-2,2,3,3-d_4 acid sodium salt (TSP-d_4) as chemical shift reference. For the extraction of the lipophilic metabolites, the pellets from the previous extraction were mixed with 1 mL of chloroform: methanol (2:1) and extracted as commented above. Lipidic extracts were dried under a gentle N2 stream and reconstituted with 700 µL of a

mixture of $CDCl_3$, CD_3OD and D_2O (64:32:4) containing 1.18 mM tetramethylsilane (TMS). Following centrifugation, 650 µL of each extract was transferred into a 5 mm NMR tube for NMR analysis. Liver extracts (aqueous and lipidic) were analyzed using a Bruker ADVANCE III 600 instrument (Bruker Biospin GmBH, Rheinstetten, Germany). 1H NMR spectra were recorded at 310 K on a spectrometer operating at a proton frequency of 600.20 MHz. For the aqueous extracts, one-dimensional 1H pulse experiments were carried out using a nuclear Overhauser effect spectroscopy (NOESY)-presaturation sequence to suppress the residual water peak at around 4.7 ppm for aqueous extract. The relaxation delay between scans was set to 5 s. Spectral width was 16 ppm and a total of 256 transients were collected for each spectrum. In the case of lipophilic extracts, a 90° pulse with presaturation sequence (zgpr) was used. Spectral width was 18.6 ppm and a total of 128 transients were collected for each spectrum.

The acquired one dimensional (1D) 1H NMR spectra were phased, baseline-corrected and referenced to glucose signal (5.23 ppm) for the aqueous extracts and to TMS signal for the lipidic extracts with TopSpin from Bruker. After baseline correction, peaks in the 1D spectra were integrated using the AMIX 3.8 software package (Bruker). Metabolites were annotated with level 1 confidence following the Rank and AssigN Confidence to Metabolites (RANCM) proposed by Joetsen et al. (Joesten and Kennedy, 2019), by comparing their chemical shifts with those for the standard compounds from Chenomx NMR Suite Professional database (Chenomx Inc., Edmonton, Canada), BBioref AMIX database (Bruker), Human metabolome database, version 3.0 (Wishart et al., 2012) and previous bibliography (Vinaixa et al., 2010). Relative concentrations derived from both aqueous and lipidic and extracts were arranged together in one single data matrix, which was used as the input matrix to perform the

statistical analysis using RStudio (version 3.3.2, Boston, MA). Student's t-test FDR-adjusted p-value < 0.05 and absolute fold change (FC) ≥ 1.1 were considered to indicate statistically significant differences between the experimental groups.

Based on previous literature, aliquots of the extracts prepared for the NMR analysis were directly analyzed by LC-MS (Beltran et al., 2012). Three L of the aqueous extracts were injected into a 1290 Infinity LC System coupled to a 6230 ESI-QTOF mass spectrometer (both from Agilent Technologies, Palo Alto, CA, USA), using an ACQUITY UHPLC HSS T3 C18 column (2.1mm x 150 mm, 1.8 m) from Waters (Eschborn, Germany), kept at 30C during the whole analysis. The mobile phases consisted of ultrapure water containing 0.1% formic acid (A) and acetonitrile with 0.1% formic acid (B) at a flow rate of 0.45 mL min-1. The gradient elution program was as follows: 100% A for 2 min, 100% A to 100% B from 2 to 9 min, 100% B from 9 to 10 min, and 100% A from 10 to 12 min.

Fifty µL of the lipidic extracts used for the NMR analysis were evaporated to dryness and reconstituted with 100 l of methanol: toluene (9:1). Three µL of these reconstituted extracts were injected into the same LC-MS instrument. Separation was performed as described by Pi et al. (Pi et al., 2016) using an ACQUITY UHPLC BEH C18 column (2.1 mm x 150 mm, 1.7 mm; Waters), and mobile phases: A: acetonitrile: water (60:40) with 10mM of ammonium formate and B: isopropanol: acetonitrile (90:10) with 10 mM of ammonium formate.

For both analyses, the mass spectrometer operated in positive electrospray ionization (ESI+) mode in the following conditions: gas temperature, 150 °C; drying gas, 11 L min−1; nebulizer, 35 psi; fragmentor, 120 V; and skimmer, 65 V. The instrument was set to acquire over the m/z range 100-1000 for the

aqueous extracts and 50−1200 for the lipidic ones, at an acquisition rate of 3 spectra s-1. To assure the quality of the analysis, the extracts were injected in randomized order and quality control (QC) samples (prepared by pooling equal volumes of all aqueous and lipidic extracts, respectively) were injected every 5 samples.

LC- MS data was processed using the XCMS software, version 2.9.2 (Smith et al., 2006) to detect and align features. Those features with intensity lower than 5,000 spectral counts and variation lower than those found in the QC samples were discarded. Features found in at least 80% of samples were used for univariate statistical analysis. Those filtered features that were statistically different between the studied groups (p-value < 0.05, Student's t-test, FDR corrected, and FC > 2) were putatively annotated by searching against the HMDB, version 3.0 (Wishart et al., 2012) within 5 ppm mass error threshold. The putatively annotated features with a candidate for the [M+H]+ adduct and relevant biological interest were confirmed by Tandem MS (MS/MS) performed in targeted mode, acquiring over the m/z range 50−1000, with a narrow isolation width (~1.3 m/z) and a fixed collision energy of 20 V. Annotation was carried out by comparing the obtained experimental mass fragmentation spectra with those experimental spectra from open access databases (HMDB, METLIN (Smith et al., 2005) and LipidMaps (Fahy et al., 2007), with a level 2 identification confidence, accordingly with Schymanski et al. (coincidence of exact mass of the precursor ion (MS) and fragmentation pattern (MS2)) (Schymanski et al., 2014). More information about relevant feature selection and metabolite annotation can be found in the Supplementary Material, Section S2. Two-way hierarchical clustering was performed using MetaboAnalyst software (Chong et al., 2019).

NMR and LC-MS data are accessible at the Zenodo Open Access Repository (https://zenodo.org), under DOI: 10.5281/zenodo.3986136

5.3.3 Pathway analysis

The statistically relevant metabolites annotated by untargeted metabolomics in the liver extracts (including both, aqueous and lipidic extracts) were used to determine the metabolic pathways altered by THS exposure. Pathway enrichment analysis was performed using MBROLE 2.0 (Chagoyen and Pazos, 2011), selecting mus musculus as organism-based background. Only pathways over enriched with a p-value < 0.05 (FDR-corrected) were considered for the biological interpretation of the results. Fold enrichment (FE) of each altered metabolic pathway was calculated using the following formula FE = (m/n)/(M/N) (Huang et al., 2009), being m: metabolites annotated in our study that belong to a specific metabolic pathway; n: the total number of metabolites annotated in our study; M: the total number of metabolites in a pathway; and N: all the metabolites of mice (mus musculus) reported in the database.

5.3.4 Mass Spectrometry Imaging

Mass spectrometry images were acquired using a matrix-free laser desorption/ionization methodology developed in our research group that is based on the deposition of gold sputtered nanolayers on tissue sections (Ràfols et al., 2018). Briefly, liver tissues were sectioned at -20°C into 10 µm thick sections using a Leica CM-1950 cryostat (Leica Biosystems Nussloch GmbH) and mounted on indium-tin oxide-coated (ITO) glass slides by directly placing the

glass slide at ambient temperature onto the section. Gold nanolayers were deposited onto the 10 µm tissue sections using a sputtering system ATC Orion 8-HV (AJA International, N. Scituate, MA, USA). Histological images were acquired by examining serial liver sections stained with Oil Red O (ORA) using standard protocols. MSI images were acquired using a MALDI TOF/TOF UltrafleXtreme instrument with SmartBeam II Nd:YAG/355 nm laser from Bruker Daltonics (Massachusetts, USA) and a raster size of 20 m.

LDI-MSI spectra data handling, alignment, calibration, peak picking (selecting peaks with signal-to-noise ratio > 5) and peak binning were carried out using the in-house developed R package rMSIproc (Ràfols et al., 2020). MS images reconstruction and visual inspection was performed with rMSI package (Ràfols et al., 2017), which allows the reconstruction of the ion intensity images and the calculation of average spectra of regions of interest.

5.4 Results

5.4.1 Untargeted metabolomics results

Combining untargeted metabolomics analysis by 1H NMR and LC-MS, we were able to annotate 108 relevant metabolites in the aqueous (52) and lipidic (56) liver extracts. Supplementary Material, Section S1 and Section S2 present detailed information about the selection of relevant features and metabolite annotation by both analytical platforms.

Table 1 shows the complete list of statistically different metabolites annotated in the aqueous extracts, including their p-values (FDR corrected) and FC for the different comparisons between the experimental groups (CTRL vs.

THS, THS vs. THS-AO) and the analytical platform that allowed the annotation. As it can be seen in Table 1, the annotated metabolites in the aqueous extracts included amino acids, coenzymes, nucleotides, peptides and organic acids, among others. Adenosine monophosphate (AMP) and glutamine were annotated by both analytical platforms, giving consistent results in both cases. For these two metabolites we present the results obtained by LC-MS, because this analytical platform provided the lower p values. Exposure to THS resulted in the alteration of forty-nine aqueous metabolites (Table 1, "CTRL vs. THS" columns), evidencing the impact of THS exposure in liver at the molecular level. Treatment with antioxidants was able to regulate the concentrations of twenty of the aqueous metabolites (Table 1, "THS vs. THS-AO" columns). As an example, serotonin, which is recognized to affect various liver diseases (Lesurtel et al., 2012), was the most upregulated metabolite annotated in THS mice livers (FC (CTRL vs. THS)= 12.4, but the levels of serotonin decreased under the antioxidant treatment of THS exposed mice (FC (THS vs. THS-AO)= -13.1). Nevertheless, we found that the antioxidant treatment was not able to revert the alterations induced by THS exposure in twenty-nine metabolites. This was the case, for instance, of the levels of some acylcarnitines (i.e. Octanoylcarnitine, Decanoylcarnitine, Hexanoylcarnitine), that were increased by THS exposure and remained increased with the antioxidant treatment. Antioxidant treatment was also not able to revert the decrease of the nucleotides cytidine and cytosine, as well as, tryptophan and adenosine diphosphate (ADP), among others.

Table 1. Metabolites annotated in the aqueous extracts that were statistically relevant between THS-exposed and non-exposed liver samples (CTRL vs. THS), between THS-exposed mice and those exposed to THS and treated with antioxidants (THS vs. THS-AO). For each metabolite, the FDR corrected p-value and fold change (FC) of each comparison and the determination technique is also indicated. (Abbreviations: NAD: Nicotinamide adenine nucleotide; NADP: Nicotinamide adenine nucleotide phosphate; AMP: Adenosine monophosphate; ADP: Adenosine diphosphate).

Metabolite	CTRL vs THS		THS vs THS-AO		*Technique*
	p-value (FDR)	*FC*	*p-value (FDR)*	*FC*	
Serotonin	2.87×10^{-03}	12.4	2.90×10^{-02}	-13.1	LC-MSMS
Octanoylcarnitine	1.65×10^{-02}	11.6			LC-MSMS
Decanoylcarnitine	4.49×10^{-02}	6.9			LC-MSMS
N-α-Acetyl-arginine	5.13×10^{-03}	6.8			LC-MSMS
N6-Acetyl-lysine	9.20×10^{-03}	5.1			LC-MSMS
NAD	7.67×10^{-03}	4.7			LC-MSMS
Leucyl-Isoleucine	1.51×10^{-02}	3.8			LC-MSMS
Adenosine diphosphate ribose	6.82×10^{-03}	3.5			LC-MSMS
Hexanoyl carnitine	2.22×10^{-02}	2.9			LC-MSMS
Nα-Acetyl-glutamine	2.62×10^{-02}	2.9			LC-MSMS
AMP	8.83×10^{-03}	2.4	3.63×10^{-03}	-1.3	LC-MSMS
Isobutyrylglycine	1.09×10^{-02}	2.3			LC-MSMS
5-Methylcytidine	3.24×10^{-02}	2.2	3.24×10^{-02}	2.2	LC-MSMS
Xanthine	5.92×10^{-04}	2.2			LC-MSMS
Adenine	8.81×10^{-04}	2.1			LC-MSMS
γ-Glutamylglycine	7.32×10^{-04}	1.8			LC-MSMS
Argininic Acid	1.01×10^{-02}	1.6			LC-MSMS
Glutamine	2.21×10^{-03}	1.6			LC-MSMS
Pyrrolidonecarboxylic	2.19×10^{-03}	1.6			LC-MSMS

acid					
NADP	1.80 x10^{-02}	1.5	1.06 x10^{-02}	-1.4	NMR
Xanthosine	3.67 x10^{-03}	1.5			LC-MSMS
Glycine	1.80 x10^{-02}	1.1			NMR
Glutathione	1.96 x10^{-03}	-1.2			NMR
3-Hydroxybutyrate	8.51 x10^{-03}	-1.3			NMR
Isoleucine	4.30 x10^{-03}	-1.3	2.97 x10^{-02}	1.4	NMR
Phenylalanine	1.02 x10^{-02}	-1.3	1.77 x10^{-02}	-1.3	NMR
Succinate	1.59 x10^{-02}	-1.3	3.41 x10^{-05}	1.5	NMR
Valine	1.96 x10^{-03}	-1.3			NMR
Acetate	1.02 x10^{-03}	-1.4	2.27 x10^{-02}	1.3	NMR
Creatine	4.30 x10^{-03}	-1.4	2.68 x10^{-02}	1.3	NMR
Tyrosine	3.70 x10^{-03}	-1.4			NMR
3-Methylxanthyne	7.50 x10^{-03}	-1.5	1.46 x10^{-02}	1.3	NMR
Niacinamide	9.12 x10^{-03}	-1.6	4.45 x10^{-02}	1.4	NMR
Glutamate	6.48 x10^{-04}	-1.7	7.69 x10^{-05}	1.4	NMR
Uridine	1.67 x10^{-03}	-1.7	5.67 x10^{-06}	1.9	NMR
Betaine	4.44 x10^{-04}	-1.8	2.19 x10^{-02}	1.4	NMR
Choline	8.65 x10^{-04}	-2	3.97 x10^{-03}	1.3	NMR
Pantothenic Acid	4.66 x10^{-02}	-2			LC-MSMS
Inosine	1.09 x10^{-02}	-2.1	6.52 x10^{-04}	1.7	NMR
Tryptophan	1.94 x10^{-03}	-2.2			LC-MSMS
1,7-Dimethylguanosine	2.05 x10^{-02}	-2.5			LC-MSMS
Glutamyl-Lysine	3.15 x10^{-03}	-2.6			LC-MSMS
O-phosphocholine	4.44 x10^{-04}	-2.9	2.41 x10^{-02}	1.4	NMR
Cytidine	6.25 x10^{-03}	-3			LC-MSMS

Glycogen	3.36×10^{-02}	-3			LC-MSMS
Cytosine	9.54×10^{-03}	-3.1			LC-MSMS
5- Glutamyl-alanine	6.48×10^{-03}	-3.6			LC-MSMS
Aminoadipic acid	4.89×10^{-03}	-9.1			LC-MSMS
ADP	2.82×10^{-03}	-12.9			LC-MSMS
Glucose			4.33×10^{-02}	1.2	NMR
Lactate			3.07×10^{-02}	-1.1	NMR
Taurine			2.99×10^{-02}	1.4	NMR

The untargeted analysis of the lipidic extracts lead to the annotation of fifty-six metabolites statistically different between the studied groups. ^{1}H-NMR analysis also allowed the annotation of five differential groups of lipids (monounsaturated fatty acids (MUFAs), polyunsaturated fatty acids (PUFAs), total and free cholesterol and triglycerides (TG)). The complete list of these metabolites can be found at Table 2, including the analytical platform that allowed their annotation, as well as, the p values and FC of each statistical comparison between groups. As it can be seen in Table 2, thirty-nine of the metabolites annotated in the lipidic extracts were altered because of THS exposure (Table 2, "CTRL vs. THS" columns). In accordance with previous works, THS exposure increased lipid concentrations, being triglycerides the lipid family that presented higher concentrations in the THS liver samples (Flores et al., 2016; Martins-Green et al., 2014). The comprehensive untargeted metabolomics approach presented here allowed the annotation of 21 different triglycerides, as well as other types of lipids such as oleic, linoleic and docosahexaenoic acids (DHA), MUFAs, PUFAs, seven unsaturated phosphocholines (PC) and two lysopophoscholines (lysoPC) that were increased by THS exposure. Conversely, we found that some saturated phosphocholines

(PC) (i.e. PC(36:0), PC(34:0)), sphingomyelins (SM) (i.e. SM(42:2), SM (36:1)), Coenzyme Q9 and free and total cholesterol decreased by THS exposure. Interestingly, the concentration of esterified cholesterol was not affected by THS exposure. In agreement with previous studies (Flores et al., 2016), the antioxidant treatment of THS exposed mice, decreased the total concentrations of lipids in liver, including the total concentration of triglycerides, DHA, and sphingomyelin. Nevertheless, the antioxidant treatment could not regulate the THS induced alterations of twenty-seven of the altered lipids including coenzyme Q9, MUFAs, oleic and linoleic acids and different kind of TGs, PCs and SMs. It also intensified the increase of PUFAs.

Table 2. Metabolites annotated in the lipidic extracts that were statistically relevant between THS-exposed and non-exposed liver samples (CTRL vs. THS) and between THS-exposed mice and those exposed to THS and treated with antioxidants (THS vs. THS-AO). For each metabolite, the FDR corrected p-value and fold change (FC) of each comparison and the determination technique is also indicated. (Abbreviations: TG: triglyceride, PC: phosphocholine, LysoPC: Lysophosphocholine, DHA: Docosahexaenoic acid, SM: sphingomyelin).

Metabolites	CTRL vs THS		THS vs THS-AO		*Technique*
	p-value FDR	*Fold Change*	*p-value (FDR)*	*Fold Change*	
TG (52:6)	4.70×10^{-03}	9.2	2.90×10^{-02}	-3.5	LC-MSMS
PC (42:6)	4.60×10^{-04}	6.9			LC-MSMS
TG (54:7)	5.06×10^{-03}	5	7.11×10^{-03}	-2.1	LC-MSMS
TG (50:4)	1.62×10^{-02}	4.9			LC-MSMS
TG (32:2)	3.81×10^{-03}	4.5	1.65×10^{-02}	-2.7	LC-MSMS
TG (50:2)	3.17×10^{-03}	3.4			LC-MSMS
TG (54:8)	1.80×10^{-02}	3.4	4.46×10^{-03}	-3.6	LC-MSMS
TG (54:6)	7.37×10^{-03}	3.3			LC-MSMS
PE (36:6)	3.32×10^{-04}	3.3			LC-MSMS
TG (50:2)	1.19×10^{-03}	3.2	2.21×10^{-04}	-2.6	LC-MSMS
TG (56:6)	3.44×10^{-03}	3.1			LC-MSMS
TG (52:5)	8.81×10^{-03}	2.9			LC-MSMS
PC (32:1)	8.08×10^{-04}	2.9			LC-MSMS
LysoPC (16:1)	7.32×10^{-03}	2.9			LC-MSMS
PC (36:6)	1.96×10^{-03}	2.9			LC-MSMS
Triglycerides	5.80×10^{-03}	2.7	2.09×10^{-02}	-1.8	NMR
TG (51:3)	5.43×10^{-03}	2.7			LC-MSMS
LysoPC (18:1)	1.60×10^{-02}	2.7			LC-MSMS
PC (17:1)	1.15×10^{-02}	2.7			LC-MSMS
PC (36:4)	1.07×10^{-03}	2.5			LC-MSMS

TG (51:1)	2.94×10^{-03}	2.4			LC-MSMS
PC (34:3)	4.47×10^{-04}	2.3			LC-MSMS
TG (49:2)	4.31×10^{-03}	2.3			LC-MSMS
TG (48:1)	1.47×10^{-03}	2.3			LC-MSMS
TG (54:2)	1.49×10^{-03}	2.2			LC-MSMS
PC (38:7)	1.22×10^{-04}	2.1			LC-MSMS
Oleic acid	7.56×10^{-03}	1.7			NMR
Linoleic acid	1.25×10^{-02}	1.3			NMR
DHA	8.03×10^{-03}	1.2	1.87×10^{-02}	1.2	NMR
Monounsaturated Fatty Acids	5.80×10^{-03}	1.2			NMR
Polyunsaturated Fatty Acids	4.37×10^{-02}	1.1	2.09×10^{-02}	1.2	NMR
Free Cholesterol	8.77×10^{-03}	-1.2	1.16×10^{-03}	1.5	NMR
Total Cholesterol	5.80×10^{-03}	-1.3	2.68×10^{-03}	1.5	NMR
Coenzyme Q9	1.06×10^{-03}	-2			LC-MSMS
PC (36:0)	5.93×10^{-04}	-2.3	1.37×10^{-02}	3.2	LC-MSMS
SM (42:2)	3.27×10^{-04}	-2.3			LC-MSMS
SM (36:1)	2.45×10^{-04}	-2.3			LC-MSMS
PC (34:0)	9.55×10^{-03}	-3.7	5.67×10^{-03}	2.1	LC-MSMS
PC (34:1)	2.53×10^{-02}	-3.8			LC-MSMS
Esterified Cholesterol			3.58×10^{-04}	2.8	NMR
PC (35:2)			1.56×10^{-03}	2	LC-MSMS
PC (36:5)			3.21×10^{-03}	-2.5	LC-MSMS
PC (38:1)			2.99×10^{-02}	2.3	LC-MSMS
PC (39:4)			9.29×10^{-04}	-2.5	LC-MSMS
PC (40:4)			6.20×10^{-04}	-3.3	LC-MSMS

PC(41:7)		1.97×10^{-04}	-7.4	LC-MSMS
Phosphatidylcholine		7.48×10^{-03}	1.3	NMR
Phosphatidylethanolamine		6.49×10^{-03}	1.2	NMR
Phosphatidylserine		2.67×10^{-04}	2.7	NMR
SM (16:1)		1.96×10^{-03}	2.9	LC-MSMS
Sphingomyelin		8.51×10^{-04}	2.4	NMR
TG (36:2)		1.55×10^{-02}	-2	LC-MSMS
*TG(48:2)**		1.12×10^{-03}	-3.7	LC-MSMS
TG (51:2)		3.14×10^{-03}	-2.3	LC-MSMS
TG(56:2)		1.12×10^{-02}	-4.8	LC-MSMS
TG (56:3)		9.58×10^{-03}	-2.3	LC-MSMS

The aqueous and lipidic annotated metabolites significantly different in the CTRL vs THS and THS vs. THS-AO comparisons were subject to hierarchical clustering, to illustrate the variation of concentrations in the three studied groups. The obtained heatmap of the relative concentrations is represented in Figure 1. For the metabolites represented here, CTRL and THS-AO groups cluster together. This figure also shows the groups of metabolites that cluster together, such as the represented TGs, NADP and serotonin (increased by THS exposure and reverted by the antioxidant treatment), acetate, total and free cholesterol, isoleucine, uridine and succinate (decreased by THS exposure, but increased by the antioxidant treatment), or phenylalanine and AMP, whose deficiency caused by THS exposure is more pronounced by antioxidants.

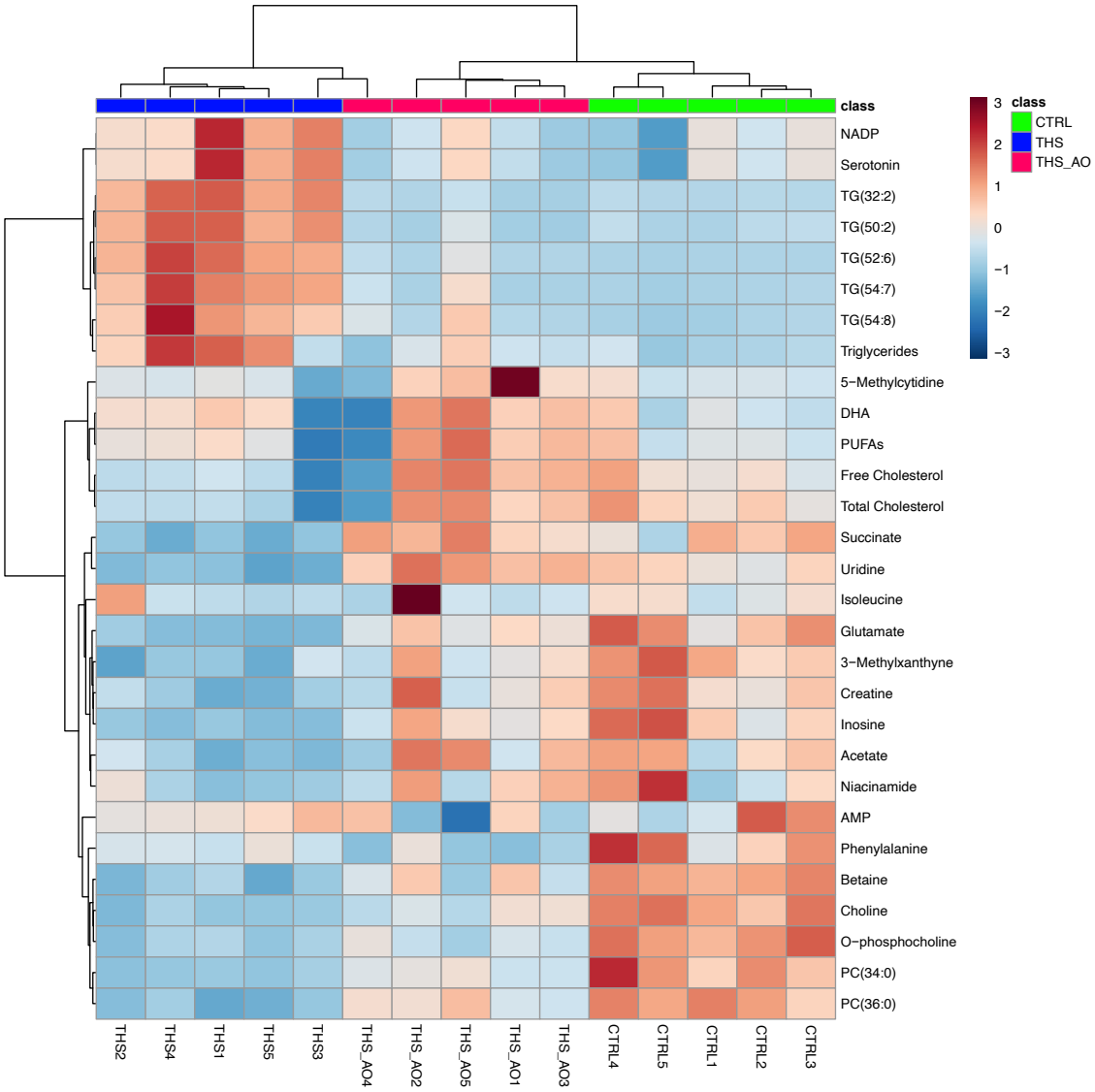

Figure 1. Heatmap representing two-way hierarchical cluster analysis of the statistically relevant metabolites in both, aqueous and lipidic extracts, for the exposure to THS (CTRL vs. THS) and for the effect of the antioxidant intake of THS-exposed mice (THS vs. THS-AO). Clustering of samples is shown on the top axis and clustering of features on the left axis. Colors represent median relative intensity of each studied group.

Finally, to illustrate the differences between the studied groups commented during this section, Supplementary material, Figure S1 shows the average 1H NMR spectra of the aqueous extracts and the individual spectra of some metabolites (Figure S1a). The differences between the 3 studied groups

can also be seen in the chromatographic peaks of the acquired LC-MS chromatograms shown in Figure S1b. Analogously, Supplementary material, Figure S2 shows the acquired 1H-NMR spectra (Figure S2a) and LC-MS chromatograms (Figure S2b) of the liver lipidic extracts. The detailed signals of some annotated lipids clearly show how the antioxidant treatment decrease the concentration of some types of lipids, such as triglycerides. However, it also shows that the concentrations of other lipids, such as sphingomyelins, are higher in liver samples of THS-AO mice than in those from CTRL and THS mice, indicating that the concentrations of these types of lipids were more influenced by the antioxidant treatment rather than THS-exposure. The combined effects of THS exposure and the antioxidant treatment against the non-treated group are presented at the Supplementary material, Section S3 and Table S2.

The findings presented so far suggest, that although the antioxidant treatment would be able to balance some of the metabolic alterations in liver induced by THS, the possible side effects associated to the combination of THS exposure and antioxidants must be object of further study.

5.4.2 Spatial distribution of lipids

The histological images of liver sections representative of CTRL, THS and THS-AO, respectively, stained with oil red O (ORO) at two magnifications (×40 and ×100 zoom) are shown in Figures 2a-f. As it could be seen from these figures, lipid droplet sizes were between 1.2-2.0 µm in CTRL liver sections, from 2.5 to 3.9 µm in THS and between 1.6 and 3.0 µm in THS-AO liver sections (Figs. 2d-f). In accordance with previous studies (Martins-Green et al., 2014), lipid droplets were more abundant and larger in the THS-exposed mice (Figs. 2b & 2e). Furthermore, these images show that the antioxidant treatment reduced the number and size of lipid droplets regarding the THS group, but not at the levels of the CTRL group. The average LDI-MS spectra in the m/z region 750-1000 Da (corresponding to the majority of lipids) is represented in Figs. 2g-i. In agreement with the histological images, average MS signals of THS-exposed liver sections (Fig. 2h) were higher than the MS signals of the lipids of CTRL and THS-AO liver samples (up to 6-fold higher than those in the CTRL liver), thus confirming the lipidomic results obtained by untargeted metabolomics. Similarly, MS signals of THS-AO liver sections (Fig. 2i) were lower than those for THS, but higher than those in the control one (up to 2-fold higher).

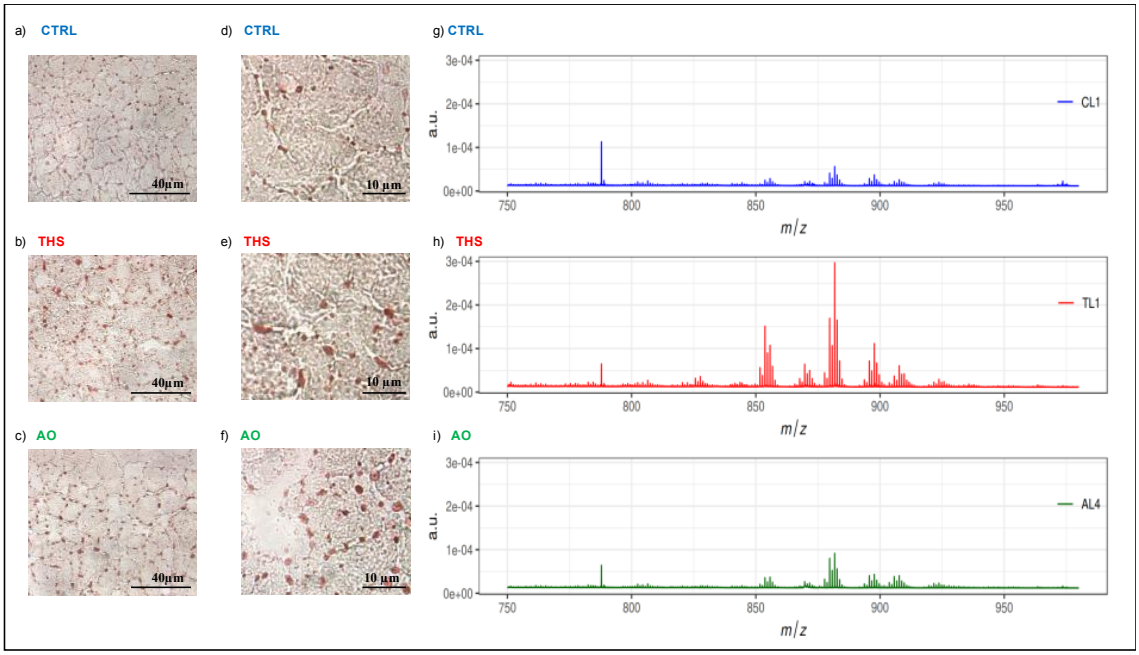

Figure 2. (A-F) Oil red O stained sections (10 µm of thickness) of liver from CTRL, THS and THS-AO mice, at zooms ×40 (A-C) and ×100 (D-F). (G-I) Average LDI-MSI mass spectra in the lipid range area (m/z 750-1000) of consecutive liver slices, the y-axis represents relative intensity in arbitrary units (a.u).

MS images of liver sections were analyzed to determine the spatial distribution of the lipids annotated by LC-MS that were statistically relevant between the experimental groups. Figure 3 shows the spatial distribution of four selected ions (m/z 758.47, m/z 800.51, m/z 873.69 and m/z 899.70, (Figs. 3a, 3b, 3c and 3d, respectively) that were annotated as PE(36:6), PC(36:6), TG(52:6) and TG(54:7) by LC-MS/MS. These lipids were found in the form of their corresponding [M+Na]+ adduct in the MSI spectra of the liver sections within a mass error up to 14 ppm, in agreement with previous observations (Ràfols et al. 2018). These figures represent the relative abundance of the selected ions in a color scale (showed to the right of the figure), where red represents the zones with higher ion signals and dark blue the minimum ones. As seen in these Figures, the relative intensities of these four ions were higher in THS-exposed liver, thus confirming the results obtained by LC-MS/MS. Images also show that

the different lipid classes represented here (PE, PC and TG) were similarly distributed in the THS-exposed liver forming comparable images. Since the spatial resolution of the MS images was between 10-20 µm, these images cannot draw individual lipid droplets, but areas with higher density of them are represented as red dots. From these images it could be derived that in THS-exposed liver, PE(36:6) and PC(36:6) might be part of the PC layer that forms lipid droplets and that TG (52:6), TG (54:7) and TG (52:6) might be in the core of the lipids droplets, usually formed by TG and stearyl esters (SE) (Bartz et al., 2007). Figure 3 also confirms that the treatment with antioxidants drastically reduces the TG accumulation induced by THS exposure, but cannot completely revert the accumulation of other kind of lipids, such as PE(36:6) or PC(36:6).

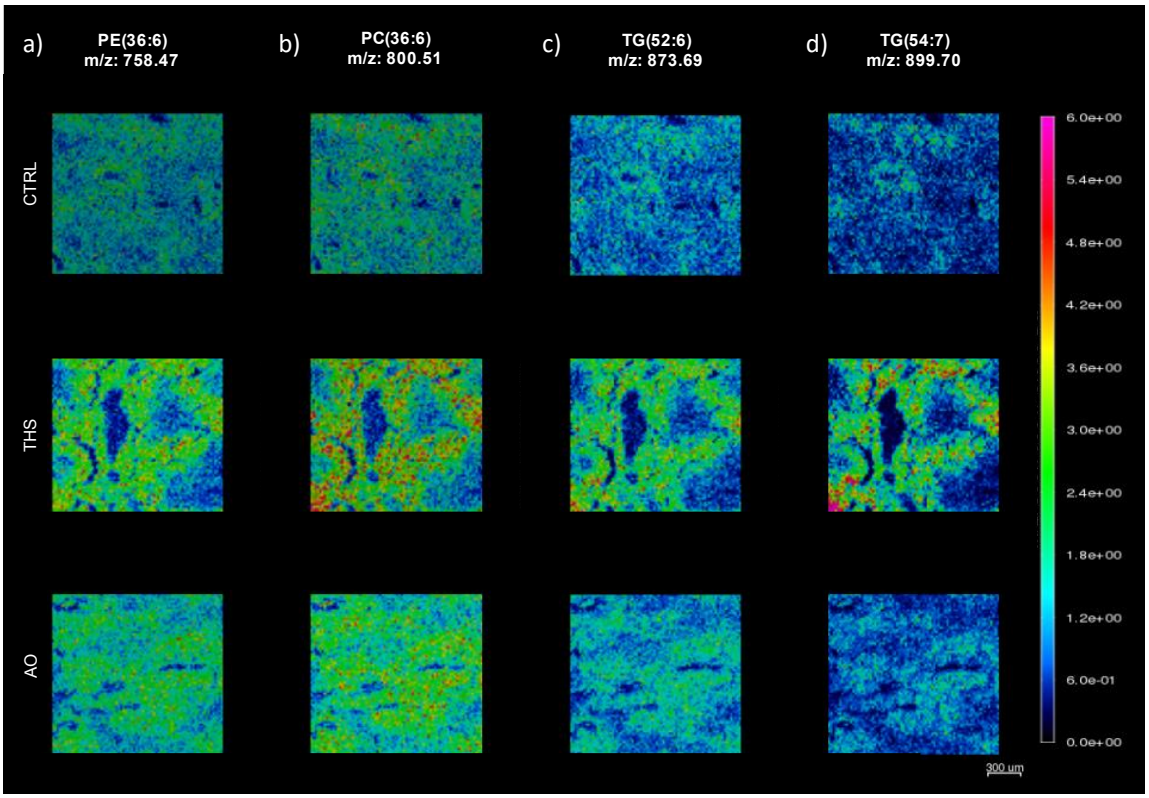

Figure 3. LDI-MS images of mice liver samples acquired at pixel size of 20 µm. Figures A to D plots the relative abundance of four of lipids (758.47 Da, 800.51 Da, 873.69 Da and 899.70 Da, respectively), annotated as the [M+Na]+ adducts of (A) PE (36:6), (B) PC(36:6), (C) TG(52:6) and (D) TG(54:7).

5.4.3 Effects of THS exposure in liver metabolism

Pathway enrichment analysis of the relevant metabolites altered in THS-exposed mice revealed that the exposure to THS significantly dysregulated twenty-one metabolic pathways (p-value (FDR corrected) < 0.05) vs. non-exposed mice. Figure 4a represents these dysregulated pathways, their p-value and fold enrichment (FE). The most affected metabolic pathways were purine, glutathione, D-glutamine and D-glutamate, glycerophospholipid, glycine, serine and threonine, and oxidative phosphorylation metabolisms. Figure 4c maps the annotated dysregulated metabolites involved in the most altered pathways by THS exposure. D-glutamine and D-glutamate metabolism, oxidative phosphorylation, glutathione and glycerophospholipid metabolism were the metabolic pathways that presented higher FE and, therefore, that have a higher proportion of dysregulated metabolites.

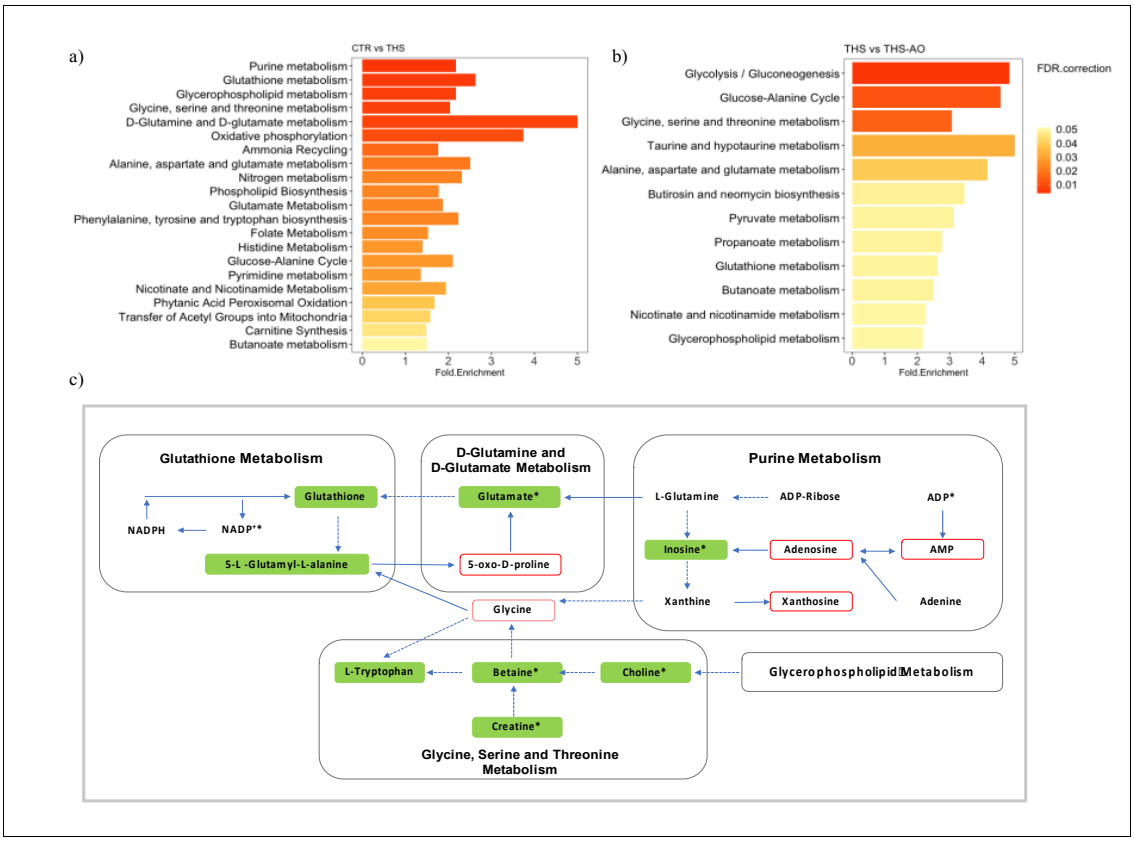

Figure 4. (A) Metabolic pathways significantly dysregulated due to THS exposure (CTRL vs. THS) ordered from lowest to higher p value (FDR-adjusted p<0.05). The color degradation represents the p-value obtained from the enrichment analysis in MBROLE 2.0 software, and bar length represent the fold enrichment score. (B) Dysregulated pathways between THS-exposed and THS-exposed treated with antioxidants mice (THS vs. THS-AO). (C) Representation of the altered metabolites included in the metabolic pathways most altered by THS exposure. Red color is used for metabolites up regulated and green for metabolites down regulated in THS-exposed liver samples. Asterisks indicate those metabolites balanced by the antioxidant treatment. Continuous lines express direct relation between metabolites and dashed lines that there are intermediate metabolites not shown in the figure.

Pathway enrichment between THS and THS-AO groups showed twelve dysregulated metabolic pathways (see Figure 4b). As seen in this graphic, the most altered pathways because of the antioxidant treatment were glycolysis and gluconeogenesis, glucose-alanine cycle, glycine, serine and threonine and taurine and hypotaurine metabolisms. We can also observe that the antioxidant treatment, could only affect five of the metabolic pathways altered by THS exposure (glutathione; glycerophospholipid; glycine, serine and threonine; alanine, aspartate and glutamate; and nicotinate and nicotinamide metabolisms), suggesting that the antioxidant treatment was not able to balance sixteen of the metabolic pathways altered by THS exposure. The metabolic pathways not reverted by antioxidants, include pathways related to lipid regulation, such as phospholipid biosynthesis, oxidative phosphorylation and carnitine synthesis metabolisms and also purine, D-glutamine and D-glutamate and phenylalanine, tyrosine and tryptophan metabolisms.

5.5 Discussion

Hepatic triglyceride accumulation in liver samples of THS-exposed mice clearly reveals that THS causes abnormal lipid metabolism known as NAFLD, as it has been previously suggested (Martins-Green et al., 2014). NASH liver

characterizes for oxidative stress and lipid accumulation, among others (Rein-Fischboeck et al., 2018). The oxidative stress suffered in liver of THS-exposed mice was demonstrated in previous studies that observed higher superoxide dismutase (SOD) activity and, as a result, increased levels of H2O2 and reactive oxygen species (ROS) (Adhami et al., 2017; Chen et al., 2018; Flores et al., 2016). Flores et al., also found that there was no significant increase in catalase or GPx (glutathione peroxidase) activity, in consequence H2O2 was not properly processed and the levels of reactive oxygen species (ROS) remained high in the liver. They also found that NADP+/NADPH ratio in mice liver, which is an indicator of the cell reducing potential because GPx activity is coupled to the reduction of NADPH to NADP+, was decreased significantly because of THS exposure, showing that the reduction potential of these animals was decreased and might result in their inability to reduce the oxidative stress levels induced by the THS toxins. The increase of oxidative stress was in accordance with the increased levels of aspartate aminotransferase (AST) activity found in THS-exposed mice. (Flores et al., 2016).

Our multiplatform untargeted metabolomic approach allowed the annotation of eighty-eight metabolites altered by THS exposure, reporting for the first time some hepatic metabolic alterations caused by THS. At a metabolic level, glutamate and glutathione deficiency found in liver of THS-exposed mice could be indicatives of increased liver oxidative stress (Wu et al., 2004). Dysregulation of glutathione metabolism induced by THS exposure, agrees with previous findings in reproductive male cells (Hang et al., 2017). Lipidomic results also confirmed the increased oxidative stress in THS-exposed liver, corroborated, for example, by the higher levels of some lysophosphatidylcholines (LPCs) (Pyttel et al., 2012), PUFAs and DHA that are linked to higher risks of lipid peroxidation (Reis and Spickett, 2012).

Our findings also suggest impairment on the hepatic mitochondrial function including decreased levels of AMP and increased levels of some acylcarnitines in the THS-exposed liver samples (Hara et al., 2013; Koves et al., 2008). Besides, THS-exposed mice presented decreased levels of Coenzyme Q9, which plays an important role in mitochondrial energy and serves as a potent endogenous antioxidant.

We also found metabolic markers of NAFL and NASH in the THS-exposed group. For instance, the increased levels of hepatic acylcarnitines and linoleic acid found in the THS group were in agreement with previous findings in human liver samples at the stage of NASH (Lake et al., 2015). Acylcarnitines are considered potential biomarkers for liver disease (Flanagan et al., 2010) since they are a key factor regulating the balance of intracellular sugar and lipid metabolism (Li et al., 2019). In addition, several studies have demonstrated the link of acylcarnitines with the development of insulin resistance, glucose deterioration and type I and type II diabetes (Koves et al., 2008) (Sun et al., 2016). Specifically, decanoylcarnitine and hexanolylcarnitine, which were increased in THS-exposed liver samples, have been significantly associated with diabetes (Sun et al., 2016), increased body fat and waist to hip ratio (Mai et al., 2013). We have also found that all the annotated metabolites related to phosphatidylcholine synthesis including choline, betaine, phosphocholine, PCs and some sphingomyelins (SMs) were decrease in liver samples of the THS group, in agreement with reduced total hepatic phosphatidylcholine (PC) content associated to NAFL and NASH (Jacobs et al., 2013; Rein-Fischboeck et al., 2018). Choline deficiency has an important role in NAFLD, not only in the deposition of triacylglycerol in liver and reduced phospholipid synthesis (Sherriff et al., 2016)(Michel et al., 2006), but also in the expression of genes

involved in cell proliferation, differentiation and apoptosis, liver dysfunction (Michel et al., 2006) and cancer (Kwee et al., 2017).

The altered fatty acid profile found in THS exposed liver samples was in accordance with the profile of smokers plasma developed by Müller et al. (Müller et al., 2014) where the metabolomics analysis revealed that MUFA and oleic acid significantly increased in smokers plasma. The same study also concluded that PC mostly containing MUFA were up regulated in smokers' samples and that saturated PC were down regulated in smokers. Our results also show this trend, as the annotated saturated PCs (PC (36:0) and PC (34:0)) were decreased in THS-exposed mice and phosphocholines containing mono and polyunsaturated fatty acids (e.g. PC (32:1), (36:6), (17:1), (36:4), (34:3) and (38:7)) were upregulated in liver of THS-exposed mice. Furthermore, our MS images showed that the lipids forming lipid droplets were unsaturated species consistently with previous observations in yeast cells by Grillitsch et al. (Grillitsch et al., 2011). The same authors also observed a higher accumulation of TGs in lipid droplets when cells were grown in oleic acid. Therefore, the increased levels of oleic acid of THS-exposed mice might be also related with the increase of triglycerides and unsaturated lipids in lipid droplets in the liver samples of the THS group.

Considering that previous studies found that oxidative stress might be responsible for most of the THS induced dysregulations in liver, a treatment with antioxidant should be able to mitigate the effects induced by this exposure. In fact, Flores et al. found that mice treated with antioxidants presented H_2O_2 levels similar to non-exposed mice and significantly lower than THS-exposed ones, and higher GPx activity (Flores et al., 2016). The results of our metabolomics study revealed that although the antioxidant treatment mitigate some of the reported metabolic alterations caused by THS exposure, it

was not able to completely revert all of them. This was the case, for instance of glutamate, which is essential in the rate-limiting step of the of glutathione biosynthesis (Franklin et al., 2009). We found that glutamate levels decreased because of THS exposure and although it increased under the antioxidant treatment, did not returned to the levels found in the control group. Moreover D-glutamine and D-glutamate metabolisms were highly altered in THS exposed mice, but not all the annotated metabolites of this pathway were balanced by the antioxidant treatment, including glutathione that is key in the pathogenesis of liver disease. Furthermore, decreased ADP and Coenzyme Q9 levels, and phospholipid biosynthesis were also not balanced by antioxidants. Further, although antioxidant treatment was able to reduce lipid droplets and generally decrease the accumulation of triglycerides, it could not decrease some lipid levels such as PUFAs, DHA and some carnitines, neither the dysregulation of the carnitine synthesis metabolism found in THS exposed mice, and the health consequences associated to them.

Besides, the THS-AO group presented increased levels of glucose and unbalanced glycolysis and gluconeogenesis metabolism. This metabolic pathway was only altered in the THS vs THS-AO comparison suggesting that a treatment with antioxidants affects this pathway more than THS exposure. Accordingly, we have found that the antioxidant treatment increased glucose levels. This result agrees with increased glucose levels in fasting blood glucose of THS-AO mice (Adhami et al., 2016), suggesting that the combined effect of THS exposure with antioxidants may imbalance other metabolic pathways not specifically altered by THS toxicants.

The results presented here, indicate that THS exposure affects liver metabolism in a complex way and could be the basis of further research to

elucidate the molecular mechanisms underlaying the toxic effects of THS exposure in liver.

5.6 Conclusions

The exposure to THS toxicants caused metabolic disorders in liver of exposed mice, producing the dysregulation of dozens of metabolites and several metabolic pathways. Our untargeted metabolomics multiplatform approach has been revealed as a powerful tool for the annotation of metabolites that can potentially serve as biomarkers of early biological effects involved in THS exposure. We annotated 88 significant metabolites included in 21 metabolic pathways dysregulated because of THS exposure. The exposure to THS toxicants significantly increased the accumulation of triglycerides in liver, altered the fatty acid, phosphocholine and acylcarnitine profiles, increasing the size and occurrence of lipid droplets. These findings support the relationship between THS exposure and NAFLD risk, in addition to the possible evolution to NASH due to the acute oxidative stress suffered in liver. The results found in THS exposed livers treated with antioxidants confirmed that oxidative stress is one of the major causes of THS-induced liver disease. The intake of antioxidants balanced some metabolite alterations induced by THS, but it was unable to revert all the molecular damage, including key metabolites in mitochondrial function and the hepatic metabolism of phospholipids and carnitines. Our study demonstrates the merit of multiple analytical platform-based metabolomics as a valuable approach for the annotation of biomarkers involved in NAFLD as well as dysregulated metabolites involved in THS exposure.

5.7 Supplementary Information

Section S1. Untargeted results by NMR analysis

1H NMR analysis of the aqueous extracts resulted in the annotation of 33 metabolites, 22 of them statistically different between CTRL and THS groups, and 17 of them between THS and THS-AO (Student's t-test p value, FDR corrected < 0.05, FC > 1.1). Analysis of the lipidic extracts resulted in the annotation of 13 metabolites, 8 of them significantly different between CTRL and THS, and 10 of them between THS and THS-AO groups. The metabolites annotated in the NMR spectra without statistical significance are presented in Table S1.

Table S1. Identified metabolites in the 1H NMR spectra without statistical significance between the studied groups. FDR corrected p values for each comparison, are also shown in this Table.

Metabolite	*CTRL vs. THS*	*THS vs. AO*
	p-value (FDR)	*p-value (FDR)*
Alanine	$8.71x10^{-02}$	$3.76x10^{-01}$
Methionine	$4.12x10^{-01}$	$1.50x10^{-01}$
Histidine	$7.67x10^{-01}$	$1.20x10^{-01}$
Cholic Acid	$4.10x10^{-01}$	$9.41x10^{-01}$
Phospholipids	$1.43x10^{-01}$	$2.39x10^{-01}$
Diglycerids	$2.46x10^{-01}$	$4.77x10^{-01}$
Plasmalogen	$8.67x10^{-01}$	$5.36x10^{-01}$

Section S2. Untargeted results by LC-MS analysis

Aqueous extracts: LC-MS analysis of the aqueous extracts resulted in a matrix of 9344 features after filtering by intensity and analytical variation (as explained in the methods section). The number of relevant features after preforming a Student's t-test between CTRL and THS groups was 2583 (FDR-adjusted p-value < 0.05, FC > 2), of them only features with an absolute fold change higher than 2 (1560 features) were selected for putative annotation against the HMBD. A total of 119 features presented a candidate for the [M+H] + adduct and had relevant biological interest, thus selected for further MS/MS analysis resulting in the annotation of 29 metabolites. Metabolite annotation was performed manually by a qualified analyst. The experimental spectra were compared to those provided by the Metlin and HMDB databases, which were obtained by analysing pure chemical standards, in the same ionization mode (ESI (+)), mass spectrometer instrument (QTOF), and the same collision energy for the fragmentation of precursor ions (20 ev). We performed the search by selecting the exact mass of the precursor ion, within a mass error of 5 ppm. We annotated the metabolites by comparing the available MS/MS spectra for each precursor mass with our experimental MS/MS spectrum looking at the coincidence of the exact mass of the fragments and their relative abundance. In case of minimal doubt, we did not annotate the metabolite to avoid false positive identifications. For the THS vs AO comparison, 566 features presented differences by LC-MS analysis (FDR-adjusted P<0.05, Fold Change > 2), of those 34 were putatively annotated against the HMDB within 5 ppm of mass error and selected for MSMS analysis. This process resulted in 2 annotated metabolites.

Lipidic extracts: The LC/MS data analysis of the lipidic extracts resulted in a matrix of 5498 filtered features. After filtering, 1541features presented

significant difference between CTRL vs THS (FDR-adjusted p-value < 0.05, FC > 2)). Of those 114 resulted in a possible annotation against the HMDB and LipidMaps data bases, with candidate for the [M+H]+ (69) and [M+NH4]+ (45) adducts to perform the MS/MS analysis. In the case of lipids, we also included the ammonium adduct [M+NH4]+ since it is the most abundant adduct of some lipids including triglycerides. Thirty-one metabolites could be annotated following our criteria. In the THS vs AO comparison, 278 features in the LC-MS analysis presented significant differences between groups, of those 39 resulted in a possible annotation against the HMDB and LipidMaps data bases and 19 lipids were identified by MS/MS spectra.

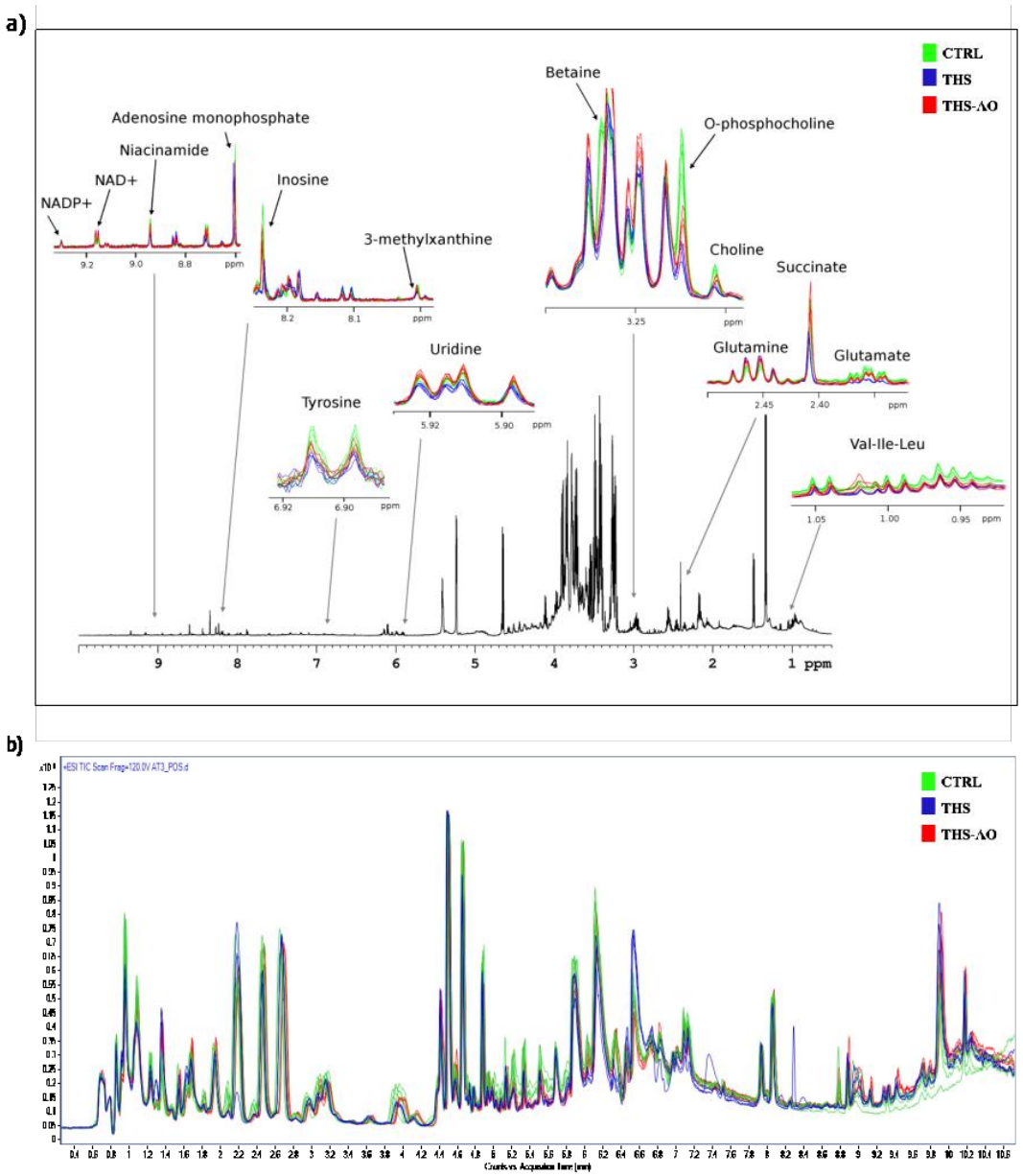

Figure S1. a) Annotated one dimensional 1H-NMR spectra and b) UHPLC-QTOF chromatograms of the aqueous extracts from CTRL (green), THS (blue) and THS-AO (red) liver mice.

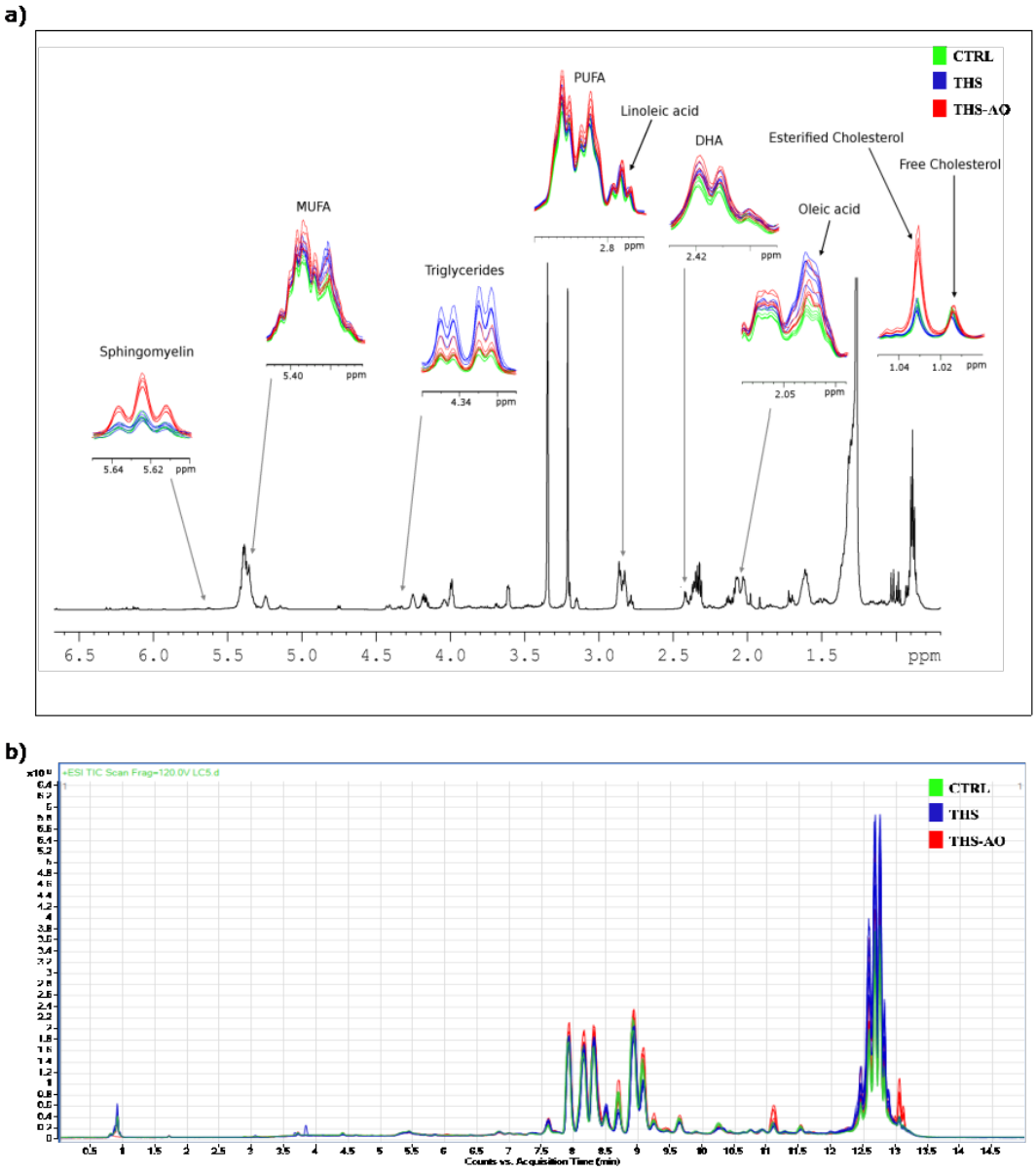

Figure S2. a) Annotated one dimensional 1H-NMR spectra and b) UHPLC-QTOF chromatograms of the lipidic extracts from CTRL (green), THS (blue) and THS-AO (red) liver mice.

Section S3. Relevant metabolites between CRTL and THS-AO groups

Table S2 shows the 12 metabolites that were found altered by the combined effect of THS exposure and antioxidant treatment, regarding the non-treated group (CTRL vs. THS-AO). Of those the ones more affected by the antioxidant treatment are isoleucine and uridine, those metabolites are down regulated due to THS exposure and completely revert due to the antioxidant treatment to levels even higher than in CTRL group. For the case of phenylalanine and glutamine the antioxidant treatment aggravates the effect of the THS exposure, decreasing even more the levels of phenylaniline and raising the levels of glutamine. With this comparison we can also see that for five of the most altered metabolites; glutamate, betaine, choline, o-phosphocholine and 3-metylxanthine the antioxidant treatment helps to ameliorate the metabolic alterations caused by THS exposure, but it cannot revert the concentrations of these metabolites to the levels found in the CTRL group.

Regarding lipidic extracts, only three phosphocholines (PC (34:0), PC (34:1) and PC (36:0)) presented significant differences between the groups. The antioxidant treatment reverts THS exposure effect, increasing the PCs concentration to higher levels than those found in the CTRL group.

Table S2. Metabolites statistically relevant between CTRL and THS-AO groups. For each metabolite, we also provide the FDR corrected p-value and fold change (FC). (Abbreviations: PC: phosphocholine)

CTRL vs THS-AO		
Metabolite	p value (FDR)	FC
O-phosphocholine	1.05×10^{-3}	-2.0
Choline	1.05×10^{-3}	-1.5
Phenylalanine	1.05×10^{-3}	-1.4
Betaine	2.16×10^{-2}	-1.3
3- methylxanthine	4.04×10^{-2}	-1.2
Glutamate	1.64×10^{-2}	-1.1
Uridine	1.71×10^{-3}	1.2
Isoleucine	4.49×10^{-2}	1.3
PC (34:0)	2.99×10^{-2}	1.8
PC (36:0)	3.45×10^{-2}	1.3
Glucose	2.81×10^{-2}	1.3
Taurine	1.08×10^{-2}	1.5
PC (34:1)	2.99×10^{-2}	2.9
Tyrosine	2.01×10^{-5}	-1.3
Glutamine	1.71×10^{-3}	1.3
Histidine	6.86×10^{-3}	-1.2

5.8 References

Adam, R., Karam, V., Delvart, V., O'Grady, J., Mirza, D., Klempnauer, J., Castaing, D., Neuhaus, P., Jamieson, N., Salizzoni, M., Pollard, S., Lerut, J., Paul, A., Garcia-Valdecasas, J.C., Rodríguez, F.S.J., Burroughs, A., 2012. Evolution of indications and results of liver transplantation in Europe. A report from the European Liver Transplant Registry (ELTR). J. Hepatol. 57, 675–688. https://doi.org/10.1016/j.jhep.2012.04.015

Adhami, N., Chen, Y., Martins-Green, M., 2017. Biomarkers of disease can be detected in mice as early as 4 weeks after initiation of exposure to third-hand smoke levels equivalent to those found in homes of smokers. Clin. Sci. 131, 2409–2426. https://doi.org/10.1042/CS20171053

Adhami, N., Starck, S.R., Flores, C., Green, M.M., 2016. A health threat to bystanders living in the homes of smokers: How smoke toxins deposited on surfaces can cause insulin resistance. PLoS One 11, 1–20. https://doi.org/10.1371/journal.pone.0149510

Akhavan Rezayat, A., Dadgar Moghadam, M., Ghasemi Nour, M., Shirazinia, M., Ghodsi, H., Rouhbakhsh Zahmatkesh, M.R., Tavakolizadeh Noghabi, M., Hoseini, B., Akhavan Rezayat, K., 2018. Association between smoking and non-alcoholic fatty liver disease: A systematic review and meta-analysis. SAGE Open Med. https://doi.org/10.1177/2050312117745223

Bartz, R., Zehmer, J.K., Zhu, M., Chen, Y., Serrero, G., Zhao, Y., Liu, P., 2007. Dynamic Activity of Lipid Droplets: Protein Phosphorylation and GTP-Mediated Protein Translocation. https://doi.org/10.1021/pr070158j

Beltran, A., Suarez, M., Rodr??guez, M.A., Vinaixa, M., Samino, S., Arola, L., Correig, X., Yanes, O., 2012. Assessment of compatibility between extraction methods for NMR- and LC/MS-based metabolomics. Anal. Chem. https://doi.org/10.1021/ac3005567

Bertuccio, P., Turati, F., Carioli, G., Rodriguez, T., La Vecchia, C., Malvezzi, M., Negri, E., 2017. Global trends and predictions in hepatocellular carcinoma mortality. J. Hepatol. 67, 302–309. https://doi.org/10.1016/j.jhep.2017.03.011

Chagoyen, M., Pazos, F., 2011. MBRole: enrichment analysis of metabolomic data. Bioinformatics 27, 730–731. https://doi.org/10.1093/bioinformatics/btr001

Chen, Y., Adhami, N., Martins-Green, M., 2018. Biological markers of harm can be detected in mice exposed for two months to low doses of Third Hand Smoke under conditions that mimic human exposure. Food Chem. Toxicol. 122, 95–103. https://doi.org/10.1016/j.fct.2018.09.048

Chong, J., Wishart, D.S., Xia, J., 2019. Using MetaboAnalyst 4.0 for Comprehensive and Integrative Metabolomics Data Analysis. Curr. Protoc. Bioinforma. https://doi.org/10.1002/cpbi.86

ELPA [WWW Document], n.d. URL https://www.elpa-info.org

EPA, 2004. US National Survey on Environmental Management, Estimation of Environmental Tobacco Smoke Exposure.

Fahy, E., Sud, M., Cotter, D., Subramaniam, S., 2007. LIPID MAPS online tools for lipid research. Nucleic Acids Res. 35, W606-12. https://doi.org/10.1093/nar/gkm324

Flanagan, J.L., Simmons, P.A., Vehige, J., Willcox, M.D., Garrett, Q., 2010. Role of carnitine in disease. Nutr. Metab. 7, 1–14. https://doi.org/10.1186/1743-7075-7-30

Flores, C., Adhami, N., Green, M.M., 2016. THS Toxins Induce Hepatic Steatosis by Altering Oxidative Stress and SIRT1 Levels. J. Clin. Toxicol. 06, 1–11. https://doi.org/10.4172/2161-0495.1000318

Flores, C., Adhami, N., Martins Green, M., 2017. The Role of Fatty Acid Metabolism and Apolipoproteins in Ths-Induced Hepatic Steatosis in Mice. Ferment. Technol. 07. https://doi.org/10.4172/2167-7972.1000359

Franklin, C.C., Backos, D.S., Mohar, I., White, C.C., Forman, H.J., Kavanagh, T.J., 2009. Structure, function, and post-translational regulation of the catalytic and modifier subunits of glutamate cysteine ligase. Mol. Aspects Med. 30, 86–98. https://doi.org/10.1016/j.mam.2008.08.009

Grillitsch, K., Connerth, M., Köfeler, H., Arrey, T.N., Rietschel, B., Wagner, B., Karas, M., Daum, G., 2011. Lipid particles/droplets of the yeast Saccharomyces cerevisiae revisited: Lipidome meets Proteome. Biochim. Biophys. Acta - Mol. Cell Biol. Lipids 1811, 1165–1176. https://doi.org/10.1016/j.bbalip.2011.07.015

Haas, J.T., Francque, S., Staels, B., 2016. Pathophysiology and Mechanisms of Nonalcoholic Fatty Liver Disease. Annu. Rev. Physiol. 78, 181–205. https://doi.org/10.1146/annurev-physiol-021115-105331

Hamabe, A., Uto, H., Imamura, Y., Kusano, K., Mawatari, S., Kumagai, K., Kure, T., Tamai, T., Moriuchi, A., Sakiyama, T., Oketani, M., Ido, A., Tsubouchi, H., 2011. Impact of cigarette smoking on onset of nonalcoholic fatty liver disease over a 10-year period. J. Gastroenterol. 46, 769–778. https://doi.org/10.1007/s00535-011-0376-z

Hang, B., Sarker, A.H., Havel, C., Saha, S., Hazra, T.K., Schick, S., Jacob, P., Rehan, V.K., Chenna, A., Sharan, D., Sleiman, M., Destaillats, H., Gundel, L.A., 2013. Thirdhand smoke causes DNA damage in human cells. Mutagenesis 28, 381–391. https://doi.org/10.1093/mutage/get013

Hang, B., Wang, P., Zhao, Y., Sarker, A., Chenna, A., Xia, Y., Snijders, A.M., Mao, J.H., 2017. Adverse health effects of thirdhand smoke: From cell to animal models. Int. J. Mol. Sci. 18. https://doi.org/10.3390/ijms18050932

Hara, H., Araya, J., Ito, S., Kobayashi, K., Takasaka, N., Yoshii, Y., Wakui, H., Kojima, J., Shimizu, K., Numata, T., Kawaishi, M., Kamiya, N., Odaka, M., Morikawa, T., Kaneko, Y., Nakayama, K., Kuwano, K., 2013. Mitochondrial fragmentation in cigarette smoke-induced bronchial epithelial cell senescence. Am. J. Physiol. - Lung Cell. Mol. Physiol. 305. https://doi.org/10.1152/ajplung.00146.2013

Huang, D.W., Sherman, B.T., Lempicki, R.A., 2009. Systematic and integrative analysis of large gene lists using DAVID bioinformatics resources. Nat. Protoc. https://doi.org/10.1038/nprot.2008.211

IARC, n.d. RISK OF CHEMICALS TO HUMANS. Tobacco Smoking 38.

Jacob, P., Benowitz, N.L., Destaillats, H., Gundel, L., Hang, B., Martins-Green, M., Matt, G.E., Quintana, P.J.E., Samet, J.M., Schick, S.F., Talbot, P., Aquilina, N.J., Hovell, M.F., Mao, J.H., Whitehead, T.P., 2017. Thirdhand smoke: New evidence, challenges, and future directions. Chem. Res. Toxicol. 30, 270–294. https://doi.org/10.1021/acs.chemrestox.6b00343

Jacobs, R.L., van der Veen, J.N., Vance, D.E., 2013. Finding the balance: The role of S-adenosylmethionine and phosphatidylcholine metabolism in development of nonalcoholic fatty liver disease. Hepatology 58, 1207–1209. https://doi.org/10.1002/hep.26499

Joesten, W.C., Kennedy, M.A., 2019. RANCM: a new ranking scheme for assigning confidence levels to metabolite assignments in NMR-based metabolomics studies. Metabolomics 15. https://doi.org/10.1007/s11306-018-1465-2

Kim, N.H., Jung, Y.S., Hong, H.P., Park, J.H., Kim, H.J., Park, D. Il, Cho, Y.K., Sohn, C. Il, Jeon, W.K., Kim, B.I., 2018. Association between cotinine-verified smoking status and risk of nonalcoholic fatty liver disease. Liver Int. 1–8. https://doi.org/10.1111/liv.13701

Koves, T.R., Ussher, J.R., Noland, R.C., Slentz, D., Mosedale, M., Ilkayeva, O., Bain, J., Stevens, R., Dyck, J.R.B., Newgard, C.B., Lopaschuk, G.D., Muoio, D.M., 2008. Mitochondrial Overload and Incomplete Fatty Acid Oxidation Contribute to Skeletal Muscle Insulin Resistance. Cell Metab. 7, 45–56. https://doi.org/10.1016/j.cmet.2007.10.013

Kwee, S.A., Sato, M.M., Kuang, Y., Franke, A., Custer, L., Miyazaki, K., Wong, L.L., 2017. [18F]Fluorocholine PET/CT Imaging of Liver Cancer: Radiopathologic Correlation with Tissue Phospholipid Profiling. Mol. Imaging Biol. 19, 446–455. https://doi.org/10.1007/s11307-016-1020-3

Lake, A.D., Novak, P., Shipkova, P., Aranibar, N., Robertson, D.G., Reily, M.D., Lehman-Mckeeman, L.D., Vaillancourt, R.R., Cherrington, N.J., 2015. Branched chain amino acid metabolism profiles in progressive human nonalcoholic fatty liver disease. Amino Acids 47, 603–615. https://doi.org/10.1007/s00726-014-1894-9

Lesurtel, M., Soll, C., Humar, B., Clavien, P.A., 2012. Serotonin: A double-edged sword for the liver? Surgeon 10, 107–113. https://doi.org/10.1016/j.surge.2011.11.002

Li, S., Gao, D., Jiang, Y., 2019. Function, detection and alteration of acylcarnitine metabolism in hepatocellular carcinoma. Metabolites 9. https://doi.org/10.3390/metabo9020036

Liu, Y., Dai, M., Bi, Y., Xu, M., Xu, Y., Li, M., Wang, T., Huang, F., Xu, B., Zhang, J., Li, X., Wang, W., Ning, G., 2013. Active Smoking, Passive Smoking, and Risk of Nonalcoholic Fatty Liver Disease (NAFLD): A Population-Based Study in China. J. Epidemiol. 23, 115–121. https://doi.org/10.2188/jea.JE20120067

Mai, M., Tönjes, A., Kovacs, P., Stumvoll, M., Fiedler, G.M., Leichtle, A.B., 2013. Serum levels of acylcarnitines are altered in prediabetic conditions. PLoS One 8. https://doi.org/10.1371/journal.pone.0082459

Martins-Green, M., Adhami, N., Frankos, M., Valdez, M., Goodwin, B., Lyubovitsky, J., Dhall, S., Garcia, M., Egiebor, I., Martinez, B., Green, H.W., Havel, C., Yu, L., Liles, S., Matt, G., Destaillats, H., Sleiman, M., Gundel, L.A., Benowitz, N., Jacob, P., Hovell, M., Winickoff, J.P., Curras-Collazo, M., 2014. Cigarette smoke toxins deposited on surfaces: Implications for human health. PLoS One 9, 1–12. https://doi.org/10.1371/journal.pone.0086391

Matt, G.E., Quintana, P.J.E., Destaillats, H., Gundel, L.A., Sleiman, M., Singer, B.C., Jacob, P., Benowitz, N., Winickoff, J.P., Rehan, V., Talbot, P., Schick, S., Samet, J., Wang, Y., Hang, B., Martins-Green, M., Pankow, J.F., Hovell, M.F., 2011. Thirdhand Tobacco Smoke: Emerging Evidence and Arguments for a Multidisciplinary Research Agenda. Environ. Health Perspect. 119, 1218–1226. https://doi.org/10.1289/ehp.1103500

Michel, V., Yuan, Z., Ramsubir, S., Bakovic, M., 2006. Choline transport for phospholipid synthesis. Exp. Biol. Med. (Maywood). 231, 490–504. https://doi.org/231/5/490 [pii]

Müller, D.C., Degen, C., Scherer, G., Jahreis, G., Niessner, R., Scherer, M., 2014. Metabolomics using GC-TOF-MS followed by subsequent GC-FID and HILIC-MS/MS analysis revealed significantly altered fatty acid and phospholipid species profiles in plasma of smokers. J. Chromatogr. B Anal. Technol. Biomed. Life Sci. https://doi.org/10.1016/j.jchromb.2014.02.044

Ott, W., Klepeis, N., Switzer, P., 2008. Air change rates of motor vehicles and in-vehicle pollutant concentrations from secondhand smoke. J. Expo. Sci. Environ. Epidemiol. https://doi.org/10.1038/sj.jes.7500601

PeiYi, L., YanYan, X., YuHan, T., Min, D., Xiao, Y., Jian, S., Lin, X., Meian, H., Sheng, W., Jing, Y., YouJie, W., Yuan, L., TangChun, W., XiaoPing, M., Ping, Y., Liu, P., Xu, Y., Tang, Y., Du, M., Yu, X., Sun, J., Xiao, L., He, M., Wei, S., Yuan, J., Wang, Y., Liang, Y., Wu, T., Miao, X., Yao, P., 2017. Independent and joint effects of moderate alcohol consumption and smoking on the risks of non-alcoholic fatty liver disease in elderly Chinese men. PLoS One 12, e0181497. https://doi.org/10.1371/journal.pone.0181497

Pi, J., Wu, X., Feng, Y., 2016. Fragmentation patterns of five types of phospholipids by ultra-high-performance liquid chromatography electrospray ionization quadrupole time-of-flight tandem mass spectrometry. Anal. Methods. https://doi.org/10.1039/C5AY00776C

Pirola, C.J., Sookoian, S., 2018. Multiomics biomarkers for the prediction of nonalcoholic fatty liver disease severity. World J. Gastroenterol. 24, 1601–1615. https://doi.org/10.3748/wjg.v24.i15.1601

Pyttel, S., Zschörnig, K., Nimptsch, A., Paasch, U., Schiller, J., 2012. Enhanced lysophosphatidylcholine and sphingomyelin contents are characteristic of spermatozoa from obese men - A MALDI mass spectrometric study. Chem. Phys. Lipids 165, 861–865. https://doi.org/10.1016/j.chemphyslip.2012.11.001

Ràfols, P., Heijs, B., del Castillo, E., Yanes, O., McDonnell, L.A., Brezmes, J., Pérez-Taboada, I., Vallejo, M., García-Altares, M., Correig, X., 2020. rMSIproc: an R package for mass spectrometry imaging data processing. Bioinformatics. https://doi.org/10.1093/bioinformatics/btaa142

Ràfols, P., Torres, S., Ramírez, N., Del Castillo, E., Yanes, O., Brezmes, J., Correig, X., 2017. RMSI: An R package for MS imaging data handling and visualization. Bioinformatics 33, 2427–2428. https://doi.org/10.1093/bioinformatics/btx182

Ràfols, P., Vilalta, D., Torres, S., Calavia, R., Heijs, B., McDonnell, L.A., Brezmes, J., del Castillo, E., Yanes, O., Ramírez, N., Correig, X., 2018. Assessing the potential of sputtered gold nanolayers in mass spectrometry imaging for metabolomics applications. PLoS One 13, e0208908. https://doi.org/10.1371/journal.pone.0208908

Rein-Fischboeck, L., Haberl, E.M., Pohl, R., Schmid, V., Feder, S., Krautbauer, S., Liebisch, G., Buechler, C., 2018. Alpha-syntrophin null mice are protected from non-alcoholic steatohepatitis in the methionine-choline-deficient diet model but not the atherogenic diet model. Biochim. Biophys. Acta - Mol. Cell Biol. Lipids 1863, 526–537. https://doi.org/10.1016/j.bbalip.2018.02.006

Reis, A., Spickett, C.M., 2012. Chemistry of phospholipid oxidation. Biochim. Biophys. Acta - Biomembr. 1818, 2374–2387. https://doi.org/10.1016/j.bbamem.2012.02.002

Schymanski, E.L., Jeon, J., Gulde, R., Fenner, K., Ruff, M., Singer, H.P., Hollender, J., 2014. Identifying small molecules via high resolution mass spectrometry: Communicating confidence. Environ. Sci. Technol. 48, 2097–2098. https://doi.org/10.1021/es5002105

Sherriff, J.L., Properzi, C., Oddo, J., Adams, L.A., 2016. Choline , Its Potential Role in Nonalcoholic Fatty Liver Disease , and the Case for Human and Bacterial Genes 1 , 2 5–13. https://doi.org/10.3945/an.114.007955.N

Siuzdak, G., Patti, G.J., Yanes, O., 2012. Innovation: Metabolomics: the apogee of the omics trilogy. Nat. Rev. Mol. Cell Biol. 13, 263–269.

Sleiman, M., Gundel, L.A., Pankow, J.F., Jacob, P., Singer, B.C., Destaillats, H., 2010. Formation of carcinogens indoors by surface-mediated reactions of nicotine with nitrous acid, leading to potential thirdhand smoke hazards. Proc. Natl. Acad. Sci. 107, 6576–6581. https://doi.org/10.1073/pnas.0912820107

Smith, C.A., O'Maille, G., Want, E.J., Qin, C., Trauger, S.A., Brandon, T.R., Custodio, D.E., Abagyan, R., Siuzdak, G., 2005. METLIN: a metabolite mass spectral database. Ther. Drug Monit. 27, 747–51.

Smith, C.A., Want, E.J., O'Maille, G., Abagyan, R., Siuzdak, G., 2006. XCMS: Processing Mass Spectrometry Data for Metabolite Profiling Using Nonlinear Peak Alignment, Matching, and Identification. Anal. Chem. 78, 779–787. https://doi.org/10.1021/ac051437y

Sun, L., Liang, L., Gao, X., Zhang, H., Yao, P., Hu, Y., Ma, Y., Wang, F., Jin, Q., Li, H., Li, R., Liu, Y., Hu, F.B., Zeng, R., Lin, X., Wu, J., 2016. Early prediction of developing type 2 diabetes by plasma acylcarnitines: A population-based study. Diabetes Care 39, 1563–1570. https://doi.org/10.2337/dc16-0232

Torres, S., Merino, C., Paton, B., Correig, X., Ramírez, N., 2018. Biomarkers of exposure to secondhand and thirdhand Tobacco smoke: Recent advances and future perspectives. Int. J. Environ. Res. Public Health. https://doi.org/10.3390/ijerph15122693

Vinaixa, M., Miguel, A., Rull, A., Joven, J., Correig, X., 2010. Metabolomic Assessment of the Effect of Dietary Cholesterol in the Progressive Development of Fatty Liver Disease research articles 2527–2538.

Wishart, D.S., Jewison, T., Guo, A.C., Wilson, M., Knox, C., Liu, Y., Djoumbou, Y., Mandal, R., Aziat, F., Dong, E., Bouatra, S., Sinelnikov, I., Arndt, D., Xia, J., Liu, P., Yallou, F., Bjorndahl, T., Perez-Pineiro, R., Eisner, R., Allen, F., Neveu, V., Greiner, R., Scalbert, A., 2012. HMDB 3.0—The Human Metabolome Database in 2013. Nucleic Acids Res. 41, D801–D807. https://doi.org/10.1093/nar/gks1065

Wu, G., Fang, Y.-Z., Yang, S., Lupton, J.R., Turner, N.D., 2004. Glutathione Metabolism and Its Implications for Health. J. Nutr. https://doi.org/10.1093/jn/134.3.489

Yuan, H., Shyy, J.Y.J., Martins-Green, M., 2009. Second-hand smoke stimulates lipid accumulation in the liver by modulating AMPK and SREBP-1. J. Hepatol. 51, 535–547. https://doi.org/10.1016/j.jhep.2009.03.026

6. General discussion and conclusions

UNIVERSITAT ROVIRA I VIRGILI
ADVANCES ON THIRDHAND SMOKE USING TARGETED AND UNTARGETED APPROACHES
Sònia Torres Gené

This thesis aimed to advance on the current knowledge about a new poorly studied way of exposure to tobacco smoke toxicants: thirdhand smoke. To accomplish that, this thesis has been divided in two main objectives: to improve the chemical characterization of THS, and to advance on the health effects derived from THS exposure.

In order to contribute on the advance on THS exposure we have gathered the available information to date to understand the advantages and limitations of the performed exposure studies to provide the community with an overview of the issue and to be able to move in the right direction. To achieve the second objective, we have applied classical approaches, such as the targeted study of the tobacco-specific compounds in THS, in combination with untargeted approaches usually used in other fields such as metabolomics but applied for the first time to the chemical characterization of THS. For the achievement of the third objective the health impact of THS has been studied conducting a metabolomic study using a murine model exposed to THS in conditions that mimic children's exposure in smokers' homes.

In this section we will discuss the advances and achievements presented in this thesis as well as the limitations and the future research regarding THS and the methodologies used.

6.1 SHS and THS biomarkers

In Chapter 2 we present a review with the recent advances and future perspectives of the assessment of SHS and THS exposure that has been published in the International journal of environmental research and public

health. The relevance of the topic is supported by the high number of citations; 18 to date.

One of the main limitations in assessing the risk of exposure to THS is the lack of specific biomarkers. Several authors, have stablished threshold values for cotinine concentrations in urine and blood as an attempt to differentiate SHS exposure from active smoking, based on the data obtained from large epidemiological studies such as the National Health and Nutrition Examination Survey [NHANES] [1–3] of the US. However, THS is a relatively recently known route of exposure and it is not considered in most of the surveys. Consequently, the measured exposure is usually a combination of SHS and THS.

In order to shed light on this issue and summarize the concentration ranges found in the research made up to date, SHS and THS exposure values have been discussed in this thesis. As an example, we observed that urinary concentration of both cotinine and NNAL do not serve to differentiate between low exposure to SHS and THS exposure, being the concentration range of low SHS exposure for cotinine (0.05 – 5ng/mL), and (0.25-30 ng/mL) for THS and (0.95-2.21 pg/mL) and (2.7-6.7 pg/mL) for NNAL respectively [4]. However, it has been observed that the urinary ratio NNAL/cotinine is higher in THS exposed than in SHS or active smokers [5]. Certainly, the simultaneous determination of nicotine and TSNAs related biomarkers as well as the search of specific THS biomarkers would be key to estimate the level of exposure to THS. Although the simultaneous determination of more than one tobacco biomarker would help to a better characterization of THS exposure, complementary approaches are needed to determine the health effects derived from THS exposure.

6.2 Analytical procedures and characterization of the chemical composition of THS in indoor dust

Regarding the chemical characterization of THS, previous research was mainly focused on the application of targeted approaches to determine tobacco smoke toxicants in dust. In most of the studies the concentration of nicotine deposited in dust have been used as THS marker in order to study the levels of THS contamination in indoor environments [6–11]. Although it is known for the community that nicotine reacts to form secondary pollutants, few studies have simultaneously analyzed other tobacco-specific markers, such as tobacco-specific nitrosamines (TSNAs), making a partial THS characterization. Nicotine is directly related to tobacco use, however, once released into the air and absorbed into indoor surfaces, it reacts to form TSNA, so its isolated analysis provides limited information about a household's smoking habits. However, the analysis of different THS markers as well as the ratio TSNAs/nicotine provides a clearer idea. As an example it has been found that the NNK/nicotine ratio is higher in house dust samples of non-smokers homes [5].

In the last decades different methods have been developed for the analysis of nicotine [9,12–15] or nicotine and TSNAs in dust [6,11,16]. Targeted approaches are suitable for the development of methods to simultaneously determine nicotine and TSNAs in dust. However, a big analytical effort needs to be done in order to develop reproducible methods that reach the limits of quantification required for the determination of compounds, such as NNAL and NNA. These compounds are found in dust at very low concentrations (ng/g of NNAL/NNA vs. µg/g for nicotine). This wide range of concentrations as well as the different chemical properties of the targeted compounds makes more difficult the development of one single method for the simultaneous determination of

these compounds in dust samples. Consequently, the development of robust and sensible methods for the simultaneous determination of the different tobacco-specific compounds (THS markers) is essential for the assessment of THS exposure.

To date THS has not been fully characterized since its analysis has been limited to the targeted analysis of tobacco specific compounds. To the best of our knowledge, untargeted approaches have been never used to enhance the chemical characterization of THS. Thus, untargeted approaches and new methodologies are very welcome since they would allow an advance in the search for new tracers and would help to understand how THS compounds behave together with other tobacco-specific and non-specific contaminants present in house dust.

The ultimate goal in untargeted approaches is the comprehensive characterization and quantification of compounds. However, due to the large chemical diversity and the number of existing compounds and the emerging contaminants, the achievement of this goal will depend on the analytical methods and platforms used and the data processing strategies applied. Regarding the analytical methods, several studies for the non-target screening of dust have been described, using comprehensive two-dimensional liquid chromatography-coupled to TOFMS [17] and two dimensional gas chromatography coupled to TOFMS[18] as analytical techniques. Although these techniques have shown its strength in resolving complex environmental matrices they not provide a real advance on the compound identification. In the last decades the advance of the HRMS instruments have played an important role for the identification of unknowns due to the exact mass and/or the possibility to perform MSMS experiments. However, few studies have been performed for the untargeted analysis of indoor dust using HRMS [19–21].

In this context, to improve the chemical characterization of THS, the results of this thesis present two complementary strategies: a) the development of an enhanced analytical method for the simultaneous quantification of seven tobacco-specific toxicants in house dust, including NNA as a good candidate of exclusive marker of environmental THS contamination (Chapter 3);and b) the characterization of indoor dust samples from smokers' and non-smokers' homes, by combining the targeted analysis of tobacco-specific toxicants with a non-target screening approach followed by a novel workflow of compound annotation (Chapter 4).

The developed targeted method for the trace analysis of nicotine, cotinine and four TSNAs presented in Chapter 3 is in accordance with the main trends in the analytical chemistry field including the use of high-throughput methods, with minimum time and solvent consumption and little sample manipulation. The method is based on a QuEChERS extraction, uses only 2 mL of solvent per sample, it is easy to automatize and doesn't require specific and expensive equipment making it a method accessible to any laboratory. The proposed method reaches the limits of quantification necessary for the analysis of Nicotine and TSNAs which are lower compared to the limits obtained in previous studies [6,11,16]. Despite not being an exclusive method for nicotine analysis, the limit of quantification is up to two orders of magnitude lower compared to a method frequently used for nicotine quantification (0.06 vs 10) ng g^{-1} [18]. Comparing with a method developed for the simultaneous quantification of nicotine and TSNAs, our LODs are lower for both nicotine (15.6 vs 0.2) ng g^{-1} and TSNAs ranges (2.5-15 ng g^{-1}) vs (0.12-2.66 ng g^{-1}) [16]. To the best of our knowledge this is the first time that nicotine and NNA are determined together using the same analytical workflow and instrumental platform. As an example in a previous study nicotine was analyzed using GC-MS

and the rest of TSNAs using LC-MS [11]. The extraction method proposed also accomplishes the demanded characteristics for the development of extraction methods used in untargeted approaches, thus providing the extraction of a wide variety of organic compounds, minimizing sample manipulation. Moreover, the matrix effect has been reduced with the use of a sorbent that retains the big amount of lipids present in dust.

The workflow developed for the untargeted analysis of dust samples presented in Chapter 4 combines the acquisition and data processing strategies from our group expertise on untargeted metabolomics, with a novel strategy for environmental toxicants identification applied as part of the research stay at the Environmental Cheminformatics Group at the Luxembourg Centre for systems Biomedicine.

Analysis were performed using an orbitrap (Exactive) which is one of the mass analyzers with higher resolving power. For compound identification we explore the possibility of acquiring MSMS data using DDA mode. For feature prioritization we applied two different strategies, first features were selected when were found at least in 80% of the same group which is a common strategy in environmental analysis. Secondly, univariant statistics were applied in order to assess the quality of the experiment, and select relevant features between groups, which is a strategy commonly used in metabolomic studies. MS/MS data obtained was used for compound annotation by in silico fragmentation using Metfrag and library search against PubChem database. To the best of our knowledge only one previous study has used MSMS data and this methodology for the identification of toxicants in plastic toys [20]. For other studies performed in dust, suspect chemicals with elevated exposure and/or toxicity potential were selected and used for further examination [19,21,24]. Typically, suspect compounds are confirmed with the use of standards or

reacquiring the sample performing MS/MS experiments which imply long periods of time and several sample acquisition datasets. These methods present its own limitations, even though samples can be stored at -80°C, when reacquiring the sample for MS/MS confirmation deviations in retention time and instrument drift affects the reliability of the analysis. This kind of strategies are not in accordance with the most advanced methods proposed either in other fields such as metabolomics or the current methods proposed by environmental scientist [25]. Current strategies are focus on finding automated methods for compound identification. Auto MSMS strategies allow the MSMS acquisition of hundreds of compounds in the same run allowing the identification of unknown compounds in a sample. However, the selection of the acquisition mode is not easy. DIA methods result in spectra that may potentially result from multiple precursor ions and DDA methods prioritize the compounds with higher intensity. Although in our case the acquisition in DDA mode allowed the annotation 152 features including nicotine, this kind of acquisition causes the loss of identifying compounds that are found in the sample at low concentration which is the common case when analyzing emergent pollutants such as those found in THS. Consequently, the TSNAs present in the samples were not automatically identified. Since this work is still in progress, new approaches for enhance the annotation of the compounds are being done.

6.3 Advance on the health impact of THS exposure

In the last decades, several studies has focused on unraveling the toxicity and the health impact of active smoking and passive smoking[26]. However, THS health effects at the molecular level and health impact on human beings are largely unknown. Regarding the health effects related to THS, different studies

have been conducted mainly using animal models and cells. Typically, that kind of studies measure changes in specific genes, proteins or metabolites to evaluate health damage [27]. With these approaches it has been demonstrated that THS causes several alterations, including cellular damage in human cells [28] and increased lipid levels in liver, excess of collagen production and high levels of inflammatory cytokines in lungs, poor wound healing and hyperactivity in mice[29].

Although these approaches provide valuable data, the information obtained from targeted approaches is limited and non-expected effects are not captured. Metabolomics is a highly appropriate tool to study organism-environment interactions and therefore it is ideal for the characterization of the response to THS exposure. As far as we know, only one previous study has used metabolomics to assess THS exposure using cells [30] and the authors suggested that applying metabolomics to animal models would be useful to better characterize the alterations suffered by THS exposure. To the best of our knowledge, the study presented in Chapter 5 is the first metabolomics study to animal models for the characterization of the health effects associated to THS exposure. Although previous studies had characterized some of the alterations induced in liver of mice exposed to THS [31–33], several molecular alterations and the variety of the dysregulated metabolic pathways due to THS exposure are reported here for the first time.

Using the multiplatform-metabolomics approach described in this thesis, eighty-eight metabolites altered by THS exposure were annotated. We also detected the dysregulation of twenty-one metabolic pathways including purine, glutathione, glutamine and glutamate, glycerophospholipid, glycine, serine and threonine, and oxidative phosphorylation metabolisms. The main health effect associated with THS exposure was abnormal lipid metabolism known as NAFLD,

being oxidative stress the main mechanism for the alterations suffered, as it has been previously suggested [29]. MSI permitted the visualization of the lipid accumulation suffered in liver and the discovery of the different distribution of lipids in liver, thus opening a new field of research beyond THS exposure. Since the oxidative stress suffered in liver of mice exposed to THS was already known, the effect of a treatment with antioxidants had been previously studied. Authors found that that the oxidative stress markers measured improved with antioxidant treatment [31,32]. With our untargeted study we were able to capture unexpected alterations finding that some alterations were not reverted with the administration of the antioxidant treatment. Since these results would not have been reported with a targeted approach, we strongly believe that by applying metabolomics to different organs and biofluids would help to better understand the health effects related to THS.

6.4 Future trends and perspectives

THS exposure is still a relatively new phenomenon, although many advances have been done the last years, future research must focus on facilitating hazards identification and exposure and carry out robust risk assessment to address THS impact on susceptible populations. The implementation of non-targeted methods would facilitate a complete characterization of THS and the search for new specific environmental markers.

In order to advance on the THS chemical characterization future research must be focused on improving identification strategies, searching for common workflows and reducing analysis time. Relying on already working strategies such the ones used in metabolomics studies may be key for the untargeted

environmental analysis to advance rapidly. Regarding the optimization of the identification workflow, improvements on sample acquisition must be applied. Advanced strategies aim to perform MS and MSMS experiments at a time in order to reduce analysis time and sample manipulation. Consequently, methods that prioritize features of interest must be key. This would probably involve the implementation of rapid and exploratory data analysis at the time the sample is being acquired.

For the health impact caused by THS, metabolomic studies would be key for the search of new biomarkers to assess THS exposure and facilitate the differentiation between THS, active smoking and SHS. The application of metabolomics to animal models would reveal the possible health effects related to THS. However, in order to identify the hazards caused by THS results must be validated using human datasets. Finally, a big effort on communication must be done by the community to bring awareness of this risk to the population and the authorities so new policies must be implemented to prevent exposure to THS and avoid THS contamination in public spaces.

6.5 References

(1) Jacob, P.; Benowitz, N. L.; Destaillats, H.; Gundel, L.; Hang, B.; Martins-Green, M.; Matt, G. E.; Quintana, P. J. E.; Samet, J. M.; Schick, S. F.; Talbot, P.; Aquilina, N. J.; Hovell, M. F.; Mao, J. H.; Whitehead, T. P. Thirdhand Smoke: New Evidence, Challenges, and Future Directions. *Chem. Res. Toxicol.* **2017**, *30* (1), 270–294. https://doi.org/10.1021/acs.chemrestox.6b00343.

(2) Kim, S.; Aung, T.; Berkeley, E.; Diette, G. B.; Breysse, P. N. Measurement of Nicotine in Household Dust. *Environ. Res.* **2008**, *108* (3), 289–293. https://doi.org/10.1016/j.envres.2008.07.004.

(3) Whitehead, T. P.; Metayer, C.; Park, J. S.; Does, M.; Buffler, P. A.; Rappaport, S. M. Levels of Nicotine in Dust from Homes of Smokeless Tobacco Users. *Nicotine Tob. Res.* **2013**, *15* (12), 2045–2052. https://doi.org/10.1093/ntr/ntt096.

(4) Whitehead, T.; Metayer, C.; Ward, M. H.; Nishioka, M. G.; Gunier, R.; Colt, J. S.; Reynolds, P.; Selvin, S.; Buffler, P.; Rappaport, S. M. Is House-Dust Nicotine a Good Surrogate for Household Smoking? *Am. J. Epidemiol.* **2009**, *169* (9), 1113–1123. https://doi.org/10.1093/aje/kwp021.

(5) Matt, G. E.; Quintana, P. J. E.; Hovell, M. F.; Bernert, J. T.; Song, S.; Novianti, N.; Juarez, T.; Floro, J.; Gehrman, C.; Garcia, M.; Larson, S. Households Contaminated by Environmental Tobacco Smoke: Sources of Infant Exposures. *Tob. Control* **2004**, *13* (1), 29–37. https://doi.org/10.1136/tc.2003.003889.

(6) Matt, G. E.; Mahabee-Gittens, E. M.; Zakarian, J. M.; Quintana, P. J. E.; Hoh, E.; Myers, M. Nicotine in Thirdhand Smoke Residue Predicts Relapse from Smoking Cessation: A Pilot Study. *Addict. Behav.* **2019**, *98* (June), 106041. https://doi.org/10.1016/j.addbeh.2019.106041.

(7) Whitehead, T. P.; Havel, C.; Metayer, C.; Benowitz, N. L.; Jacob, P. Tobacco Alkaloids and Tobacco-Specific Nitrosamines in Dust from Homes of Smokeless Tobacco Users, Active Smokers, and Nontobacco Users. *Chem. Res. Toxicol.* **2015**, *28* (5), 1007–1014. https://doi.org/10.1021/acs.chemrestox.5b00040.

(8) Ramírez, N.; Özel, M. Z.; Lewis, A. C.; Marcé, R. M.; Borrull, F.; Hamilton, J. F. Determination of Nicotine and N-Nitrosamines in House Dust by Pressurized Liquid Extraction and Comprehensive Gas Chromatography-Nitrogen Chemiluminiscence Detection. *J. Chromatogr. A* **2012**, *1219*, 180–187. https://doi.org/10.1016/j.chroma.2011.11.017.

(9) Matt, G. E.; Quintana, P. J. E.; Zakarian, J. M.; Hoh, E.; Hovell, M. F.; Mahabee-Gittens, M.; Watanabe, K.; Datuin, K.; Vue, C.; Chatfield, D. A. When Smokers Quit: Exposure to Nicotine and Carcinogens Persists from Thirdhand Smoke Pollution. *Tob. Control* **2017**, *26* (5), 548–556. https://doi.org/10.1136/tobaccocontrol-2016-053119.

(10) Ouyang, X.; Weiss, J. M.; de Boer, J.; Lamoree, M. H.; Leonards, P. E. G. Non-Target Analysis of Household Dust and Laundry Dryer Lint Using Comprehensive Two-Dimensional Liquid Chromatography Coupled with Time-of-Flight Mass Spectrometry. *Chemosphere* **2017**, *166*, 431–437. https://doi.org/10.1016/j.chemosphere.2016.09.107.

(11) Hilton, D. C.; Jones, R. S.; Sjödin, A. A Method for Rapid, Non-Targeted Screening for Environmental Contaminants in Household Dust. *J. Chromatogr. A* **2010**, *1217* (44), 6851–6856. https://doi.org/10.1016/j.chroma.2010.08.039.

(12) Rager, J. E.; Strynar, M. J.; Liang, S.; McMahen, R. L.; Richard, A. M.; Grulke, C. M.; Wambaugh, J. F.; Isaacs, K. K.; Judson, R.; Williams, A. J.; Sobus, J. R. Linking High Resolution Mass Spectrometry Data with Exposure and Toxicity Forecasts to Advance High-Throughput Environmental Monitoring. *Environ. Int.* **2016**, *88*, 269–280. https://doi.org/10.1016/j.envint.2015.12.008.

(13) Moschet, C.; Anumol, T.; Lew, B. M.; Bennett, D. H.; Young, T. M. Household Dust as a Repository of Chemical Accumulation: New Insights from a Comprehensive High-Resolution Mass Spectrometric Study. *Environ. Sci. Technol.* **2018**, *52* (5), 2878–2887. https://doi.org/10.1021/acs.est.7b05767.

(14) Shin, H. M.; Moschet, C.; Young, T. M.; Bennett, D. H. Measured Concentrations of Consumer Product Chemicals in California House Dust: Implications for Sources, Exposure, and Toxicity Potential. *Indoor Air* **2020**, *30* (1), 60–75. https://doi.org/10.1111/ina.12607.

(15) Newton, S. R.; Sobus, J. R.; Ulrich, E. M.; Singh, R. R.; Chao, A.; McCord, J.; Laughlin-Toth, S.; Strynar, M. Examining NTA Performance and Potential Using Fortified and Reference House Dust as Part of EPA's Non-Targeted Analysis Collaborative Trial (ENTACT). *Anal. Bioanal. Chem.* **2020**, *412* (18), 4221–4233. https://doi.org/10.1007/s00216-020-02658-w.

(16) Rostkowski, P.; Haglund, P.; Aalizadeh, R.; Alygizakis, N.; Thomaidis, N.; Arandes, J. B.; Nizzetto, P. B.; Booij, P.; Budzinski, H.; Brunswick, P.; Covaci, A.; Gallampois, C.; Grosse, S.; Hindle, R.; Ipolyi, I.; Jobst, K.; Kaserzon, S. L.; Leonards, P.; Lestremau, F.; Letzel, T.; Magnér, J.; Matsukami, H.; Moschet, C.; Oswald, P.; Plassmann, M.; Slobodnik, J.; Yang, C. The Strength in Numbers: Comprehensive Characterization of House Dust Using Complementary Mass Spectrometric Techniques. *Anal. Bioanal. Chem.* **2019**, *411* (10), 1957–1977. https://doi.org/10.1007/s00216-019-01615-6.

(17) Dong, T.; Zhang, Y.; Jia, S.; Shang, H.; Fang, W.; Chen, D.; Fang, M. Human Indoor Exposome of Chemicals in Dust and Risk Prioritization Using EPA's ToxCast Database. *Environ. Sci. Technol.* **2019**, *53* (12), 7045–7054. https://doi.org/10.1021/acs.est.9b00280.

(18) Hollender, J.; Schymanski, E. L.; Singer, H. P.; Ferguson, P. L. Nontarget Screening with High Resolution Mass Spectrometry in the Environment: Ready to Go? *Environ. Sci. Technol.* **2017**, *51* (20), 11505–11512. https://doi.org/10.1021/acs.est.7b02184.

(19) Argüder, E. Third - Hand Smoke Exposure And. **2019**. https://doi.org/10.4103/ejop.ejop.

(20) Moore, B. F.; Clark, M. L.; Bachand, A.; Reynolds, S. J.; Nelson, T. L.; Peel, J. L. Interactions between Diet and Exposure to Secondhand Smoke on Metabolic Syndrome among Children: NHANES 2007â€"2010. *J. Clin. Endocrinol. Metab.* **2016**. https://doi.org/10.1210/jc.2015-2477.

(21) Bagchi, P.; Geldner, N.; deCastro, B. R.; De Jesús, V. R.; Park, S. K.; Blount, B. C. Crotonaldehyde Exposure in U.S. Tobacco Smokers and Nonsmokers: NHANES 2005–

2006 and 2011–2012. *Environ. Res.* **2018**. https://doi.org/10.1016/j.envres.2018.01.033.

(22) Jain, R. B. Serum Cotinine and Urinary 4-(Methylnitrosamino)-1-(3-Pyridyl)-1-Butanonol Levels among Non-Hispanic Asian American Smokers and Nonsmokers as Compared to Other Race/Ethnicities: Data from NHANES 2011-2012. *Chemosphere* **2015**, *120*, 584–591. https://doi.org/10.1016/j.chemosphere.2014.09.069.

(23) Torres, S.; Merino, C.; Paton, B.; Correig, X.; Ramírez, N. Biomarkers of Exposure to Secondhand and Thirdhand Tobacco Smoke: Recent Advances and Future Perspectives. *International Journal of Environmental Research and Public Health*. 2018. https://doi.org/10.3390/ijerph15122693.

(24) Hang, B.; Wang, P.; Zhao, Y.; Sarker, A.; Chenna, A.; Xia, Y.; Snijders, A. M.; Mao, J. H. Adverse Health Effects of Thirdhand Smoke: From Cell to Animal Models. *Int. J. Mol. Sci.* **2017**, *18* (5). https://doi.org/10.3390/ijms18050932.

(25) Hang, B.; Sarker, A. H.; Havel, C.; Saha, S.; Hazra, T. K.; Schick, S.; Jacob, P.; Rehan, V. K.; Chenna, A.; Sharan, D.; Sleiman, M.; Destaillats, H.; Gundel, L. A. Thirdhand Smoke Causes DNA Damage in Human Cells. *Mutagenesis* **2013**, *28* (4), 381–391. https://doi.org/10.1093/mutage/get013.

(26) Martins-Green, M.; Adhami, N.; Frankos, M.; Valdez, M.; Goodwin, B.; Lyubovitsky, J.; Dhall, S.; Garcia, M.; Egiebor, I.; Martinez, B.; Green, H. W.; Havel, C.; Yu, L.; Liles, S.; Matt, G.; Destaillats, H.; Sleiman, M.; Gundel, L. A.; Benowitz, N.; Jacob, P.; Hovell, M.; Winickoff, J. P.; Curras-Collazo, M. Cigarette Smoke Toxins Deposited on Surfaces: Implications for Human Health. *PLoS One* **2014**, *9* (1), 1–12. https://doi.org/10.1371/journal.pone.0086391.

(27) Xu, B.; Chen, M.; Yao, M.; Ji, X.; Mao, Z.; Tang, W.; Qiao, S.; Schick, S. F.; Mao, J. H.; Hang, B.; Xia, Y. Metabolomics Reveals Metabolic Changes in Male Reproductive Cells Exposed to Thirdhand Smoke. *Sci. Rep.* **2015**, *5*, 1–10. https://doi.org/10.1038/srep15512.

(28) Flores, C.; Adhami, N.; Martins Green, M. The Role of Fatty Acid Metabolism and Apolipoproteins in Ths-Induced Hepatic Steatosis in Mice. *Ferment. Technol.* **2017**, *07* (04). https://doi.org/10.4172/2167-7972.1000359.

(29) Flores, C.; Adhami, N.; Green, M. M. THS Toxins Induce Hepatic Steatosis by Altering Oxidative Stress and SIRT1 Levels. *J. Clin. Toxicol.* **2016**, *06* (05), 1–11. https://doi.org/10.4172/2161-0495.1000318.

(30) Adhami, N.; Chen, Y.; Martins-Green, M. Biomarkers of Disease Can Be Detected in Mice as Early as 4 Weeks after Initiation of Exposure to Third-Hand Smoke Levels Equivalent to Those Found in Homes of Smokers. *Clin. Sci.* **2017**, *131* (19), 2409–2426. https://doi.org/10.1042/CS20171053.

UNIVERSITAT
ROVIRA i VIRGILI